The synthetic multivulva genes and their suppressors regulate opposing cell fates through chromatin remodeling

by
Erik C. Andersen

B.S., Biological Sciences
Stanford University, 2000

Submitted to the Department of Biology
in partial fulfillment of the requirements for the degree of

DOCTOR OF PHILOSOPHY

at the
MASSACHUSETTS INSTITUTE OF TECHNOLOGY

June 2007

Signature of Author: _____
Department of Biology

Certified by: _____
H. Robert Horvitz
Professor of Biology
Thesis Supervisor

Accepted by: _____
Stephen P. Bell
Chairman of the Graduate Committee
Department of Biology

The synthetic multivulva genes and their suppressors regulate opposing cell fates by remodeling chromatin

Erik Andersen

ABSTRACT

The synthetic multivulva (synMuv) genes act redundantly to inhibit vulval fates in *Caenorhabditis elegans*. These genes are grouped into three classes called A, B and C. The class A genes encode putative transcription factors. The class B and C genes encode presumptive transcriptional repressors and chromatin-remodeling factors. The synMuv genes likely repress the transcription of the Ras pathway ligand *lin-3* EGF. Some class B synMuv proteins are homologs of a Nucleosome Remodeling and Deacetylase (NuRD)-like complex and heterochromatin protein 1 (HP1). In addition to a NuRD-like complex, which deacetylates lysine nine of histone H3 (H3K9), and HP1, we found two histone methyltransferase (HMT) genes (*met-1* and *met-2*) that act as class B synMuv genes and repress *lin-3* transcription. *met-1* encodes a *C. elegans* homolog of yeast Set2, an H3K36 HMT that inhibits the ectopic initiation of transcription, and *met-2* encodes a homolog of human SETDB1, an H3K9 HMT involved in transcriptional repression. Our results link H3K36 methylation to a transcriptional repression cascade composed of the NuRD complex, H3K9 methylation and HP1 in the inhibition of ectopic transcriptional initiation. We found that not only do the class A and B synMuv genes act redundantly to inhibit vulval fates, but most genes within each class act in parallel. Pairs of genes, which act together biochemically, function in a single activity in vulval cell-fate specification. Our findings offer an opportunity to determine molecular activities for uncharacterized but conserved synMuv proteins. We identified the *isw-1* synMuv suppressor gene, a homolog of the *Drosophila* ATP-dependent chromatin-remodeling enzyme ISWI. ISW-1 likely acts as part of a NURF-like complex with at least the *C. elegans* NURF301 homolog, to antagonize the synMuv genes in the control of multiple cell-fate decisions. Our results suggest that the NURF-like complex is required in the absence of the synMuv genes to promote the expression of *lin-3* EGF. We found an *lst-3* gain-of-function mutation that suppresses the synMuv phenotype perhaps by repressing *lin-3* EGF transcription. *lst-3* encodes a homolog of the mammalian transcription factor CARP-1. Our results suggest that CARP-1 is a tumor-suppressor gene acting by Ras pathway inhibition.

Thesis Supervisor: H. Robert Horvitz
Title: Professor of Biology

ACKNOWLEDGMENTS

To be honest, I didn't want to join the Horvitz lab at first. After a few conversations with Brendan Galvin and a rotation with Craig Ceol, I caved. I would like to thank both of them for those roles. My advisor, Bob Horvitz created a fertile environment by attracting great scientists and more than adequate funding. For that environment, teaching effective oral and visual presentation skills and grammar, I thank him. Dr. Eileen Furlong and Dr. Matthew Scott at Stanford positively influenced my early scientific pursuits – I owe them much for exciting me about biology and helping to get me to MIT.

My work over the past seven years would have been far less enjoyable and productive if it weren't for my friends in the Horvitz lab: Namiko Abe, Mark Alkema, Kostas Boulias, Craig Ceol, Ewa Davison, Dan Denning, Allan Froelich, Brendan Galvin, Megan Gustafson, Dave Harris, Melissa Harrison, Brad Hersh, Takashi Hirose, Mike Hurwitz, Yin Li, Long Ma, Eric Miska, Shunji Nakano, Bob O'Hagan, Dan Omura, Ignacio Perez de la Cruz, Hillel Schwartz, Johanna Varner and Melanie Worley. I especially thank Ezequiel Alvarez-Saavedra, Peter Reddien, Niels Ringstad and Adam Saffer for continuing to question and inspire me. My path through science would have drastically different without their influence.

It has been a pleasure to be a part of such a tight-knit group of collegues and friends in the BioGrad Class of 2000. This long arduous trip would have been far more painful had it not been for all of them, especially Ezequiel, Lucila and Tomás Alvarez-Saavedra, Andy and Gretchen Baltus, Seth Berman, John Doench, Phil Iaquinta, Chris Petersen and Mark Rosenzweig. Thanks for the games, drinks and fun.

I have been extremely lucky to have a wonderful group of friends outside of the lab to provide stimulating dinner conversations, Buffy the Vampire Slayer indulgence, SCUBA, many beers, vacations and so much more: 31 Miller St. and Visor Enterprises, Aileen Carrigan, Stef Carter, Bryan Baesel, Gloria Brar, Amy Christie, Renuka George, Joe Goebel, Supper Club and Dinner Group. Thank you for still being there regardless of how long it has been since we last spoke.

Not a single day goes by that I don't think about how lucky I am to have a family like mine. My parents, Chris and Mary Andersen, are constantly engaging, caring, concerned and helpful. I've tried to live by their examples and make them proud. My brother, Mark Andersen, is my biggest competitor, most trusted confidant and my best friend. Most of who I am is because of his constant presence.

For most of the past seven years, I have shared my life with Robyn Tanny. She has dealt with an absent and distracted companion with unending patience and unconditional love, and for that I owe her my greatest thanks. My days rise and set with her, and my accomplishments were made possible by her.

TABLE OF CONTENTS

CHAPTER ONE

The synthetic multivulva genes and their suppressors regulate opposing cell fates by remodeling chromatin

Prologue

My interests have focused on the control of cell-fate decisions, specifically the cells fates of the *Caenorhabditis elegans* vulva. My introductory chapter will begin with a discussion of the vulva and the genes controlling vulval fates. Because many of the proteins encoded by the genes that regulate vulval development are involved in the regulation of transcription by chromatin, I will discuss chromatin and how transcription is regulated by chromatin, particularly histone methylation and ATP-dependent chromatin remodeling.

The *Caenorhabditis elegans* vulva

The roundworm *C. elegans* is sexually dimorphic with both males and self-fertilizing hermaphrodites (BRENNER 1974). The hermaphrodite has a vulva, which is the structure through which male sperm enter and embryos exit the animal. The vulva connects the uterus to the outside environment. The vulva is not essential for viability, and mutants defective in vulval cell fates are easily observed using the dissecting microscope (HORVITZ and SULSTON 1980).

The specification of vulval cell fates occurs during the second larval stage. There are six hypodermal blast cells (P3.p to P8.p) on the ventral side of the animal (SULSTON and HORVITZ 1977) named the vulval equivalence group, and each cell has an equal capacity to express vulval fates (Figure 1). A secreted signal from a nearby gonadal cell, named the anchor cell (AC), induces the three closest cells (P5.p, P6.p and P7.p) of the equivalence group to adopt vulval cell fates (SULSTON and WHITE 1980; KIMBLE 1981). The remaining three cells (P3.p, P4.p and P8.p) adopt non-vulval cell fates and fuse with the neighboring hypodermal syncytium called hyp7 (SULSTON and HORVITZ 1977). The three cells receiving the inductive signal from the AC adopt one of two vulval cell fates, named primary (1º) or secondary (2º) (STERNBERG and HORVITZ 1986). P6.p is closest to the AC and normally adopts the 1º vulval fate, where it divides three times to generate eight descendants. P5.p and P7.p adopt 2º vulval fates; each of these cells generate seven descendants. Pair-wise combinations of the 22

descendants of P5.p, P6.p and P7.p ultimately fuse to generate a complex tube composed of concentric cellular rings (PODBILEWICZ and WHITE 1994).

The Ras, Notch and Wnt cell-signaling pathways promote vulval fates

Mutants defective in vulval-fate specification are grouped broadly into two classes (HORVITZ and SULSTON 1980). In vulvaless (Vul) mutants, none of the cells of the vulval equivalence group adopts a vulval fate. By contrast in multivulva (Muv) mutants, all six cells of the vulval equivalence group express vulval fates. Mutants of these two types are defective in the complex signaling initiated by cell-cell interactions. Vul mutants have loss-of-function mutations of genes that promote vulval fates or gain-of-function mutations that inhibit vulval fates. The Muv phenotype is caused by loss-of-function mutations of genes that inhibit vulval fates or gain-of-function mutations of genes that promote vulval fates. Mutants of these two types led to the identification and characterization of both intercellular (cell-cell) signaling pathways and intracellular signaling cascades that direct vulval cell-fate specification.

The conserved Ras cell-signaling pathway was identified and characterized by studies of the *C. elegans* vulva (STERNBERG 2006), *Drosophila* compound eye (SIMON 1994) and mammalian cells. In *C. elegans*, the Ras pathway promotes vulval fates (BEITEL *et al.* 1990; HAN *et al.* 1990). Loss-of-function mutations of genes in the Ras pathway cause Vul phenotypes, and gain-of-function mutations cause Muv phenotypes. The AC initiates Ras pathway activation by expressing the Ras pathway ligand *lin-3* epidermal growth factor (EGF) (HILL and STERNBERG 1992). This inductive signal is secreted and also membrane-bound (DUTT *et al.* 2004). The *let-23* EGF receptor (EGFR) receives the inductive signal and like the mammalian EGFRs (SCHLESSINGER 2000) is thought to dimerize in response to EGF binding. EGF binding causes EGFRs to autophosphorylate and activate the intracellular Ras pathway components. Because the LET-23 EGFR receptor must be expressed on the cell surface in proximity to the LIN-3 EGF ligand, proper localization of LET-23 is crucial to

vulval development. The LIN-2/LIN-7/LIN-10 complex promotes basolateral membrane localization of LET-23 EGFR in *C. elegans* (KAECH *et al.* 1998). After autophosphorylation of LET-23 EGFR, the SEM-5/Grb2 adaptor protein binds and brings the guanine nucleotide exchange factor SOS-1 in close proximity to LET-60 Ras (CLARK *et al.* 1992; LOWENSTEIN *et al.* 1992; OLIVIER *et al.* 1993; CHANG *et al.* 2000). Subsequently, the LET-60 Ras GTPase switch controlling vulval development is activated (BEITEL *et al.* 1990; HAN *et al.* 1990), and then the downstream conserved MPK-1 MAPK amplifies the Ras pathway signal (LACKNER *et al.* 1994; LACKNER and KIM 1998). The Ras pathway terminates in the control of transcription. The heterodimeric transcription factor LIN-1/LIN-31 acts as a transcriptional repressor. After MPK-1 MAPK phosphorylates LIN-1 and LIN-31 (BEITEL *et al.* 1995; TAN *et al.* 1998; MILLER *et al.* 2000), this heterodimer disassociates. LIN-1 and LIN-31 then separately promote the transcription of genes important for the adoption of the 1º vulval fate in P6.p (INOUE *et al.* 2002; CUI and HAN 2003; TIENSUU *et al.* 2005; WAGMAISTER *et al.* 2006). The *lin-1* mutant is Muv because the primary role of LIN-1 is to inhibit vulval fates (BEITEL *et al.* 1995).

Studies of vulval cell-fate mutants also revealed two roles for a Notch signaling pathway in the control of vulval fates. *lin-12* encodes the Notch receptor (YOCHEM *et al.* 1988), which binds Delta/Serrate/LAG-2 (DSL) ligands to activate Notch signaling in different cell types (HENDERSON *et al.* 1994; CHEN and GREENWALD 2004). LIN-12 Notch first influences vulval fates in the fate specification of the AC (GREENWALD *et al.* 1983), the source of the Ras pathway ligand *lin-3* EGF (HILL and STERNBERG 1992). The AC and ventral uterine (VU) cell are determined by cell-cell interactions mediated by Notch. Loss-of-function mutations of *lin-12* Notch cause two AC to be specified, and gain-of-function mutations of *lin-12* cause two VU to be specified (GREENWALD *et al.* 1983). In the vulval cells, *lin-12* Notch promotes the 2º vulval fate (STERNBERG and HORVITZ 1989). Too much Notch pathway activity causes ectopic 2º cells, and too little causes no 2º cells to be specified. Like LET-23 EGFR, membrane localization of

LIN-12 Notch is crucial for its signaling (SHAYE and GREENWALD 2002; SHAYE and GREENWALD 2005). The 1º vulval cell expresses several different DSL ligands to initiate the pathway (CHEN and GREENWALD 2004). Studies of *Drosophila* and mammalian cells reported that after activation by DSL ligands Notch is cleaved in the membrane, and the cytoplasmic domain enters the nucleus to promote transcription (PAN and RUBIN 1997; ANNAERT and DE STROOPER 1999). In the control of vulval fates the cytoplasmic domain of LIN-12 binds to and acts with the CBF1/Su(H)/LAG-1 (CSL) transcription cofactor LAG-1 (CHRISTENSEN *et al.* 1996) to promote the expression of 2º vulval fates in P5.p and P7.p (YOO *et al.* 2004; YOO and GREENWALD 2005).

In addition to Ras and Notch pathways, at least four Wnt ligands and downstream pathway components control vulval-fate specification. First discovered as a pathway required for the asymmetric cell divisions of 2º cell descendants (SAWA *et al.* 1996; INOUE *et al.* 2004), subsequent studies have reported a role in the control of vulval-fate specification (GLEASON *et al.* 2002; GLEASON *et al.* 2006). An identical pathway to that discovered in *Drosophila* promotes vulval fates in *C. elegans*, composed of BAR-1 β-catenin, PRY-1 axin and APR-1 APC. There are at least four Wnt pathway ligands controlling vulval fates (GLEASON *et al.* 2006). Unlike the Ras and Notch pathway, which promote the 1º or 2º vulval cell fates, respectively, the Wnt pathway promotes the adoption of both vulval fates through the prevention of Pn.p fusion with the hypodermal syncytium hyp7 (EISENMANN *et al.* 1998; EISENMANN and KIM 2000). Additionally upstream of the Wnt receptor, many Wnts have been reported to act redundantly to promote vulval cell-fate specification (GLEASON *et al.* 2006).

The interplay between the Ras, Notch and Wnt signaling pathways

The three cell-signaling cascades that control vulval fates interact with each other in different ways. The Ras and Notch pathways oppose each other to specify either 1º or 2º vulval fates, respectively. The Ras and Wnt pathways likely promote induced vulval cell fates cooperatively.

Specifically, the Ras pathway promotes the 1º vulval fate and inhibits the 2º vulval fate (STERNBERG 2006). The Notch pathway down-regulates Ras pathway activity thereby promoting the 2º vulval fate and inhibiting the 1º vulval fate (SUNDARAM 2005). In P6.p where the Ras pathway is normally most active, DSL ligands are produced at higher levels than in other Pn.p cells. This DSL expression leads to greater Notch pathway activity in the neighboring P5.p and P7.p cells. Concurrently, the Ras pathway activates a mechanism to internalize LIN-12 Notch receptors expressed in P6.p. In this way, Notch is inactivated in P6.p, the future 1º vulval cell. The Notch pathway increases transcription of genes whose proteins inhibit Ras pathway activity in P5.p and P7.p, the future 2º cells. These mechanisms ensure that P5.p – P6.p – P7.p adopt the respective 2º - 1º - 2º vulval cell fates in wild-type animals (SULSTON and HORVITZ 1977; STERNBERG and HORVITZ 1986; SUNDARAM 2005).

In addition to the Ras pathway, a Wnt pathway is required for normal vulval cell-fate specification (EISENMANN *et al.* 1998; EISENMANN and KIM 2000). The Wnt pathway inhibits the adoption of the fused (F) fate, in which cells of the vulval equivalence group fuse with the underlying hypodermis (EISENMANN *et al.* 1998) and cannot be induced to become vulval cells. In *bar-1* β-catenin mutants, the vulval equivalence group cells P3.p through P8.p ectopically adopt the F fate, resulting in a hypo-induced phenotype similar to the Vul phenotype. The Wnt pathway promotes the expression of the *lin-39* Hox transcription factor (CLARK *et al.* 1993), which inhibits the F fate through the EGL-18 and ELT-6 GATA transcription factors (KOH *et al.* 2002).

In this model, sequential signaling pathways determine the cells that will ultimately adopt vulval cell fates. First, Wnt signaling determines which vulval equivalence group cells adopt the F fate and fuse with the underlying

hypodermis. The P3.p, P4.p and P8.p cells adopt the F fate in the wild type. Subsequently, the Ras and Notch pathways interact to determine the type of induced vulval cell fate that will be expressed, as described above. An increase in Wnt signaling causes more vulval equivalence group cells to be induced (GLEASON *et al.* 2002) likely because fusion with hyp7 has been inhibited. Additionally, mutations in Wnt genes suppress Muv phenotypes caused by an increase in Ras pathway activity. These results suggest that Wnt might also regulate vulval induction. Assays to separate vulval induction from cell fusion are required to separate an effect on vulval induction from a cell-fusion defects that leaves Pn.p cells unfused and able to be induced.

Some genes negatively regulate vulval fates by inhibiting the Ras pathway

Equally important to the cell-signaling pathways that promote vulval fates in *C. elegans* are the pathways that inhibit vulval fates. Vulval cell-fate mutants with a Muv phenotype are candidates for being defective in such inhibitory signals. Muv mutants from early genetic screens had loss-of-function mutations in genes that act in the Ras pathway to inhibit vulval cell fates, like *lin-1* or *lin-31* (BEITEL *et al.* 1995; TAN *et al.* 1998; MILLER *et al.* 2000). Subsequently, screens were designed to look for genes that inhibit vulval fates in sensitized genetic backgrounds, such as suppressors of the *lin-3* Vul phenotype or enhancers of incompletely penetrant Muv phenotypes caused by mutations of identified Ras pathway negative regulators.

Screens for suppressor of the *lin-3* Vul phenotype identified three genes that inhibit vulval fates, *sli-1*, *sli-3* and *unc-101* (LEE *et al.* 1994; JONGEWARD *et al.* 1995; YOON *et al.* 1995; GUPTA *et al.* 2006). Because *lin-3* EGF is the ligand for LET-23 RTK and the most upstream member of the Ras pathway, negative regulators could affect Ras pathway activity at any step downstream. *sli-3* is uncloned (GUPTA *et al.* 2006) and it is not known how *unc-101* inhibits vulval fates (LEE *et al.* 1994). *sli-1* c-Cbl might act through binding LET-23 EGFR and inhibiting its functions (JONGEWARD *et al.* 1995; YOON *et al.* 1995; YOON *et al.*

2000). LET-60 Ras is similar to GTPases that act as switches in developmental and cellular processes (BEITEL *et al.* 1990; HAN *et al.* 1990). Ras GTPase activating proteins (RasGAPs) inhibit LET-60 by promoting its GTPase activity. The *gap-1* RasGAP is one such negative regulator identified as a suppressor of an incompletely penetrant Vul phenotype (HAJNAL *et al.* 1997). Some negative regulators were identified based on homologies to other organisms, like LIP-1, a phosphatase that inhibits MAPK functions by removing phosphates from MAPK (HAJNAL and BERSET 2002). Mutations in two negative regulatory genes, *dep-1* and *ark-1*, were identified in screens for enhancers of the Muv phenotypes of other negative regulators. DEP-1, a receptor protein tyrosine phosphatase (BERSET *et al.* 2005), and ARK-1, an Ack-related kinase (HOPPER *et al.* 2000), are thought to regulate LET-23 autophosphorylation or inhibitory phosphorylation, respectively. Additionally, the Notch pathway might inhibit the Ras pathway by activating the transcription of Ras pathway inhibitors. The *lst* (lateral signal target) genes, *lip-1*, *ark-1* and *dpy-23* are each activated by the Notch pathway to inhibit Ras pathway activity (YOO *et al.* 2004) thereby promoting the 2º vulval fate. Each of these genes is hypothesized to act in the Pn.p cells to inhibit Ras pathway activity.

The synthetic multivulva genes inhibit vulval fates

The Muv phenotype of one vulval mutant was dependent on two unlinked loss-of-function mutations (HORVITZ and SULSTON 1980; FERGUSON and HORVITZ 1989). These two genes were the founding synthetic multivulva (synMuv) genes. The synMuv genes act in parallel to inhibit vulval fates within three classes, called A, B and C (FERGUSON and HORVITZ 1989; CEOL and HORVITZ 2004). Single mutants or animals multiply mutant for genes in the same class are non-Muv. By contrast, mutations in any two genes in different classes cause a Muv phenotype (Figure 3). In Chapter Three, I discuss why the class C genes are a subset of the class B genes. Many synMuv genes have been identified in several genetic screens (FERGUSON and HORVITZ 1985; THOMAS *et al.* 2003; POULIN *et al.*

2005; CEOL *et al.* 2006). A list of class A and B synMuv genes identified by our laboratory and others can be found in Table 1.

There are five class A synMuv genes: *lin-8*, *lin-15A*, *lin-38*, *lin-56* and *mcd-1*. I describe *mcd-1* in Chapter Six and the accompanying addendum. *lin-8* encodes a nuclear protein that might interact with the class B synMuv protein LIN-35 Rb (DAVISON *et al.* 2005). *lin-15A*, *lin-38* and *lin-56* encode nuclear proteins, containing either THAP domains (*lin-15A* and *lin-56*) or a zinc-finger domain (*lin-38*) (A.M. Saffer, E.M. Davison and H.R. Horvitz, unpublished results). Both of these domains have been shown to bind DNA and influence transcription or chromatin structure (REDDY and VILLENEUVE 2004; CLOUAIRE *et al.* 2005). The class A mutants do not have any reported defects in any tissue besides the vulva (DAVISON *et al.* 2005). Because the proteins encoded by the synMuv genes contain DNA-binding domains, we believe that they modulate transcription through DNA interactions.

There are at least 26 class B synMuv genes, including the class C genes in the class B genes (see Chapter Three). Many of the class B genes encode proteins that in other organisms regulate chromatin, including Rb (LU and HORVITZ 1998), the heterodimeric transcription factor E2F/DP (CEOL and HORVITZ 2001), a nucleosome remodeling and deacetylase (NuRD)-like complex (LU and HORVITZ 1998; SOLARI and AHRINGER 2000; UNHAVAITHAYA *et al.* 2002), heterochromatin protein 1 (HP1) (COUTEAU *et al.* 2002) and the DRM complex (HARRISON *et al.* 2006). The class C gene subclass of the class B genes might form a histone-acetyltransferase (HAT) complex similar to NuA4/Tip60 (CEOL and HORVITZ 2004). The list of class B genes in Table 1 includes proteins with the closest homology to the synMuv proteins and the predicted chromatin-remodeling complexes. We believe that the class B proteins form a number of separable complexes or activities to inhibit vulval fates by regulating chromatin (Figure 4). I will introduce chromatin remodeling in a later section.

Recently, Cui *et al.* (2006a) identified *lin-3* EGF as a putative synMuv target gene. The authors reported that in class A or class B single mutants *lin-3*

transcription levels do not differ from that in the wild type, but in class AB double mutants, *lin-3* transcription is increased. An increase in *lin-3* EGF levels can cause a Muv phenotype by over-activating the Ras pathway in cells that normally adopt non-vulval fates (KATZ *et al.* 1995). Additionally, the authors reported evidence that *lin-3* might be ectopically expressed in the syncytial hypoderm cell hyp7 in class AB double mutants. Because of the proximity of hyp7 to the vulval equivalence group, increased hyp7 levels of LIN-3 might induce ectopic vulval fates. The authors suggested that the class A and class B synMuv proteins might inhibit vulval fates by repressing the transcription of *lin-3* EGF in hyp7.

The class B synMuv genes control other cell-fate decisions

Over the past eight years, the class B synMuv genes have been implicated in the control of many different aspects of *C. elegans* biology. These results suggest that distinct subsets of synMuv genes regulate specific biological processes**.** For example, the subset of class B genes controlling G_1 cell-cycle progression (BOXEM and VAN DEN HEUVEL 2001; BOXEM and VAN DEN HEUVEL 2002) is different from the subset controlling viability (FAY *et al.* 2002; FAY *et al.* 2003; FAY *et al.* 2004; CERON *et al.* 2007; REDDIEN *et al.* 2007). In addition to G_1 cell-cycle progression and viability, synMuv genes control programmed cell death (REDDIEN *et al.* 2007), *mat-3* APC transcriptional repression (GARBE *et al.* 2004), *lag-2* transcriptional repression (DUFOURCQ *et al.* 2002; POULIN *et al.* 2005), initiation of meiotic recombination (REDDY and VILLENEUVE 2004), female development (GROTE and CONRADT 2006) and the inhibition of germline fates in the soma (HSIEH *et al.* 1999; UNHAVAITHAYA *et al.* 2002; WANG *et al.* 2005; LEHNER *et al.* 2006). Most work recently has focused on the germline/soma cell-fate decision, which I will describe below.

The germline of *C. elegans* is separated from the soma starting at the 16-cell stage (SULSTON and HORVITZ 1977; SULSTON *et al.* 1983). The germline employs a variety of mechanisms that protect the integrity of the genetic material to be passed on to the next generation. Transcription from repetitive DNA

elements is repressed perhaps to avoid the deleterious effects of transposon mobilization in the germline (HSIEH *et al.* 1999; SIJEN and PLASTERK 2003; VASTENHOUW *et al.* 2003), and this transcriptional repression might be RNAi-mediated (WANG *et al.* 2005; LEHNER *et al.* 2006). Class B synMuv mutants contain somatic cells transformed to be more like germline cells in both appearance, expression of germline markers and function (UNHAVAITHAYA *et al.* 2002). These mutants are sensitive to RNAi, perhaps because they express both germline and somatic RNAi machinery (WANG *et al.* 2005; LEHNER *et al.* 2006), and have increased silencing of repetitive transgenes (HSIEH *et al.* 1999) mediated by a germline mechanism (KELLY *et al.* 1997; KELLY and FIRE 1998; WANG *et al.* 2005). Currently, we understand little about the identity or function of the germline genes repressed by synMuv proteins.

We believe that in each of the defects associated with class B synMuv loss-of-function mutations chromatin structure is altered and transcriptional repression is reduced. This ectopic transcription phenotype is most readily seen in suppression of *mat-3* vulval defects. *mat-3(ku233)* is a partial loss-of-function promoter mutation that causes an abnormal vulval phenotype; the mutant phenotype can be suppressed by loss of some class B synMuv genes, which increases transcription of *mat-3*. In the regulation of other cell-fate decisions, distinct sets of genes are likely regulated by different groups of synMuv proteins. For example, the group of synMuv genes that when mutated cause defects in programmed cell death (REDDIEN *et al.* 2007) is different than those causing *mat-3* suppression (GARBE *et al.* 2004).

Genes that oppose the functions of the synMuv genes

The synMuv genes inhibit vulval fates, so genes that oppose the activities of the synMuv genes will promote vulval fates. Mutations in such genes can cause suppression of the synMuv phenotype. Three screens for synMuv suppressors have been carried out in two different synMuv strains. In the Horvitz laboratory, a previous graduate student, Scott Clark, screened for suppressors of the *lin-15AB(n765)* synMuv phenotype (CLARK 1992). His screen identified mutants that defined members of the Ras pathway and a Hox transcription factor (CLARK *et al.* 1992; CLARK *et al.* 1993; KORNFELD *et al.* 1995a; KORNFELD *et al.* 1995b). I discuss the mapping, cloning and characterization of one isolate from Scott Clark's screen, *n2070*, in Chapter Five. Cui *et al.* (2006b) screened for suppressors of the *lin-15AB(n765)* synMuv phenotype using a whole-genome RNAi library (FRASER *et al.* 2000; KAMATH *et al.* 2003). These authors reported that 70 genes opposed the synMuv genes in vulval development, 32 of which encode homologs predicted to remodel chromatin. In a different synMuv suppressor screen, a previous graduate student in the Horvitz laboratory, Xiaowei Lu, identified 43 suppressors of the *lin-53; lin-15A* synMuv phenotype (X. Lu and H.R. Horvitz, unpublished results). She cloned one suppressor, *isw-1*, which encodes an ATP-dependent chromatin-remodeling enzyme (ANDERSEN *et al.* 2006). I discuss the characterization of *isw-1* in Chapter Four.

From the synMuv suppressors identified to date, two general groups emerge: (1) Ras pathway effectors or positive regulators, and (2) chromatin-remodeling factors. Scott Clark and Cui *et al.* (2006b) identified genes that when their function is reduced or eliminated suppress the synMuv phenotype of *lin-15AB(n765)*. Many of these genes are regulators of the Ras pathway, which potentiate or transduce Ras pathway signaling, including the zinc-cation diffusion facilitator *cdf-1* (BRUINSMA *et al.* 2002), *lin-3* EGF (FERGUSON and HORVITZ 1985), protein tyrosine phosphatase *ptp-2* (SIEBURTH *et al.* 1999) and *lin-45* Raf (HAN *et al.* 1993). Previous studies reported that the Ras pathway is required for the synMuv phenotype (FERGUSON *et al.* 1987), and the cloned synMuv suppressor genes as Ras pathway positive regulators confirm those results. The

suppressors of the synMuv phenotype encoding chromatin-remodeling factors, include *isw-1* ISWI (ANDERSEN *et al.* 2006; CUI *et al.* 2006b), a Polycomb complex similar to E(z) containing *mes-2*, *mes-3* and *mes-6* (XU *et al.* 2001; BENDER *et al.* 2004; CUI *et al.* 2006b), the histone methyltransferase *mes-4* (FONG *et al.* 2002; BENDER *et al.* 2006). Additionally, genetic screens identified many genes predicted to encode chromatin-remodeling factors (ANDERSEN *et al.* 2006; CUI *et al.* 2006b), including a complex similar to *Drosophila* NURF. These chromatin-remodeling activities might oppose the synMuv proteins in the regulation of genes important for vulval fates. Therefore, an understanding of how chromatin regulates transcription will teach us much about how cell-fate decisions are controlled by specific temporal and spatial gene expression.

Chromatin structure affects transcription

The DNA within the nucleus of the average eukaryotic cell would be two meters long if stretched from end to end. To fit the DNA into the nucleus, about 150 base pairs of DNA are wrapped around an octamer of proteins called histones two and half times (WOLFFE 1998). This DNA/histone complex is called the nucleosome. Nucleosome spaced along the DNA is sometimes referred to as "beads-on-a-string" chromatin. This first-order compaction of DNA is then followed by wrapping of the "beads-on-a-string" around itself to form a fiber 30-nm in diameter (second-order compaction). The formation of the 30-nm fiber might depend on histone H1 or the linker histone that can bind two nucleosomes to each other. The DNA template on which the transcriptional machinery assembles and produces mRNA is thought to be in the first-order of DNA compaction. Areas of repressed transcription or heterochromatin are compacted at least to the 30-nm fiber or further compaction by looping of the 30-nm fiber around scaffolding proteins (third-order compaction).

Because the nucleosome contains DNA wrapped around the histone octamer, occluding the sites where proteins interact with the DNA can inhibit DNA-mediated processes. Cells have exploited this situation by using the

positions of nucleosomes to regulate a variety of cellular processes, including transcription, recombination (YAMADA *et al.* 2004), DNA repair and replication (GROTH *et al.* 2007). Nucleosome positioning and structure are changed to influence transcription through a process called chromatin remodeling. Many of the synMuv proteins likely regulate transcription. I describe below the regulation of transcription by chromatin.

There are three general ways to alter chromatin to affect transcription: covalent mechanisms (KOUZARIDES 2007) and non-covalent mechanisms composed of ATP-dependent chromatin remodeling (LANGST and BECKER 2004) and replacement of core histones with histone variants (BERNSTEIN and HAKE 2006).

The covalent modification of histones regulates transcription

From crystallographic studies of the nucleosome, the unstructured amino-termini of the histone proteins can be detected projecting out from the histone octamer core (LUGER *et al.* 1997). Clues as to the importance of these histone tails were revealed after an enzyme was identified that post-translationally modified histone-tail residues by acetylation (BROWNELL *et al.* 1996). This enzyme from *Tetrahymena* is similar to the yeast protein *GCN5* known to be involved in transcriptional regulation. Subsequently, enzymes known to regulate transcriptional repression and heterochromatin in *Drosophila* were reported to modify histone-tail residues (TSCHIERSCH *et al.* 1994; DE RUBERTIS *et al.* 1996). The connection between modification of histone tails and the repression of transcription was solidified when genes known to affect heterochromatin formation were found to encode proteins that bind to the covalent chromatin modifications (JAMES and ELGIN 1986; EISSENBERG *et al.* 1990; BANNISTER *et al.* 2001; LACHNER *et al.* 2001).

To date, there are eight different types of modifications that decorate histones, including acetylation, methylation (of arginines and lysines), phosphorylation, ubquitylation, sumoylation, ADP ribosylation and deimination

(KOUZARIDES 2007). Each of these modifications affects transcription and other processes that require DNA-binding activities. Generally, acetylation is associated with transcriptional activation. Methylation either activates or represses transcription. In some cases, the covalent modification of histones has been shown to disrupt the higher-order structures of chromatin (SHOGREN-KNAAK *et al.* 2006), create binding sites for proteins that regulate the higher-order structure of chromatin (BANNISTER *et al.* 2001) or change nucleosome positions (HASSAN *et al.* 2001). In the following section, I will focus on methylation of residues on the amino-terminal tail or globular core domain of the histones.

Histone methylation can either promote or inhibit transcription

Histones can be methylated on lysines (K) or arginines (R) (KOUZARIDES 2002). Lysines can be mono-, di- or trimethylated, and arginines can be mono- or dimethylated. Histone methyltransferases (HMTs) are grouped broadly into three different classes. (1) HMTs that methylate lysines on the histone amino-terminal tails, (2) HMTs that methylate lysines in the globular core domain and (3) HMTs that methylate arginines. The HMTs that methylate lysines on the histone amino-terminal tails contain the enzymatic SET domain, named for a domain in common among the Su(var)3-9, E(z) and Trithorax enzymes – the first three well characterized HMTs. DOT1 is a conserved HMT that methylates histone H3K79 in the globular core domain and is associated with transcriptional activation (NG *et al.* 2002; VAN LEEUWEN *et al.* 2002). DOT1 does not have a SET domain but does have a binding site for S-adenosyl-L-methionine (SAM) similar to SET-domain proteins (MIN *et al.* 2003a). Arginine-specific HMTs are involved in transcriptional activation (TEYSSIER *et al.* 2002; HUANG *et al.* 2005). Like DOT1, these enzymes do not have SET domains, and arginine methylation is often correlated with histone acetylation in actively transcribed chromatin regions. Because the class B synMuv genes *met-1* and *met-2* encode presumptive lysine-specific histone-tail HMTs (Chapter Two), I will focus on the methylation of lysines on the histone H3 amino-terminal tail.

There are four lysines on the histone H3 tail methylated by different HMTs: H3K4, H3K9, H3K27 and H3K36 (KOUZARIDES 2007). To date, all HMTs that methylate lysine residues on histone amino-terminal tails have a SET domain (KOUZARIDES 2002; PIRROTTA 2006; SHILATIFARD 2006). The presence or absence of cysteine-rich domains in HMTs determines the specificity of which lysine will be methylated (Table 2). I will discuss only methylation of the histone H3 tail on lysines four (H3K4), nine (H3K9), 27 (H3K27) and 36 (H3K36). Proteins with SET domains and the C-terminal cysteine-rich domain called PostSET methylate histone H3K4. HMTs with SET domains flanked by PreSET and PostSET domains methylate histone H3K9. The associated with SET domain (AWS) and PostSET domains flank SET domains found in HMTs specific for histone H3K36. The HMTs specific for histone H3K27 do not have flanking cysteine-rich domains. Investigation of the primary amino-acid sequence of an HMT can be predictive of which residue on the histone might be methylated.

The methylation of specific residues on the histone tail is thought to influence transcription. The methylation of H3K4 is associated with regions of active transcription (SIMS and REINBERG 2006). In *S. cerevisiae*, the methylation of H3K4 creates a binding site for the CHD1 and NURF complexes to open chromatin and increase transcription (WYSOCKA *et al.* 2005; WYSOCKA *et al.* 2006). The methylation of H3K9 is associated with transcriptional repression (KOUZARIDES 2002). One of the first characterized HMTs, *Drosophila* Su(var)3-9, and its human counterparts SUV39H1 and SUV39H2, regulate transcriptional repression and heterochromatin formation through H3K9 methylation. In Chapter Two, I discuss the *C. elegans* homolog of a human HMT SETDB1, which is an H3K9 trimethylase involved in transcriptional repression (SCHULTZ *et al.* 2002). The *Drosophila* Polycomb chromatin-remodeling complex E(z) and homologs from the worm (BENDER *et al.* 2004) to humans (CAO *et al.* 2002) methylate H3K27 to repress transcription (CAO and ZHANG 2004). These complexes share a conserved role in repressing Hox gene expression during development. Although H3K27 methylation and H3K9 methylation are involved in transcriptional

repression, each seems to share non-redundant roles during transcriptional repression (LINDROTH *et al.* 2004; RINGROSE *et al.* 2004; ROUGEULLE *et al.* 2004). Histone H3K36 methylation is associated with chromatin regions of active transcription (EISSENBERG and SHILATIFARD 2006). The *S. cerevisiae* H3K36 HMT, Set2, binds to elongating RNA polymerase II phosphorylated on serine five of the carboxyl-terminal domain (CTD) (LI *et al.* 2002; KROGAN *et al.* 2003; LI *et al.* 2003; XIAO *et al.* 2003) and is thought to close chromatin after the transcriptional machinery has initiated and started elongating the mRNA transcript by deacetylating H3K9 (CARROZZA *et al.* 2005; JOSHI and STRUHL 2005; KEOGH *et al.* 2005). This mechanism is hypothesized to prevent reinitiation of transcription and possible interference between multiple elongating polymerases. The initial characterization of Set2 reported that *in vitro* it could repress transcription (STRAHL *et al.* 2002), and Landry *et al.* (2003) found that SET2 repressed basal transcription from GAL4 promoters. Because *S. cerevisiae* lacks most mechanisms of transcriptional repression found in other organisms and H3K36 methylation has been most investigated in this organism, a role of H3K36 methylation in euchromatic transcriptional repression has not been widely investigated. Although the Set2 homologs in chicken (BANNISTER *et al.* 2005) and human (SUN *et al.* 2005) regulate transcriptional elongation, a recent report suggested that an H3K36 HMT can mediate transcriptional repression through the deacetylation of histone H3K9 (BROWN *et al.* 2006).

Some regulators of transcription bind methylated histones

The modification of histone-tail residues has been suggested to represent a code for the regulation of DNA-mediated processes, a histone code (JENUWEIN and ALLIS 2001). Specific domains found within proteins or enzymes that change chromatin structure recognize these different post-translational modifications. I will discuss the proteins that bind to methylated histone-tail lysines (Table 2), as these are most similar to synMuv proteins.

The methylation of lysine four of the histone H3 (H3K4) tail is bound by proteins that activate transcription, and the methylation of lysine 36 of histone H3 is associated with transcriptional elongation though no proteins that bind H3K36 methylation have been identified to date. The best understood domain that binds methylated lysines is the chromodomain (NIELSEN *et al.* 2002). Proteins with this domain, which bind H3K4 are found in complexes that also regulate transcriptional elongation (PRAY-GRANT *et al.* 2005). A WD40 domain-containing protein binds methylated H3K4 (WYSOCKA *et al.* 2005) to enhance transcription.

Methylation of H3K9 and H3K27 is associated with transcriptional repression (KOUZARIDES 2002; KOUZARIDES 2007). Different effecter proteins bind these marks. The methylation of H3K9 has long been associated with transcriptional repression, because studies of position-effect variegation from *Drosophila* implicated many genes encoding these activities in repression. The methylation of H3K9 is bound by the chromodomain of heterochromatin protein 1 (HP1) (BANNISTER *et al.* 2001; LACHNER *et al.* 2001). The binding of HP1 creates a more compact chromatin configuration called heterochromatin, but HP1 binding also inactivates genes within actively transcribed regions, called euchromatin (AYYANATHAN *et al.* 2003). Polycomb factors, which remodel chromatin, bind to H3K27 methylation to repress transcription (FISCHLE *et al.* 2003; MIN *et al.* 2003b). After binding of these proteins, chromatin compaction occurs occluding the binding of transcription factors to target DNA sequences (FRANCIS *et al.* 2004). H3K9- and H3K27-associated repressive chromatin modifications independently cause the inactivation of transcription.

Using protein-array technology, Kim *et al.* (2006) found interactions among Tudor domains, MBT domains and chromodomains with methylated histone residues. Specifically, they report that Tudor and MBT domains, which are structurally similar to chromodomains, interact with H3K4, H3K9 and H4K20 methylated peptides. Unfortunately, no interactions with H3K27 or H3K36 methylated peptides were tested. The PHD domain has also been reported to bind to methylated histones (PALACIOS *et al.* 2006; SHI *et al.* 2007) and might participate in the binding of acetylated histone (RAGVIN *et al.* 2004). Additionally, the WD-40 domain has been reported to bind to a methylated H3K4 as does the PHD domain (WYSOCKA *et al.* 2005; WYSOCKA *et al.* 2006). These studies show that we have much to learn about what proteins bind to methylated histone residues and what those proteins do to chromatin structure.

Histone lysine demethylases regulate transcription

The methylation of histone tails was once considered a stable modification that could be the long-term epigenetic mark long sought in the chromatin field. Recently, lysine demethylases have been identified for some lysine residues and reported to be crucial regulators of chromatin structure and transcription (SHI *et al.* 2004; KLOSE *et al.* 2006; TSUKADA *et al.* 2006; WHETSTINE *et al.* 2006). With these discoveries, it became clear that the methylation of histones is a reversible process. In the same way that histone methylation affects both transcriptional activation and repression, histone demethylation, particularly lysine demethylation, both promotes and prevents transcription depending on the residue affected. Many of the characterized lysine demethylases have the conserved JmjC domain, which promotes the amine oxidation required to remove methyl groups from lysines. Some histone demethylases have dual specificity, enzymatically removing methyl groups from both H3K9 and H3K36, suggesting shared functions for H3K9 and H3K36 methylation (KLOSE *et al.* 2006; WHETSTINE *et al.* 2006). Not surprisingly, these histone demethylases are involved in transcriptional activation (YAMANE *et al.* 2006). Very little is known about how

histone demethylase activities associate with known chromatin-remodeling complexes or their effects on development. Recently, a H3K4 demethylase was shown to inhibit vulval cell fates in *C. elegans* (CHRISTENSEN *et al.* 2007). Additionally, not all methylation marks have associated demethylases. For example, H3K27 methylation has no known demethylases and could be a long-term epigenetic mark.

ATP-dependent chromatin remodeling enzymes slide nucleosomes to allow or prevent access of the transcriptional apparatus to the DNA

There are multiple mechanisms to move nucleosomes along the DNA to regulate DNA-mediated processes, such as transcription. There are four general classes of ATP-dependent chromatin-remodeling enzymes named after their founding members: Swi2/Snf2, ISWI, Mi-2 and INO80 (LANGST and BECKER 2004). These different classes are segregated based upon different domains found in each family member within a group. The Swi2/Snf2 family has bromodomains, which bind acetylated histones (HUDSON *et al.* 2000; JACOBSON *et al.* 2000). The ISWI family has SANT domains. The Mi-2 family has chromodomains and PHD domains, both of which bind methylated histones. The INO80 family has split ATPase domains. I will discuss the first three types of ATP-dependent chromatin remodelers, as each of these classes contains synMuv proteins or synMuv suppressor proteins.

The Swi2/Snf2 ATPase was the first identified ATP-dependent chromatin-remodeling enzyme (HIRSCHHORN *et al.* 1992). Its implication in non-covalent chromatin remodeling led to the purification and characterization of the Swi/Snf complex (PETERSON and WORKMAN 2000; VIGNALI *et al.* 2000). This complex regulates transcription by altering the structure of the nucleosome, thereby allowing its movement to different positions. After first being characterized as a transcriptional activator complex, roles for the Swi/Snf complex have been identified in transcriptional repression (MURPHY *et al.* 1999; SUDARSANAM *et al.* 2000). The ATPase activity of Swi2/Snf2 is stimulated by both free and

nucleosomal DNA (AALFS *et al.* 2001), suggesting a mechanism of chromatin remodeling distinct from those of the enzymes discussed below.

In an effort to identify homologs of Swi2/Snf2 in *Drosophila*, Elfring *et al.* (1994) identified a gene encoding an ATP-dependent chromatin-remodeling enzyme related to but distinct from Swi2/Snf2 named Imitation of Switch (ISWI). Subsequently, several laboratories found ISWI was the ATPase subunit of several non-covalent chromatin-remodeling complexes (TSUKIYAMA and WU 1995; ITO *et al.* 1997; VARGA-WEISZ *et al.* 1997). The chromatin accessibility (CHRAC) complex and the ATP-utilizing and chromatin-remodeling factor (ACF) share ISWI and ACF1 subunits, but the CHRAC complex also contains the histone-fold-like proteins CHRAC-14 and CHRAC-16. These complexes evenly space nucleosomes from an unevenly spaced nucleosomal template *in vitro*. The Nucleosome remodeling factor (NURF) slides nucleosomes to allow the binding of the GAGA transcription factor *in vitro* (TSUKIYAMA and WU 1995) and Hox gene expression *in vivo* (BADENHORST *et al.* 2002; WYSOCKA *et al.* 2006). In addition to ISWI, NURF contains an inorganic pyrophosphatase (NURF-38), a WD-repeat containing protein (NURF-55) similar to RbAp48 or CAF-1 (GDULA *et al.* 1998; MARTINEZ-BALBAS *et al.* 1998) and a large presumptive scaffolding subunit NURF301 (XIAO *et al.* 2001). ISWI has been identified in other chromatin-regulatory complexes involved in DNA repair (URA *et al.* 2001; GAILLARD *et al.* 2003) and sister-chromatid cohesion (HAKIMI *et al.* 2002). The ISWI family is the largest class of ATP-dependent chromatin-remodeling enzymes. Importantly, ISWI ATPases require the histone tails for their chromatin-remodeling activities, suggesting a link between histone modification and ATP-dependent chromatin remodeling (GEORGEL *et al.* 1997; CLAPIER *et al.* 2001; LOYOLA *et al.* 2001; CLAPIER *et al.* 2002).

The Mi-2 family of ATP-dependent chromatin-remodeling enzymes was identified first as the antigenic target in the autoimmune disease dermatomyositis (SEELIG *et al.* 1995). Mi-2 is the ATPase subunit of the nucleosome remodeling and deacetylase (NuRD) complex (XUE *et al.* 1998; ZHANG *et al.* 1998; ZHANG *et*

al. 1999), which represses transcription. The ATPase activity of Mi-2 is stimulated only by nucleosomal DNA (BOUAZOUNE *et al.* 2002), so complexes containing Mi-2 are suspected of sliding nucleosomes in *cis* along the DNA.

Many synMuv genes encode proteins similar to chromatin-remodeling and transcription factors

The extensive genetic screens for synMuv mutants led to the identification of over thirty synMuv genes. Most of these genes encode proteins similar to those that regulate chromatin structure or transcription (FAY and YOCHEM 2007). In the following sections, I will introduce the different predicted activities of the synMuv proteins based on the homologies to other organisms. The class B and C synMuv genes will be divided up into their respective predicted complexes, and the molecular functions of the homologous complexes will be described.

Most of the class A synMuv genes encode putative transcription factors

Most of the class A synMuv genes encode proteins with DNA-binding domains (E.M. Davison, A.M. Saffer and H.R. Horvitz, unpublished results). *lin-15A* and *lin-56* encode proteins that have the conserved THAP domain (E.M. Davison and H.R. Horvitz, unpublished results), reported to bind DNA (CLOUAIRE *et al.* 2005). Additionally, LIN-15A and LIN-56 likely bind each other *in vivo* and function as a heterodimeric transcription factor (E.M. Davison and H.R. Horvitz, unpublished results). *lin-8* encodes a protein similar to a family containing at least 16 other members in *C. elegans* (DAVISON *et al.* 2005), and LIN-8 might bind LIN-35 *in vitro.* Currently, *lin-38* is being investigated by Adam Saffer in the Horvitz laboratory, and it encodes a protein with a single zinc-finger domain. As described in Chapter Six and an accompanying addendum, *mcd-1* encodes a zinc-finger-containing protein thought to act with some class B synMuv proteins to regulate programmed cell death (REDDIEN *et al.* 2007).

Many of the class B synMuv proteins are homologous to proteins found in chromatin-regulatory complexes

Beginning with the identification of *lin-35* Rb, *lin-53* RbAp48 and *hda-1* HDAC1 as class B synMuv genes (LU and HORVITZ 1998), the class B synMuv proteins have been predicted to be chromatin-regulatory factors, because of homology to the mammalian NuRD complex (XUE *et al.* 1998; ZHANG *et al.* 1998; ZHANG *et al.* 1999). Subsequently, a homolog of another NuRD complex component Mi-2 was found to be a class B synMuv gene named *let-418* (VON ZELEWSKY *et al.* 2000). Similar results were reported using RNAi (SOLARI and AHRINGER 2000). Homologs of other NuRD complex members were implicated in vulval development, but after careful analysis of vulval cell-fate specification were excluded as synMuv genes (CHEN and HAN 2001). The *C. elegans* NuRD-like complex that regulates vulval development is likely different from the mammalian NuRD complex, as it lacks MTA1 subunits and methylated DNA-binding MBD subunits. The NuRD complex mediates transcriptional repression once recruited to target genes by interaction with Rb (BREHM *et al.* 1998; LUO *et al.* 1998; MAGNAGHI-JAULIN *et al.* 1998). A transcriptional repression cassette described in *S. pombe* and *Drosophila* cells functions in the following stepwise fashion to inactivate transcription (NAKAYAMA *et al.* 2001; AYYANATHAN *et al.* 2003). Histone H3K9 is deacetyated by NuRD, methylated by an H3K9-specific HMT and that methyl mark is bound by heterochromatin protein one (HP1), which forms a heterochromatin domain refractory to transcription.

Subsequent to the discovery of *lin-35* Rb as a class B synMuv gene, the heterodimeric transcription factors *efl-1* E2F4 and *dpl-1* DP were identified as class B synMuv genes (CEOL and HORVITZ 2001). *efl-1* encodes a protein most similar to E2F4, a repressive E2F family member (RAYMAN *et al.* 2002). Therefore in the control of vulval cell-fate inhibition by the synMuv genes, *efl-1* E2F4, *dpl-1* DP and *lin-35* Rb likely act together to inhibit transcription. EFL-1, DPL-1 and LIN-35 might form a complex in *C. elegans*, supporting a role for a shared function in vulval fate inhibition.

Two complexes, called Myb-MuvB and dREAM, were purified from *Drosophila* and are composed of homologs of class B synMuv proteins (KORENJAK *et al.* 2004; LEWIS *et al.* 2004). Using co-immunoprecipitation experiments, the DRM complex, more similar to Myb-MuvB than dREAM, was identified from *C. elegans* embryonic extracts. It contains LIN-9 Mip130/aly LIN-35 pRb, LIN-37 Mip40, LIN-52 dLin52, LIN-53 RbAp48, LIN-54 Mip120/tesmin and DPL-1 DP (HARRISON *et al.* 2006). The Myb-MuvB and dREAM complexes repress the transcription of cell-cycle progression genes bound by the Myb transcription factor (KORENJAK *et al.* 2004; LEWIS *et al.* 2004).

The class C synMuv proteins are similar to the conserved NuA4/Tip60 histone acetyltransferase complexes (ALLARD *et al.* 1999; IKURA *et al.* 2000; LOEWITH *et al.* 2000; EISEN *et al.* 2001). NuA4 is composed of a histone acetyltransferase subunit ESA1, which acetylates all four lysines on the histone H4 tail to promote transcriptional activation (ALLARD *et al.* 1999). A similar complex, Tip60, identified in mammalian cells has the same histone acetylase activity and promotes transcription (IKURA *et al.* 2000). The presumptive class C complex might act in transcriptional repression or could promote the expression of a vulval transcriptional repressor.

What can we learn from the synMuv genes?

The information stored within the genome of an organism must be read and interpreted by the transcriptional apparatus. The dynamic structure of chromatin uses the complexity of the genome to create another layer of transcriptional regulation. Each cell in a metazoan must make specific decisions as to what fate it will adopt and the function(s) that it will carry out. Because the genome is the same from cell to cell (except for immune cells), the genes that are activated, at what level and when help to determine the ultimate fates of every cell. If we understand how the transcriptional apparatus reads the genome to determine cell fate, we will know more about how each cell contributes to the development and function of an organism.

The inappropriate specification of cell fate can lead to rapid overproliferation and carcinogenesis in humans (HANAHAN and WEINBERG 2000). Two of the most common perturbations of human cells that cause carcinogenesis are an increase in Ras pathway activity or a loss of the tumor-suppressor gene Retinoblastoma (Rb). The control of the vulval cell fate in *C. elegans* has a similar genetic relationship to carcinogenesis in humans. An increase in *let-60* Ras function leads to an increase in the vulval cell fate, and a loss of *lin-35* Rb can also cause an increase in the vulval cell fate. Learning more about how *lin-35* Rb (or other synMuv genes) affects the vulval cell fate might teach us more about how tumor-suppressor genes inhibit carcinogenesis in humans. Additionally, the interplay between oncogenes (like Ras) and tumor-suppressor genes (like Rb) could be directly modeled by control of the vulval cell fate in *C. elegans*.

The synMuv genes generally inhibit vulval fates in *C. elegans*. This inhibition of the vulval fate might be through the transcriptional repression of the Ras pathway ligand *lin-3* EGF by chromatin remodeling. So not only might we learn about the contributory genes to human carcinogenesis, but we might also learn about the regulation of transcription by chromatin structure. In the following chapters, I will describe some new synMuv genes that act as chromatin regulators (Chapter Two), how the synMuv genes act either together or separably in different molecular functions to regulate chromatin structure (Chapter Three), genes that oppose the actions of the synMuv genes in a putative ATP-dependent chromatin-remodeling complex (Chapter Four) or as a novel transcriptional regulator conserved in humans (Chapter Five) and finally how the synMuv genes regulate the fate of a cell to live or die (Chapter Six). I will conclude this thesis with a discussion of where we should go from here. I believe exciting days are ahead when we directly connect chromatin structure to transcriptional readout, as we can finally use the nearly 30 years of *C. elegans* vulval research to address issues of the chromatin regulation of cell fate.

ACKNOWLEDGMENTS

I thank Mike Hurwitz and Shunji Nakano for critically reading of this chapter.

LITERATURE CITED

AALFS, J. D., G. J. NARLIKAR and R. E. KINGSTON, 2001 Functional differences between the human ATP-dependent nucleosome remodeling proteins BRG1 and SNF2H. J Biol Chem **276:** 34270-34278.

ALLARD, S., R. T. UTLEY, J. SAVARD, A. CLARKE, P. GRANT, C. J. BRANDL, L. PILLUS, J. L. WORKMAN and J. COTE, 1999 NuA4, an essential transcription adaptor/histone H4 acetyltransferase complex containing Esa1p and the ATM-related cofactor Tra1p. Embo J **18:** 5108-5119.

ANDERSEN, E. C., X. LU and H. R. HORVITZ, 2006 *C. elegans* ISWI and NURF301 antagonize an Rb-like pathway in the determination of multiple cell fates. Development **133:** 2695-2704.

ANNAERT, W., and B. DE STROOPER, 1999 Presenilins: molecular switches between proteolysis and signal transduction. Trends Neurosci **22:** 439-443.

AYYANATHAN, K., M. S. LECHNER, P. BELL, G. G. MAUL, D. C. SCHULTZ, Y. YAMADA, K. TANAKA, K. TORIGOE and F. J. RAUSCHER, 3RD, 2003 Regulated recruitment of HP1 to a euchromatic gene induces mitotically heritable, epigenetic gene silencing: a mammalian cell culture model of gene variegation. Genes Dev **17:** 1855-1869.

BADENHORST, P., M. VOAS, I. REBAY and C. WU, 2002 Biological functions of the ISWI chromatin remodeling complex NURF. Genes Dev **16:** 3186-3198.

BANNISTER, A. J., R. SCHNEIDER, F. A. MYERS, A. W. THORNE, C. CRANE-ROBINSON and T. KOUZARIDES, 2005 Spatial distribution of di- and tri-methyl lysine 36 of histone H3 at active genes. J Biol Chem **280:** 17732-17736.

BANNISTER, A. J., P. ZEGERMAN, J. F. PARTRIDGE, E. A. MISKA, J. O. THOMAS, R. C. ALLSHIRE and T. KOUZARIDES, 2001 Selective recognition of methylated lysine 9 on histone H3 by the HP1 chromo domain. Nature **410:** 120-124.

BEITEL, G. J., S. G. CLARK and H. R. HORVITZ, 1990 *Caenorhabditis elegans* ras gene *let-60* acts as a switch in the pathway of vulval induction. Nature **348:** 503-509.

BEITEL, G. J., S. TUCK, I. GREENWALD and H. R. HORVITZ, 1995 The *Caenorhabditis elegans* gene *lin-1* encodes an ETS-domain protein and defines a branch of the vulval induction pathway. Genes Dev **9:** 3149-3162.

BENDER, L. B., R. CAO, Y. ZHANG and S. STROME, 2004 The MES-2/MES-3/MES-6 complex and regulation of histone H3 methylation in *C. elegans*. Curr Biol **14:** 1639-1643.

BENDER, L. B., J. SUH, C. R. CARROLL, Y. FONG, I. M. FINGERMAN, S. D. BRIGGS, R. CAO, Y. ZHANG, V. REINKE and S. STROME, 2006 MES-4: an autosome-associated histone methyltransferase that participates in silencing the X chromosomes in the *C. elegans* germ line. Development **133:** 3907-3917.

BERNSTEIN, E., and S. B. HAKE, 2006 The nucleosome: a little variation goes a long way. Biochem Cell Biol **84:** 505-517.

BERSET, T. A., E. F. HOIER and A. HAJNAL, 2005 The *C. elegans* homolog of the mammalian tumor suppressor Dep-1/Scc1 inhibits EGFR signaling to regulate binary cell fate decisions. Genes Dev **19:** 1328-1340.

BOUAZOUNE, K., A. MITTERWEGER, G. LANGST, A. IMHOF, A. AKHTAR, P. B. BECKER and A. BREHM, 2002 The dMi-2 chromodomains are DNA binding modules important for ATP-dependent nucleosome mobilization. Embo J **21:** 2430-2440.

BOXEM, M., and S. VAN DEN HEUVEL, 2001 *lin-35* Rb and *cki-1* Cip/Kip cooperate in developmental regulation of G1 progression in *C. elegans*. Development **128:** 4349-4359.

BOXEM, M., and S. VAN DEN HEUVEL, 2002 *C. elegans* class B synthetic multivulva genes act in G(1) regulation. Curr Biol **12:** 906-911.

BREHM, A., E. A. MISKA, D. J. MCCANCE, J. L. REID, A. J. BANNISTER and T. KOUZARIDES, 1998 Retinoblastoma protein recruits histone deacetylase to repress transcription. Nature **391:** 597-601.

BRENNER, S., 1974 The genetics of *Caenorhabditis elegans*. Genetics **77:** 71-94.

BROWN, M. A., R. J. SIMS, 3RD, P. D. GOTTLIEB and P. W. TUCKER, 2006 Identification and characterization of Smyd2: a split SET/MYND domain-containing histone H3 lysine 36-specific methyltransferase that interacts with the Sin3 histone deacetylase complex. Mol Cancer **5:** 26.

BROWNELL, J. E., J. ZHOU, T. RANALLI, R. KOBAYASHI, D. G. EDMONDSON, S. Y. ROTH and C. D. ALLIS, 1996 *Tetrahymena* histone acetyltransferase A: a

homolog to yeast Gcn5p linking histone acetylation to gene activation. Cell **84:** 843-851.

BRUINSMA, J. J., T. JIRAKULAPORN, A. J. MUSLIN and K. KORNFELD, 2002 Zinc ions and cation diffusion facilitator proteins regulate Ras-mediated signaling. Dev Cell **2:** 567-578.

CAO, R., L. WANG, H. WANG, L. XIA, H. ERDJUMENT-BROMAGE, P. TEMPST, R. S. JONES and Y. ZHANG, 2002 Role of histone H3 lysine 27 methylation in Polycomb-group silencing. Science **298:** 1039-1043.

CAO, R., and Y. ZHANG, 2004 The functions of E(Z)/EZH2-mediated methylation of lysine 27 in histone H3. Curr Opin Genet Dev **14:** 155-164.

CARROZZA, M. J., B. LI, L. FLORENS, T. SUGANUMA, S. K. SWANSON, K. K. LEE, W. J. SHIA, S. ANDERSON, J. YATES, M. P. WASHBURN and J. L. WORKMAN, 2005 Histone H3 methylation by Set2 directs deacetylation of coding regions by Rpd3S to suppress spurious intragenic transcription. Cell **123:** 581-592.

CEOL, C. J., and H. R. HORVITZ, 2001 *dpl-1* DP and *efl-1* E2F act with *lin-35* Rb to antagonize Ras signaling in *C. elegans* vulval development. Mol Cell **7:** 461-473.

CEOL, C. J., and H. R. HORVITZ, 2004 A new class of *C. elegans* synMuv genes implicates a Tip60/NuA4-like HAT complex as a negative regulator of Ras signaling. Dev Cell **6:** 563-576.

CEOL, C. J., F. STEGMEIER, M. M. HARRISON and H. R. HORVITZ, 2006 Identification and classification of genes that act antagonistically to *let-60*

Ras signaling in *Caenorhabditis elegans* vulval development. Genetics **173:** 709-726.

CERON, J., J. F. RUAL, A. CHANDRA, D. DUPUY, M. VIDAL and S. VAN DEN HEUVEL, 2007 Large-scale RNAi screens identify novel genes that interact with the *C. elegans* retinoblastoma pathway as well as splicing-related components with synMuv B activity. BMC Dev Biol **7:** 30.

CHANG, C., N. A. HOPPER and P. W. STERNBERG, 2000 *Caenorhabditis elegans* SOS-1 is necessary for multiple RAS-mediated developmental signals. Embo J **19:** 3283-3294.

CHEN, N., and I. GREENWALD, 2004 The lateral signal for LIN-12/Notch in *C. elegans* vulval development comprises redundant secreted and transmembrane DSL proteins. Dev Cell **6:** 183-192.

CHEN, Z., and M. HAN, 2001 Role of *C. elegans lin-40* MTA in vulval fate specification and morphogenesis. Development **128:** 4911-4921.

CHRISTENSEN, J., K. AGGER, P. A. CLOOS, D. PASINI, S. ROSE, L. SENNELS, J. RAPPSILBER, K. H. HANSEN, A. E. SALCINI and K. HELIN, 2007 RBP2 belongs to a family of demethylases, specific for tri-and dimethylated lysine 4 on histone 3. Cell **128:** 1063-1076.

CHRISTENSEN, S., V. KODOYIANNI, M. BOSENBERG, L. FRIEDMAN and J. KIMBLE, 1996 *lag-1*, a gene required for *lin-12* and *glp-1* signaling in *Caenorhabditis elegans*, is homologous to human CBF1 and *Drosophila* Su(H). Development **122:** 1373-1383.

CLAPIER, C. R., G. LANGST, D. F. CORONA, P. B. BECKER and K. P. NIGHTINGALE, 2001 Critical role for the histone H4 N terminus in nucleosome remodeling by ISWI. Mol Cell Biol **21:** 875-883.

CLAPIER, C. R., K. P. NIGHTINGALE and P. B. BECKER, 2002 A critical epitope for substrate recognition by the nucleosome remodeling ATPase ISWI. Nucleic Acids Res **30:** 649-655.

CLARK, S. G., 1992 Intercellular signalling and homeotic genes required during vulval development in *C. elegans*. Ph. D. Thesis, Massachusetts Institute of Technology.

CLARK, S. G., A. D. CHISHOLM and H. R. HORVITZ, 1993 Control of cell fates in the central body region of *C. elegans* by the homeobox gene *lin-39*. Cell **74:** 43-55.

CLARK, S. G., M. J. STERN and H. R. HORVITZ, 1992 *C. elegans* cell-signalling gene *sem-5* encodes a protein with SH2 and SH3 domains. Nature **356:** 340-344.

CLOUAIRE, T., M. ROUSSIGNE, V. ECOCHARD, C. MATHE, F. AMALRIC and J. P. GIRARD, 2005 The THAP domain of THAP1 is a large C2CH module with zinc-dependent sequence-specific DNA-binding activity. Proc Natl Acad Sci U S A **102:** 6907-6912.

COUTEAU, F., F. GUERRY, F. MULLER and F. PALLADINO, 2002 A heterochromatin protein 1 homologue in *Caenorhabditis elegans* acts in germline and vulval development. EMBO Rep **3:** 235-241.

CUI, M., J. CHEN, T. R. MYERS, B. J. HWANG, P. W. STERNBERG, I. GREENWALD and M. HAN, 2006a SynMuv genes redundantly inhibit *lin-3*/EGF expression to prevent inappropriate vulval induction in *C. elegans*. Dev Cell **10:** 667-672.

CUI, M., and M. HAN, 2003 *Cis* regulatory requirements for vulval cell-specific expression of the *Caenorhabditis elegans* fibroblast growth factor gene *egl-17*. Dev Biol **257:** 104-116.

CUI, M., E. B. KIM and M. HAN, 2006b Diverse chromatin remodeling genes antagonize the Rb-involved SynMuv pathways in *C. elegans*. PLoS Genet **2:** e74.

DAVISON, E. M., M. M. HARRISON, A. J. WALHOUT, M. VIDAL and H. R. HORVITZ, 2005 *lin-8*, which antagonizes *C. elegans* Ras-mediated vulval induction, encodes a novel nuclear protein that interacts with the LIN-35 Rb protein. Genetics.

DE RUBERTIS, F., D. KADOSH, S. HENCHOZ, D. PAULI, G. REUTER, K. STRUHL and P. SPIERER, 1996 The histone deacetylase RPD3 counteracts genomic silencing in *Drosophila* and yeast. Nature **384:** 589-591.

DUFOURCQ, P., M. VICTOR, F. GAY, D. CALVO, J. HODGKIN and Y. SHI, 2002 Functional requirement for histone deacetylase 1 in *Caenorhabditis elegans* gonadogenesis. Mol Cell Biol **22:** 3024-3034.

DUTT, A., S. CANEVASCINI, E. FROEHLI-HOIER and A. HAJNAL, 2004 EGF signal propagation during *C. elegans* vulval development mediated by ROM-1 rhomboid. PLoS Biol **2:** e334.

EISEN, A., R. T. UTLEY, A. NOURANI, S. ALLARD, P. SCHMIDT, W. S. LANE, J. C. LUCCHESI and J. COTE, 2001 The yeast NuA4 and *Drosophila* MSL complexes contain homologous subunits important for transcription regulation. J Biol Chem **276:** 3484-3491.

EISENMANN, D. M., and S. K. KIM, 2000 Protruding vulva mutants identify novel loci and Wnt signaling factors that function during *Caenorhabditis elegans* vulva development. Genetics **156:** 1097-1116.

EISENMANN, D. M., J. N. MALOOF, J. S. SIMSKE, C. KENYON and S. K. KIM, 1998 The beta-catenin homolog BAR-1 and LET-60 Ras coordinately regulate the Hox gene *lin-39* during *Caenorhabditis elegans* vulval development. Development **125:** 3667-3680.

EISSENBERG, J. C., T. C. JAMES, D. M. FOSTER-HARTNETT, T. HARTNETT, V. NGAN and S. C. ELGIN, 1990 Mutation in a heterochromatin-specific chromosomal protein is associated with suppression of position-effect variegation in *Drosophila melanogaster*. Proc Natl Acad Sci U S A **87:** 9923-9927.

EISSENBERG, J. C., and A. SHILATIFARD, 2006 Leaving a mark: the many footprints of the elongating RNA polymerase II. Curr Opin Genet Dev **16:** 184-190.

ELFRING, L. K., R. DEURING, C. M. MCCALLUM, C. L. PETERSON and J. W. TAMKUN, 1994 Identification and characterization of *Drosophila* relatives of the yeast transcriptional activator SNF2/SWI2. Mol Cell Biol **14:** 2225-2234.

FAY, D. S., S. KEENAN and M. HAN, 2002 *fzr-1* and *lin-35*/Rb function redundantly to control cell proliferation in *C. elegans* as revealed by a nonbiased synthetic screen. Genes Dev **16:** 503-517.

FAY, D. S., E. LARGE, M. HAN and M. DARLAND, 2003 *lin-35*/Rb and *ubc-18*, an E2 ubiquitin-conjugating enzyme, function redundantly to control pharyngeal morphogenesis in *C. elegans*. Development **130:** 3319-3330.

FAY, D. S., X. QIU, E. LARGE, C. P. SMITH, S. MANGO and B. L. JOHANSON, 2004 The coordinate regulation of pharyngeal development in *C. elegans* by *lin-35*/Rb, *pha-1*, and *ubc-18*. Dev Biol **271:** 11-25.

FAY, D. S., and J. YOCHEM, 2007 The synMuv genes of *Caenorhabditis elegans* in vulval development and beyond. Dev Biol.

FERGUSON, E. L., and H. R. HORVITZ, 1985 Identification and characterization of 22 genes that affect the vulval cell lineages of the nematode *Caenorhabditis elegans*. Genetics **110:** 17-72.

FERGUSON, E. L., and H. R. HORVITZ, 1989 The multivulva phenotype of certain *Caenorhabditis elegans* mutants results from defects in two functionally redundant pathways. Genetics **123:** 109-121.

FERGUSON, E. L., P. W. STERNBERG and H. R. HORVITZ, 1987 A genetic pathway for the specification of the vulval cell lineages of *Caenorhabditis elegans*. Nature **326:** 259-267.

FISCHLE, W., Y. WANG, S. A. JACOBS, Y. KIM, C. D. ALLIS and S. KHORASANIZADEH, 2003 Molecular basis for the discrimination of repressive methyl-lysine marks in histone H3 by Polycomb and HP1 chromodomains. Genes Dev **17:** 1870-1881.

FONG, Y., L. BENDER, W. WANG and S. STROME, 2002 Regulation of the different chromatin states of autosomes and X chromosomes in the germ line of *C. elegans*. Science **296:** 2235-2238.

FRANCIS, N. J., R. E. KINGSTON and C. L. WOODCOCK, 2004 Chromatin compaction by a polycomb group protein complex. Science **306:** 1574-1577.

FRASER, A. G., R. S. KAMATH, P. ZIPPERLEN, M. MARTINEZ-CAMPOS, M. SOHRMANN and J. AHRINGER, 2000 Functional genomic analysis of *C. elegans* chromosome I by systematic RNA interference. Nature **408:** 325-330.

GAILLARD, H., D. J. FITZGERALD, C. L. SMITH, C. L. PETERSON, T. J. RICHMOND and F. THOMA, 2003 Chromatin remodeling activities act on UV-damaged nucleosomes and modulate DNA damage accessibility to photolyase. J Biol Chem **278:** 17655-17663.

GARBE, D., J. B. DOTO and M. V. SUNDARAM, 2004 *Caenorhabditis elegans lin-35*/Rb, *efl-1*/E2F and other synthetic multivulva genes negatively regulate the anaphase-promoting complex gene *mat-3*/APC8. Genetics **167:** 663-672.

GDULA, D. A., R. SANDALTZOPOULOS, T. TSUKIYAMA, V. OSSIPOW and C. WU, 1998 Inorganic pyrophosphatase is a component of the *Drosophila* nucleosome remodeling factor complex. Genes Dev **12:** 3206-3216.

GEORGEL, P. T., T. TSUKIYAMA and C. WU, 1997 Role of histone tails in nucleosome remodeling by *Drosophila* NURF. Embo J **16:** 4717-4726.

GLEASON, J. E., H. C. KORSWAGEN and D. M. EISENMANN, 2002 Activation of Wnt signaling bypasses the requirement for RTK/Ras signaling during *C. elegans* vulval induction. Genes Dev **16:** 1281-1290.

GLEASON, J. E., E. A. SZYLEYKO and D. M. EISENMANN, 2006 Multiple redundant Wnt signaling components function in two processes during *C. elegans* vulval development. Dev Biol **298:** 442-457.

GREENWALD, I. S., P. W. STERNBERG and H. R. HORVITZ, 1983 The *lin-12* locus specifies cell fates in *Caenorhabditis elegans*. Cell **34:** 435-444.

GROTE, P., and B. CONRADT, 2006 The PLZF-like protein TRA-4 cooperates with the Gli-like transcription factor TRA-1 to promote female development in *C. elegans*. Dev Cell **11:** 561-573.

GROTH, A., W. ROCHA, A. VERREAULT and G. ALMOUZNI, 2007 Chromatin challenges during DNA replication and repair. Cell **128:** 721-733.

GUPTA, B. P., J. LIU, B. J. HWANG, N. MOGHAL and P. W. STERNBERG, 2006 *sli-3* negatively regulates the LET-23/epidermal growth factor receptor-mediated vulval induction pathway in *Caenorhabditis elegans*. Genetics **174:** 1315-1326.

HAJNAL, A., and T. BERSET, 2002 The *C.elegans* MAPK phosphatase LIP-1 is required for the G(2)/M meiotic arrest of developing oocytes. Embo J **21:** 4317-4326.

HAJNAL, A., C. W. WHITFIELD and S. K. KIM, 1997 Inhibition of *Caenorhabditis elegans* vulval induction by *gap-1* and by *let-23* receptor tyrosine kinase. Genes Dev **11:** 2715-2728.

HAKIMI, M. A., D. A. BOCHAR, J. A. SCHMIESING, Y. DONG, O. G. BARAK, D. W. SPEICHER, K. YOKOMORI and R. SHIEKHATTAR, 2002 A chromatin remodelling complex that loads cohesin onto human chromosomes. Nature **418:** 994-998.

HAN, M., R. V. AROIAN and P. W. STERNBERG, 1990 The *let-60* locus controls the switch between vulval and nonvulval cell fates in *Caenorhabditis elegans*. Genetics **126:** 899-913.

HAN, M., A. GOLDEN, Y. HAN and P. W. STERNBERG, 1993 *C. elegans lin-45* raf gene participates in *let-60* ras-stimulated vulval differentiation. Nature **363:** 133-140.

HANAHAN, D., and R. A. WEINBERG, 2000 The hallmarks of cancer. Cell **100:** 57-70.

HARRISON, M. M., C. J. CEOL, X. LU and H. R. HORVITZ, 2006 Some *C. elegans* class B synthetic multivulva proteins encode a conserved LIN-35 Rb-containing complex distinct from a NuRD-like complex. Proc Natl Acad Sci U S A **103:** 16782-16787.

HASSAN, A. H., K. E. NEELY and J. L. WORKMAN, 2001 Histone acetyltransferase complexes stabilize swi/snf binding to promoter nucleosomes. Cell **104:** 817-827.

HENDERSON, S. T., D. GAO, E. J. LAMBIE and J. KIMBLE, 1994 *lag-2* may encode a signaling ligand for the GLP-1 and LIN-12 receptors of *C. elegans*. Development **120:** 2913-2924.

HILL, R. J., and P. W. STERNBERG, 1992 The gene *lin-3* encodes an inductive signal for vulval development in *C. elegans*. Nature **358:** 470-476.

HIRSCHHORN, J. N., S. A. BROWN, C. D. CLARK and F. WINSTON, 1992 Evidence that SNF2/SWI2 and SNF5 activate transcription in yeast by altering chromatin structure. Genes Dev **6:** 2288-2298.

HOPPER, N. A., J. LEE and P. W. STERNBERG, 2000 ARK-1 inhibits EGFR signaling in *C. elegans*. Mol Cell **6:** 65-75.

HORVITZ, H. R., and J. E. SULSTON, 1980 Isolation and genetic characterization of cell-lineage mutants of the nematode *Caenorhabditis elegans*. Genetics **96:** 435-454.

HSIEH, J., J. LIU, S. A. KOSTAS, C. CHANG, P. W. STERNBERG and A. FIRE, 1999 The RING finger/B-box factor TAM-1 and a retinoblastoma-like protein LIN-35 modulate context-dependent gene silencing in *Caenorhabditis elegans*. Genes Dev **13:** 2958-2970.

HUANG, S., M. LITT and G. FELSENFELD, 2005 Methylation of histone H4 by arginine methyltransferase PRMT1 is essential in vivo for many subsequent histone modifications. Genes Dev **19:** 1885-1893.

HUDSON, B. P., M. A. MARTINEZ-YAMOUT, H. J. DYSON and P. E. WRIGHT, 2000 Solution structure and acetyl-lysine binding activity of the GCN5 bromodomain. J Mol Biol **304:** 355-370.

IKURA, T., V. V. OGRYZKO, M. GRIGORIEV, R. GROISMAN, J. WANG, M. HORIKOSHI, R. SCULLY, J. QIN and Y. NAKATANI, 2000 Involvement of the TIP60 histone acetylase complex in DNA repair and apoptosis. Cell **102:** 463-473.

INOUE, T., H. S. OZ, D. WILAND, S. GHARIB, R. DESHPANDE, R. J. HILL, W. S. KATZ and P. W. STERNBERG, 2004 *C. elegans* LIN-18 is a Ryk ortholog and functions in parallel to LIN-17/Frizzled in Wnt signaling. Cell **118:** 795-806.

INOUE, T., D. R. SHERWOOD, G. ASPOCK, J. A. BUTLER, B. P. GUPTA, M. KIROUAC, M. WANG, P. Y. LEE, J. M. KRAMER, I. HOPE, T. R. BURGLIN and P. W. STERNBERG, 2002 Gene expression markers for *Caenorhabditis elegans* vulval cells. Gene Expr Patterns **2:** 235-241.

ITO, T., M. BULGER, M. J. PAZIN, R. KOBAYASHI and J. T. KADONAGA, 1997 ACF, an ISWI-containing and ATP-utilizing chromatin assembly and remodeling factor. Cell **90:** 145-155.

JACOBSON, R. H., A. G. LADURNER, D. S. KING and R. TJIAN, 2000 Structure and function of a human TAFII250 double bromodomain module. Science **288:** 1422-1425.

JAMES, T. C., and S. C. ELGIN, 1986 Identification of a nonhistone chromosomal protein associated with heterochromatin in *Drosophila melanogaster* and its gene. Mol Cell Biol **6:** 3862-3872.

JENUWEIN, T., and C. D. ALLIS, 2001 Translating the histone code. Science **293:** 1074-1080.

JONGEWARD, G. D., T. R. CLANDININ and P. W. STERNBERG, 1995 *sli-1*, a negative regulator of *let-23*-mediated signaling in *C. elegans*. Genetics **139:** 1553-1566.

JOSHI, A. A., and K. STRUHL, 2005 Eaf3 chromodomain interaction with methylated H3-K36 links histone deacetylation to Pol II elongation. Mol Cell **20:** 971-978.

KAECH, S. M., C. W. WHITFIELD and S. K. KIM, 1998 The LIN-2/LIN-7/LIN-10 complex mediates basolateral membrane localization of the *C. elegans* EGF receptor LET-23 in vulval epithelial cells. Cell **94:** 761-771.

KAMATH, R. S., A. G. FRASER, Y. DONG, G. POULIN, R. DURBIN, M. GOTTA, A. KANAPIN, N. LE BOT, S. MORENO, M. SOHRMANN, D. P. WELCHMAN, P. ZIPPERLEN and J. AHRINGER, 2003 Systematic functional analysis of the *Caenorhabditis elegans* genome using RNAi. Nature **421:** 231-237.

KATZ, W. S., R. J. HILL, T. R. CLANDININ and P. W. STERNBERG, 1995 Different levels of the *C. elegans* growth factor LIN-3 promote distinct vulval precursor fates. Cell **82:** 297-307.

KELLY, W. G., and A. FIRE, 1998 Chromatin silencing and the maintenance of a functional germline in *Caenorhabditis elegans*. Development **125:** 2451-2456.

KELLY, W. G., S. XU, M. K. MONTGOMERY and A. FIRE, 1997 Distinct requirements for somatic and germline expression of a generally expressed *Caernorhabditis elegans* gene. Genetics **146:** 227-238.

KEOGH, M. C., S. K. KURDISTANI, S. A. MORRIS, S. H. AHN, V. PODOLNY, S. R. COLLINS, M. SCHULDINER, K. CHIN, T. PUNNA, N. J. THOMPSON, C. BOONE, A. EMILI, J. S. WEISSMAN, T. R. HUGHES, B. D. STRAHL, M. GRUNSTEIN, J. F. GREENBLATT, S. BURATOWSKI and N. J. KROGAN, 2005 Cotranscriptional

set2 methylation of histone H3 lysine 36 recruits a repressive Rpd3 complex. Cell **123:** 593-605.

KIM, J., J. DANIEL, A. ESPEJO, A. LAKE, M. KRISHNA, L. XIA, Y. ZHANG and M. T. BEDFORD, 2006 Tudor, MBT and chromo domains gauge the degree of lysine methylation. EMBO Rep **7:** 397-403.

KIMBLE, J., 1981 Alterations in cell lineage following laser ablation of cells in the somatic gonad of *Caenorhabditis elegans*. Dev Biol **87:** 286-300.

KLOSE, R. J., K. YAMANE, Y. BAE, D. ZHANG, H. ERDJUMENT-BROMAGE, P. TEMPST, J. WONG and Y. ZHANG, 2006 The transcriptional repressor JHDM3A demethylates trimethyl histone H3 lysine 9 and lysine 36. Nature **442:** 312-316.

KOH, K., S. M. PEYROT, C. G. WOOD, J. A. WAGMAISTER, M. F. MADURO, D. M. EISENMANN and J. H. ROTHMAN, 2002 Cell fates and fusion in the *C. elegans* vulval primordium are regulated by the EGL-18 and ELT-6 GATA factors -- apparent direct targets of the LIN-39 Hox protein. Development **129:** 5171-5180.

KORENJAK, M., B. TAYLOR-HARDING, U. K. BINNE, J. S. SATTERLEE, O. STEVAUX, R. AASLAND, H. WHITE-COOPER, N. DYSON and A. BREHM, 2004 Native E2F/RBF complexes contain Myb-interacting proteins and repress transcription of developmentally controlled E2F target genes. Cell **119:** 181-193.

KORNFELD, K., K. L. GUAN and H. R. HORVITZ, 1995a The *Caenorhabditis elegans* gene *mek-2* is required for vulval induction and encodes a protein similar to the protein kinase MEK. Genes Dev **9:** 756-768.

KORNFELD, K., D. B. HOM and H. R. HORVITZ, 1995b The *ksr-1* gene encodes a novel protein kinase involved in Ras-mediated signaling in *C. elegans*. Cell **83:** 903-913.

KOUZARIDES, T., 2002 Histone methylation in transcriptional control. Curr Opin Genet Dev **12:** 198-209.

KOUZARIDES, T., 2007 Chromatin modifications and their function. Cell **128:** 693-705.

KROGAN, N. J., M. KIM, A. TONG, A. GOLSHANI, G. CAGNEY, V. CANADIEN, D. P. RICHARDS, B. K. BEATTIE, A. EMILI, C. BOONE, A. SHILATIFARD, S. BURATOWSKI and J. GREENBLATT, 2003 Methylation of histone H3 by Set2 in *Saccharomyces cerevisiae* is linked to transcriptional elongation by RNA polymerase II. Mol Cell Biol **23:** 4207-4218.

LACHNER, M., D. O'CARROLL, S. REA, K. MECHTLER and T. JENUWEIN, 2001 Methylation of histone H3 lysine 9 creates a binding site for HP1 proteins. Nature **410:** 116-120.

LACKNER, M. R., and S. K. KIM, 1998 Genetic analysis of the *Caenorhabditis elegans* MAP kinase gene *mpk-1*. Genetics **150:** 103-117.

LACKNER, M. R., K. KORNFELD, L. M. MILLER, H. R. HORVITZ and S. K. KIM, 1994 A MAP kinase homolog, *mpk-1*, is involved in ras-mediated induction of vulval cell fates in *Caenorhabditis elegans*. Genes Dev **8:** 160-173.

LANDRY, J., A. SUTTON, T. HESMAN, J. MIN, R. M. XU, M. JOHNSTON and R. STERNGLANZ, 2003 Set2-catalyzed methylation of histone H3 represses

basal expression of GAL4 in *Saccharomyces cerevisiae*. Mol Cell Biol **23:** 5972-5978.

LANGST, G., and P. B. BECKER, 2004 Nucleosome remodeling: one mechanism, many phenomena? Biochim Biophys Acta **1677:** 58-63.

LEE, J., G. D. JONGEWARD and P. W. STERNBERG, 1994 *unc-101*, a gene required for many aspects of *Caenorhabditis elegans* development and behavior, encodes a clathrin-associated protein. Genes Dev **8:** 60-73.

LEHNER, B., A. CALIXTO, C. CROMBIE, J. TISCHLER, A. FORTUNATO, M. CHALFIE and A. G. FRASER, 2006 Loss of LIN-35, the *Caenorhabditis elegans* ortholog of the tumor suppressor p105Rb, results in enhanced RNA interference. Genome Biol **7:** R4.

LEWIS, P. W., E. L. BEALL, T. C. FLEISCHER, D. GEORLETTE, A. J. LINK and M. R. BOTCHAN, 2004 Identification of a *Drosophila* Myb-E2F2/RBF transcriptional repressor complex. Genes Dev **18:** 2929-2940.

LI, B., L. HOWE, S. ANDERSON, J. R. YATES, 3RD and J. L. WORKMAN, 2003 The Set2 histone methyltransferase functions through the phosphorylated carboxyl-terminal domain of RNA polymerase II. J Biol Chem **278:** 8897-8903.

LI, J., D. MOAZED and S. P. GYGI, 2002 Association of the histone methyltransferase Set2 with RNA polymerase II plays a role in transcription elongation. J Biol Chem **277:** 49383-49388.

LINDROTH, A. M., D. SHULTIS, Z. JASENCAKOVA, J. FUCHS, L. JOHNSON, D. SCHUBERT, D. PATNAIK, S. PRADHAN, J. GOODRICH, I. SCHUBERT, T.

JENUWEIN, S. KHORASANIZADEH and S. E. JACOBSEN, 2004 Dual histone H3 methylation marks at lysines 9 and 27 required for interaction with CHROMOMETHYLASE3. Embo J **23:** 4286-4296.

LOEWITH, R., M. MEIJER, S. P. LEES-MILLER, K. RIABOWOL and D. YOUNG, 2000 Three yeast proteins related to the human candidate tumor suppressor p33(ING1) are associated with histone acetyltransferase activities. Mol Cell Biol **20:** 3807-3816.

LOWENSTEIN, E. J., R. J. DALY, A. G. BATZER, W. LI, B. MARGOLIS, R. LAMMERS, A. ULLRICH, E. Y. SKOLNIK, D. BAR-SAGI and J. SCHLESSINGER, 1992 The SH2 and SH3 domain-containing protein GRB2 links receptor tyrosine kinases to ras signaling. Cell **70:** 431-442.

LOYOLA, A., G. LEROY, Y. H. WANG and D. REINBERG, 2001 Reconstitution of recombinant chromatin establishes a requirement for histone-tail modifications during chromatin assembly and transcription. Genes Dev **15:** 2837-2851.

LU, X., and H. R. HORVITZ, 1998 *lin-35* and *lin-53*, two genes that antagonize a *C. elegans* Ras pathway, encode proteins similar to Rb and its binding protein RbAp48. Cell **95:** 981-991.

LUGER, K., A. W. MADER, R. K. RICHMOND, D. F. SARGENT and T. J. RICHMOND, 1997 Crystal structure of the nucleosome core particle at 2.8 A resolution. Nature **389:** 251-260.

LUO, R. X., A. A. POSTIGO and D. C. DEAN, 1998 Rb interacts with histone deacetylase to repress transcription. Cell **92:** 463-473.

MAGNAGHI-JAULIN, L., R. GROISMAN, I. NAGUIBNEVA, P. ROBIN, S. LORAIN, J. P. LE VILLAIN, F. TROALEN, D. TROUCHE and A. HAREL-BELLAN, 1998 Retinoblastoma protein represses transcription by recruiting a histone deacetylase. Nature **391:** 601-605.

MARTINEZ-BALBAS, M. A., T. TSUKIYAMA, D. GDULA and C. WU, 1998 *Drosophila* NURF-55, a WD repeat protein involved in histone metabolism. Proc Natl Acad Sci U S A **95:** 132-137.

MILLER, L. M., H. A. HESS, D. B. DOROQUEZ and N. M. ANDREWS, 2000 Null mutations in the *lin-31* gene indicate two functions during *Caenorhabditis elegans* vulval development. Genetics **156:** 1595-1602.

MIN, J., Q. FENG, Z. LI, Y. ZHANG and R. M. XU, 2003a Structure of the catalytic domain of human DOT1L, a non-SET domain nucleosomal histone methyltransferase. Cell **112:** 711-723.

MIN, J., Y. ZHANG and R. M. XU, 2003b Structural basis for specific binding of Polycomb chromodomain to histone H3 methylated at Lys 27. Genes Dev **17:** 1823-1828.

MURPHY, D. J., S. HARDY and D. A. ENGEL, 1999 Human SWI-SNF component BRG1 represses transcription of the *c-fos* gene. Mol Cell Biol **19:** 2724-2733.

NAKAYAMA, J., J. C. RICE, B. D. STRAHL, C. D. ALLIS and S. I. GREWAL, 2001 Role of histone H3 lysine 9 methylation in epigenetic control of heterochromatin assembly. Science **292:** 110-113.

NG, H. H., Q. FENG, H. WANG, H. ERDJUMENT-BROMAGE, P. TEMPST, Y. ZHANG and K. STRUHL, 2002 Lysine methylation within the globular domain of histone H3 by Dot1 is important for telomeric silencing and Sir protein association. Genes Dev **16:** 1518-1527.

NIELSEN, P. R., D. NIETLISPACH, H. R. MOTT, J. CALLAGHAN, A. BANNISTER, T. KOUZARIDES, A. G. MURZIN, N. V. MURZINA and E. D. LAUE, 2002 Structure of the HP1 chromodomain bound to histone H3 methylated at lysine 9. Nature **416:** 103-107.

OLIVIER, J. P., T. RAABE, M. HENKEMEYER, B. DICKSON, G. MBAMALU, B. MARGOLIS, J. SCHLESSINGER, E. HAFEN and T. PAWSON, 1993 A *Drosophila* SH2-SH3 adaptor protein implicated in coupling the sevenless tyrosine kinase to an activator of Ras guanine nucleotide exchange, Sos. Cell **73:** 179-191.

PALACIOS, A., P. GARCIA, D. PADRO, E. LOPEZ-HERNANDEZ, I. MARTIN and F. J. BLANCO, 2006 Solution structure and NMR characterization of the binding to methylated histone tails of the plant homeodomain finger of the tumour suppressor ING4. FEBS Lett **580:** 6903-6908.

PAN, D., and G. M. RUBIN, 1997 Kuzbanian controls proteolytic processing of Notch and mediates lateral inhibition during *Drosophila* and vertebrate neurogenesis. Cell **90:** 271-280.

PETERSON, C. L., and J. L. WORKMAN, 2000 Promoter targeting and chromatin remodeling by the SWI/SNF complex. Curr Opin Genet Dev **10:** 187-192.

PIRROTTA, V., 2006 Polycomb silencing mechanisms and genomic programming. Ernst Schering Res Found Workshop**:** 97-113.

PODBILEWICZ, B., and J. G. WHITE, 1994 Cell fusions in the developing epithelial of *C. elegans*. Dev Biol **161:** 408-424.

POULIN, G., Y. DONG, A. G. FRASER, N. A. HOPPER and J. AHRINGER, 2005 Chromatin regulation and sumoylation in the inhibition of Ras-induced vulval development in *Caenorhabditis elegans*. Embo J **24:** 2613-2623.

PRAY-GRANT, M. G., J. A. DANIEL, D. SCHIELTZ, J. R. YATES, 3RD and P. A. GRANT, 2005 Chd1 chromodomain links histone H3 methylation with SAGA- and SLIK-dependent acetylation. Nature **433:** 434-438.

RAGVIN, A., H. VALVATNE, S. ERDAL, V. ARSKOG, K. R. TUFTELAND, K. BREEN, O. Y. AM, A. EBERHARTER, T. J. GIBSON, P. B. BECKER and R. AASLAND, 2004 Nucleosome binding by the bromodomain and PHD finger of the transcriptional cofactor p300. J Mol Biol **337:** 773-788.

RAYMAN, J. B., Y. TAKAHASHI, V. B. INDJEIAN, J. H. DANNENBERG, S. CATCHPOLE, R. J. WATSON, H. TE RIELE and B. D. DYNLACHT, 2002 E2F mediates cell cycle-dependent transcriptional repression *in vivo* by recruitment of an HDAC1/mSin3B corepressor complex. Genes Dev **16:** 933-947.

REDDIEN, P. W., E. C. ANDERSEN, M. C. HUANG and H. R. HORVITZ, 2007 DPL-1 DP, LIN-35 Rb and EFL-1 E2F Act With the MCD-1 Zinc-Finger Protein to Promote Programmed Cell Death in *Caenorhabditis elegans*. Genetics **175:** 1719-1733.

REDDY, K. C., and A. M. VILLENEUVE, 2004 *C. elegans* HIM-17 links chromatin modification and competence for initiation of meiotic recombination. Cell **118:** 439-452.

RINGROSE, L., H. EHRET and R. PARO, 2004 Distinct contributions of histone H3 lysine 9 and 27 methylation to locus-specific stability of polycomb complexes. Mol Cell **16:** 641-653.

ROUGEULLE, C., J. CHAUMEIL, K. SARMA, C. D. ALLIS, D. REINBERG, P. AVNER and E. HEARD, 2004 Differential histone H3 Lys-9 and Lys-27 methylation profiles on the X chromosome. Mol Cell Biol **24:** 5475-5484.

SAWA, H., L. LOBEL and H. R. HORVITZ, 1996 The *Caenorhabditis elegans* gene *lin-17*, which is required for certain asymmetric cell divisions, encodes a putative seven-transmembrane protein similar to the *Drosophila* frizzled protein. Genes Dev **10:** 2189-2197.

SCHLESSINGER, J., 2000 Cell signaling by receptor tyrosine kinases. Cell **103:** 211-225.

SCHULTZ, D. C., K. AYYANATHAN, D. NEGOREV, G. G. MAUL and F. J. RAUSCHER, 3RD, 2002 SETDB1: a novel KAP-1-associated histone H3, lysine 9-specific methyltransferase that contributes to HP1-mediated silencing of euchromatic genes by KRAB zinc-finger proteins. Genes Dev **16:** 919-932.

SEELIG, H. P., I. MOOSBRUGGER, H. EHRFELD, T. FINK, M. RENZ and E. GENTH, 1995 The major dermatomyositis-specific Mi-2 autoantigen is a presumed helicase involved in transcriptional activation. Arthritis Rheum **38:** 1389-1399.

SHAYE, D. D., and I. GREENWALD, 2002 Endocytosis-mediated downregulation of LIN-12/Notch upon Ras activation in *Caenorhabditis elegans*. Nature **420:** 686-690.

SHAYE, D. D., and I. GREENWALD, 2005 LIN-12/Notch trafficking and regulation of DSL ligand activity during vulval induction in *Caenorhabditis elegans*. Development **132:** 5081-5092.

SHI, X., I. KACHIRSKAIA, K. L. WALTER, J. H. KUO, A. LAKE, F. DAVRAZOU, S. M. CHAN, D. G. MARTIN, I. M. FINGERMAN, S. D. BRIGGS, L. HOWE, P. J. UTZ, T. G. KUTATELADZE, A. A. LUGOVSKOY, M. T. BEDFORD and O. GOZANI, 2007 Proteome-wide analysis in *Saccharomyces cerevisiae* identifies several PHD fingers as novel direct and selective binding modules of histone H3 methylated at either lysine 4 or lysine 36. J Biol Chem **282:** 2450-2455.

SHI, Y., F. LAN, C. MATSON, P. MULLIGAN, J. R. WHETSTINE, P. A. COLE, R. A. CASERO and Y. SHI, 2004 Histone demethylation mediated by the nuclear amine oxidase homolog LSD1. Cell **119:** 941-953.

SHILATIFARD, A., 2006 Chromatin modifications by methylation and ubiquitination: implications in the regulation of gene expression. Annu Rev Biochem **75:** 243-269.

SHOGREN-KNAAK, M., H. ISHII, J. M. SUN, M. J. PAZIN, J. R. DAVIE and C. L. PETERSON, 2006 Histone H4-K16 acetylation controls chromatin structure and protein interactions. Science **311:** 844-847.

SIEBURTH, D. S., M. SUNDARAM, R. M. HOWARD and M. HAN, 1999 A PP2A regulatory subunit positively regulates Ras-mediated signaling during *Caenorhabditis elegans* vulval induction. Genes Dev **13:** 2562-2569.

SIJEN, T., and R. H. PLASTERK, 2003 Transposon silencing in the *Caenorhabditis elegans* germ line by natural RNAi. Nature **426:** 310-314.

SIMON, M. A., 1994 Signal transduction during the development of the *Drosophila* R7 photoreceptor. Dev Biol **166:** 431-442.

SIMS, R. J., 3RD, and D. REINBERG, 2006 Histone H3 Lys 4 methylation: caught in a bind? Genes Dev **20:** 2779-2786.

SOLARI, F., and J. AHRINGER, 2000 NURD-complex genes antagonise Ras-induced vulval development in *Caenorhabditis elegans*. Curr Biol **10:** 223-226.

STERNBERG, P. W., 2006 Pathway to RAS. Genetics **172:** 727-731.

STERNBERG, P. W., and H. R. HORVITZ, 1986 Pattern formation during vulval development in *C. elegans*. Cell **44:** 761-772.

STERNBERG, P. W., and H. R. HORVITZ, 1989 The combined action of two intercellular signaling pathways specifies three cell fates during vulval induction in *C. elegans*. Cell **58:** 679-693.

STRAHL, B. D., P. A. GRANT, S. D. BRIGGS, Z. W. SUN, J. R. BONE, J. A. CALDWELL, S. MOLLAH, R. G. COOK, J. SHABANOWITZ, D. F. HUNT and C. D. ALLIS, 2002 Set2 is a nucleosomal histone H3-selective methyltransferase that mediates transcriptional repression. Mol Cell Biol **22:** 1298-1306.

SUDARSANAM, P., V. R. IYER, P. O. BROWN and F. WINSTON, 2000 Whole-genome expression analysis of *snf/swi* mutants of *Saccharomyces cerevisiae*. Proc Natl Acad Sci U S A **97:** 3364-3369.

SULSTON, J. E., and H. R. HORVITZ, 1977 Post-embryonic cell lineages of the nematode, *Caenorhabditis elegans*. Dev Biol **56:** 110-156.

SULSTON, J. E., E. SCHIERENBERG, J. G. WHITE and J. N. THOMSON, 1983 The embryonic cell lineage of the nematode *Caenorhabditis elegans*. Dev Biol **100:** 64-119.

SULSTON, J. E., and J. G. WHITE, 1980 Regulation and cell autonomy during postembryonic development of *Caenorhabditis elegans*. Dev Biol **78:** 577-597.

SUN, X. J., J. WEI, X. Y. WU, M. HU, L. WANG, H. H. WANG, Q. H. ZHANG, S. J. CHEN, Q. H. HUANG and Z. CHEN, 2005 Identification and characterization of a novel human histone H3 lysine 36-specific methyltransferase. J Biol Chem **280:** 35261-35271.

SUNDARAM, M. V., 2005 The love-hate relationship between Ras and Notch. Genes Dev **19:** 1825-1839.

TAN, P. B., M. R. LACKNER and S. K. KIM, 1998 MAP kinase signaling specificity mediated by the LIN-1 Ets/LIN-31 WH transcription factor complex during *C. elegans* vulval induction. Cell **93:** 569-580.

TEYSSIER, C., D. CHEN and M. R. STALLCUP, 2002 Requirement for multiple domains of the protein arginine methyltransferase CARM1 in its transcriptional coactivator function. J Biol Chem **277:** 46066-46072.

THOMAS, J. H., C. J. CEOL, H. T. SCHWARTZ and H. R. HORVITZ, 2003 New genes that interact with *lin-35* Rb to negatively regulate the *let-60* ras pathway in *Caenorhabditis elegans*. Genetics **164:** 135-151.

TIENSUU, T., M. K. LARSEN, E. VERNERSSON and S. TUCK, 2005 *lin-1* has both positive and negative functions in specifying multiple cell fates induced by Ras/MAP kinase signaling in *C. elegans*. Dev Biol **286:** 338-351.

TSCHIERSCH, B., A. HOFMANN, V. KRAUSS, R. DORN, G. KORGE and G. REUTER, 1994 The protein encoded by the *Drosophila* position-effect variegation suppressor gene *Su(var)3-9* combines domains of antagonistic regulators of homeotic gene complexes. Embo J **13:** 3822-3831.

TSUKADA, Y., J. FANG, H. ERDJUMENT-BROMAGE, M. E. WARREN, C. H. BORCHERS, P. TEMPST and Y. ZHANG, 2006 Histone demethylation by a family of JmjC domain-containing proteins. Nature **439:** 811-816.

TSUKIYAMA, T., and C. WU, 1995 Purification and properties of an ATP-dependent nucleosome remodeling factor. Cell **83:** 1011-1020.

UNHAVAITHAYA, Y., T. H. SHIN, N. MILIARAS, J. LEE, T. OYAMA and C. C. MELLO, 2002 MEP-1 and a homolog of the NURD complex component Mi-2 act together to maintain germline-soma distinctions in *C. elegans*. Cell **111:** 991-1002.

URA, K., M. ARAKI, H. SAEKI, C. MASUTANI, T. ITO, S. IWAI, T. MIZUKOSHI, Y. KANEDA and F. HANAOKA, 2001 ATP-dependent chromatin remodeling facilitates nucleotide excision repair of UV-induced DNA lesions in synthetic dinucleosomes. Embo J **20:** 2004-2014.

VAN LEEUWEN, F., P. R. GAFKEN and D. E. GOTTSCHLING, 2002 Dot1p modulates silencing in yeast by methylation of the nucleosome core. Cell **109:** 745-756.

VARGA-WEISZ, P. D., M. WILM, E. BONTE, K. DUMAS, M. MANN and P. B. BECKER, 1997 Chromatin-remodelling factor CHRAC contains the ATPases ISWI and topoisomerase II. Nature **388:** 598-602.

VASTENHOUW, N. L., S. E. FISCHER, V. J. ROBERT, K. L. THIJSSEN, A. G. FRASER, R. S. KAMATH, J. AHRINGER and R. H. PLASTERK, 2003 A genome-wide screen identifies 27 genes involved in transposon silencing in *C. elegans*. Curr Biol **13:** 1311-1316.

VIGNALI, M., A. H. HASSAN, K. E. NEELY and J. L. WORKMAN, 2000 ATP-dependent chromatin-remodeling complexes. Mol Cell Biol **20:** 1899-1910.

VON ZELEWSKY, T., F. PALLADINO, K. BRUNSCHWIG, H. TOBLER, A. HAJNAL and F. MULLER, 2000 The *C. elegans* Mi-2 chromatin-remodelling proteins function in vulval cell fate determination. Development **127:** 5277-5284.

WAGMAISTER, J. A., G. R. MILEY, C. A. MORRIS, J. E. GLEASON, L. M. MILLER, K. KORNFELD and D. M. EISENMANN, 2006 Identification of *cis*-regulatory elements from the *C. elegans* Hox gene *lin-39* required for embryonic expression and for regulation by the transcription factors LIN-1, LIN-31 and LIN-39. Dev Biol **297:** 550-565.

WANG, D., S. KENNEDY, D. CONTE, JR., J. K. KIM, H. W. GABEL, R. S. KAMATH, C. C. MELLO and G. RUVKUN, 2005 Somatic misexpression of germline P granules and enhanced RNA interference in retinoblastoma pathway mutants. Nature **436:** 593-597.

WHETSTINE, J. R., A. NOTTKE, F. LAN, M. HUARTE, S. SMOLIKOV, Z. CHEN, E. SPOONER, E. LI, G. ZHANG, M. COLAIACOVO and Y. SHI, 2006 Reversal of

histone lysine trimethylation by the JMJD2 family of histone demethylases. Cell **125:** 467-481.

WOLFFE, A., 1998 Chromatin: Structure and Function.

WYSOCKA, J., T. SWIGUT, T. A. MILNE, Y. DOU, X. ZHANG, A. L. BURLINGAME, R. G. ROEDER, A. H. BRIVANLOU and C. D. ALLIS, 2005 WDR5 associates with histone H3 methylated at K4 and is essential for H3 K4 methylation and vertebrate development. Cell **121:** 859-872.

WYSOCKA, J., T. SWIGUT, H. XIAO, T. A. MILNE, S. Y. KWON, J. LANDRY, M. KAUER, A. J. TACKETT, B. T. CHAIT, P. BADENHORST, C. WU and C. D. ALLIS, 2006 A PHD finger of NURF couples histone H3 lysine 4 trimethylation with chromatin remodelling. Nature **442:** 86-90.

XIAO, H., R. SANDALTZOPOULOS, H. M. WANG, A. HAMICHE, R. RANALLO, K. M. LEE, D. FU and C. WU, 2001 Dual functions of largest NURF subunit NURF301 in nucleosome sliding and transcription factor interactions. Mol Cell **8:** 531-543.

XIAO, T., H. HALL, K. O. KIZER, Y. SHIBATA, M. C. HALL, C. H. BORCHERS and B. D. STRAHL, 2003 Phosphorylation of RNA polymerase II CTD regulates H3 methylation in yeast. Genes Dev **17:** 654-663.

XU, L., Y. FONG and S. STROME, 2001 The *Caenorhabditis elegans* maternal-effect sterile proteins, MES-2, MES-3, and MES-6, are associated in a complex in embryos. Proc Natl Acad Sci U S A **98:** 5061-5066.

XUE, Y., J. WONG, G. T. MORENO, M. K. YOUNG, J. COTE and W. WANG, 1998 NURD, a novel complex with both ATP-dependent chromatin-remodeling and histone deacetylase activities. Mol Cell **2:** 851-861.

YAMADA, T., K. MIZUNO, K. HIROTA, N. KON, W. P. WAHLS, E. HARTSUIKER, H. MUROFUSHI, T. SHIBATA and K. OHTA, 2004 Roles of histone acetylation and chromatin remodeling factor in a meiotic recombination hotspot. Embo J **23:** 1792-1803.

YAMANE, K., C. TOUMAZOU, Y. TSUKADA, H. ERDJUMENT-BROMAGE, P. TEMPST, J. WONG and Y. ZHANG, 2006 JHDM2A, a JmjC-containing H3K9 demethylase, facilitates transcription activation by androgen receptor. Cell **125:** 483-495.

YOCHEM, J., K. WESTON and I. GREENWALD, 1988 The *Caenorhabditis elegans lin-12* gene encodes a transmembrane protein with overall similarity to *Drosophila* Notch. Nature **335:** 547-550.

YOO, A. S., C. BAIS and I. GREENWALD, 2004 Crosstalk between the EGFR and LIN-12/Notch pathways in *C. elegans* vulval development. Science **303:** 663-666.

YOO, A. S., and I. GREENWALD, 2005 LIN-12/Notch activation leads to microRNA-mediated down-regulation of Vav in *C. elegans*. Science **310:** 1330-1333.

YOON, C. H., C. CHANG, N. A. HOPPER, G. M. LESA and P. W. STERNBERG, 2000 Requirements of multiple domains of SLI-1, a *Caenorhabditis elegans* homologue of c-Cbl, and an inhibitory tyrosine in LET-23 in regulating vulval differentiation. Mol Biol Cell **11:** 4019-4031.

YOON, C. H., J. LEE, G. D. JONGEWARD and P. W. STERNBERG, 1995 Similarity of *sli-1*, a regulator of vulval development in *C. elegans*, to the mammalian proto-oncogene c-cbl. Science **269:** 1102-1105.

ZHANG, Y., G. LEROY, H. P. SEELIG, W. S. LANE and D. REINBERG, 1998 The dermatomyositis-specific autoantigen Mi2 is a component of a complex containing histone deacetylase and nucleosome remodeling activities. Cell **95:** 279-289.

ZHANG, Y., H. H. NG, H. ERDJUMENT-BROMAGE, P. TEMPST, A. BIRD and D. REINBERG, 1999 Analysis of the NuRD subunits reveals a histone deacetylase core complex and a connection with DNA methylation. Genes Dev **13:** 1924-1935.

Table 1. The synthetic multivulva genes

class A genes	Homolog(s) or domain	Complex
lin-8		
lin-15A	THAP domain	LIN-15A/LIN-56
lin-38	zinc finger	
lin-56	THAP domain	LIN-15A/LIN-56
mcd-1	zinc finger	
class B genes	**Homolog(s) or domain**	**Complex(es)**
ark-1	Ack	
dpl-1	DP	DP/E2F
efl-1	E2F	DP/E2F
epc-1	E(Pc)	Tip60 or NuA4
gap-1	RasGAP	
hda-1	HDAC1	NuRD
hpl-2	HP1	
let-418	Mi-2	NuRD
lin-9	Mip130 or aly	DRM
lin-13	zinc fingers	
lin-15B	THAP domain	
lin-35	Rb	DRM
lin-36	THAP domain	
lin-37	Mip40	DRM
lin-52	dLin52	DRM
lin-53	RbAp48 or CAF-1	DRM and NuRD
lin-54	Mip120 or tesmin	DRM
lin-61	l(3)MBT	
lin-65		
lst-3	CARP-1	
mep-1	zinc finger	NuRD
met-1	Set2 HMT	
met-2	SETDB1 HMT	
mys-1	MYST HAT	Tip60 and NuA4
tam-1	TRIM	
trr-1	TRRAP	Tip60 and NuA4

Table 2. Histone methyltransferases, effects on transcription and proteins that bind to methylated lysines (see text for relevant references)

Domains	Lysine modified	Most common enzyme(s)	Associated with transcriptional…	Protein(s) that bind methylated residue
SET and PostSET	H3K4	Set1	activation	Chd1, WDR5
PreSET, SET and PostSET	H3K9	SUVARH1, SETDB1	repression	HP1
SET	H3K27	E(z)	repression	Pc?
AWS, SET and PostSET	H3K36	Set2	activation	Eaf3

FIGURE DESCRIPTIONS

Figure 1. Pn.p cells can adopt any one of three fates.
A cartoon of the early third larval stage hermaphrodite animal is shown. In green the anchor cell (AC), is the source of the LIN-3 EGF Ras pathway inducer, and in orange, is the syncytial hypodermal cell, hyp7, the source of an inhibitory vulval signal. The Pn.p cells are labeled in either blue or yellow. Blue denotes the cells that in the wild-type animal adopt non-vulval cell fates. The yellow denotes the cells that in the wild-type animal adopt vulval fates. The fate that the vulval equivalence group cell adopts in the wild type is shown with the respective cell lineage below.

Figure 1.

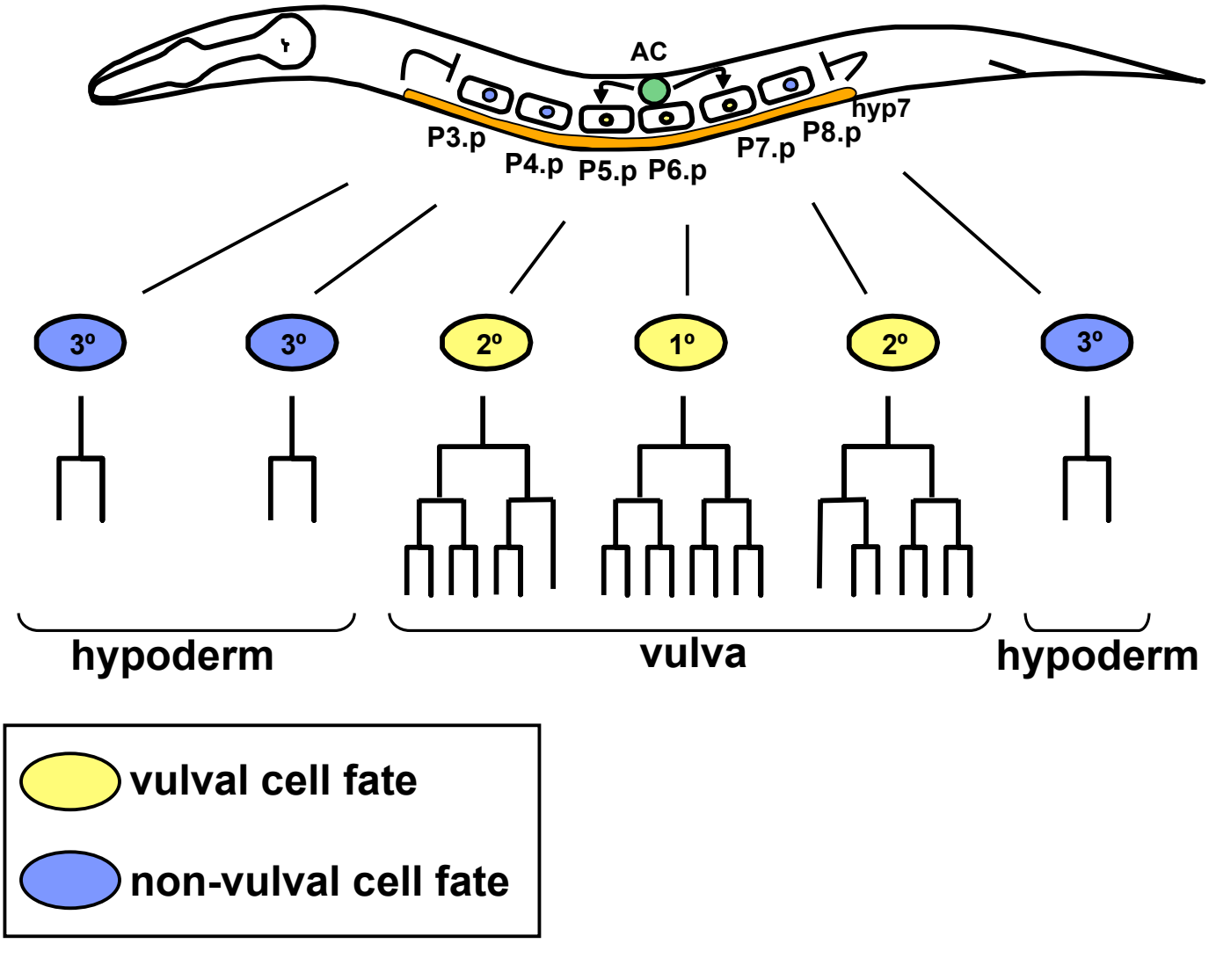
AC
hyp7
P3.p
P4.p
P5.p
P6.p
P7.p
P8.p
3º
3º
2º
1º
2º
3º
hypoderm
vulva
hypoderm
vulval cell fate
non-vulval cell fate

Figure 2. There are two general classes of mutant vulval phenotypes
The wild-type and vulval mutant phenotypes in adult animals are shown. Top, in wild-type hermaphrodites, three of the six cells of the vulval equivalence group adopt vulval fates and the remaining three cells fuse with the hypodermis. The vulva is indicated with a yellow arrow. Middle, in vulvaless or Vul mutants (*let-23(sy1)*), all six cells adopt non-vulval fates and fuse with the hypodermis causing the "bag of worms" phenotype. Bottom, in multivulva or Muv mutants (*lin-15AB(n765)*), all six cells adopt vulval fates, and ectopic vulval tissue can be observed on the ventral side of the animal. The extra vulval tissue is indicated with yellow arrows. The fates that the Pn.p cells adopted during the third larval stage are shown above each picture. Blue denotes the cells that in the wild-type animal adopt non-vulval cell fates. The yellow denotes the cells that in the wild-type animal adopt vulval fates.

Figure 2.

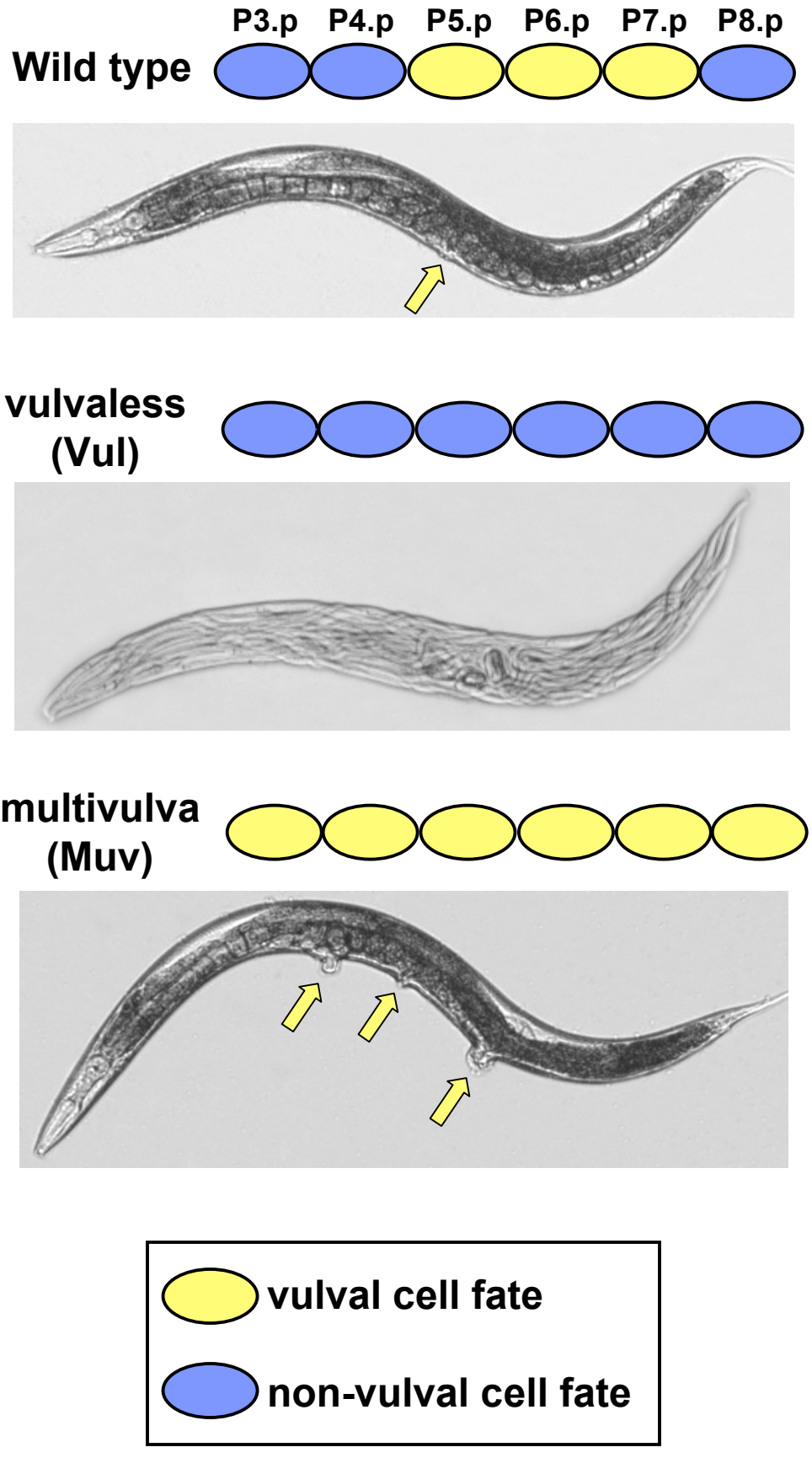
P3.p
P4.p
P5.p
P6.p
P7.p
P8.p
Wild type
vulvaless
(Vul)
multivulva
(Muv)
vulval cell fate
non-vulval cell fate

Figure 3. The synthetic multivulva genes act redundantly to inhibit vulval cell fates

A micrograph of a *lin-53(n833); lin-15A(n767)* synMuv mutant is shown on top. The yellow arrows indicate the ventral protrusions of ectopic vulval tissue. Below are two genetic pathways that inhibit vulval cell fates composed of the class A and class B synMuv genes.

Figure 3.

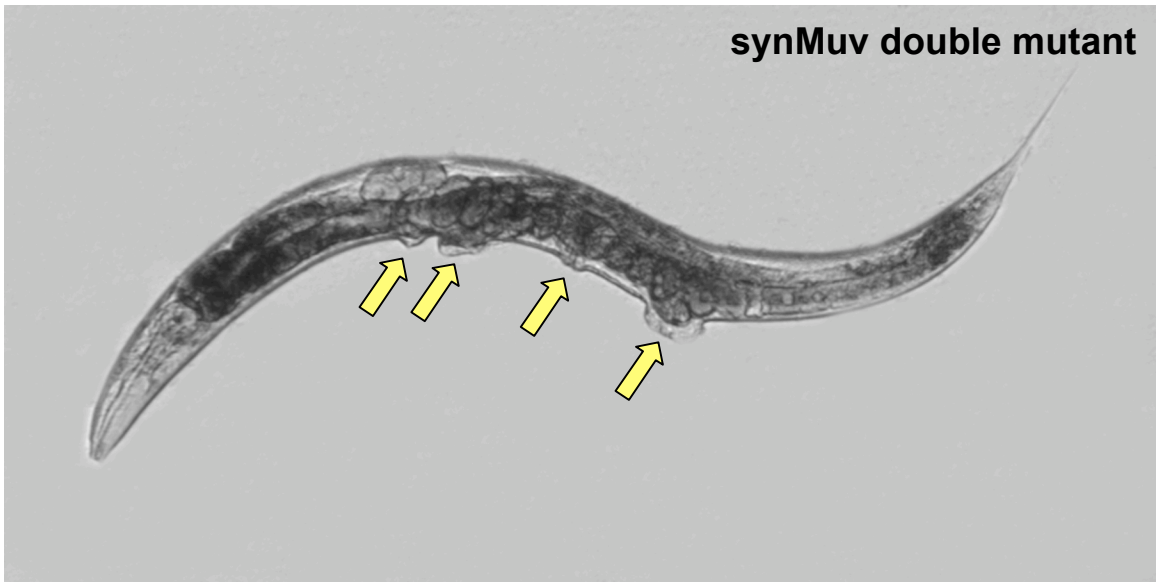

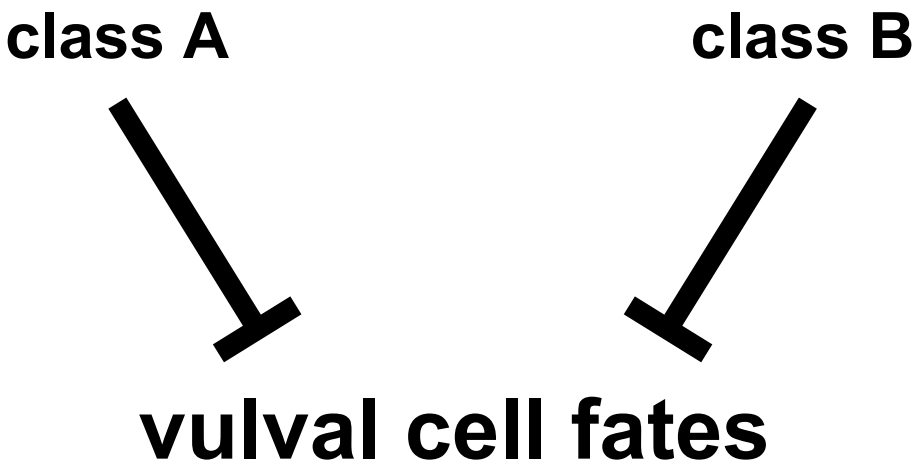

Figure 4. The synthetic multivulva proteins might form as many as three distinct chromatin-remodeling complexes

A model of the actions of some synMuv protein complexes is shown. The NuRD-like complex (colored orange) might deacetylate histones in the promoters of vulval genes to repress transcription. The DRM complex (colored green) might repress transcription through chromatin remodeling. LIN-53 is colored orange and green because it is thought to act in both the NuRD-like complex and the DRM complex. The NuA4-like complex (colored purple) could acetylate histones in the promoters of vulval genes to cause transcriptional repression.

Figure 4.

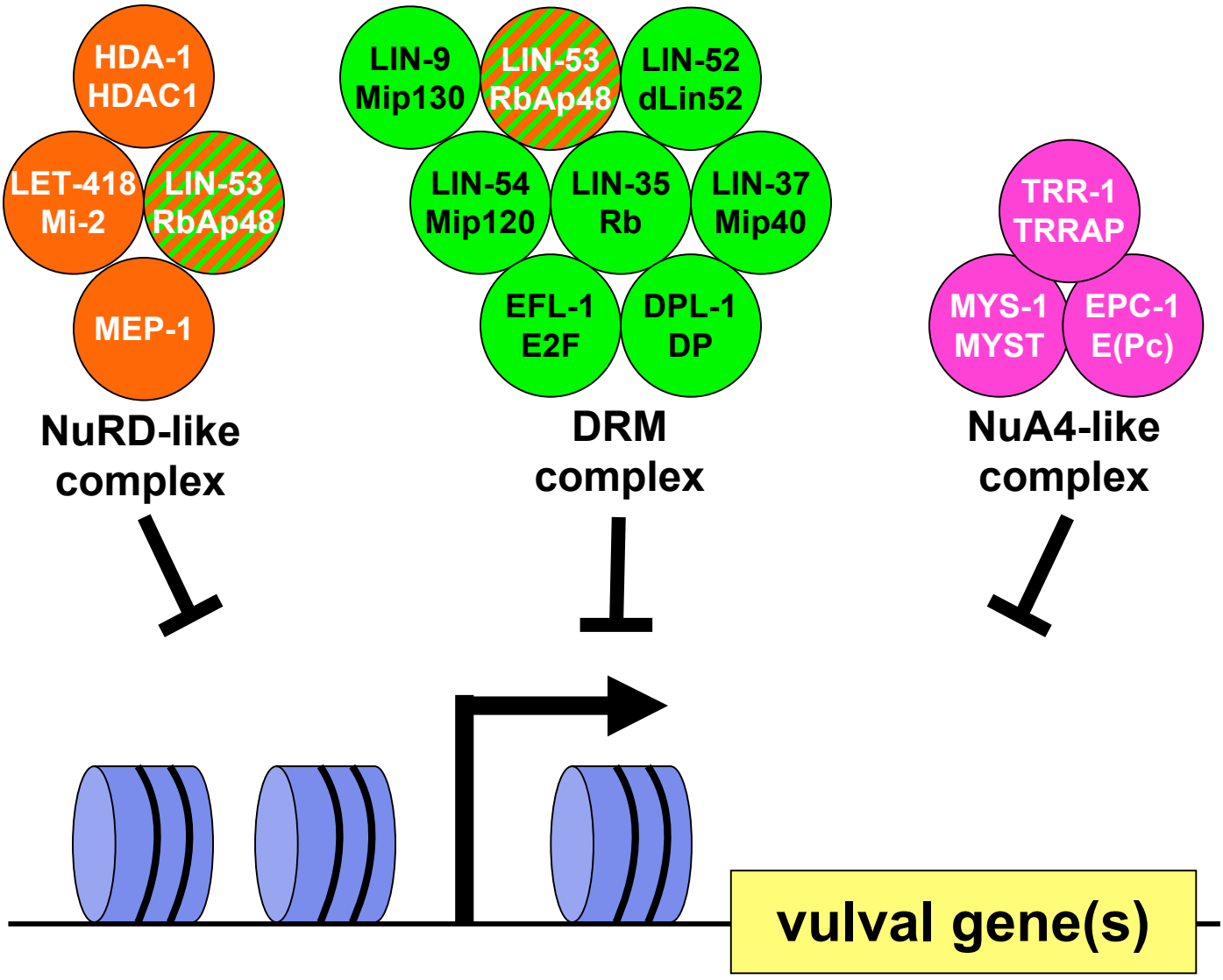
HDA-1
HDAC1
LET-418
Mi-2
LIN-53
RbAp48
MEP-1
NuRD-like
complex
LIN-9
Mip130
LIN-53
RbAp48
LIN-52
dLin52
LIN-54
Mip120
LIN-35
Rb
LIN-37
Mip40
EFL-1
E2F
DPL-1
DP
DRM
complex
TRR-1
TRRAP
MYS-1
MYST
EPC-1
E(Pc)
NuA4-like
complex
vulval gene(s)

CHAPTER TWO

The *C. elegans* Set2 and SETDB1 histone methyltransferases independently repress *lin-3* EGF transcription

Erik C. Andersen and H. Robert Horvitz

This chapter was edited and published as Andersen and Horvitz (2007) Development 134(16) 2991-2999.

SUMMARY

Studies of *Schizosaccharomyces pombe* and mammalian cells revealed a series of histone modifications that results in transcriptional repression. Lysine 9 of histone H3 (H3K9) is deacetylated by the NuRD complex, methylated by a histone methyltransferase (HMT) and then bound by a chromodomain-containing protein, such as heterochromatin protein 1 (HP1), leading to transcriptional repression. A *Caenorhabditis elegans* NuRD-like complex and HP1 homologs regulate vulval development, but no HMT is known to act in this process. We surveyed all 38 putative HMT genes in *C. elegans* and identified *met-1* and *met-2* as negative regulators of vulval cell-fate specification. *met-1* is homologous to *Saccharomyces cerevisiae* Set2, an H3K36 HMT that prevents the reinitiation of transcription. *met-2* is homologous to human SETDB1, an H3K9 HMT that represses transcription. *met-1* and *met-2* (1) are each required for the normal trimethylation of both H3K9 and H3K36, (2) act redundantly with each other as well as with the *C. elegans* HP1 homologs and (3) repress transcription of the gene *lin-3* EGF, which encodes the signal that induces vulval development. We propose that as in yeast MET-1 prevents the reinitiation of transcription. However, our results suggest that in the inhibition of vulval development homologs of SETDB1, HP1 and the NuRD complex also prevent ectopic transcriptional initiation.

INTRODUCTION

The diversity of cell types in an organism is generated by cell-fate decisions made throughout development. Cell-signaling cascades, such as the receptor tyrosine kinase (RTK)/Ras, Notch and Wnt pathways, direct many of these cell-fate decisions. Each of these pathways regulates the activity of one or more transcription factors, which in turn regulate the transcription of genes that determine cell fates (KORSWAGEN 2002; SUNDARAM 2005). Transcription can be controlled through changes in chromatin structure, altering accessibility of the DNA template to the transcriptional machinery (JENUWEIN and ALLIS 2001). Thus, chromatin-remodeling factors can control cell-fate determination through the transcriptional regulation of cell-fate specification genes (FISHER 2002).

The development of the *Caenorhabditis elegans* vulva is an excellent system for the study of cell-fate determination. The vulva is dispensable for viability, and cell-fate defects are easily observed using a dissecting microscope (STERNBERG and HORVITZ 1991). An epidermal growth factor (EGF)-like signal from a neighboring gonadal cell induces three of a set of six equipotent cells (the vulval equivalence group) located on the ventral surface of the animal to form the vulva (SULSTON and HORVITZ 1977; SULSTON and WHITE 1980; KIMBLE 1981; HILL and STERNBERG 1992). This EGF signal is transduced by a conserved RTK/Ras pathway that causes those three cells to divide and generate the 22 descendants of the vulva (KORNFELD 1997). Mutations that reduce or eliminate the activity of the RTK/Ras pathway can result in a vulvaless (Vul) animal in which no cells of the vulval equivalence group express vulval fates; by contrast, mutations that increase the activity of this pathway can cause ectopic adoption of vulval cell fates by the other cells of the vulval equivalence group and result in a multivulva (Muv) animal (BEITEL *et al.* 1990; HAN and STERNBERG 1990). The RTK/Ras pathway terminates in the control of at least two transcription factors, LIN-1 and LIN-31 (BEITEL *et al.* 1995; TAN *et al.* 1998), which regulate the transcription of an unknown set of genes to control the expression of the vulval cell fate.

The vulval cell-fate decision is antagonized by the actions of the synthetic multivulva (synMuv) genes. These genes have been grouped into three classes: A, B and C. Animals defective in genes in any two classes have a Muv phenotype, whereas animals defective in genes from a single class are not Muv (FERGUSON and HORVITZ 1989; CEOL and HORVITZ 2004). Many synMuv genes encode homologs of chromatin-remodeling proteins and transcriptional repressors. A subset of the class B synMuv proteins are homologs of a conserved transcriptional repression cascade, including LIN-35 Rb (LU and HORVITZ 1998), the NuRD-like complex HDA-1 HDAC1, LET-418 Mi2, LIN-53 RbAp48 (VON ZELEWSKY *et al.* 2000; UNHAVAITHAYA *et al.* 2002) and HPL-2 Heterochromatin Protein 1 (HP1) (COUTEAU *et al.* 2002). In mammalian cells, the activity of this transcriptional repression cascade is initiated by the recruitment of the NuRD complex by Rb to target genes (BREHM *et al.* 1998; BREHM *et al.* 1999). Subsequent deacetylation of histone H3 lysine 9 (H3K9) by a histone deacetylase, methylation of H3K9 by a histone methyltransferase (HMT) and binding of the chromodomain-containing protein HP1 creates a region of repressive chromatin that inhibits transcription (NAKAYAMA *et al.* 2001; AYYANATHAN *et al.* 2003). Of this transcriptional repression cascade, only a gene predicted to encode an HMT is not represented within the cloned synMuv genes.

All lysine-specific histone-tail HMTs contain a SET domain, which is the enzymatic core of these proteins (KOUZARIDES 2002; PIRROTTA 2006; SHILATIFARD 2006). On the histone H3 N-terminal tail, four lysine residues can be methylated: K4, K9, K27 and K36. The methylation of histone H3 lysines K4 and K36 is generally associated with actively transcribed genes, although H3K36 methylation functions in repression to prevent transcriptional initiation downstream of the promoter (KROGAN *et al.* 2003; CARROZZA *et al.* 2005). The methylation of histone H3 lysines K9 and K27 is generally associated with repressed transcription. The cysteine-rich domains flanking the SET domain determine the specificity of the HMT. HMTs with a SET domain flanked by PreSET and PostSET domains methylate H3K9. HMTs with a SET domain

flanked by AWS and PostSET domains methylate H3K36. HMTs with only a PostSET domain flanking the SET domain methylate H3K4. Enzymes that methylate H3K27 do not have cysteine-rich domains flanking the SET domain. The methylated histone-tail lysines and other modifications have been proposed to regulate the transcription of nearby genes (JENUWEIN and ALLIS 2001).

To identify HMTs that act in vulval development, we used deletion alleles and RNAi to examine the loss-of-function phenotypes of all 38 *C. elegans* genes predicted to encode lysine-specific histone-tail HMTs. We discovered that two HMT genes, which we named *met-1* and *met-2*, caused a synMuv phenotype when inactivated in a class A synMuv mutant background. MET-1 is homologous to *S. cerevisiae* Set2, a histone H3 lysine 36 (H3K36) HMT, and MET-2 is homologous to mammalian SETDB1, an H3K9 HMT. We determined that these two putative HMTs act redundantly with each other and with the presumptive downstream HP1 homologs during vulval development. Additionally, we found that transcription of the synMuv target gene *lin-3* EGF is increased in *met-1*, *met-2* and *hpl-2* mutants. Our results suggest that in *C. elegans* the trimethylation of histone H3 lysine 36 by MET-1 Set2 promotes a transcriptional repression cascade mediated by a NuRD-like complex and by the trimethylation of histone H3K9 by a SETDB1-like HMT. This cascade leads to the recruitment of HP1 and the inhibition of ectopic *lin-3* transcription during vulval development. This model suggests that, in addition to an H3K36 HMT like MET-1, the NuRD complex, SETDB1 and HP1 inhibit the ectopic initiation of transcription downstream of the promoter in humans.

MATERIALS AND METHODS

Strains and genetics

C. elegans was grown as described by Brenner (1974) and maintained at 20ºC unless otherwise noted. N2 was the wild-type strain. The mutations and integrants used were: LGI: *met-1(n4337)* (this study), *lin-35(n745)*, LGII: *lin-8(n2731)* (DAVISON *et al.* 2005), *dpl-1(n2994)* (CEOL and HORVITZ 2001), *lin-38(n751)*, *trr-1(n3712)* (CEOL and HORVITZ 2004), *lin-56(n2728)* (THOMAS *et al.* 2003); LGIII: *lin-37(n4903)* (ANDERSEN *et al.* 2006), *met-2(n4256)* (this study); LGV: *mys-1(n3681)* (CEOL and HORVITZ 2004) LGX: *hpl-1(n4317)* (this study), *lin-15A(n433*, *n767)*, *lin-15B(n744)*, *lin-15AB(n765)*.

Information about *tm* (kindly provided by S. Mitani), *gk* and *ok* alleles can be found at www.wormbase.org. Information about all *n* deletion alleles generated in this study (Table 1) is presented in Table S1. The following balancer chromosomes were used: *hT2 [qIs48]* LGI; LGIII, *nT1 [qIs51]* LGIV; LGV, *mIn1 [mIs14]* and *qC1 [nIs189]*. Mutant alleles for which no citation is given are described by Riddle (1997).

Determination of gene structures and generation of cDNA constructs

For *met-1*, the sequences of the cDNA clones yk27f9, yk152a5, yk154f7, yk1128b1 and yk1327b12 were determined. 5' rapid amplification of cDNA ends (5' RACE, Invitrogen) was used to determine the 5' end of *met-1*, and an SL1 splice-leader sequence was identified. Clones yk1128b1 and yk1327b12 were generated from a PCR product that inappropriately terminated in a 3' A-rich sequence. Both clones contained a transcriptional start different from that identified in the 5' RACE experiments (data not shown). The 5' RACE products did not contain exon six, indicating that there are two alternatively spliced *met-1* transcripts. Using yeast-mediated ligation (OLDENBURG *et al.* 1997), yk27f9 and the 5' RACE product were combined to make a presumptive full-length *met-1* clone (pEA130), which was transferred to the Gateway system (Invitrogen). For

met-2, the sequences of three independent cDNA clones, yk6f10, yk29g5 and yk249d10, were determined. 5' RACE identified the same 5' sequence as found in the cDNA clones. Using yeast-mediated ligation, yk249d10 and the 5' RACE product were combined to make a presumptive full-length *met-2* clone (pEA109), which was transferred to the Gateway system. Quickchange (Stratagene) was used to create the clones pEA181 (*met-1*) and pEA110 (*met-2*), which contain two SET-domain mutations that abolish the HMT activities of homologous enzymes: RFVNHSC to GFVNHSA.

Quantitative western blot analysis

Protein samples were prepared from embryonic extracts as described by Harrison *et al.* (2006). The linear range of reactivity for the antisera used in these studies was determined using wild-type extracts with total protein concentrations from 6.25 μg/μl to 50 μg/μl. 12.5 μg of total protein was loaded in quadruplicate for each strain tested using quantitative western blots. Levels of histone H3 antibody reactivity (1:1000, Abcam) were normalized to levels of both tubulin (1:1000, DM1A, Sigma) and histone H2A (1:500, Abcam) using fluorescent secondary antibodies (1:500, Cy3 and Cy5, Jackson ImmunoResearch Inc.) and a Typhoon Imaging System (GE Healthcare Life Sciences). For each assay, the levels of histone H3 trimethylation were normalized to the levels of total histone H3. The levels of histone H3 lysine 4 trimethylation (H3K4tri, 1:5000, Abcam), H3K9tri (1:1000, Upstate), H3K27tri (1:3000, Upstate) and H3K36tri (1:2000, Abcam) were determined. The data shown are representative of data from at least two independent embryonic protein preparations.

Quantitative PCR assays

Synchronized wild-type and mutant animals were grown, and larvae were harvested at or near the L2-to-L3 larval transition, when vulval induction occurs. Total RNA was extracted using Trizol (Invitrogen). First-strand cDNA was prepared from 1 μg total RNA using the SuperScript III First-strand Synthesis

Supermix for qRT-PCR (Invitrogen). Each real-time reverse transcriptase (RT)-PCR mix contained 10 ng of RT products, 25 μL of 2X SyBR Green PCR Master Mix (Applied Biosystems) and 0.4 μM of each primer. The real-time PCR was performed in triplicate on a DNA Engine Opticon System (BioRad). Three independent samples of each genotype were prepared, and levels of *lin-3* and *rpl-26* were quantified from each biological replicate. The ΔC_T values for *lin-3* were determined using *rpl-26* as the internal reference, and the $\Delta\Delta C_T$ values were calculated for each genotype compared to the wild type (as described in the Applied Biosystems real-time PCR manual). All changes were normalized to the wild type. The error shown are the ranges of relative *lin-3*/*rpl-26* ratios for three trials determined from the standard deviation of the $\Delta\Delta C_T$ values.

RESULTS

A survey of all 38 *C. elegans* putative HMT genes identified three genes required for viability

To characterize the *in vivo* roles of the HMT genes, we generated or collected loss-of-function mutations for 29 of the 38 predicted *C. elegans* genes encoding proteins with SET domains and inactivated each of the remaining nine genes by RNAi. We found that loss of function of only six of the 38 HMT genes caused obvious abnormalities (Table 1). It was known previously that mutations in *mes-2* and *mes-4* cause maternal-effect sterility (HOLDEMAN *et al.* 1998; FONG *et al.* 2002), and that RNAi of *set-1* causes embryonic lethality (TERRANOVA *et al.* 2002). We found that null mutations in *lin-59, set-16* and *set-23* caused lethality. LIN-59 is required for hindgut development and is similar to *Drosophila* ASH1 (CHAMBERLIN and THOMAS 2000), a histone H3 lysine 4 (H3K4) HMT. ASH1 is a Trithorax gene that opposes Polycomb group genes in the transcriptional regulation of Hox genes (KLYMENKO and MULLER 2004). SET-16 is homologous to human MLL3, which is mutated in mixed-lineage leukemias (RUAULT *et al.* 2002) and is associated with H3K4 methylation (LEE *et al.* 2006). *set-23* is homologous to the ancestral gene into which a mariner transposon inserted in primates. This ancestral gene encodes a SET-domain protein (CORDAUX *et al.* 2006), and the primate gene is named SETMAR for the SET-mariner fusion (ROBERTSON and ZUMPANO 1997).

Four HMT genes regulate vulval cell-fate specification

We also investigated possibly more subtle roles for the HMT genes during vulval development. We constructed multiple mutants carrying HMT deletions and loss-of-function mutations in the class A synMuv gene *lin-15A*, the class B synMuv gene *lin-15B* or both. For the nine genes without deletion alleles, we used RNAi to inactivate them, as above (Table 1). Because the synMuv phenotype is

temperature-sensitive (FERGUSON and HORVITZ 1989), we also scored the vulval phenotypes of our mutant strains at 25ºC (Table S1).

This survey identified two synMuv genes, which we named *met-1* and *met-2* (*met* = histone methyltransferase-like, Table 1). Previously, *met-2* but not *met-1* was identified as a class B synMuv gene in a whole-genome RNAi feeding screen (POULIN *et al.* 2005). We found that a role for *met-1* in vulval development can be observed using RNAi by injection (data not shown) or in a deletion mutant but not using RNAi by feeding. Additionally, we identified two genes that when inactivated suppressed the synMuv phenotype, *mes-2* and *mes-4* (Table 1). Subsequently, *mes-2*, *mes-3*, *mes-4* and *mes-6* were reported to be suppressors of the synMuv phenotype (Table S2 and CUI *et al.* 2006b).

met-1 Set2 and *met-2* SETDB1 are synMuv genes

Deletion mutations of *met-1* or *met-2* caused no vulval abnormalities (Table 2). A synMuv phenotype resulted when each deletion was combined with a loss-of-function mutation of each class A gene. Loss of *met-2* function caused a more severe synMuv phenotype than did loss of *met-1* in combination with null mutations in each of the class A genes, indicating that *met-2* might more strongly inhibit the vulval cell-fate decision. Double mutants of a *met-1* or *met-2* mutation and one of several class B mutations did not have a synMuv phenotype. A *met-2* deletion but not a *met-1* deletion enhanced the incompletely penetrant Muv phenotype of the class C synMuv mutant *trr-1(n3712)* and caused a synMuv phenotype with the class C synMuv mutation *mys-1(n3681)*. Because it is synMuv in combination with mutations in both class A and C genes, *met-2* is a class B synMuv gene. Unlike the class C genes, the *met-1* deletion did not cause a synMuv phenotype in combination with class B synMuv mutations. Because a *met-1* mutation did not cause a synMuv phenotype with class B or class C mutations but did cause a synMuv phenotype with class A mutations, *met-1* might define a novel class of synMuv gene.

Using database searches, we determined that MET-1 is similar to yeast Set2 and human HYPB, both of which are H3K36 HMTs (STRAHL *et al.* 2002; SUN *et al.* 2005). Set2 prevents spurious transcription from genes that are actively being transcribed (CARROZZA *et al.* 2005; KEOGH *et al.* 2005). Specifically, Set2 prevents transcription from initiating downstream of the promoter region by recruiting the Rpd3S histone deacetylase (HDAC) complex through interaction of trimethylated H3K36 with the chromodomain-containing protein Eaf3 (JOSHI and STRUHL 2005). The Rpd3S complex removes acetyl groups from histone H3K9, thereby preventing transcription. Set2 is recruited to actively transcribed genes by interaction with the carboxyl-terminal domain (CTD) of RNA polymerase II phosphorylated on serine five (LI *et al.* 2002; KROGAN *et al.* 2003; LI *et al.* 2003; XIAO *et al.* 2003). HYPB and MET-1 are similar throughout their lengths (27% identity), especially in the AWS, SET and PostSET domains (46% identity, Figure 1).

MET-2 is similar to human SETDB1, which is an H3K9 methyltransferase that plays a role in euchromatic transcriptional repression and the formation of heterochromatin (SCHULTZ *et al.* 2002). MET-2 and SETDB1 share homology throughout the length of each protein (19% identity) but are most similar in the SET, PreSET and PostSET domains (Figure 1, 50% identity) . Like SETDB1, MET-2 has a methyl-DNA binding domain (MBD). The methylation of DNA has not been observed in *C. elegans* (SIMPSON *et al.* 1986), so this domain might be unimportant for MET-2 function or might function differently.

met-1 and *met-2* might act redundantly to inhibit vulval cell fates through the trimethylation of the N-terminal tail of histone H3

We observed that a *met-1; met-2* double mutant had an incompletely penetrant synMuv phenotype (Table 3). The *met-1; met-2* synMuv phenotype is recapitulated by RNAi of either *met* gene combined with a deletion of the other, indicating that this synMuv phenotype was caused specifically by loss of *met-1* and *met-2* gene function and by not a linked mutation. Additionally, we found that

the HMT genes most similar to *met-1* and *met-2* (*set-12* and *set-11*, respectively) did not act redundantly with either *met* gene during vulval development (Table S3). Thus, not all predicted H3K9 and H3K36 HMT genes act redundantly with *met-1* or *met-2*. Additionally, the *met-1; met-2* double mutant displayed a mortal germline (Mrt) phenotype (AHMED and HODGKIN 2000) in which the strain became sterile after 3-11 generations (Figure S3). By contrast, *met-2* mutants were Mrt after 18-28 generations and *met-1* mutants were not Mrt (data not shown). We conclude that *met-1* and *met-2* act partially redundantly in the inhibition of vulval cell fates and in promoting the immortality of the germline.

The class B synMuv defects of *met-1* or *met-2* mutants could be rescued by expressing *met-1* or *met-2*, respectively, under the control of the *dpy-7* promoter (see Supplemental Materials and Methods for details), which is expressed in the hypodermal tissue that neighbors the vulval cells. Specifically, in eight independent lines expression of *met-1* reduced the penetrance of the *met-1(n4337); lin-15A(n767)* synMuv phenotype from 81% to 2, 6, 14, 14, 15, 15, 32 and 34%, and in seven independent lines expression of *met-2* reduced the penetrance of the *met-2(n4256); lin-15A(n433)* synMuv phenotype from 94% to 0, 0, 0, 3, 3, 6 and 9%. The addition of two missense mutations known to abolish enzymatic function of homologous HMTs (REA *et al.* 2000; LANDRY *et al.* 2003) reduced this phenotypic rescue of either *met-1* or *met-2*. Specifically, in seven independent lines expression of such a *met-1* SET mutant gene caused a synMuv phenotype that was 44, 50, 51, 52, 54, 60 and 70% penetrant, and in eight independent lines expression of such a *met-2* SET mutant gene caused a synMuv phenotype that was 91, 91, 93, 94, 95, 97, 98 and 100% penetrant. Therefore, the methylation activity of the SET domain is necessary for most of the functions of *met-1* and *met-2* during vulval development. The rescue of the *met-1; lin-15A* synMuv phenotype was not disrupted completely by the SET-domain mutations, suggesting that *met-1* might have other functions in addition to histone methylation. Our results indicate that histone methylation mediated by the SET domains of MET-1 and MET-2 regulates vulval development.

Using quantitative western blots, we tested which residues on the histone H3 tail are methylated in the wild type and in *met-1* and *met-2* mutants. MET-1 is predicted to methylate histone H3K36 based on its homology to yeast Set2, and MET-2 is predicted to methylate histone H3K9 based on its homology to mammalian SETDB1. We probed embryonic protein extracts for levels of histone H3 lysine trimethylation (Figure 2), because HP1 has been shown to bind more strongly to trimethylated than to dimethylated or monomethylated histone tails (BANNISTER *et al.* 2001; NIELSEN *et al.* 2002). Our results suggest that levels of H3K4 and H3K27 trimethylation were not significantly different from those in the wild type. However, *met-1* embryos showed a striking defect in histone H3K36 trimethylation and a roughly 50% decrease in histone H3K9 trimethylation. *met-2* mutants showed a defect in H3K9 trimethylation and a roughly 40% decrease in H3K36 trimethylation. We conclude that consistent with their homologies MET-1 likely trimethylates H3K36, and MET-2 likely trimethylates H3K9. Because of the synthetic sterility of the *met-1; met-2* double mutant (Table S3), we were unable to collect sufficient quantities of histones to measure the levels of lysine trimethylation in the double mutant.

met-1 and *met-2* act redundantly with the *C. elegans* HP1 homologs in vulval cell-fate determination

Because the trimethylation of lysines on histone H3 tails creates binding sites for HP1, we investigated the role of the two *C. elegans* HP1 homologs HPL-1 and HPL-2 in vulval cell-fate specification. The *C. elegans* HP1 homolog *hpl-2* has been reported to be a class B synMuv gene (COUTEAU *et al.* 2002). We found that although an *hpl-2* single mutant did not have a Muv phenotype at 20ºC (Table 4), at 25ºC it had a 99% penetrant Muv phenotype (Table S4). At 20ºC, a presumptive null allele of *hpl-2* caused a class B synMuv phenotype with null or strong mutations of each of the class A synMuv genes (Table S4). By contrast, an *hpl-1* deletion did not cause a synMuv phenotype when combined with class A or B mutations nor did it enhance a synMuv double mutant phenotype. At 20ºC,

hpl-2; hpl-1 double mutants had a 24% penetrant synMuv phenotype (Table 4), showing that *hpl-1* and *hpl-2* act redundantly during vulval development (SCHOTT *et al.* 2006).

If *met-1* or *met-2* act in the same pathway as the *C. elegans* HP1 homologs, then one would not expect mutations in the *hpl* and *met* genes to enhance the synMuv phenotypes of other *hpl* or *met* mutants when combined in multiple mutants. However, null mutations in *met-1* or *met-2* enhanced the Muv phenotype of *hpl-2* (Table 4). Triple mutants in which the *met-1; met-2* double mutant was combined with either *hpl-1* or *hpl-2* had a more severe phenotype than each of the *met hpl*, *met-1; met-2* or *hpl-2; hpl-1* double mutant combinations. Triple mutants in which the *hpl-2; hpl-1* double mutant was combined with either *met-1* or *met-2* had a more severe phenotype than each *met hpl, met* or *hpl* double mutant combination. The quadruple mutant *met-1; met-2 hpl-2; hpl-1* had a more severe synMuv phenotype than any double or triple mutant combination. The synMuv phenotype of the quadruple mutant was completely penetrant when derived from the *met-2 hpl-2* heterozygote, unlike the triple mutant synMuv phenotypes, which were maternally rescued (Table 4 and data not shown).

We conclude that the *C. elegans* MET-1 and MET-2 HMTs and the proteins thought to be recruited to the methylated residues created by these HMTs can act independently to inhibit the adoption of ectopic vulval cell fates.

met-1, met-2 and *hpl-2* regulate the transcriptional repression of the synMuv target gene *lin-3* EGF

Recently, it was reported that some synMuv proteins repress the transcription of the gene *lin-3* in the hypodermis surrounding the vulval cells (CUI *et al.* 2006a). *lin-3* EGF is normally expressed in the gonadal anchor cell, and LIN-3 activates the RTK/Ras pathway in the cells of the vulval equivalence group closest to the anchor cell to cause these cells to adopt vulval cell fates (HILL and STERNBERG 1992; KORNFELD 1997). Cui *et al.* (2006a) proposed that the synMuv mutants

cause ectopic vulval induction because increased levels of *lin-3* EGF in the neighboring hypodermis drives the induction of the three remaining cells of the vulval equivalence group to become vulval cells. Single class A or class B mutants do not have significantly increased levels of *lin-3*, whereas class AB double mutants have greater levels than does the wild type or either single synMuv mutant (Cui *et al.* 2006a).

We quantified *lin-3* expression from *met-1*, *met-2* and *hpl-2* synMuv mutants (*hpl-1* mutants are not synMuv) during the time of vulval induction (Figure 3). *met-1* and *met-2* single mutants did not have increased levels of *lin-3*. However, *met-1*, *met-2* or *hpl-2* mutations combined with the synMuv class A mutation *lin-15A(n767)* showed increased levels of *lin-3* as compared to that in the wild type. The *met-1; met-2* double mutant had slightly higher levels of *lin-3* than the wild type. *lin-3* expression was lower in the *met-1; met-2* double mutant than in the *met* double mutants with *lin-15A*. This result might reflect the less penetrant Muv phenotype of *met-1; met-2* animals (Table 2). Alternatively, the *met-1; met-2* double mutant Muv phenotype might not be caused by an increase in *lin-3* expression.

In short, the vulval HMT genes *met-1* and *met-2* as well as the HP1 gene *hpl-2* control the transcriptional repression of the synMuv target gene *lin-3* redundantly with the class A synMuv genes, and mutations of each of these genes can cause increased levels of *lin-3* transcription. That MET-1, MET-2 and HPL-2 are homologous to transcriptional repressors suggests that these proteins control *lin-3* levels by acting directly as transcriptional repressors of *lin-3*.

DISCUSSION

The class B synMuv genes *met-1* Set2 and *met-2* SETDB1 regulate both H3K9 and H3K36 trimethylation

Whereas *met-1* and *met-2* single mutants are normal in vulval development, *met-1; met-2* double mutants have an incompletely penetrant Muv phenotype, indicating that these two genes act redundantly to inhibit the adoption of vulval cell fates. Because both *met-1* and *met-2* encode presumptive HMTs and because an active HMT enzymatic domain is required for the function of each, *met-1* and *met-2* might function similarly *in vivo*. Furthermore, *met-1* and *met-2* mutants are both defective in both H3K9 and H3K36 trimethylation. These observations are all consistent with the hypothesis that *met-1* and *met-2* control functionally redundant activities. We discuss below several hypotheses that could explain the redundancy observed between *met-1* and *met-2*.

First, MET-1 and MET-2 might each methylate both H3K9 and H3K36. However, MET-1 Set2 and MET-2 SETDB1 are homologous to an H3K36 HMT and an H3K9 HMT, respectively. One simple model is that MET-1 methylates primarily H3K36 but also methylates H3K9, and MET-2 methylates primarily H3K9 but also methylates H3K36. In the absence of either MET-1 or MET-2 function, the activity of the other results in a sufficient level of methylation for some biological function. Thus, neither single mutant has a Muv phenotype. However, *in vitro* studies of Set2 and SETDB1 have not shown such dual specificity (SCHULTZ *et al.* 2002; STRAHL *et al.* 2002), suggesting either that the *in vitro* results do not recapitulate the functions of these proteins *in vivo*, that MET-1 and MET-2 function differently than their homologs or that this simple model is incorrect.

Second, the transcriptional repression of vulval target genes could depend on the concerted actions of MET-1 and MET-2 to methylate H3K9 and H3K36. For example in *met-1* mutants, H3K36 trimethylation is strongly reduced. The

trimethylation of H3K9 also could be impaired because the H3K9-HMT activity of MET-2 is dependent on the methylation of H3K36 by MET-1. The reciprocal methylation activity of MET-1 might also require the H3K9 activity of MET-2. Although partially deficient in both H3K9 and H3K36 methylation, the single mutants might not show a Muv phenotype because their levels of methylation are sufficient for wild-type vulval development. Methylation of H3K36 has been associated with transcriptional repression in mammalian cells (STRAHL *et al.* 2002), and the possible dependence of this repression on H3K9 methylation has not been investigated.

Third, the redundancy between *met-1* and *met-2* could be caused solely by defects in the level of either H3K9 or H3K36 trimethylation. One possibility is that the level of H3K9 trimethylation is the major methylation event for inhibiting the vulval cell fate, with MET-2 primarily methylating H3K9 and MET-1 indirectly providing some H3K9 trimethylation by promoting the expression of another H3K9-specific HMT. In support of this hypothesis, the severity of the *met-1* or *met-2* class B synMuv defect is more closely correlated with the level of H3K9 trimethylation than with the level of H3K36 trimethylation (Table 2 and Figure 2). Thus, the redundancy between *met-1* and *met-2* might be caused by a reduction in H3K9 trimethylation below the threshold needed to prevent ectopic vulval development. In *met-1* or *met-2* single mutants, there would still be sufficient H3K9 trimethylation to repress *lin-3* expression in the hypodermis, so wild-type vulval development would occur. In the *met-1; met-2* double mutant, H3K9 trimethylation would drop below the threshold needed to repress *lin-3* transcription, and a synMuv phenotype would result.

The *C. elegans* HP1 homologs can act independently of histone methylation mediated by MET-1 and MET-2

Because HP1 is an effecter of methylation-dependent transcriptional repression (HEDIGER and GASSER 2006), we expected the HP1 homologs to act downstream of either or both of the *met* genes. However, we found that the *met* genes could

act redundantly with the *hpl* genes. Perhaps the *C. elegans* HP1 proteins act at sites other than the methylated histone tails generated by MET-1 and MET-2. One observation indicates that HP1 proteins might act independently of histone methylation: in *Drosophila*, HP1 can bind naked DNA and nucleosomal DNA with histones without N-terminal tails *in vitro* (ZHAO *et al.* 2000).

Alternatively, the functional redundancy between the *met* and *hpl* genes during vulval cell-fate determination could be caused an incomplete loss of HMT or HP1-like gene functions. For example in the *met-1; met-2* double mutant, a third HMT could provide some histone methylation important for the localization of the HPL proteins. Besides *met-1* and *met-2*, one or more of the other 36 HMT genes could have subtle roles not detected in our assays. For example, we note that we could not assess the roles of the four HMT genes required for viability in vulval development. Furthermore, there are 20 genes in *C. elegans* that encode proteins with at least one chromodomain (E.C. Andersen and H.R. Horvitz, unpublished results). Other chromodomain-encoding genes could function redundantly with the *hpl* genes in vulval cell-fate determination.

H3K9 deacetylation by a NuRD-like complex, trimethylation by MET-2 SETDB1 and HP1 binding might act with H3K36 trimethylation to prevent ectopic initiation of *lin-3* EGF transcription

In *S. cerevisiae*, Set2 is localized to actively transcribed genes and methylates H3K36 through interactions with RNA polymerase II (LI *et al.* 2002; KROGAN *et al.* 2003; LI *et al.* 2003; XIAO *et al.* 2003). Methylated H3K36 is bound by Eaf3 (JOSHI and STRUHL 2005) and subsequently recruits an HDAC complex to prevent inappropriate transcriptional initiation downstream of the promoter (CARROZZA *et al.* 2005; KEOGH *et al.* 2005). Eaf3 is a part of the NuA4 complex, which through a distinct mechanism also prevents ectopic transcriptional initiation (MORILLON *et al.* 2005).

This mechanism of inhibiting inappropriate transcriptional initiation might be identical to that controlling *lin-3* expression during vulval development. In

addition, our data indicate that other processes are also involved, including H3K9 trimethylation, the binding of a NuRD-like complex and HP1-like proteins. Specifically, we propose that MET-1 inhibits transcriptional initiation downstream of the *lin-3* promoter, acting much as Set2 does in *S. cerevisiae.* H3K36 methylated by MET-1 is bound by the *C. elegans* NuRD-like complex, which contains the chromodomain-containing LET-418 Mi-2 subunit and the HDA-1 histone deacetylase subunit (VON ZELEWSKY *et al.* 2000; UNHAVAITHAYA *et al.* 2002). Subsequently, the NuRD-like complex deacetylates histone H3K9, and MET-2 SETDB1 methylates H3K9, thereby creating a site for HPL-1 and HPL-2 to bind and prevent the inappropriate initiation of *lin-3* EGF transcription. The methylation of H3K36 might also recruit the *C. elegans* NuA4-like complex, which contains class C synMuv proteins (CEOL *et al.* 2006), to inhibit inappropriate transcriptional initiation of *lin-3*. Consistent with this model, H3K9 trimethylation and HP1gamma recently have been found to be enriched in actively transcribed genes in mammalian cells (VAKOC *et al.* 2005).

An unidentified human HMT mediates H3K9 trimethylation in the inhibition of ectopic transcriptional initiation (VAKOC *et al.* 2005). We propose that this HMT is the MET-2 homolog SETDB1. Additionally, human homologs of the *C. elegans* NURF-like complex act oppositely to the synMuv proteins and promote vulval fates (ANDERSEN *et al.* 2006). In mammalian cells, the NURF complex has been shown promote the initiation of transcription (WYSOCKA *et al.* 2006). Perhaps the synMuv suppressor NURF-like complex and the synMuv proteins antagonize each other by oppositely regulating the initiation of *lin-3* transcription during vulval development. Such pathways involving H3K36 trimethylation, NuRD histone deacetylase activity, SETDB1 H3K9 trimethylation and HP1 opposed by a NURF complex might be conserved in other organisms, including humans, and serve as important and general mechanisms for the regulation of transcriptional initiation.

ACKNOWLEDGMENTS

We thank Beth Castor for DNA sequence determinations, Na An for strain management, Andrew Hellman, Shannon McGonagle, Beth Castor and Tove Ljungars for deletion allele screening, and Dan Denning, Megan Gustafson, David Harris, Shunji Nakano, Adam Saffer, and Robyn Tanny for critical reading of this manuscript. Strains were provided by the *Caenorhabditis* Genetics Center, which is supported by the NIH National Center for Research Resources, and by Shohei Mitani of Tokyo Women's Medical University. We thank Yuji Kohara for EST clones. E.C.A. was an Anna Fuller Cancer Research Fellow, and H.R.H. is the David H. Koch Professor of Biology at MIT and an Investigator of the Howard Hughes Medical Institute. This work was supported by NIH grant GM24663.

LITERATURE CITED

AHMED, S., and J. HODGKIN, 2000 MRT-2 checkpoint protein is required for germline immortality and telomere replication in *C. elegans*. Nature **403:** 159-164.

ANDERSEN, E. C., X. LU and H. R. HORVITZ, 2006 *C. elegans* ISWI and NURF301 antagonize an Rb-like pathway in the determination of multiple cell fates. Development **133:** 2695-2704.

AYYANATHAN, K., M. S. LECHNER, P. BELL, G. G. MAUL, D. C. SCHULTZ, Y. YAMADA, K. TANAKA, K. TORIGOE and F. J. RAUSCHER, 3RD, 2003 Regulated recruitment of HP1 to a euchromatic gene induces mitotically heritable, epigenetic gene silencing: a mammalian cell culture model of gene variegation. Genes Dev **17:** 1855-1869.

BANNISTER, A. J., P. ZEGERMAN, J. F. PARTRIDGE, E. A. MISKA, J. O. THOMAS, R. C. ALLSHIRE and T. KOUZARIDES, 2001 Selective recognition of methylated lysine 9 on histone H3 by the HP1 chromo domain. Nature **410:** 120-124.

BEITEL, G. J., S. G. CLARK and H. R. HORVITZ, 1990 *Caenorhabditis elegans* ras gene *let-60* acts as a switch in the pathway of vulval induction. Nature **348:** 503-509.

BEITEL, G. J., S. TUCK, I. GREENWALD and H. R. HORVITZ, 1995 The *Caenorhabditis elegans* gene *lin-1* encodes an ETS-domain protein and defines a branch of the vulval induction pathway. Genes Dev **9:** 3149-3162.

BREHM, A., E. A. MISKA, D. J. MCCANCE, J. L. REID, A. J. BANNISTER and T. KOUZARIDES, 1998 Retinoblastoma protein recruits histone deacetylase to repress transcription. Nature **391:** 597-601.

BREHM, A., S. J. NIELSEN, E. A. MISKA, D. J. MCCANCE, J. L. REID, A. J. BANNISTER and T. KOUZARIDES, 1999 The E7 oncoprotein associates with Mi2 and histone deacetylase activity to promote cell growth. Embo J **18:** 2449-2458.

BRENNER, S., 1974 The genetics of *Caenorhabditis elegans*. Genetics **77:** 71-94.

CARROZZA, M. J., B. LI, L. FLORENS, T. SUGANUMA, S. K. SWANSON, K. K. LEE, W. J. SHIA, S. ANDERSON, J. YATES, M. P. WASHBURN and J. L. WORKMAN, 2005 Histone H3 methylation by Set2 directs deacetylation of coding regions by Rpd3S to suppress spurious intragenic transcription. Cell **123:** 581-592.

CEOL, C. J., and H. R. HORVITZ, 2001 *dpl-1* DP and *efl-1* E2F act with *lin-35* Rb to antagonize Ras signaling in *C. elegans* vulval development. Mol Cell **7:** 461-473.

CEOL, C. J., and H. R. HORVITZ, 2004 A new class of *C. elegans* synMuv genes implicates a Tip60/NuA4-like HAT complex as a negative regulator of Ras signaling. Dev Cell **6:** 563-576.

CEOL, C. J., F. STEGMEIER, M. M. HARRISON and H. R. HORVITZ, 2006 Identification and classification of genes that act antagonistically to *let-60* Ras signaling in *Caenorhabditis elegans* vulval development. Genetics **173:** 709-726.

CHAMBERLIN, H. M., and J. H. THOMAS, 2000 The bromodomain protein LIN-49 and trithorax-related protein LIN-59 affect development and gene expression in *Caenorhabditis elegans*. Development **127:** 713-723.

CORDAUX, R., S. UDIT, M. A. BATZER and C. FESCHOTTE, 2006 Birth of a chimeric primate gene by capture of the transposase gene from a mobile element. Proc Natl Acad Sci U S A **103:** 8101-8106.

COUTEAU, F., F. GUERRY, F. MULLER and F. PALLADINO, 2002 A heterochromatin protein 1 homologue in *Caenorhabditis elegans* acts in germline and vulval development. EMBO Rep **3:** 235-241.

CUI, M., J. CHEN, T. R. MYERS, B. J. HWANG, P. W. STERNBERG, I. GREENWALD and M. HAN, 2006a SynMuv genes redundantly inhibit *lin-3*/EGF expression to prevent inappropriate vulval induction in *C. elegans*. Dev Cell **10:** 667-672.

CUI, M., E. B. KIM and M. HAN, 2006b Diverse chromatin remodeling genes antagonize the Rb-involved SynMuv pathways in *C. elegans*. PLoS Genet **2:** e74.

DAVISON, E. M., M. M. HARRISON, A. J. WALHOUT, M. VIDAL and H. R. HORVITZ, 2005 *lin-8*, which antagonizes *C. elegans* Ras-mediated vulval induction, encodes a novel nuclear protein that interacts with the LIN-35 Rb protein. Genetics.

FERGUSON, E. L., and H. R. HORVITZ, 1989 The multivulva phenotype of certain *Caenorhabditis elegans* mutants results from defects in two functionally redundant pathways. Genetics **123:** 109-121.

FISHER, A. G., 2002 Cellular identity and lineage choice. Nat Rev Immunol **2:** 977-982.

FONG, Y., L. BENDER, W. WANG and S. STROME, 2002 Regulation of the different chromatin states of autosomes and X chromosomes in the germ line of *C. elegans*. Science **296:** 2235-2238.

HAN, M., and P. W. STERNBERG, 1990 *let-60*, a gene that specifies cell fates during *C. elegans* vulval induction, encodes a ras protein. Cell **63:** 921-931.

HARRISON, M. M., C. J. CEOL, X. LU and H. R. HORVITZ, 2006 Some *C. elegans* class B synthetic multivulva proteins encode a conserved LIN-35 Rb-containing complex distinct from a NuRD-like complex. Proc Natl Acad Sci U S A **103:** 16782-16787.

HEDIGER, F., and S. M. GASSER, 2006 Heterochromatin protein 1: don't judge the book by its cover! Curr Opin Genet Dev **16:** 143-150.

HILL, R. J., and P. W. STERNBERG, 1992 The gene *lin-3* encodes an inductive signal for vulval development in *C. elegans*. Nature **358:** 470-476.

HOLDEMAN, R., S. NEHRT and S. STROME, 1998 MES-2, a maternal protein essential for viability of the germline in *Caenorhabditis elegans*, is homologous to a *Drosophila* Polycomb group protein. Development **125:** 2457-2467.

JENUWEIN, T., and C. D. ALLIS, 2001 Translating the histone code. Science **293:** 1074-1080.

JOSHI, A. A., and K. STRUHL, 2005 Eaf3 chromodomain interaction with methylated H3-K36 links histone deacetylation to Pol II elongation. Mol Cell **20:** 971-978.

KEOGH, M. C., S. K. KURDISTANI, S. A. MORRIS, S. H. AHN, V. PODOLNY, S. R. COLLINS, M. SCHULDINER, K. CHIN, T. PUNNA, N. J. THOMPSON, C. BOONE, A. EMILI, J. S. WEISSMAN, T. R. HUGHES, B. D. STRAHL, M. GRUNSTEIN, J. F. GREENBLATT, S. BURATOWSKI and N. J. KROGAN, 2005 Cotranscriptional set2 methylation of histone H3 lysine 36 recruits a repressive Rpd3 complex. Cell **123:** 593-605.

KIMBLE, J., 1981 Alterations in cell lineage following laser ablation of cells in the somatic gonad of *Caenorhabditis elegans*. Dev Biol **87:** 286-300.

KLYMENKO, T., and J. MULLER, 2004 The histone methyltransferases Trithorax and Ash1 prevent transcriptional silencing by Polycomb group proteins. EMBO Rep **5:** 373-377.

KORNFELD, K., 1997 Vulval development in *Caenorhabditis elegans*. Trends Genet **13:** 55-61.

KORSWAGEN, H. C., 2002 Canonical and non-canonical Wnt signaling pathways in *Caenorhabditis elegans*: variations on a common signaling theme. Bioessays **24:** 801-810.

KOUZARIDES, T., 2002 Histone methylation in transcriptional control. Curr Opin Genet Dev **12:** 198-209.

KROGAN, N. J., M. KIM, A. TONG, A. GOLSHANI, G. CAGNEY, V. CANADIEN, D. P. RICHARDS, B. K. BEATTIE, A. EMILI, C. BOONE, A. SHILATIFARD, S.

BURATOWSKI and J. GREENBLATT, 2003 Methylation of histone H3 by Set2 in *Saccharomyces cerevisiae* is linked to transcriptional elongation by RNA polymerase II. Mol Cell Biol **23:** 4207-4218.

LANDRY, J., A. SUTTON, T. HESMAN, J. MIN, R. M. XU, M. JOHNSTON and R. STERNGLANZ, 2003 Set2-catalyzed methylation of histone H3 represses basal expression of GAL4 in *Saccharomyces cerevisiae*. Mol Cell Biol **23:** 5972-5978.

LEE, S., D. K. LEE, Y. DOU, J. LEE, B. LEE, E. KWAK, Y. Y. KONG, S. K. LEE, R. G. ROEDER and J. W. LEE, 2006 Coactivator as a target gene specificity determinant for histone H3 lysine 4 methyltransferases. Proc Natl Acad Sci U S A **103:** 15392-15397.

LI, B., L. HOWE, S. ANDERSON, J. R. YATES, 3RD and J. L. WORKMAN, 2003 The Set2 histone methyltransferase functions through the phosphorylated carboxyl-terminal domain of RNA polymerase II. J Biol Chem **278:** 8897-8903.

LI, J., D. MOAZED and S. P. GYGI, 2002 Association of the histone methyltransferase Set2 with RNA polymerase II plays a role in transcription elongation. J Biol Chem **277:** 49383-49388.

LU, X., and H. R. HORVITZ, 1998 *lin-35* and *lin-53*, two genes that antagonize a *C. elegans* Ras pathway, encode proteins similar to Rb and its binding protein RbAp48. Cell **95:** 981-991.

MORILLON, A., N. KARABETSOU, A. NAIR and J. MELLOR, 2005 Dynamic lysine methylation on histone H3 defines the regulatory phase of gene transcription. Mol Cell **18:** 723-734.

NAKAYAMA, J., J. C. RICE, B. D. STRAHL, C. D. ALLIS and S. I. GREWAL, 2001 Role of histone H3 lysine 9 methylation in epigenetic control of heterochromatin assembly. Science **292:** 110-113.

NIELSEN, P. R., D. NIETLISPACH, H. R. MOTT, J. CALLAGHAN, A. BANNISTER, T. KOUZARIDES, A. G. MURZIN, N. V. MURZINA and E. D. LAUE, 2002 Structure of the HP1 chromodomain bound to histone H3 methylated at lysine 9. Nature **416:** 103-107.

OLDENBURG, K. R., K. T. VO, S. MICHAELIS and C. PADDON, 1997 Recombination-mediated PCR-directed plasmid construction *in vivo* in yeast. Nucleic Acids Res **25:** 451-452.

PIRROTTA, V., 2006 Polycomb silencing mechanisms and genomic programming. Ernst Schering Res Found Workshop**:** 97-113.

POULIN, G., Y. DONG, A. G. FRASER, N. A. HOPPER and J. AHRINGER, 2005 Chromatin regulation and sumoylation in the inhibition of Ras-induced vulval development in *Caenorhabditis elegans*. Embo J **24:** 2613-2623.

REA, S., F. EISENHABER, D. O'CARROLL, B. D. STRAHL, Z. W. SUN, M. SCHMID, S. OPRAVIL, K. MECHTLER, C. P. PONTING, C. D. ALLIS and T. JENUWEIN, 2000 Regulation of chromatin structure by site-specific histone H3 methyltransferases. Nature **406:** 593-599.

RIDDLE, D. L., BLUMENTHAL T., MEYER, B.J., PRIESS, J.R., 1997 *C. elegans II*. Cold Spring Harbor Laboratory Press, Cold Spring Harbor.

ROBERTSON, H. M., and K. L. ZUMPANO, 1997 Molecular evolution of an ancient mariner transposon, *Hsmar1*, in the human genome. Gene **205:** 203-217.

RUAULT, M., M. E. BRUN, M. VENTURA, G. ROIZES and A. DE SARIO, 2002 MLL3, a new human member of the TRX/MLL gene family, maps to 7q36, a chromosome region frequently deleted in myeloid leukaemia. Gene **284:** 73-81.

SCHOTT, S., V. COUSTHAM, T. SIMONET, C. BEDET and F. PALLADINO, 2006 Unique and redundant functions of *C. elegans* HP1 proteins in post-embryonic development. Dev Biol **298:** 176-187.

SCHULTZ, D. C., K. AYYANATHAN, D. NEGOREV, G. G. MAUL and F. J. RAUSCHER, 3RD, 2002 SETDB1: a novel KAP-1-associated histone H3, lysine 9-specific methyltransferase that contributes to HP1-mediated silencing of euchromatic genes by KRAB zinc-finger proteins. Genes Dev **16:** 919-932.

SHILATIFARD, A., 2006 Chromatin modifications by methylation and ubiquitination: implications in the regulation of gene expression. Annu Rev Biochem **75:** 243-269.

SIMPSON, V. J., T. E. JOHNSON and R. F. HAMMEN, 1986 *Caenorhabditis elegans* DNA does not contain 5-methylcytosine at any time during development or aging. Nucleic Acids Res **14:** 6711-6719.

STERNBERG, P. W., and H. R. HORVITZ, 1991 Signal transduction during *C. elegans* vulval induction. Trends Genet **7:** 366-371.

STRAHL, B. D., P. A. GRANT, S. D. BRIGGS, Z. W. SUN, J. R. BONE, J. A. CALDWELL, S. MOLLAH, R. G. COOK, J. SHABANOWITZ, D. F. HUNT and C. D. ALLIS, 2002

Set2 is a nucleosomal histone H3-selective methyltransferase that mediates transcriptional repression. Mol Cell Biol **22:** 1298-1306.

SULSTON, J. E., and H. R. HORVITZ, 1977 Post-embryonic cell lineages of the nematode, *Caenorhabditis elegans*. Dev Biol **56:** 110-156.

SULSTON, J. E., and J. G. WHITE, 1980 Regulation and cell autonomy during postembryonic development of *Caenorhabditis elegans*. Dev Biol **78:** 577-597.

SUN, X. J., J. WEI, X. Y. WU, M. HU, L. WANG, H. H. WANG, Q. H. ZHANG, S. J. CHEN, Q. H. HUANG and Z. CHEN, 2005 Identification and characterization of a novel human histone H3 lysine 36-specific methyltransferase. J Biol Chem **280:** 35261-35271.

SUNDARAM, M. V., 2005 The love-hate relationship between Ras and Notch. Genes Dev **19:** 1825-1839.

TAN, P. B., M. R. LACKNER and S. K. KIM, 1998 MAP kinase signaling specificity mediated by the LIN-1 Ets/LIN-31 WH transcription factor complex during *C. elegans* vulval induction. Cell **93:** 569-580.

TERRANOVA, R., N. PUJOL, L. FASANO and M. DJABALI, 2002 Characterisation of *set-1*, a conserved PR/SET domain gene in *Caenorhabditis elegans*. Gene **292:** 33-41.

THOMAS, J. H., C. J. CEOL, H. T. SCHWARTZ and H. R. HORVITZ, 2003 New genes that interact with *lin-35* Rb to negatively regulate the *let-60* ras pathway in *Caenorhabditis elegans*. Genetics **164:** 135-151.

UNHAVAITHAYA, Y., T. H. SHIN, N. MILIARAS, J. LEE, T. OYAMA and C. C. MELLO, 2002 MEP-1 and a homolog of the NURD complex component Mi-2 act together to maintain germline-soma distinctions in *C. elegans*. Cell **111:** 991-1002.

VAKOC, C. R., S. A. MANDAT, B. A. OLENCHOCK and G. A. BLOBEL, 2005 Histone H3 lysine 9 methylation and HP1gamma are associated with transcription elongation through mammalian chromatin. Mol Cell **19:** 381-391.

VON ZELEWSKY, T., F. PALLADINO, K. BRUNSCHWIG, H. TOBLER, A. HAJNAL and F. MULLER, 2000 The *C. elegans* Mi-2 chromatin-remodelling proteins function in vulval cell fate determination. Development **127:** 5277-5284.

WYSOCKA, J., T. SWIGUT, H. XIAO, T. A. MILNE, S. Y. KWON, J. LANDRY, M. KAUER, A. J. TACKETT, B. T. CHAIT, P. BADENHORST, C. WU and C. D. ALLIS, 2006 A PHD finger of NURF couples histone H3 lysine 4 trimethylation with chromatin remodelling. Nature **442:** 86-90.

XIAO, T., H. HALL, K. O. KIZER, Y. SHIBATA, M. C. HALL, C. H. BORCHERS and B. D. STRAHL, 2003 Phosphorylation of RNA polymerase II CTD regulates H3 methylation in yeast. Genes Dev **17:** 654-663.

ZHAO, T., T. HEYDUK, C. D. ALLIS and J. C. EISSENBERG, 2000 Heterochromatin protein 1 binds to nucleosomes and DNA *in vitro*. J Biol Chem **275:** 28332-28338.

Table 1: Deletion or RNAi of some genes encoding proteins with SET domains causes gross abnormalities, including synthetic multivulva and suppression of synthetic multivulva phenotypes.

Gene name	Allele or RNAi[a]	Phenotype as a single mutant	% multivulva[b] in combination with		
			lin-15A(n767)	*lin-15B(n744)*	*lin-15AB(n765)*
blmp-1	*tm548*	WT	0 (196)	0 (188)	100 (99)
lin-59	*n3425*	Lvl	NA[c]	NA	NA
mes-2	*bn11*	Mes	0 (233)	0 (258)	1 (194)
mes-4	*bn73*	Mes	0 (140)	0 (130)	7 (224)
met-1	*n4337*	WT	81 (469)	0 (216)	100 (206)
met-2	*n4256*	WT	100 (350)	0 (349)	100 (273)
set-1	*n4617*	Emb, Lvl	NA	NA	NA
set-2	*n4589*	WT	0 (291)	1 (134)	100 (281)
set-3	*n4948*	WT	0 (194)	0 (142)	100 (116)
set-4	*n4600*	WT	0 (361)	0 (236)	99 (202)
set-5	*ok1568*	WT	0 (170)	0 (157)	100 (104)
set-6	*tm1611*	WT	0 (151)	0 (139)	100 (111)
set-7	RNAi	WT	0 (186)	0 (215)	100 (116)
set-8	*tm2113*	WT	0 (122)	0 (130)	100 (131)
set-9	*n4949*	WT	0 (171)	0 (151)	100 (91)
set-10	RNAi	WT	0 (211)	0 (149)	100 (36)
set-11	*n4488*	WT	0 (473)	0 (275)	100 (241)
set-12	*n4442*	WT	0 (380	0 (204)	100 (262)
set-13	*n5012*	WT	0 (119)	0 (136)	100 (104)
set-14	RNAi	WT	0 (222)	0 (219)	100 (140)
set-15	RNAi	WT	0 (75)	0 (102)	100 (97)
set-16	*n4526*	Lvl	NA	NA	NA
set-17	*n5017*	WT	0 (147)	0 (104)	100 (146)
set-18	*gk334*	WT	1 (171)	0 (161)	100 (143)
set-19	*ok1813*	WT	0 (163)	0 (101)	100 (111)
set-20	RNAi	WT	0 (211)	0 (195)	100 (147)
set-21	RNAi	WT	0 (235)	0 (176)	100 (113)
set-22	*n5015*	WT	0 (125)	0 (130)	100 (120)
set-23	*n4496*	Emb	NA	NA	NA
set-24	*n4909*	WT	0 (151)	0 (96)	100 (103)
set-25	*n5021*	WT	0 (183)	0 (117)	100 (170)
set-26	RNAi	WT	0 (227)	0 (159)	100 (90)
set-27	RNAi	WT	0 (123)	0 (139)	100 (123)
set-28	*n4953*	WT	0 (144)	0 (99)	100 (128)
set-29	RNAi	WT	0 (163)	0 (132)	100 (107)
set-30	*gk315*	WT	0 (150)	0 (132)	100 (180)
set-31	*ok1482*	WT	0 (190)	0 (206)	100 (158)
set-32	*ok1457*	WT	0 (174)	0 (241)	100 (166)

WT, wild-type. Lvl, larval lethal. Mes, maternal-effect sterile. Emb, embryonic lethal.

[a] For each RNAi experiment, at least two independent cDNA clones were used to make dsRNA for injection.

[b] *lin-15A(n767)* and *lin-15B(n744)* single mutants are non-Muv, and *lin-15AB(n765)* mutants are 100% Muv at 20ºC.

[c] NA = Not Applicable, because the animals died prior to vulval development

Table 2: *met-1* and *met-2* are synthetic multivulva genes.

Genotype	% multivulva (n)
met-1 and *met-2* single mutants	
met-1(n4337)	0 (247)
met-2(n4256)	0 (170)
met-1 and *met-2* interactions with class A mutations	
met-1(n4337); lin-8(n2731)	89 (185)
met-1(n4337); lin-15A(n433)	20 (291)
met-1(n4337); lin-15A(n767)	81 (469)
*met-1(*RNAi*); lin-15A(n767)*	50 (263)
met-1(n4337); lin-38(n751)	52 (313)
met-1(n4337); lin-56(n2728)	78 (330)
lin-8(n2731); met-2(n4256)	89 (341)
met-2(n4256); lin-15A(n433)	94 (234)
met-2(n4256); lin-15A(n767)	100 (350)
*met-2(*RNAi*); lin-15A(n767)*	99 (347)
lin-38(n751); met-2(n4256)	100 (349)
lin-56(n2728); met-2(n4256)	100 (263)
met-1 and *met-2* interactions with class B mutations	
met-1(n4337); lin-15B(n744)	0 (216)
met-1(n4337) lin-35(n745)	0 (146)
met-1(n4337); lin-37(n4903)	0 (131)
met-1(n4337); dpl-1(n2994)	0 (435)
met-2(n4256); lin-15B(n744)	0 (349)
lin-35(n745); met-2(n4256)	0 (391)
lin-37(n4903) met-2(n4256)	0 (114)
dpl-1(n2994); met-2(n4256)	0 (105)
met-1 and *met-2* interactions with class C mutations	
met-1(n4337); mys-1(n3681)[a]	0 (241)
met-1(n4337); trr-1(n3712)[b]	12 (22)
met-2(n4256); mys-1(n3681)[a]	24 (93)
trr-1(n3712); met-2(n4256)[b]	29 (36)

[a] The vulval phenotypes of these animals were scored at 25ºC, at which temperature the single mutants *met-1(n4337)*, *met-2(n4256)* and *mys-1(n3681)* are 0% Muv.

[b] *trr-1(n3712)* is 11% Muv as a single mutant.

Table 3: *met-1* and *met-2* act redundantly to control the vulval cell-fate decision.

Genotype	% multivulva (n)
met-1(n4337)	0 (247)
met-2(n4256)	0 (170)
met-1(n4337); met-2(n4256)[a]	29 (126)
*met-1(n4337); met-2(*RNAi*)*	22 (34)
*met-1(*RNAi*); met-2(n4256)*	11 (48)

[a] The *met-1; met-2* double mutant is synthetically sterile with a Mrt germline phenotype, so these animals were descended from *met-1*/+*; met-2*/+ heterozygotes.

Table 4: The *C. elegans* HP1 homologs act redundantly with each other and with the *met* genes to control the vulval cell-fate decision

Genotype	% multivulva (n)[a]
hpl and *met* single mutants are not Muv at 20ºC	
hpl-1(n4317)	0 (312)
hpl-2(tm1489)	0 (161)
met-1(n4337)	0 (247)
met-2(n4256)	0 (170)
hpl-2 acts redundantly with *hpl-1, met-1* and *met-2*	
hpl-2(tm1489); hpl-1(n4317)	24 (203)
met-1(n4337); hpl-1(n4317)	0 (165)
met-2(n4256); hpl-1(n4317)	0 (276)
met-1(n4337); hpl-2(tm1489)	17 (81)
met-2(n4256) hpl-2(tm1489)	87 (286)
met-1 and *met-2* act redundantly with the *C. elegans* HP1 homologs	
met-1(n4337); met-2(n4256)	29 (126)
met-1(n4337); hpl-2(tm1489); hpl-1(n4317)	84 (205)
met-2(n4256) hpl-2(tm1489); hpl-1(n4317)	100 (52)
met-1(n4337); met-2(n4256); hpl-1(n4317)	57 (7)
met-1(n4337); met-2(n4256) hpl-2(tm1489)	100 (126)
met-1(n4337); met-2(n4256) hpl-2(tm1489); hpl-1(n4317)	100 (68)[b]

[a] These vulval phenotypes were scored at 20ºC.

[b] These homozygotes were derived from *met-2*/+ *hpl-2*/+ heterozygotes, because the quadruple mutant is synthetically sterile. This mutant did not show any maternal rescue of the synMuv phenotype, unlike the *met-2(n4256) hpl-2(tm1489); hpl-1(n4317)* and *met-1(n4337); met-2(n4256) hpl-2(tm1489)* triple mutants.

FIGURE DESCRIPTIONS

Figure 1. *met-1* and *met-2* gene structures, mutations and predicted protein structures.

(A) The genomic structures of *met-1* and *met-2*. Exons are indicated by black boxes, and 3' untranslated regions are indicated by white boxes. The alternatively spliced exon six of *met-1* is depicted as a white-dotted box. The locations of the deletion alleles are shown.

(B) Representations of the domain structures of the MET-1 and MET-2 proteins.

Figure 1

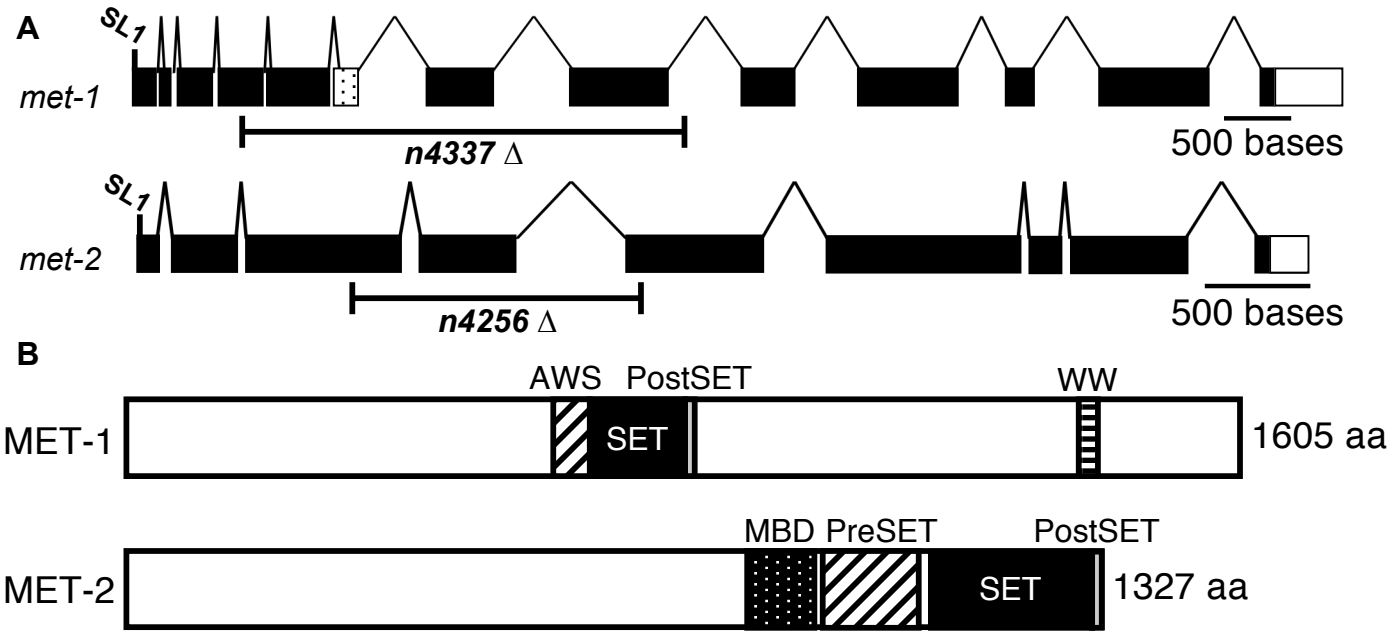
A
SL1
met-1
n4337 Δ
500 bases
SL1
met-2
n4256 Δ
500 bases
B
AWS
PostSET
WW
MET-1
SET
1605 aa
MBD
PreSET
PostSET
MET-2
SET
1327 aa

Figure 2. *met-1* and *met-2* are required *in vivo* for normal levels of histone H3K36 and H3K9 trimethylation, respectively.

(A) The levels of histone H3 trimethylation at K4, K9, K27 and K36 were assayed using quantitative western blots and normalized to levels of histone H3 (see Materials and Methods). Relative histone H3 trimethylation levels of *met-1(n4337)* mutants (white bars) and *met-2(n4256)* mutants (grey bars) were normalized to the trimethylation levels of the wild type (black bars) for each experiment. The levels of histone H3 were measured (Figure S1), and the specificity of the H3K9 and H3K36 trimethylation antisera were confirmed using dot blots of methylated histone tail peptides (Figure S2). Normalized units of fluorescence and standard deviations are shown.

Figure 2

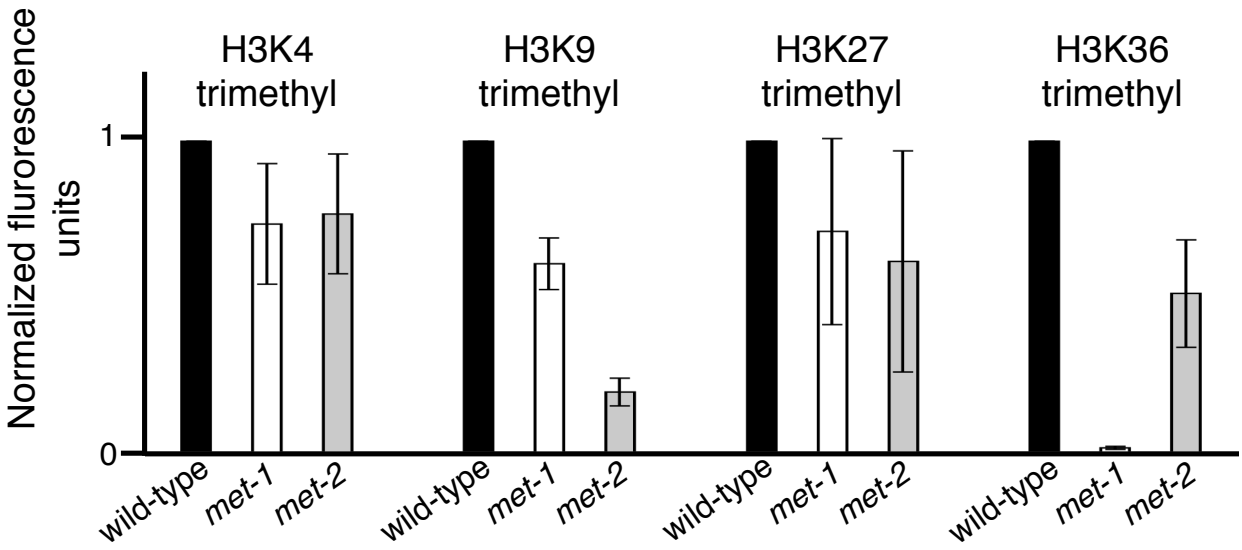
Normalized flurorescence units
1
0
H3K4 trimethyl
H3K9 trimethyl
H3K27 trimethyl
H3K36 trimethyl
wild-type
met-1
met-2
wild-type
met-1
met-2
wild-type
met-1
met-2
wild-type
met-1
met-2

Figure 3. *met-1* and *met-2* are each required to prevent ectopic *lin-3* expression in a *lin-15A(n767)* mutant background. Real-time RT-PCR experiments were performed using RNA samples from animals of the genotypes shown. Mean $\Delta\Delta C_T$ values were used to calculate relative changes in *lin-3* expression normalized to levels of *rpl-26* (see Materials and Methods). Mean values and ranges of relative *lin-3*/*rpl-26* ratios for three trials are shown.

Figure 3

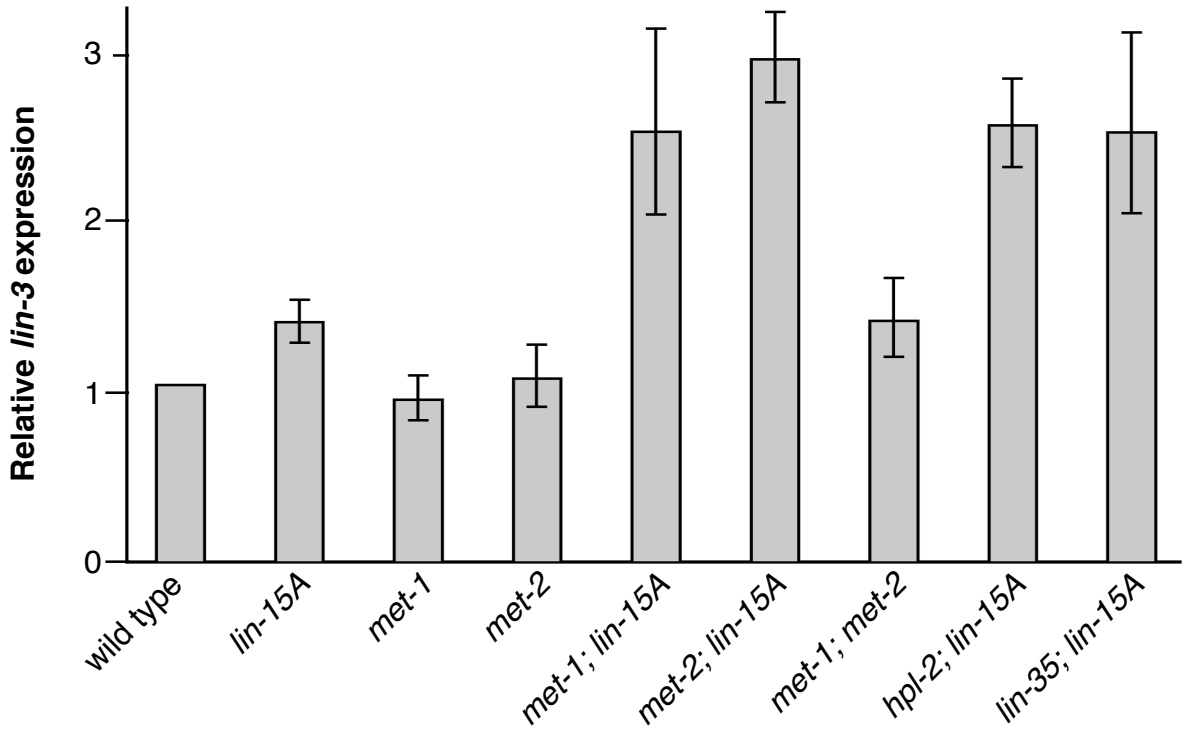
Relative lin-3 expression
0
1
2
3
wild type
lin-15A
met-1
met-2
met-1; lin-15A
met-2; lin-15A
met-1; met-2
hpl-2; lin-15A
lin-35; lin-15A

Supplemental Materials and Methods

RNAi analyses

RNAi by injection was performed as described by Andersen *et al.* (2006). For RNAi studies of putative histone methyltransferase genes, the clones used to generate dsRNA are described in Table S1. Yuji Kohara kindly provided all yk clones.

Isolation of deletion alleles

Genomic DNA pools from the progeny of EMS or UV-TMP mutagenized animals were screened for deletions using PCR as described by Ceol and Horvitz (2001). *hpl-1(n4317)* removes nucleotides 20092 to 21648 of cosmid K08H2. A complete list of the positions of all HMT deletion alleles can be found in Table S1.

Germline transformation experiments

Germline transformation experiments were performed as described by Mello *et al.* (1991). For rescue of the *met-1(n4337); lin-15A(n767)* synMuv phenotype, we injected pEA182 (50 ng/μl). For rescue of the *met-2(n4256); lin-15A(n433)* synMuv phenotype, we injected pEA115 (50 ng/μl). pEA182 and pEA115 have the *met-1* and *met-2* cDNAs, respectively, cloned downstream of the *dpy-7* promoter, which drives expression in the hyp7 syncytium (GILLEARD *et al.* 1997). Each injection included a 1 kb ladder (Invitrogen) at 100 μg/μl and *sur-5::gfp* (YOCHEM *et al.* 1998) at 20 ng/μl.

Supplemental Information

met-1, *met-2* and *hpl-2* mutants display pleiotropic defects distinct from canonical class B synMuv mutants

Many of the class B synMuv genes control aspects of a germline-versus-soma cell-fate decision process (UNHAVAITHAYA *et al.* 2002; WANG *et al.* 2005). Defects in this process can be observed as the ectopic expression of germline markers in the soma, enhanced sensitivity to RNAi, silencing of repetitive transgenes (Tam phenotype) and the germline-like appearance of somatic cells in *mep-1* and *let-418* arrested larvae. We found that *met-1*, *met-2, hpl-1* and *hpl-2* single mutants were not hypersensitive to RNAi (Figure S3) and did not have a Tam phenotype (data not shown). However, *met-1; met-2* and *hpl-2; hpl-1* double mutants were sensitive to RNAi (Figure S4) but were not Tam (data not shown).

We also tested the ectopic activation of a *lag-2::gfp* reporter construct; some class B mutants show such activation (DUFOURCQ *et al.* 2002; POULIN *et al.* 2005; COUSTHAM *et al.* 2006; SCHOTT *et al.* 2006). *met-1*, *met-2* and *hpl-2* but not *hpl-1* mutations caused ectopic activation of a *lag-2* reporter in the intestine and the posterior of the animal (data not shown), suggesting that these genes might normally repress transcription from the *lag-2* promoter. Additionally, some class B synMuv mutations suppress the vulval defects of *mat-3(ku233)* mutants, presumably through the ectopic activation of *mat-3* transcription from the promoter mutant *ku233* (GARBE *et al.* 2004). We found that the *met* and *hpl* null mutations suppressed the cell-cycle-like vulval defects of *mat-3(ku233)* mutants (Table S5). Many class B synMuv mutants are hypersensitive to RNAi, have a Tam phenotype, ectopically express GFP from a *lag-2* reporter and suppress *mat-3(ku233)* vulval defects. Given that *met-1*, *met-2* and *hpl-2* mutations all cause strong mutant phenotypes and share only the last two attributes, these genes likely represent a distinct subset of class B synMuv genes.

Supplemental References

ANDERSEN, E. C., X. LU and H. R. HORVITZ, 2006 *C. elegans* ISWI and NURF301 antagonize an Rb-like pathway in the determination of multiple cell fates. Development **133:** 2695-2704.

CEOL, C. J., and H. R. HORVITZ, 2001 *dpl-1* DP and *efl-1* E2F act with *lin-35* Rb to antagonize Ras signaling in *C. elegans* vulval development. Mol Cell **7:** 461-473.

COUSTHAM, V., C. BEDET, K. MONIER, S. SCHOTT, M. KARALI and F. PALLADINO, 2006 The *C. elegan*s HP1 homologue HPL-2 and the LIN-13 zinc finger protein form a complex implicated in vulval development. Dev Biol **297:** 308-322.

DUFOURCQ, P., M. VICTOR, F. GAY, D. CALVO, J. HODGKIN and Y. SHI, 2002 Functional requirement for histone deacetylase 1 in *Caenorhabditis elegans* gonadogenesis. Mol Cell Biol **22:** 3024-3034.

GARBE, D., J. B. DOTO and M. V. SUNDARAM, 2004 *Caenorhabditis elegans lin-35*/Rb, *efl-1*/E2F and other synthetic multivulva genes negatively regulate the anaphase-promoting complex gene *mat-3*/APC8. Genetics **167:** 663-672.

GILLEARD, J. S., J. D. BARRY and I. L. JOHNSTONE, 1997 *cis* regulatory requirements for hypodermal cell-specific expression of the *Caenorhabditis elegans* cuticle collagen gene *dpy-7*. Mol Cell Biol **17:** 2301-2311.

MELLO, C. C., J. M. KRAMER, D. STINCHCOMB and V. AMBROS, 1991 Efficient gene transfer in *C.elegans*: extrachromosomal maintenance and integration of transforming sequences. Embo J **10:** 3959-3970.

POULIN, G., Y. DONG, A. G. FRASER, N. A. HOPPER and J. AHRINGER, 2005 Chromatin regulation and sumoylation in the inhibition of Ras-induced vulval development in *Caenorhabditis elegans*. Embo J **24:** 2613-2623.

SCHOTT, S., V. COUSTHAM, T. SIMONET, C. BEDET and F. PALLADINO, 2006 Unique and redundant functions of *C. elegans* HP1 proteins in post-embryonic development. Dev Biol **298:** 176-187.

UNHAVAITHAYA, Y., T. H. SHIN, N. MILIARAS, J. LEE, T. OYAMA and C. C. MELLO, 2002 MEP-1 and a homolog of the NURD complex component Mi-2 act together to maintain germline-soma distinctions in *C. elegans*. Cell **111:** 991-1002.

WANG, D., S. KENNEDY, D. CONTE, JR., J. K. KIM, H. W. GABEL, R. S. KAMATH, C. C. MELLO and G. RUVKUN, 2005 Somatic misexpression of germline P granules and enhanced RNA interference in retinoblastoma pathway mutants. Nature **436:** 593-597.

YOCHEM, J., T. GU and M. HAN, 1998 A new marker for mosaic analysis in *Caenorhabditis elegans* indicates a fusion between hyp6 and hyp7, two major components of the hypodermis. Genetics **149:** 1323-1334.

Table S1: Deletion or RNAi of some genes encoding proteins with SET domains causes gross abnormalities, including synthetic multivulva phenotypes at 25ºC.

Cosmid name	Named gene	Allele or RNAi	Deletion position[a]	RNAi clones used[b]	Phenotype as a single mutant[c]	% multivulva[d] in combination with	
						lin-15A(n767)	*lin-15B(n744)*
C07A9.7	*set-3*	*n4948*	29557-30494	-	WT	2 (148)	0 (109)
C15H11.5	*set-31*	*ok1482*	-	-	WT	0 (218)	0 (193)
C26E6.9	*set-2*	*n4589*	11822-12718	-	WT	0 (238)	0 (138)
C32D5.5	*set-4*	*n4600*	18605-19750	-	WT	0 (376)	0 (354)
C41G7.4	*set-32*	*ok1457*	-	-	WT	1 (277)	0 (114)
C43E11.3	*met-1*	*n4337*	27305-29164	yk27f9, yk1128b01	WT	100 (412)	Lvl
C47E8.8	*set-5*	*ok1568*	-	-	WT	3 (154)	0 (152)
C49F5.2	*set-6*	*tm1611*	-	-	WT	1 (139)	0 (83)
D2013.9	*set-7*	RNAi	-	yk1606h6, yk1489d9	WT	6 (186)	0 (114)
F02D10.7	*set-8*	*tm2113*	-	-	WT	2 (116)	0 (63)
F15E6.1	*set-9*	*n4949*	28418-29672	-	WT	0 (114)	0 (136)
F25D7.3	*blmp-1*	*tm548*	-	-	WT	4 (285)	0 (61)
F33H2.7	*set-10*	RNAi	-	pEA213, 26g11	WT	0 (124)	0 (72)
F34D6.4	*set-11*	*n4488*	14558-15189	-	WT	0 (535)	1 (264)
K09F5.5	*set-12*	*n4442*	29664-31178	-	WT	0 (311)	0 (169)
K12H6.11	*set-13*	*n5012*	19739-21230	-	WT	2 (136)	0 (56)
R05D3.11	*met-2*	*n4256*	32838-34180	yk29g5, yk249d7	WT	100 (198)	0 (163)
R06A4.7	*mes-2*	*bn11*	-		Mes	1 (293)	0 (218)
R06F6.4	*set-14*	RNAi	-	yk1738g11, yk772g4	WT	1 (177)	0 (128)
R11E3.4	*set-15*	RNAi	-	-	WT	0 (188)	0 (211)
T12D8.1	*set-16*	*n4526*	28901-30380	-	Lvl	NA[e]	NA
T12F5.4	*lin-59*	*n3425*	3325-4739	-	Lvl	NA	NA
T21B10.5	*set-17*	*n5017*	11267-12041	-	WT	2 (168)	0 (45)
T22A3.4	*set-18*	*gk334*	-	-	WT	2 (191)	0 (158)
T26A5.7	*set-1*	*n4617*		-	Emb, Lvl	NA	NA
W01C8.3	*set-19*	*ok1813*	-	-	WT	3 (179)	0 (131)
W01C8.4	*set-20*	RNAi	-	yk772e2, 184f9	WT	0 (150)	0 (42)

Y24D9A.2	*set-21*	RNAi		pEA215	WT	0 (143)	0 (60)
Y2H9A.1	*mes-4*	*bn73*	-	-	Mes	0 (114)	0 (103)
Y32F6A.1	*set-22*	*n5015*	10355-11110	-	WT	0 (168)	0 (95)
Y41D4B.12	*set-23*	*n4496*	45994-46817	-	Emb	NA	NA
Y43F11A.5	*set-24*	*n4909*	5846-7310	-	WT	1 (207)	0 (135)
Y43F4B.3	*set-25*	*n5021*	465-2443	-	WT	0 (154)	0 (126)
Y51H4A.12	*set-26*	RNAi	-	pEA216, 119h9	WT	0 (165)	0 (100)
Y71H2AM.8	*set-27*	RNAi	-	pEA212	WT	0 (70)	0 (57)
Y73B3B.2	*set-28*	*n4953*	15866-17064	-	WT	1 (131)	0 (49)
Y92H12BR.6	*set-29*	RNAi	-	yk1541e11, pEA218	WT	6 (179)	0 (114)
ZC8.3	*set-30*	*gk315*	-	-	WT	5 (204)	0 (156)

WT, wild-type. Lvl, larval lethal. Mes, maternal-effect sterile. Emb, embryonic lethal.

[a] The deletion position numbers refer to the start and stop nucleotide of the cosmid containing that gene. Information about *ok*, *gk* and *tm* deletion alleles can be found at www.wormbase.org.

[b] Two independent RNAi experiments were performed for each gene tested. For clones starting with yk, cDNA clones kindly provided by Yuji Kohara were used to make template for dsRNA production and subsequent RNAi by injection. For clones starting with pEA, cDNA clones were made using RT-PCR to make template for dsRNA production and subsequent RNAi injection. For RNAi feeding experiments the plate number and position of the clone from the Ahringer RNAi feeding library is shown.

[c] These loss-of-function phenotypes are described in this manuscript (*met-1* and *met-2*) or previously published,

[d] *lin-15A(n767)* and *lin-15B(n744)* single mutants are not appreciably Muv at 25ºC. Because *lin-15AB(n765)* is 100% Muv at 20ºC, suppression of a more severe phenotype was not tested.

[e] NA = Not applicable, because the animals died prior to vulval development

Table S2: *mes-2*, *mes-3*, *mes-4* and *mes-6* but not *mes-1* are suppressors of the *lin-15AB(n765)* synMuv phenotype	
Genotype	% multivulva (n)[a]
lin-15AB(n765)	100 (230)
*mes-1(*RNAi*) lin-15AB(n765)*	100 (149)
mes-2(bn11); lin-15AB(n765)	61 (175)
mes-3(bn35); lin-15AB(n765)	43 (406)
mes-4(bn73); lin-15AB(n765)	7 (224)
mes-6(bn66); lin-15AB(n765)	73 (529)

[a] The vulval phenotype of every strain carrying a *mes* mutation was scored one generation after the *mes* mutation was descended from a *mes* heterozygous mutant. This assay allowed for the scoring of vulval abnormalities of the maternal-effect sterile offspring.

Table S3: *met-1* and *met-2* mutants do not act redundantly with genes that encode HMTs predicted to methylate H3K9 or H3K36.

Genotype	% multivulva (n)[a]
met-1(n4337); set-11(n4488)	0 (246)
met-2(n4256); set-12(n4442)	0 (201)
met-1(n4337); set-12(n4442)	0 (186)
set-11(n4488); met-2(n4256)	0 (205)
met-1(n4337); met-2(n4256)	29 (126)
met-1(n4337); met-2(n4256); set-12(n4442)	28 (109)
met-1(n4337); set-11(n4488); met-2(n4256)	NA[b]

set-11 encodes a putative HMT predicted to methylate H3K9, and *set-12* encodes a putative HMT predicted to methylate H3K36.

[a] The vulval phenotypes of these animals were scored at 25ºC.

[b] This combination of mutations caused embryonic lethal.

Table S4: Loss of *hpl-2* causes a Muv phenotype that is enhanced by loss of synMuv class A, B or C gene activity		
Genotype	% multivulva (n)[a]	
hpl-2 but not *hpl-1* is Muv at 25ºC as a single mutant		
	22.5ºC	25ºC
hpl-1(n4317)	0 (500)	0 (156)
hpl-2(tm1489)	0 (73)	99 (205)
The Muv phenotype of *hpl-2* at 22.5ºC is enhanced by loss of class A, B or C gene activity		
lin-8(n2731); hpl-2(tm1489)	100 (134)	
hpl-2(tm1489); lin-15A(n767)	100 (507)	
lin-35(n745); hpl-2(tm1489)	71 (94)	
hpl-2(tm1489); lin-15B(n744)	100 (43)	
hpl-2(tm1489); mys-1(n3681)	71 (210)	
hpl-1 is not a synMuv gene at 22.5ºC and does not enhance a weak synMuv class AB double mutant at 20ºC.		
hpl-1(n4317) lin-15A(n767)	0 (270)	
lin-56(n2728); hpl-1(n4317)	1 (342)	
lin-35(n745); hpl-1(n4317)	0 (251)	
dpl-1(n2994); hpl-1(n4317)	0 (62)	
mys-1(n3681); hpl-1(n4317)	0 (161)	
lin-15AB(n2993 n433)	66 (112)	
hpl-1(n4317); lin-15AB(n2993 n433)	66 (157)	

lin-8 and *lin-15A* are class A synMuv genes. *lin-35* and *lin-15B* are class B synMuv genes. *mys-1* is a class C synMuv gene. *lin-15AB(n2993 n433)* is a partial loss-of-function mutation affecting both *lin-15A* and *lin-15B*.

Table S5: *met-1*, *met-2*, *hpl-1* and *hpl-2* mutations suppress the vulval defects of *mat-3(ku233)* mutants.

Genotype	% Abnormal vulva (n)[a]
wild-type	0 (51)
mat-3(ku233)	61 (65)
met-1(n4337); mat-3(ku233)	11 (52)
mat-3(ku233) met-2(n4256)	10 (39)
mat-3(ku233); hpl-1(n4317)	38 (39)
mat-3(ku233) hpl-2(tm1489)	6 (31)

[a] These vulval phenotypes were scored at 20ºC using Nomarski optics.

Figure S1. *met-1* and *met-2* mutants appear to have approximately normal levels of histone H3.

(A) The levels of histone H3 as assayed using quantitative western blots are shown. Levels of histone H3 were normalized to levels of histone H2A. Relative levels of histone H3 in *met-1(n4337)* (white bar) and *met-2(n4256)* (grey bar) mutants were normalized to relative levels of histone H3 of the wild type (black bar). Normalized units of fluorescence and standard deviations are shown.

(B) The levels of histone H3 as assayed using quantitative western blots are shown. Levels of histone H3 were normalized to levels of tubulin. Relative levels of histone H3 in *met-1(n4337)* (white bar) and *met-2(n4256)* (grey bar) mutants were normalized to relative levels of histone H3 of the wild type (black bar). Normalized units of fluorescence and standard deviations are shown.

Figure S1

A

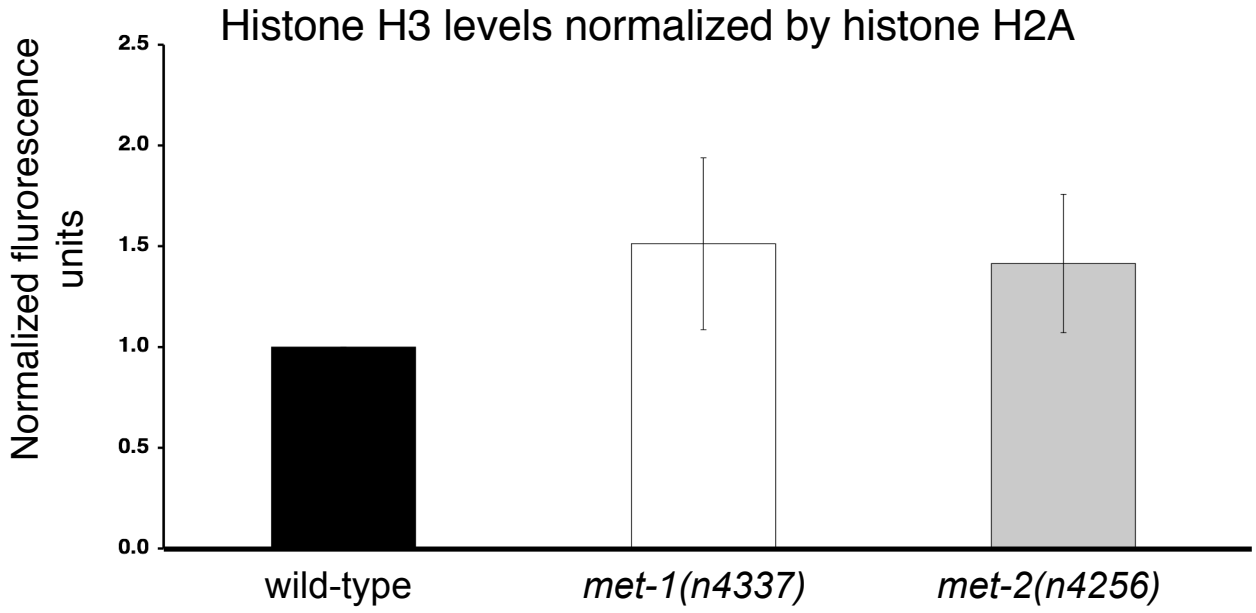
Histone H3 levels normalized by histone H2A
Normalized flurorescence units
2.5
2.0
1.5
1.0
0.5
0.0
wild-type
met-1(n4337)
met-2(n4256)

B

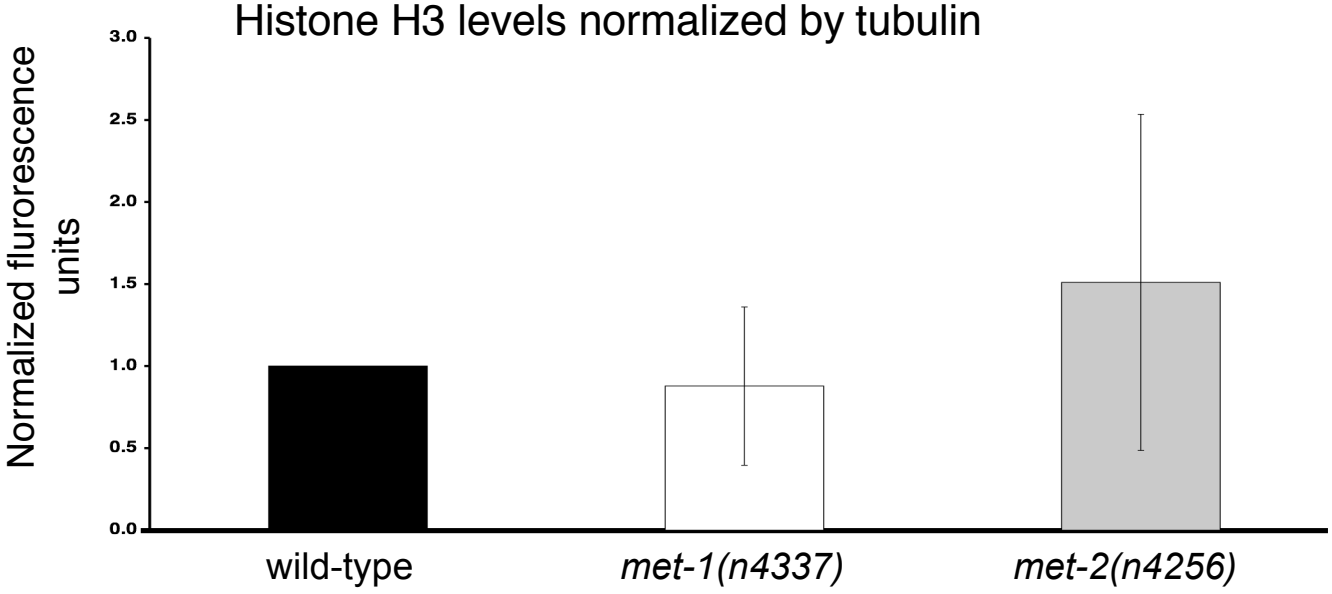
Histone H3 levels normalized by tubulin
Normalized flurorescence units
3.0
2.5
2.0
1.5
1.0
0.5
0.0
wild-type
met-1(n4337)
met-2(n4256)

Figure S2. The histone H3K9 and H3K36 trimethylation antisera are specific.

Peptides from histone H3 trimethylated at lysine 9 (Upstate) or lysine 36 (Upstate) were probed with the antisera we used to recognize levels of histone trimethylation *in vivo*. 0-25 μg of each peptide was blotted. The top row of each blot is the peptide with lysine 9 trimethylated. The bottom row of each blot is the peptide with lysine 36 trimethylated. The top blot was probed with antisera to histone H3K9 trimethylation (Upstate). The bottom blot was probed with antisera to histone H3K36 trimethylation (Abcam).

Figure S2

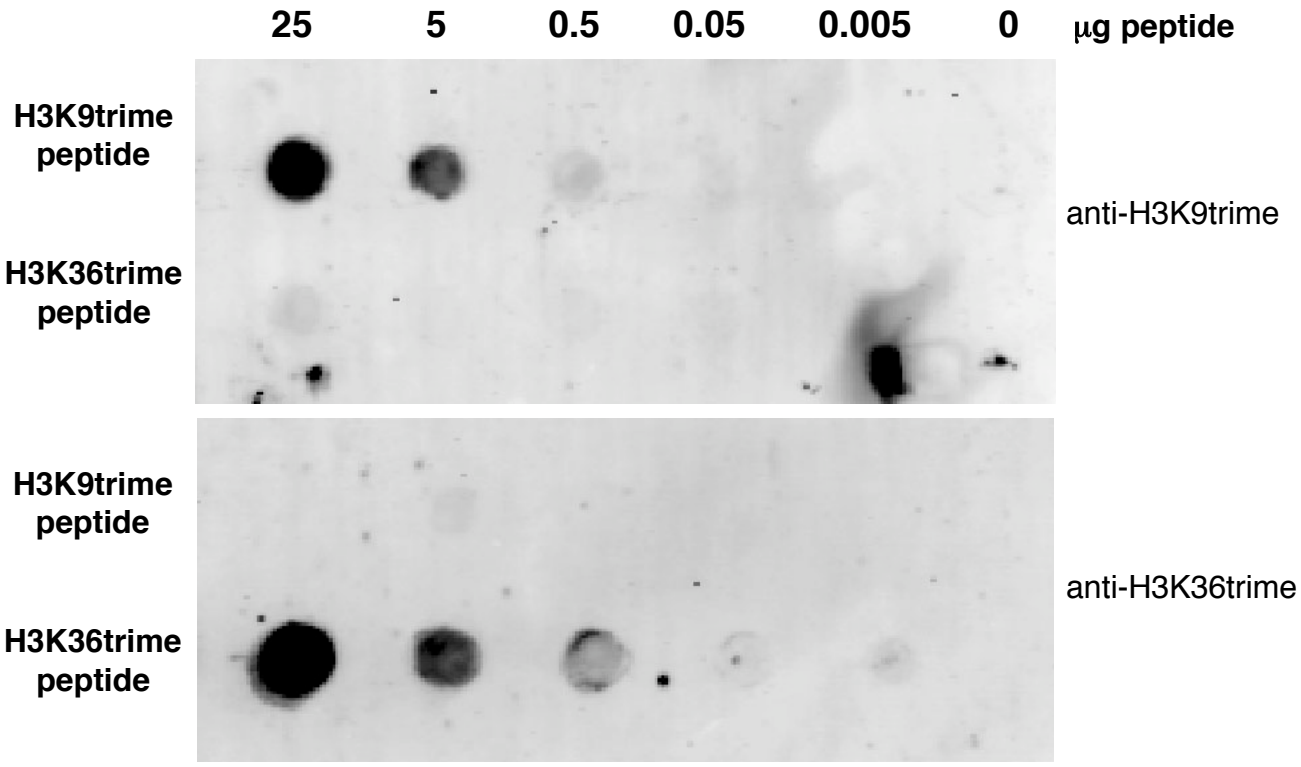
25
5
0.5
0.05
0.005
0
μg peptide
H3K9trime peptide
H3K36trime peptide
anti-H3K9trime
H3K9trime peptide
H3K36trime peptide
anti-H3K36trime

Figure S3. *met-1; met-2* double mutants have a mortal germline defect.
Seven lines of *met-1(n433); met-2(n4256)* animals were scored for sterility. The generation at which each line became 100% is shown.

Figure S3

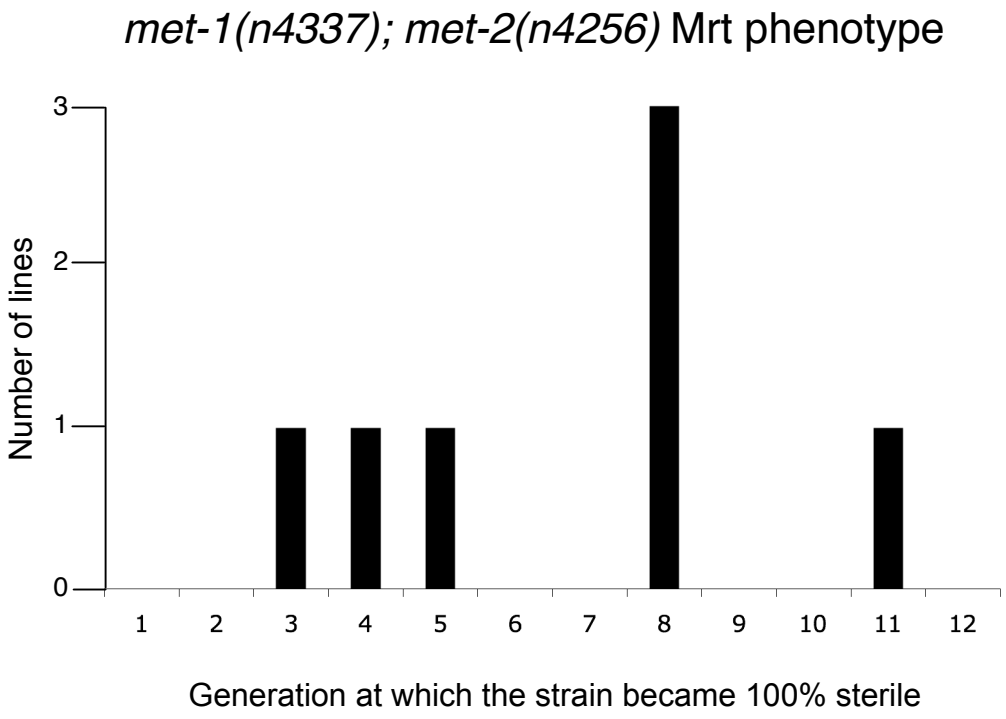
met-1(n4337); met-2(n4256) Mrt phenotype
Number of lines
0
1
2
3
1
2
3
4
5
6
7
8
9
10
11
12
Generation at which the strain became 100% sterile

Figure S4. The *met* genes and the *hpl* genes act redundantly to prevent sensitization to RNAi by feeding.

After exposure of animals to *cel-1* RNAi, the number of arrested L2 larvae was scored in at least three independent experiments. The average percent of L2 arrested larvae is shown. Error bars indicate standard deviations.

Figure S4

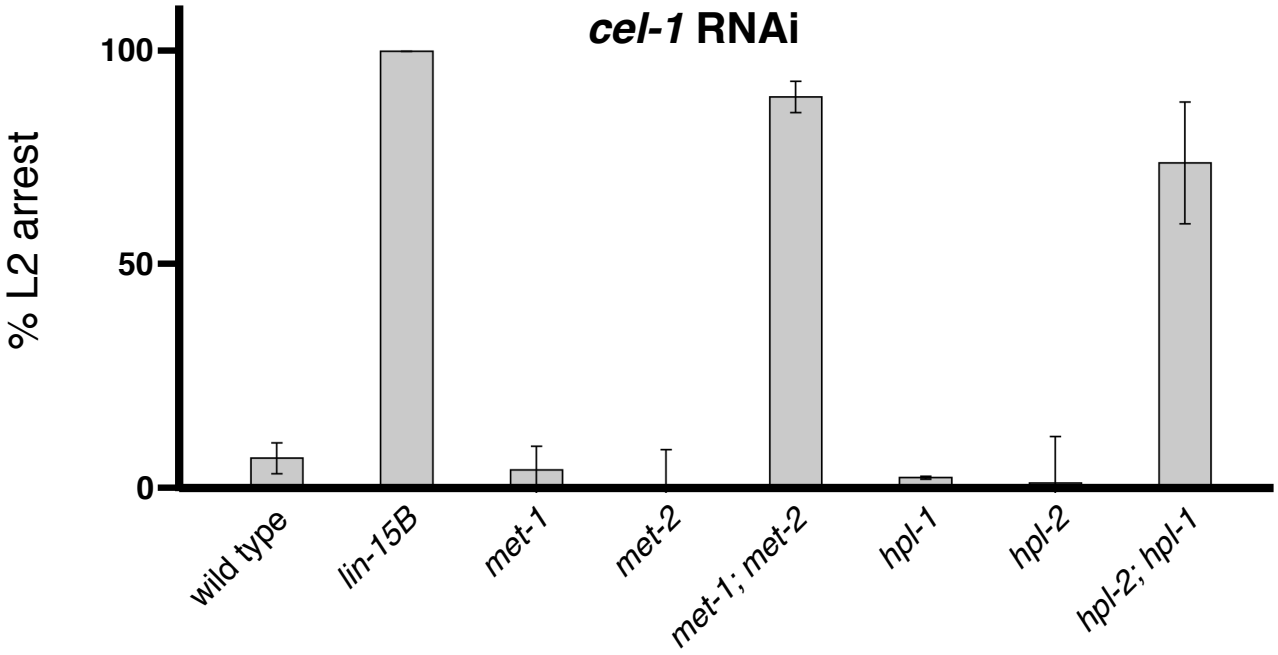
cel-1 RNAi
% L2 arrest
100
50
0
wild type
lin-15B
met-1
met-2
met-1; met-2
hpl-1
hpl-2
hpl-2; hpl-1

CHAPTER THREE

Genetic interactions reveal shared molecular activities in the inhibition of *C. elegans* vulval cell fates

Erik C. Andersen*, Adam M. Saffer* and H. Robert Horvitz

* These authors contributed equally to this work.

Graduate student Adam Saffer constructed and scored all class AA double mutants and class AAB triple mutants. He also scored the single class A mutant vulval phenotypes. I constructed and scored all class BB double mutants and class BBA triple mutants. I also scored the single class B mutant vulval phenotypes. I wrote the manuscript; Adam helped edit.

This manuscript is being prepared for publication.

SUMMARY

Many mutations do not cause any obvious abnormalities because of parallel or redundant processes. Genetic redundancy can be revealed by means of synthetic interactions, in which a double mutant has a phenotype not seen in either single mutant. In *Caenorhabditis elegans*, the synthetic multivulva (synMuv) genes redundantly inhibit vulval cell fates. The synMuv genes are grouped into three classes, A, B and C. Animals with one or more mutations of the same class have wild-type vulval development, but animals with mutations of any two classes have a multivulva phenotype. We have examined in detail possible interactions between genes in the same class and have found that redundant interactions exist within each synMuv class. However, some genes in the same class do not act redundantly and likely share the same function. Our genetic experiments can be used to determine which synMuv genes act together *in vivo*. Because many synMuv genes encode conserved proteins that are uncharacterized in other organisms, the results of these experiments might assign these genes to known molecular activities.

INTRODUCTION

Global analyses of loss-of-function mutants have revealed that many mutations do not cause any obvious phenotypic abnormalities (PARK and HORVITZ 1986; WINZELER *et al.* 1999; FRASER *et al.* 2000; KAMATH *et al.* 2003). The wild-type phenotype of such mutants could reflect genetic redundancy, which can confer phenotypic robustness to developmental and behavioral processes (HARRISON *et al.* 2007b; SIEBER *et al.* 2007). Genetic redundancy can be identified and characterized using synthetic interactions, in which a mutant defective in the functions of two genes displays a phenotype that is not seen in mutants defective in the function of either single gene. Genes that display a synthetic interaction are typically thought to function in the same broad biological process. One example of genetic redundancy is the numerous synthetic-lethal interactions uncovered in global analyses of *S. cerevisiae* (TONG *et al.* 2001; OOI *et al.* 2003; TONG *et al.* 2004). Another example is the synthetic defects in the formation of the *C. elegans* hermaphrodite vulva (FERGUSON and HORVITZ 1989). We have chosen to study the parallel activities that regulate the *C. elegans* vulva, as an example of how a complex network of genes controls cell-fate specification during development.

In *C. elegans*, three cells from among six equipotent progenitor cells are specified to adopt vulval cell fates by three cell-signaling cascades: the receptor tyrosine kinase (RTK)/Ras, Notch and Wnt pathways (SUNDARAM 2005; STERNBERG 2006). The three cells that adopt vulval fates divide several times and give rise to the vulva (SULSTON and HORVITZ 1977). The remaining three cells fail to adopt vulval fates and fuse the underlying hypodermis. The synthetic multivulva (synMuv) genes prevent the three cells that normally become non-vulval cells from adopting ectopic vulval cell fates (FERGUSON and HORVITZ 1989).

The synMuv genes originally were grouped into two classes, A and B, which were defined as follows: single loss-of-function mutants and animals mutant for two genes within the same synMuv class do not have obvious vulval

abnormalities, but a multivulva (Muv) phenotype is observed in class AB double mutants. This synthetic interaction suggests that the synMuv genes act in two parallel processes to inhibit the adoption of vulval cell fates (FERGUSON and HORVITZ 1989). The class A synMuv genes encode nuclear proteins thought to regulate transcription (CLARK *et al.* 1994; HUANG *et al.* 1994; DAVISON *et al.* 2005) (A.M. Saffer, E.M. Davison and H.R.H., unpublished results). Many class B synMuv genes encode homologs of regulators of transcription and chromatin, including a Nucleosome Remodeling and Deacetylase (NuRD) complex (SOLARI and AHRINGER 2000; UNHAVAITHAYA *et al.* 2002), Rb/E2F4/DP (LU and HORVITZ 1998; CEOL and HORVITZ 2001), two histone methyltransferases (Chapter Two), heterochromatin protein 1 (HP1) (COUTEAU *et al.* 2002) and the DRM complex (HARRISON *et al.* 2006). The recently described class C synMuv genes encode proteins similar to members of the Tip60/NuA4 histone acetyltransferase complex (CEOL and HORVITZ 2004). The effects of class C synMuv mutations on vulval development are similar to those of class B mutations, because, like AB double mutants, AC double mutants are Muv but class BC double mutants exhibit an incompletely penetrant Muv defect.

Genetic screens for mutants defective in the inhibition of vulval cell fates have identified many synMuv genes (FERGUSON and HORVITZ 1989; THOMAS *et al.* 2003; POULIN *et al.* 2005; CEOL *et al.* 2006). To date, there are at least four class A synMuv genes, 23 class B synMuv genes and three class C genes based on the original synMuv classification scheme (FERGUSON and HORVITZ 1989; VON ZELEWSKY *et al.* 2000; COUTEAU *et al.* 2002; DUFOURCQ *et al.* 2002; UNHAVAITHAYA *et al.* 2002; THOMAS *et al.* 2003; CEOL *et al.* 2006)(Chapters Two and Six). However as additional synMuv genes were identified, it became clear that the original classification scheme was not sufficient to explain all observations. In Chapter Two, it was reported that two class B synMuv genes *met-1* and *met-2* act in parallel to inhibit vulval cell fates. Mutations of *let-418* or the class C genes caused Muv phenotypes when combined with mutations in class A and class B synMuv genes (VON ZELEWSKY *et al.* 2000; CEOL and HORVITZ 2004). However,

let-418 was classified as a class B gene, and the class C genes were assigned to a separate class. Using sensitive assays of the Muv phenotype, we sought determination of whether these observations of redundancy within a class were exceptions to the synMuv classification scheme or whether they were generally applicable to other synMuv genes.

To assess whether different genes act in separable processes, we combined null or strong loss-of-function mutations and quantified the penetrance of the phenotype as compared to phenotype of either single mutant. We tried to use at least one null mutation in every comparison because those mutants have completely lost the function of that gene, and the contribution of other genes to the phenotype can be assessed. If two genes act in a shared process, they do not act in parallel. Mutations of both genes with activities in a shared process will not cause a more penetrant mutant phenotype than that caused by either single mutation. If two genes act in separable activities, they act in parallel. Mutations of two genes in separable processes will cause a more penetrant mutant phenotype than that caused by either single mutation. These activities *in vivo* could represent shared or separable molecular activites important for the process under investigation, such as histone acetylase or ATP-dependent chromatin-remodeling activity.

In this chapter, we report that redundancy exists within each of the synMuv classes. This genetic complexity within a synMuv class is an attribute of synMuv genes, suggesting a redefinition of the synMuv classification scheme. There are only two synMuv classes, A and B, defined by highly penetrant Muv phenotypes when class A and B mutations are combined. Redundancy exists within each synMuv class causing incompletely penetrant Muv phenotypes. In some cases, two genes within the same class did not act in parallel. We believe that this genetic relationship indicates that these genes act in the same process to inhibit vulval fates. Assigning conserved and uncharacterized genes to groups with known activities *in vivo* can define shared functions in a common molecular process.

MATERIALS AND METHODS

Strains and genetics

C. elegans was cultured using the bacterial strain OP50 as described previously (BRENNER 1974). N2 was the wild-type strain. The following mutations were used:
LGI: *lin-35(n745)* (LU and HORVITZ 1998), *lin-61(n3447*, *n3809)* (HARRISON *et al.* 2007a).
LGII: *lin-8(n2731)* (THOMAS *et al.* 2003), *dpl-1(n3316)* (CEOL and HORVITZ 2001), *trr-1(n3712)* (CEOL and HORVITZ 2004), *lin-56(n2728)* (THOMAS *et al.* 2003), *lin-38(n751)* (A.M.S. and H.R.H., unpublished results).
LGIII: *lin-37(n4903)* (ANDERSEN *et al.* 2006), *lin-52(n771)* (THOMAS *et al.* 2003).
LGV: *let-418(n3536)* (CEOL *et al.* 2006), *mys-1(n3681)* (CEOL and HORVITZ 2004).
LGX: *lin-15A(n433*, *n767)* (E.M. Davison *et al.*, unpublished results).
The following balancer chromosomes were used: *mIn1 [mIs14 dpy-10(e128)]* (EDGLEY and RIDDLE 2001) and *nT1 [qIs51]* (MATHIES *et al.* 2003). Other mutant strains are described previously (RIDDLE 1997).

RNAi analyses

RNAi of *efl-1* was performed by injection using clone yk617e4 to synthesize dsRNA as described previously (ANDERSEN *et al.* 2006).

Scoring the vulval cell fate

Using the dissecting microscope, the vulval phenotypes of each strain were scored from three independently grown cultures. At least 100 animals were scored for each genotype. The penetrance of the Muv phenotype was calculated as the number of Muv animals out of the total number of animals. The average percent Muv and standard deviation of the replicates were calculated.

RESULTS

Temperature can be used to sensitize the vulval phenotype

As observed previously, single loss-of-function null mutations of most synMuv genes (Table 1) did not cause a Muv phenotype at any temperature (Tables 2A and 3A). The class A mutations combined with either a class B or class C mutation caused Muv phenotypes (Table 4), confirming that the class A synMuv genes act in parallel to the class B and C genes to inhibit vulval fates. The Muv phenotype caused by synMuv mutations was temperature-sensitive: at higher temperatures the penetrance of the Muv phenotype increased. For example, the penetrance of the *lin-61(n3809); lin-56(n2728)* Muv phenotype increased from 5% at 20ºC to 81% at 22.5ºC (Table 4A), and the penetrance of the *lin-35(n745); lin-15A(n433)* Muv phenotype increased from 10% at 15ºC to 100% at 20ºC (Table 4B). Both *lin-35(n745)* and *lin-15A(n767)* are presumptive null alleles and display the phenotypes associated with a complete loss of gene function. To summarize our results: at low temperatures, most synMuv double mutants had an incompletely penetrant Muv phenotype; at high temperatures, the incompletely penetrant Muv phenotypes at low temperatures were much more penetrant. For all of our analyses, we scored the Muv phenotypes of sensitized class A strains at higher temperatures (20ºC to 22.5ºC) and sensitized class B strains at lower temperatures (15ºC to 20ºC). At these temperatures, the Muv phenotypes were not maximized and phenotypic enhancement could be quantified easily.

Some class AA double mutants have Muv phenotypes

We assayed redundancy within the class A synMuv genes, using temperature to sensitize the vulval cell-fate decision. We observed the vulval phenotypes of animals with null mutations of *lin-8*, *lin-15A* and *lin-56* and a partial loss-of-function mutation of *lin-38* (Tables 1 and 2A). As reported previously, class A single mutants did not have Muv phenotypes at 20ºC (FERGUSON and HORVITZ

1989; THOMAS *et al.* 2003; DAVISON *et al.* 2005). By contrast at 25ºC, some class A synMuv mutations caused incompletely penetrant Muv phenotypes, with less than 1% penetrance (Table 2A). We also observed the vulval phenotypes of class AA double mutants (Table 2B). Most strains were not Muv at 20ºC, but many combinations have Muv phenotypes at 25ºC, ranging from 1% to 33% penetrance. Only the class AA double mutants *lin-8 lin-56* and *lin-56; lin-15A* did not have a Muv phenotype greater than that of either single mutant at 25ºC. These results indicate that not only do the class A and B synMuv genes act in parallel but also that there are separable activities within the class A synMuv genes.

Most class BB double mutants do not have Muv phenotypes

We used the temperature-senstivity of the synMuv phenotype to similarly study the genetic interactions between class B synMuv genes. We used null mutations of the class B synMuv genes *lin-35*, *lin-61*, *dpl-1* and *lin-37,* partial loss-of-function alleles of *lin-52* and *let-418* and RNAi of *efl-1* (Table 1). Because the class C synMuv genes are similar to the class B genes in that class C mutations cause synMuv in combination with class A mutations, we also tested class C synMuv genes in these experiments, using a null allele of *trr-1* and a partial loss-of-function allele of *mys-1*. Unlike the class A genes, most single class B and class BB double synMuv mutants did not have a Muv phenotype at 20ºC or 25ºC (Table 3). The exceptions were the class C synMuv mutation *trr-1(n3712)* and the class B mutation *let-418(n3536)*, which were weakly Muv as single mutants. Many class BB double mutants had a larval-lethal phenotype at 25ºC, indicating that those genes act redundantly to control viability. Also, the null mutant combinations *lin-61(n3809) lin-35(n745)* and *lin-61(n3809); lin-37(n4903)* had weak Muv phenotypes. Because most class BB and class BC double mutants were not appreciably Muv at high temperatures, the class B and C synMuv genes might not have parallel activities or the strength of class B or class C synMuv loss-of-function was not sufficient to cause vulval defects. Because the class C

mutations likely cause a partial loss of gene function, a lack of genetic interaction with the class B genes was not surprising in this non-sensitized background.

Partial loss-of-function mutations in class A or class B synMuv genes sensitize the vulval phenotype

In addition to temperature, genetic background can be used to sensitize the detection of subtle vulval cell-fate defects. For null or strong class AA or class BB double mutants for which no synMuv defect was observed, either the two synMuv genes do not act in parallel or they do act in parallel but loss-of-function mutations of both genes are not sufficient to cause a detectable Muv phenotype. Addition of a partial loss-of-function mutation of a different synMuv class could allow for the detection of subtle parallel activities by enhancement of the incompletely penetrant Muv phenotype. For the detection of subtle parallel activities between class A genes, we used the missense mutation *lin-61(n3447)*, which causes an incompletely penetrant synMuv defect in combination with strong or null class A mutations (Table 4A). This incompletely penetrant Muv phenotype might be enhanced by other null or strong class A mutations if the genes act in parallel to inhibit vulval fates. For the detection of subtle redundancy within class B genes, we used the missense mutation *lin-15A(n433)*, which causes a weak class A synMuv defect (CLARK *et al.* 1994). In a similar way as the sensitization of class A gene function by a partial loss of *lin-61* function (Table 4B), the partial loss of *lin-15A* function might allow for the quantification of subtle differences between class B single and class BB double mutant combinations.

lin-15A and *lin-56* act together to inhibit vulval cell-fate specification

To characterize the redundancy within the class A synMuv genes further, we combined class A single or class AA double mutations with the class B synMuv mutation *lin-61(n3447)*. Single class A synMuv mutations in combination with *lin-61(n3447)* caused Muv phenotypes at 20ºC and 22.5ºC (Table 4A). These vulval phenotypes revealed that *lin-15A* and *lin-38* each have strong inhibitory inputs

into the vulval cell-fate decision, because each had strong synMuv phenotypes in sensitized genetic backgrounds using *lin-61(n3447)*. *lin-8* and *lin-56* have weaker inhibitory inputs, as indicated by the less penetrant Muv phenotypes.

Because *lin-8* and *lin-56* have relatively weak inhibitory inputs, the lack of redundancy observed in the *lin-8 lin-56* and *lin-56; lin-15A* double mutants at 25ºC could reflect the limits of the sensitivity of the assay, or it is possible that those class A genes do not act in parallel. To address redundancy within the class A synMuv genes more sensitively, we constructed triple mutants with two class A synMuv genes and the class B synMuv gene *lin-61* (Table 5). Each class AA synMuv double mutant with an appreciable 25ºC Muv phenotype had a Muv phenotype enhanced over that caused by either single mutation in a *lin-61(n3447)* background. The Muv phenotype of the *lin-61; lin-8 lin-56* triple mutant was stronger than the Muv phenotypes of either *lin-61; lin-8* or *lin-61; lin-56* at 20ºC and 22.5ºC. Thus, *lin-8* and *lin-56* act in parallel, and the lack of a Muv phenotype in the *lin-8 lin-56* double mutant likely indicates the threshold of the synMuv phenotype in the absence of sensitization by a class B mutation. The Muv phenotype of the *lin-61; lin-56; lin-15A* triple mutant was not stronger than *lin-61; lin-56* or *lin-61; lin-15A*. Thus, *lin-15A* and *lin-56* do not act in parallel, indicating that *lin-56* and *lin-15A* act together *in vivo*. This observation is consistent with the molecular data that show LIN-56 and LIN-15A are required for the stability of each other *in vivo* and bind each other *in vitro* (E.M. Davison and H.R.H., unpublished results).

Most class B synMuv genes act in parallel to inhibit vulval cell fates

To observe subtle redundancies within the class B synMuv genes and to assess the relative input of each of the class B synMuv genes into vulval cell-fate inhibition, we combined single class B and class BB double mutants with the weak class A mutation *lin-15A(n433)* (Table 4B and Figure 1). *lin-35* and *lin-37* had the strongest inhibitory inputs, as each had completely penetrant Muv phenotypes at 17.5ºC and 20ºC. *lin-61*, *lin-52*, *let-418* and *mys-1* did not have

appreciably Muv phenotypes at 17.5ºC nor 20ºC, and, therefore, had weaker inhibitory inputs into vulval cell-fate specification.

Like the class A genes, most class B genes displayed redundancy in the inhibition of vulval cell fates in a sensitized background (Figure 1). Nearly all combinations of class BB and class BC double mutants in the *lin-15A(n433)* background had Muv phenotypes greater than those found in the respective single mutants. This difference was observed most notably in strong double mutant combinations at 15ºC, intermediate combinations at 17.5ºC and weak combinations at 20ºC.

Because all tested class BBA and class BCA triple mutants had Muv phenotypes greater than the respective BA or CA double mutants, we tested genes hypothesized to with shared molecular activities. *dpl-1* DP and *efl-1* E2F interact *in vitro* in *C. elegans* (CEOL and HORVITZ 2001) and both *in vitro* and *in vivo* in other organisms (BANDARA *et al.* 1993; HELIN *et al.* 1993; KREK *et al.* 1993). RNAi of *efl-1* in a *lin-15A(n433)* background caused a Muv phenotype that was 8 ± 12% penetrant at 17.5ºC (average ± standard deviation, from assays as performed in Materials and Methods). *dpl-1(n3316); lin-15A(n433)* was 2 ± 2% penetrant at 17.5ºC. RNAi of *efl-1* in *dpl-1(n3316); lin-15A(n433)* mutants did not cause enhancement of the Muv phenotype at 17.5ºC (7 ± 10% Muv). These data indicate that *efl-1* and *dpl-1*, which act as a heterodimeric transcription factor, act together to inhibit vulval fates. Additionally, the *trr-1* TRRAP and *mys-1* MYST homologs might form a histone acetyltransferase complex in mammalian cells (IKURA *et al.* 2000). At 20ºC, the *trr-1(n3712); mys-1(n3681); lin-15A(n433)* class CCA triple mutant did not have a Muv phenotype (6 ± 6% Muv) greater than *trr-1(n3712); lin-15A(n433)* (12 ± 5% Muv) or *mys-1(n3681); lin-15A(n433)* (2 ± 1% Muv), indicating that *trr-1* and *mys-1* share the same activity to inhibit vulval fates. *dpl-1*, *efl-1*, *trr-1* and *mys-1* might not cause a complete loss of gene function because of possible maternal rescue from *dpl-1* and *trr-1* heterozygous mothers and the partial loss of gene function by RNAi of *efl-1* and *mys-1(n3681)*. Because RNAi of *efl-1* enhanced the Muv phenotype of *lin-37(n4903); lin-*

15A(n433) mutants from 59% to 100% at 17.5ºC, and *mys-1(n3681)* enhanced other Muv phenotypes (Figure 1), the decreases of gene functions caused by these mutations were detectable in our assays. Therefore, we believe our results suggest that *dpl-1*, *efl-1* and *trr-1*, *mys-1* each form single activities important for the inhibition of vulval cell fates in *C. elegans*.

DISCUSSION

How should we classify the synMuv genes?

Many synMuv genes have been identified in genetic screens and are grouped into three classes acting in parallel to inhibit vulval fates (FERGUSON and HORVITZ 1985; FERGUSON and HORVITZ 1989; THOMAS *et al.* 2003; POULIN *et al.* 2005; CEOL *et al.* 2006). There are more than 23 class B synMuv genes, whereas the class A and C synMuv genes each number less than a half dozen (THOMAS *et al.* 2003; CEOL and HORVITZ 2004; POULIN *et al.* 2005; CEOL *et al.* 2006).

Mutations of some synMuv genes have been reported to cause incompletely penetrant Muv phenotypes as single mutants, including *let-418*, *lin-13*, *hda-1*, *hpl-2* and the class C genes (FERGUSON and HORVITZ 1985; MELENDEZ and GREENWALD 2000; SOLARI and AHRINGER 2000; VON ZELEWSKY *et al.* 2000; COUTEAU *et al.* 2002; DUFOURCQ *et al.* 2002; CEOL and HORVITZ 2004). These Muv phenotypes are enhanced by loss-of-function mutations of class A synMuv genes, so many of these genes were allocated as class B synMuv genes. Many of these Muv phenotypes were not tested for enhancement by loss-of-function mutations of class B synMuv genes. The class C synMuv mutations were tested for interactions with a few class B mutations, and a weak enhancement of the single class C Muv phenotype was observed, leading to the class C synMuv genes being considered a separate class (CEOL and HORVITZ 2004). Additionally, we observed that some class A single mutants had Muv phenotypes at 25ºC (A.M.S., E.C.A. and H.R.H., unpublished observations), so the class A mutants also have Muv phenotypes as single mutants. Moreover, the class B synMuv histone methyltransferases *met-1* and *met-2* act in parallel with each other and with the class B synMuv genes *hpl-1* and *hpl-2* to inhibit vulval fates (Chapter Two). Because of these numerous exceptions to the synMuv classification scheme, we wondered how to classify new synMuv genes.

We believe that the synMuv classification scheme should be modified given the current data. To date, class A genes are defined as genes in which a

loss-of-function mutation causes a Muv phenotype in combination with one or more class B mutations, and the class B genes are defined as genes in which a loss-of-function mutation causes a Muv phenotype in combination with one or more class A mutations (FERGUSON and HORVITZ 1989). The class C genes are defined as genes in which a loss-of-function mutation causes a Muv phenotype in combination with class A or class B mutations (CEOL and HORVITZ 2004). Our data indicate that all class A genes have activities in parallel with each other to inhibit vulval fates, except *lin-15A* and *lin-56*. Additionally, many class B genes have activities in parallel with each other and single mutations some class B genes and all class C genes cause Muv phenotypes. We suggest that a class A gene should now be defined such that a loss-of-function mutation causes a more penetrant Muv phenotype with class B mutations than as a single mutant or with class A mutations. A class B gene should now be defined such that a loss-of-function mutation causes a more penetrant Muv phenotype with class A mutations than as a single mutant or with class B mutations.

Given this new classification scheme, we suggest that the class C genes should be reclassified as class B genes because these mutations cause a more penetrant Muv phenotype with class A mutations than as single mutants or with class B mutations. The class B genes *hda-1*, *hpl-2*, *let-418* and *lin-13* cause Muv phenotypes as single mutants. For this reason, each gene was thought to be an exception to the synMuv classification scheme and each gene could have merited separate synMuv class designations. Using this new synMuv classification scheme, these genes are class B genes because mutations in these genes cause more penetrant Muv phenotypes with class A mutations than as single mutants or in combination with class B mutations. With this new synMuv classification scheme, much of the controversy and confusion over which genes function in similar activities or processes can be avoided. The activities of synMuv genes in particular processes are addressed better using genetic pathway tests like those we performed in this chapter.

The synMuv classes are composed of genes acting in separable and shared processes

As shown previously, the class A and B synMuv genes have parallel activities, as class AB double mutants have almost completely penetrant Muv phenotypes at 20ºC (FERGUSON and HORVITZ 1989). However, we found that there are separable activities within each of the synMuv classes. Most class AA or class BB double mutants either have incompletely penetrant Muv phenotypes or show enhancement within a synMuv class in sensitivized assays. We believe that the class A and B synMuv genes act broadly in two parallel processes to inhibit vulval fates. However, within each synMuv class, multiple separable and shared processes act to inhibit vulval fates (Figure 2). Given this model, a comprehensive analysis of all synMuv genes will group genes into subclasses that act in separable or shared processes to inhibit vulval fates. This subclassification of the synMuv genes might assign conserved but uncharacterized genes to groups of genes with known functions. In this way, our genetic tests can implicate the homologs of synMuv proteins in well characterized molecular activities, such as specific chromatin-remodeling activities or methods of tumor suppression.

Genes that do not act in parallel within a synMuv class might act in the same process *in vivo*

Synthetic interactions, such as synthetic lethality in *S. cerevisiae* (TONG *et al.* 2001; TONG *et al.* 2004), are used to implicate genes in broad biological processes, like the DNA-damage response (OOI *et al.* 2003). Likewise, the class A and B synMuv genes are required in the same broad biological process: to inhibit vulval fates (FERGUSON and HORVITZ 1989). However, subtle synthetic interactions within a broad biological process are rarely investigated. These subtle synthetic interactions might represent a specific molecular process, such as the movement of nucleosomes important for *lin-3* EGF transcription during vulval development in *C. elegans*. In the same way that strong synthetic

interactions can be used to assign genes to broad biological processes, subtle synthetic interactions can be used to implicate genes in specific molecular activities.

The identified subgroups of the class B genes, *dpl-1*, *efl-1* and *mys-1*, *trr-1,* encode proteins with homologs that in other organisms act in complexes (BANDARA *et al.* 1993; HELIN *et al.* 1993; KREK *et al.* 1993; IKURA *et al.* 2000). The class A proteins LIN-15A and LIN-56 are required for the stability of each other *in vivo* and bind each other *in vitro* (E.M. Davison and H.R. Horvitz, unpublished results). These double mutant combinations did not have enhancement of the Muv phenotype and might represent shared activities *in vivo*. For example MYS-1 and TRR-1 might both be required to acetylate histones to inhibit vulval fates (CEOL and HORVITZ 2004). Subgroups within the synMuv classes could represent proteins that act in a shared biochemical process.

Recently, the *C. elegans* DRM complex was shown to contain many class B synMuv proteins, including LIN-9, LIN-35, LIN-37, LIN-52, LIN-53, LIN-54, DPL-1 and EFL-1 (HARRISON *et al.* 2006). However, the class BB double mutants with *lin-35*, *lin-37* and *lin-52* showed weak parallel activities, suggesting that the proteins in the DRM complex have separable functions during vulval development. It remains to be determined whether other members of the putative DRM complex act together during vulval development. For example, LIN-9 and LIN-53 are hypothesized to bind each other, based upon immunoprecipitation assays of wild-type, *lin-9* and *lin-53* mutant animals (HARRISON *et al.* 2006).

In addition to the DRM complex, there are other putative synMuv complexes based upon homology to other organisms or *in vitro* interaction studies using *C. elegans* proteins, including the LIN-35/EFL-1/DPL-1 Rb/E2F4/DP complex (CEOL and HORVITZ 2001), a NuRD-like complex composed of at least HDA-1, LET-418, LIN-53 and MEP-1 (XUE *et al.* 1998; ZHANG *et al.* 1998; ZHANG *et al.* 1999; UNHAVAITHAYA *et al.* 2002), the LIN-35/LIN-53 Rb/RbAp48 complex (HUANG *et al.* 1991; LU and HORVITZ 1998), and a putative LIN-37/LIN-53 interaction (WALHOUT *et al.* 2000). We plan to investigate whether

the genes listed above act in shared or separable processes to inhibit vulval fates.

Our results suggest that the class B synMuv genes act in separable or shared processes during vulval development. However, the class B genes also control other cell fates during *C. elegans* development. Understanding more about which genes control certain processes might elucidate the genes that act together or separably *in vivo*. Groups of synMuv genes control at least 15 biological processes in *C. elegans* (FERGUSON and HORVITZ 1989; BOXEM and VAN DEN HEUVEL 2001; CHEN and HAN 2001; PAGE *et al.* 2001; BOXEM and VAN DEN HEUVEL 2002; DUFOURCQ *et al.* 2002; FAY *et al.* 2002; UNHAVAITHAYA *et al.* 2002; FAY *et al.* 2003; CUI *et al.* 2004; FAY *et al.* 2004; GARBE *et al.* 2004; REDDY and VILLENEUVE 2004; WANG *et al.* 2005; REDDIEN *et al.* 2007). In many cases, the group of synMuv genes that controls a process is different from the group of genes that regulates other processes. In this way, synMuv proteins could regulate distinct processes by assembling different complexes to control diverse activities. A comprehensive analysis of all class B synMuv genes in a process could be highly informative about the roles of synMuv genes and the activities of their homologs during development.

Redundancy is a hallmark of tumor suppression in humans

The class B synMuv genes are similar to genes involved in tumor suppression, including *lin-35* Rb. Although the class A synMuv genes are not conserved by sequence, their function could be conserved in humans and important for negative regulation of the RTK/Ras pathway as tumor-suppressor genes. The parallel functions of genes involved in tumor suppression are crucial for prevention of inappropriate cell proliferation, a hallmark of carcinogenesis (HANAHAN and WEINBERG 2000). The separable and shared activities observed between and within the synMuv classes might be conserved in humans and relevant for the prevention of tumorigenesis.

ACKNOWLEDGMENTS

We thank Na An for strain management and Hillel Schwartz for critical reading of this manuscript. Strains were provided by the *Caenorhabditis* Genetics Center, which is supported by the National Institutes of Heath National Center for Research Resources. Yuji Kohara of the National Institute of Genetics in Japan kindly provided the *efl-1* cDNA clone. E.C.A. is an Anna Fuller Cancer Research Fellow, and H.R.H. is the David H. Koch Professor of Biology at the Massachusetts Institute of Technology and an Investigator of the Howard Hughes Medical Institute. This work was supported by National Institutes of Health grant GM24663.

LITERATURE CITED

ANDERSEN, E. C., X. LU and H. R. HORVITZ, 2006 *C. elegans* ISWI and NURF301 antagonize an Rb-like pathway in the determination of multiple cell fates. Development **133:** 2695-2704.

BANDARA, L. R., V. M. BUCK, M. ZAMANIAN, L. H. JOHNSTON and N. B. LA THANGUE, 1993 Functional synergy between DP-1 and E2F-1 in the cell cycle-regulating transcription factor DRTF1/E2F. Embo J **12:** 4317-4324.

BOXEM, M., and S. VAN DEN HEUVEL, 2001 *lin-35* Rb and *cki-1* Cip/Kip cooperate in developmental regulation of G1 progression in *C. elegans*. Development **128:** 4349-4359.

BOXEM, M., and S. VAN DEN HEUVEL, 2002 *C. elegans* class B synthetic multivulva genes act in G(1) regulation. Curr Biol **12:** 906-911.

BRENNER, S., 1974 The genetics of *Caenorhabditis elegans*. Genetics **77:** 71-94.

CEOL, C. J., and H. R. HORVITZ, 2001 *dpl-1* DP and *efl-1* E2F act with *lin-35* Rb to antagonize Ras signaling in *C. elegans* vulval development. Mol Cell **7:** 461-473.

CEOL, C. J., and H. R. HORVITZ, 2004 A new class of *C. elegans* synMuv genes implicates a Tip60/NuA4-like HAT complex as a negative regulator of Ras signaling. Dev Cell **6:** 563-576.

CEOL, C. J., F. STEGMEIER, M. M. HARRISON and H. R. HORVITZ, 2006 Identification and classification of genes that act antagonistically to *let-60*

Ras signaling in *Caenorhabditis elegans* vulval development. Genetics **173:** 709-726.

CHEN, Z., and M. HAN, 2001 *C. elegans* Rb, NuRD, and Ras regulate *lin-39*-mediated cell fusion during vulval fate specification. Curr Biol **11:** 1874-1879.

CLARK, S. G., X. LU and H. R. HORVITZ, 1994 The *Caenorhabditis elegans* locus *lin-15*, a negative regulator of a tyrosine kinase signaling pathway, encodes two different proteins. Genetics **137:** 987-997.

COUTEAU, F., F. GUERRY, F. MULLER and F. PALLADINO, 2002 A heterochromatin protein 1 homologue in *Caenorhabditis elegans* acts in germline and vulval development. EMBO Rep **3:** 235-241.

CUI, M., D. S. FAY and M. HAN, 2004 *lin-35*/Rb cooperates with the SWI/SNF complex to control *Caenorhabditis elegans* larval development. Genetics **167:** 1177-1185.

DAVISON, E. M., M. M. HARRISON, A. J. WALHOUT, M. VIDAL and H. R. HORVITZ, 2005 *lin-8*, which antagonizes *C. elegans* Ras-mediated vulval induction, encodes a novel nuclear protein that interacts with the LIN-35 Rb protein. Genetics.

DUFOURCQ, P., M. VICTOR, F. GAY, D. CALVO, J. HODGKIN and Y. SHI, 2002 Functional requirement for histone deacetylase 1 in *Caenorhabditis elegans* gonadogenesis. Mol Cell Biol **22:** 3024-3034.

EDGLEY, M. L., and D. L. RIDDLE, 2001 LG II balancer chromosomes in *Caenorhabditis elegans*: *mT1(II;III)* and the *mIn1* set of dominantly and recessively marked inversions. Mol Genet Genomics **266:** 385-395.

FAY, D. S., S. KEENAN and M. HAN, 2002 *fzr-1* and *lin-35*/Rb function redundantly to control cell proliferation in *C. elegans* as revealed by a nonbiased synthetic screen. Genes Dev **16:** 503-517.

FAY, D. S., E. LARGE, M. HAN and M. DARLAND, 2003 *lin-35*/Rb and *ubc-18*, an E2 ubiquitin-conjugating enzyme, function redundantly to control pharyngeal morphogenesis in *C. elegans*. Development **130:** 3319-3330.

FAY, D. S., X. QIU, E. LARGE, C. P. SMITH, S. MANGO and B. L. JOHANSON, 2004 The coordinate regulation of pharyngeal development in *C. elegans* by *lin-35*/Rb, *pha-1*, and *ubc-18*. Dev Biol **271:** 11-25.

FERGUSON, E. L., and H. R. HORVITZ, 1985 Identification and characterization of 22 genes that affect the vulval cell lineages of the nematode *Caenorhabditis elegans*. Genetics **110:** 17-72.

FERGUSON, E. L., and H. R. HORVITZ, 1989 The multivulva phenotype of certain *Caenorhabditis elegans* mutants results from defects in two functionally redundant pathways. Genetics **123:** 109-121.

FRASER, A. G., R. S. KAMATH, P. ZIPPERLEN, M. MARTINEZ-CAMPOS, M. SOHRMANN and J. AHRINGER, 2000 Functional genomic analysis of *C. elegans* chromosome I by systematic RNA interference. Nature **408:** 325-330.

GARBE, D., J. B. DOTO and M. V. SUNDARAM, 2004 *Caenorhabditis elegans lin-35*/Rb, *efl-1*/E2F and other synthetic multivulva genes negatively regulate

the anaphase-promoting complex gene *mat-3*/APC8. Genetics **167:** 663-672.

HANAHAN, D., and R. A. WEINBERG, 2000 The hallmarks of cancer. Cell **100:** 57-70.

HARRISON, M. M., C. J. CEOL, X. LU and H. R. HORVITZ, 2006 Some *C. elegans* class B synthetic multivulva proteins encode a conserved LIN-35 Rb-containing complex distinct from a NuRD-like complex. Proc Natl Acad Sci U S A **103:** 16782-16787.

HARRISON, M. M., X. LU and H. R. HORVITZ, 2007a LIN-61, one of two *Caenorhabditis elegans* MBT-repeat-containing proteins, acts with the DRM and NuRD-like protein complexes in vulval development but not in certain other biological processes. Genetics.

HARRISON, R., B. PAPP, C. PAL, S. G. OLIVER and D. DELNERI, 2007b Plasticity of genetic interactions in metabolic networks of yeast. Proc Natl Acad Sci U S A **104:** 2307-2312.

HELIN, K., C. L. WU, A. R. FATTAEY, J. A. LEES, B. D. DYNLACHT, C. NGWU and E. HARLOW, 1993 Heterodimerization of the transcription factors E2F-1 and DP-1 leads to cooperative *trans*-activation. Genes Dev **7:** 1850-1861.

HUANG, L. S., P. TZOU and P. W. STERNBERG, 1994 The *lin-15* locus encodes two negative regulators of *Caenorhabditis elegans* vulval development. Mol Biol Cell **5:** 395-411.

HUANG, S., W. H. LEE and E. Y. LEE, 1991 A cellular protein that competes with SV40 T antigen for binding to the retinoblastoma gene product. Nature **350:** 160-162.

IKURA, T., V. V. OGRYZKO, M. GRIGORIEV, R. GROISMAN, J. WANG, M. HORIKOSHI, R. SCULLY, J. QIN and Y. NAKATANI, 2000 Involvement of the TIP60 histone acetylase complex in DNA repair and apoptosis. Cell **102:** 463-473.

KAMATH, R. S., A. G. FRASER, Y. DONG, G. POULIN, R. DURBIN, M. GOTTA, A. KANAPIN, N. LE BOT, S. MORENO, M. SOHRMANN, D. P. WELCHMAN, P. ZIPPERLEN and J. AHRINGER, 2003 Systematic functional analysis of the *Caenorhabditis elegans* genome using RNAi. Nature **421:** 231-237.

KREK, W., D. M. LIVINGSTON and S. SHIRODKAR, 1993 Binding to DNA and the retinoblastoma gene product promoted by complex formation of different E2F family members. Science **262:** 1557-1560.

LU, X., and H. R. HORVITZ, 1998 *lin-35* and *lin-53*, two genes that antagonize a *C. elegans* Ras pathway, encode proteins similar to Rb and its binding protein RbAp48. Cell **95:** 981-991.

MATHIES, L. D., S. T. HENDERSON and J. KIMBLE, 2003 The *C. elegans* Hand gene controls embryogenesis and early gonadogenesis. Development **130:** 2881-2892.

MELENDEZ, A., and I. GREENWALD, 2000 *Caenorhabditis elegans lin-13*, a member of the LIN-35 Rb class of genes involved in vulval development, encodes a protein with zinc fingers and an LXCXE motif. Genetics **155:** 1127-1137.

OOI, S. L., D. D. SHOEMAKER and J. D. BOEKE, 2003 DNA helicase gene interaction network defined using synthetic lethality analyzed by microarray. Nat Genet **35:** 277-286.

PAGE, B. D., S. GUEDES, D. WARING and J. R. PRIESS, 2001 The *C. elegans* E2F- and DP-related proteins are required for embryonic asymmetry and negatively regulate Ras/MAPK signaling. Mol Cell **7:** 451-460.

PARK, E. C., and H. R. HORVITZ, 1986 Mutations with dominant effects on the behavior and morphology of the nematode *Caenorhabditis elegans*. Genetics **113:** 821-852.

POULIN, G., Y. DONG, A. G. FRASER, N. A. HOPPER and J. AHRINGER, 2005 Chromatin regulation and sumoylation in the inhibition of Ras-induced vulval development in *Caenorhabditis elegans*. Embo J **24:** 2613-2623.

REDDIEN, P. W., E. C. ANDERSEN, M. C. HUANG and H. R. HORVITZ, 2007 DPL-1 DP, LIN-35 Rb and EFL-1 E2F Act With the MCD-1 Zinc-Finger Protein to Promote Programmed Cell Death in *Caenorhabditis elegans*. Genetics **175:** 1719-1733.

REDDY, K. C., and A. M. VILLENEUVE, 2004 *C. elegans* HIM-17 links chromatin modification and competence for initiation of meiotic recombination. Cell **118:** 439-452.

RIDDLE, D. L., BLUMENTHAL T., MEYER, B.J., PRIESS, J.R., 1997 *C. elegans II*. Cold Spring Harbor Laboratory Press, Cold Spring Harbor.

SIEBER, P., F. WELLMER, J. GHEYSELINCK, J. L. RIECHMANN and E. M. MEYEROWITZ, 2007 Redundancy and specialization among plant microRNAs: role of the

MIR164 family in developmental robustness. Development **134:** 1051-1060.

SOLARI, F., and J. AHRINGER, 2000 NURD-complex genes antagonise Ras-induced vulval development in *Caenorhabditis elegans*. Curr Biol **10:** 223-226.

STERNBERG, P. W., 2006 Pathway to RAS. Genetics **172:** 727-731.

SULSTON, J. E., and H. R. HORVITZ, 1977 Post-embryonic cell lineages of the nematode, *Caenorhabditis elegans*. Dev Biol **56:** 110-156.

SUNDARAM, M. V., 2005 The love-hate relationship between Ras and Notch. Genes Dev **19:** 1825-1839.

THOMAS, J. H., C. J. CEOL, H. T. SCHWARTZ and H. R. HORVITZ, 2003 New genes that interact with *lin-35* Rb to negatively regulate the *let-60* ras pathway in *Caenorhabditis elegans*. Genetics **164:** 135-151.

TONG, A. H., M. EVANGELISTA, A. B. PARSONS, H. XU, G. D. BADER, N. PAGE, M. ROBINSON, S. RAGHIBIZADEH, C. W. HOGUE, H. BUSSEY, B. ANDREWS, M. TYERS and C. BOONE, 2001 Systematic genetic analysis with ordered arrays of yeast deletion mutants. Science **294:** 2364-2368.

TONG, A. H., G. LESAGE, G. D. BADER, H. DING, H. XU, X. XIN, J. YOUNG, G. F. BERRIZ, R. L. BROST, M. CHANG, Y. CHEN, X. CHENG, G. CHUA, H. FRIESEN, D. S. GOLDBERG, J. HAYNES, C. HUMPHRIES, G. HE, S. HUSSEIN, L. KE, N. KROGAN, Z. LI, J. N. LEVINSON, H. LU, P. MENARD, C. MUNYANA, A. B. PARSONS, O. RYAN, R. TONIKIAN, T. ROBERTS, A. M. SDICU, J. SHAPIRO, B. SHEIKH, B. SUTER, S. L. WONG, L. V. ZHANG, H. ZHU, C. G. BURD, S.

MUNRO, C. SANDER, J. RINE, J. GREENBLATT, M. PETER, A. BRETSCHER, G. BELL, F. P. ROTH, G. W. BROWN, B. ANDREWS, H. BUSSEY and C. BOONE, 2004 Global mapping of the yeast genetic interaction network. Science **303:** 808-813.

UNHAVAITHAYA, Y., T. H. SHIN, N. MILIARAS, J. LEE, T. OYAMA and C. C. MELLO, 2002 MEP-1 and a homolog of the NURD complex component Mi-2 act together to maintain germline-soma distinctions in *C. elegans*. Cell **111:** 991-1002.

VON ZELEWSKY, T., F. PALLADINO, K. BRUNSCHWIG, H. TOBLER, A. HAJNAL and F. MULLER, 2000 The *C. elegans* Mi-2 chromatin-remodelling proteins function in vulval cell fate determination. Development **127:** 5277-5284.

WALHOUT, A. J., R. SORDELLA, X. LU, J. L. HARTLEY, G. F. TEMPLE, M. A. BRASCH, N. THIERRY-MIEG and M. VIDAL, 2000 Protein interaction mapping in *C. elegans* using proteins involved in vulval development. Science **287:** 116-122.

WANG, D., S. KENNEDY, D. CONTE, JR., J. K. KIM, H. W. GABEL, R. S. KAMATH, C. C. MELLO and G. RUVKUN, 2005 Somatic misexpression of germline P granules and enhanced RNA interference in retinoblastoma pathway mutants. Nature **436:** 593-597.

WINZELER, E. A., D. D. SHOEMAKER, A. ASTROMOFF, H. LIANG, K. ANDERSON, B. ANDRE, R. BANGHAM, R. BENITO, J. D. BOEKE, H. BUSSEY, A. M. CHU, C. CONNELLY, K. DAVIS, F. DIETRICH, S. W. DOW, M. EL BAKKOURY, F. FOURY, S. H. FRIEND, E. GENTALEN, G. GIAEVER, J. H. HEGEMANN, T. JONES, M. LAUB, H. LIAO, N. LIEBUNDGUTH, D. J. LOCKHART, A. LUCAU-DANILA, M. LUSSIER, N. M'RABET, P. MENARD, M. MITTMANN, C. PAI, C. REBISCHUNG, J.

L. REVUELTA, L. RILES, C. J. ROBERTS, P. ROSS-MACDONALD, B. SCHERENS, M. SNYDER, S. SOOKHAI-MAHADEO, R. K. STORMS, S. VERONNEAU, M. VOET, G. VOLCKAERT, T. R. WARD, R. WYSOCKI, G. S. YEN, K. YU, K. ZIMMERMANN, P. PHILIPPSEN, M. JOHNSTON and R. W. DAVIS, 1999 Functional characterization of the *S. cerevisiae* genome by gene deletion and parallel analysis. Science **285:** 901-906.

XUE, Y., J. WONG, G. T. MORENO, M. K. YOUNG, J. COTE and W. WANG, 1998 NURD, a novel complex with both ATP-dependent chromatin-remodeling and histone deacetylase activities. Mol Cell **2:** 851-861.

ZHANG, Y., G. LEROY, H. P. SEELIG, W. S. LANE and D. REINBERG, 1998 The dermatomyositis-specific autoantigen Mi2 is a component of a complex containing histone deacetylase and nucleosome remodeling activities. Cell **95:** 279-289.

ZHANG, Y., H. H. NG, H. ERDJUMENT-BROMAGE, P. TEMPST, A. BIRD and D. REINBERG, 1999 Analysis of the NuRD subunits reveals a histone deacetylase core complex and a connection with DNA methylation. Genes Dev **13:** 1924-1935.

Table 1: synMuv alleles used in this study.

class A gene	allele	mutation	putative null?
lin-8	*n2731*	Q113ochre	Yes
lin-15A	*n767*	deletion	Yes
lin-15A	*n433*	A250V	No
lin-38	*n751*	R517C	No[a, b, c]
lin-56	*n2728*	deletion	Yes
class B gene			
lin-35	*n745*	W151opal	Yes
lin-61	*n3809*	Q159ochre	Yes
lin-61	*n3447*	S354N	No
dpl-1	*n3316*	deletion	Yes[a]
lin-37	*n4903*	deletion	Yes
lin-52	*n771*	E36K	No[c]
efl-1	RNAi	NA	No[c]
let-418	*n3536*	P675L	No[c]
class C gene			
trr-1	*n3712*	W2593amber	Yes[a]
mys-1	*n3681*	G341R	No[c]

[a] This mutation recessively causes a sterile phenotype. The homozygous animals examined could therefore possess some maternally provided gene activity.

[b] In these cases, we used non-null alleles because the null alleles cause sterility or larval arrest.

[c] A.M.S., E. Davison, and H.R.H., unpublished results.

NA, not applicable

Table 2: Many class A synMuv double mutants have a multivulva phenotype.

A. genotype[a]	**% multivulva ± s.d.**[b]	
	20ºC	**25ºC**
wild type	0 ± 0	0 ± 0
lin-8	0 ± 0	0 ± 0
lin-56	0 ± 0	1 ± 0
lin-38	0 ± 0	1 ± 1
lin-15A	0 ± 0	0 ± 0
B. genotype[a]		
lin-8 lin-56	0 ± 0	0 ± 0
lin-8 lin-38	1 ± 1	7 ± 2
lin-8; lin-15A	0 ± 0	13 ± 6
lin-56 lin-38	0 ± 0	6 ± 4
lin-56; lin-15A	0 ± 0	1 ± 0
lin-38; lin-15A	0 ± 0	33 ± 10

[a] The alleles used are described in Table 1. The null allele *lin-15A(n767)* was used for these analyses.

[b] % multivulva was determined as described in Materials and Methods. s.d., standard deviation.

Table 3: Class B and C synMuv single and class BB and BC double mutants do not have appreciably Muv phenotypes.

A. genotype[a]	**% multivulva ± s.d.**[b]	
	20ºC	**25ºC**
wild type	0 ± 0	0 ± 0
lin-35	0 ± 0	0 ± 0
lin-61	0 ± 0	0 ± 0
dpl-1[c]	0 ± 0	0 ± 0
trr-1[c]	2 ± 1	3 ± 2
lin-37	0 ± 0	0 ± 0
lin-52	0 ± 0	0 ± 0
let-418	0 ± 0	1 ± 0
mys-1	0 ± 0	0 ± 0
efl-1	0 ± 0	0 ± 0
B. genotype[a]		
lin-35 lin-61	0 ± 0	1 ± 0
lin-35; lin-37	0 ± 0	0 ± 0
lin-35; lin-52	0 ± 0	0 ± 1
lin-35; let-418	0 ± 0	Lvl
lin-35; mys-1	0 ± 0	Lvl
lin-35; efl-1	0 ± 0	0 ± 0
lin-61; lin-37	0 ± 0	1 ± 1
lin-61; lin-52	0 ± 0	0 ± 0
lin-61; let-418	2 ± 2	Lvl
lin-61; mys-1	0 ± 0	Lvl
dpl-1; efl-1[c]	0 ± 0	0 ± 0
trr-1; mys-1[c]	4 ± 3	Lvl
lin-37; let-418	0 ± 0	0 ± 0
lin-37; mys-1	0 ± 0	Lvl
lin-37; efl-1	0 ± 0	0 ± 0
lin-52; let-418	0 ± 0	0 ± 0
lin-52; mys-1	0 ± 0	Lvl
let-418 mys-1	0 ± 0	Lvl

[a] The alleles used are described in Table 1. The null allele *lin-61(n3809)* was used for these analyses.

[b] % multivulva was determined as described in Materials and Methods. s.d., standard deviation.

[c] These animals were descended from synMuv mutant heterozygotes because the mutations recessively cause sterility.

Lvl, Larval lethality

Table 4: Partial loss-of-function mutations of class A and B synMuv genes sensitize the vulval phenotype

A. genotype[a]	**% multivulva ± s.d.**[b]	
	20ºC	**22.5ºC**
wild type	0 ± 0	0 ± 0
lin-8	8 ± 6	69 ± 3
lin-56	5 ± 1	81 ± 8
lin-38	32 ± 18	99 ± 1
lin-15A	21 ± 8	97 ± 2

B. genotype[c]	**% multivulva ± s.d.**[b]		
	15ºC	**17.5ºC**	**20ºC**
wild type	0.0 ± 0.0	0.0 ± 0.0	0.0 ± 0.0
lin-35(n745)	10 ± 2.5	65 ± 9.7	100 ± 0.0
lin-61(n3809)	0.0 ± 0.0	0.5 ± 0.5	19 ± 17
dpl-1(n3316)[d]	0.0 ± 0.0	2.4 ± 2.1	70 ± 6.6
trr-1(n3712)[d]	0.6 ± 1.0	3.5 ± 5.1	12 ± 5.2
lin-37(n4903)	3.7 ± 2.9	59 ± 11	100 ± 0.0
lin-52(n771)	0.3 ± 0.5	0.0 ± 0.0	15 ± 5.9
let-418(n3536)	0.0 ± 0.0	0.0 ± 0.0	0.2 ± 0.3
mys-1(n3681)	0.2 ± 0.4	0.0 ± 0.0	1.8 ± 1.2
*efl-1(*RNAi*)*	0.0 ± 0.0	7.5 ± 12	92 ± 7.4

[a] These strains all contain the class B synMuv mutation *lin-61(n3447)*. The alleles used are described in Table 1. *lin-15A(n767)* was used in these analyses.

[b] % multivulva was determined as described in Materails and Methods. s.d., standard deviation.

[c] These strains all contain the class A synMuv mutation *lin-15A(n433)*. The alleles used are described in Table 1. *lin-61(n3809)* was used in the analyses.

[d] These animals were descended from synMuv mutant heterozygotes because the mutations cause recessive sterility.

Table 5: Most class A synMuv genes act in parallel to inhibit vulval fates

A. genotype[a]	% multivulva ± s.d.[b]	
	20ºC	22.5ºC
lin-8 lin-56	21 ± 11	95 ± 2
lin-8 lin-38	69 ± 8	100 ± 0
lin-8; lin-15A	60 ± 7	100 ± 1
llin-56 lin-38	49 ± 13	100 ± 0
lin-56; lin-15A	14 ± 7	97 ± 2
lin-38; lin-15A	78 ± 10	100 ± 0

[a] These strains all contain the class B synMuv mutation *lin-61(n3447)*. The alleles used are described in Table 1. *lin-15A(n767)* was used in these analyses.

[b] % multivulva was determined as described in Materials and Methods. s.d., standard deviation.

FIGURE DESCRIPTIONS

Figure 1: All tested class B and C genes act in parallel to inhibit vulval fates

Each strain was grown at the temperature shown in the top left magenta part of the figure. All strains contain the class A synMuv mutation *lin-15A(n433)*. The alleles used are described in Table 1. *lin-61(n3809)* was used in these analyses. The % Muv was determined as described in Materials and methods and the average % Muv and standard deviation are shown.

Figure 1

15ºC	*lin-35*	*lin-37*	*lin-52*	*lin-61*	*let-418*	*mys-1*
lin-35	10 ± 3	72 ± 6	23 ± 3	97 ± 3	50 ± 5	67 ± 9
lin-37		4 ± 3	ND	95 ± 3	33 ± 5	29 ± 5
lin-52			0 ± 1	17 ± 7	0 ± 0	1 ± 1
lin-61				0 ± 0	3 ± 1	1 ± 1
let-418					0 ± 0	ND
mys-1	All strains contain *lin-15A(n433)*					0 ± 0

17.5ºC	*lin-35*	*lin-37*	*lin-52*	*lin-61*	*let-418*	*mys-1*
lin-35	65 ± 10	100 ± 0	93 ± 10	100 ± 1	100 ± 0	99 ± 1
lin-37		59 ± 11	ND	100 ± 0	96 ± 6	92 ± 7
lin-52			0 ± 0	58 ± 18	1 ± 2	6 ± 6
lin-61				1 ± 1	9 ± 2	9 ± 6
let-418					0 ± 0	ND
mys-1	All strains contain *lin-15A(n433)*					0 ± 0

20ºC	*lin-35*	*lin-37*	*lin-52*	*lin-61*	*let-418*	*mys-1*
lin-35	100 ± 0	100 ± 0	100 ± 0	100 ± 0	100 ± 0	100 ± 0
lin-37		100 ± 0	ND	100 ± 0	100 ± 0	100 ± 0
lin-52			15 ± 6	100 ± 0	89 ± 10	97 ± 1
lin-61				19 ± 17	94 ± 5	93 ± 6
let-418					0 ± 0	ND
mys-1	All strains contain *lin-15A(n433)*					2 ± 1

Figure 2: Parallel activities between and within the synMuv classes inhibit vulval cell fates.

The class A and B synMuv genes act in separate processes to inhibit vulval cell-fate specification. Additionally, each class is composed of many separable activities, except for the following genes that act together. *lin-15A* and *lin-56* perform a single process within the class A genes, while the following gene pairs act in single process within the class B genes to inhibit vulval cell fates: *dpl-1*, *efl-1* and *mys-1*, *trr-1*.

Figure 2

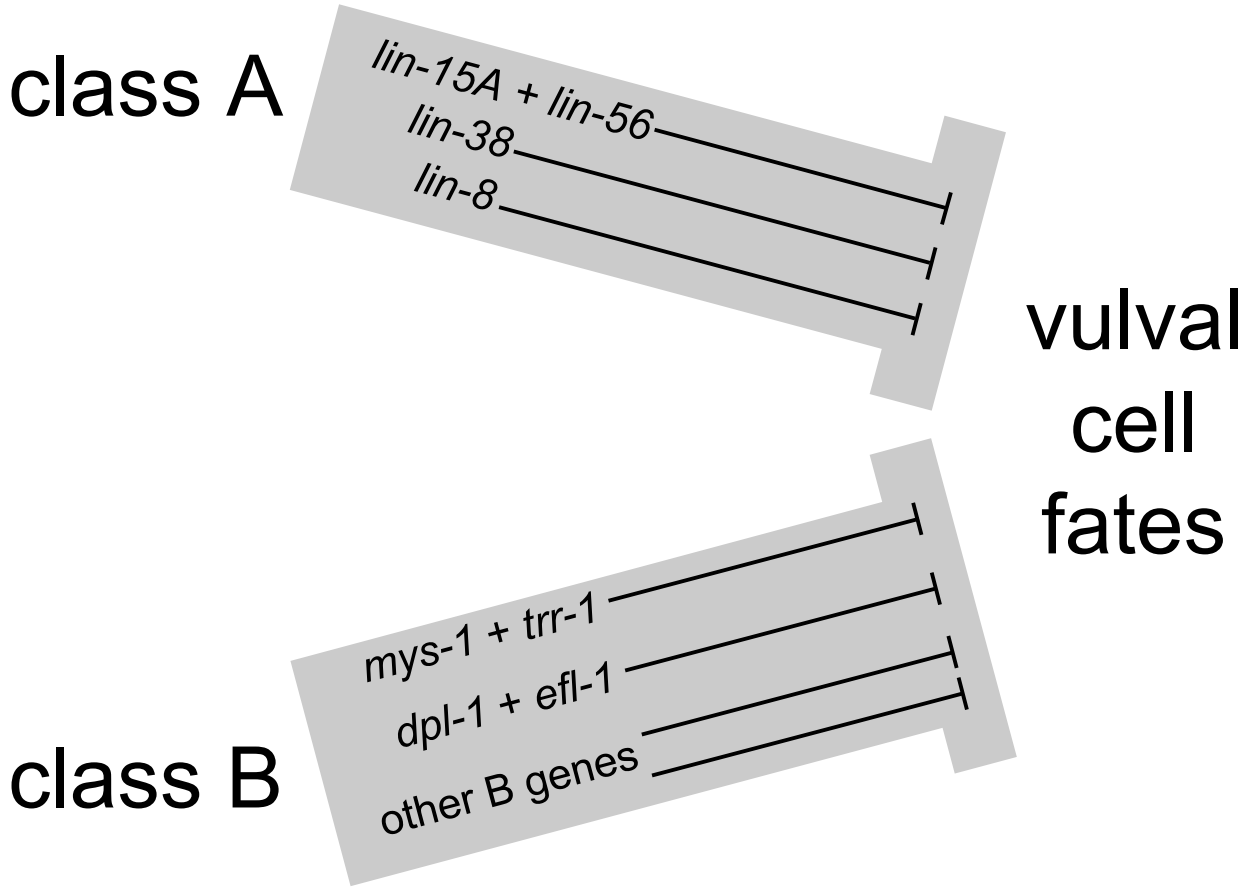
class A
lin-15A + lin-56
lin-38
lin-8
vulval
cell
fates
mys-1 + trr-1
dpl-1 + efl-1
other B genes
class B

CHAPTER FOUR

C. elegans ISWI and NURF301 antagonize an Rb-like pathway in the determination of multiple cell fates

Erik C. Andersen, Xiaowei Lu[1] and H. Robert Horvitz

[1] *Present address:* Department of Cell Biology, University of Virginia School of Medicine, Charlottesville, VA 22908

Graduate student Xiaowei Lu isolated and cloned *isw-1* as a suppressor of the synMuv phenotype. I performed all subsequent experiments and wrote the manuscript.

This chapter is published as Andersen *et al.* (2006) Development 133(14):2695-2704

SUMMARY

The class A, B and C synthetic multivulva (synMuv) genes act redundantly to negatively regulate the expression of vulval cell fates in *Caenorhabditis elegans.* The class B and C synMuv proteins include homologs of proteins that modulate chromatin and influence transcription in other organisms similar to members of the Myb-MuvB/dREAM, NuRD and Tip60/NuA4 complexes. To determine how these chromatin-remodeling activities negatively regulate the vulval cell-fate decision, we isolated a suppressor of the synMuv phenotype and found that the suppressor gene encodes the *C. elegans* homolog of *Drosophila melanogaster* ISWI. The *C. elegans* ISW-1 protein likely acts as part of a Nucleosome Remodeling Factor (NURF) complex with NURF-1, a nematode ortholog of NURF301, to promote the synMuv phenotype. *isw-1* and *nurf-1* mutations suppress both the synMuv phenotype and the multivulva phenotype caused by overactivation of the Ras pathway. Our data suggest that a NURF-like complex pomotes the expression of vulval cell fates by antagonizing the transcriptional and chromatin-remodeling activities of complexes similar to Myb-MuvB/dREAM, NuRD and Tip60/NuA4. Because the phenotypes caused by a null mutation in the tumor-suppressor and class B synMuv gene *lin-35* Rb and a gain-of-function mutation in *let-60* Ras are suppressed by reduction of *isw-1* function, NURF complex proteins might be effective targets for cancer therapy.

INTRODUCTION

The ordered recruitment of factors required for proper gene expression is crucial for animal development. For example, sequence-specific transcription factors recruit a variety of protein complexes that remodel chromatin to regulate the transcription of target genes either by using the energy of ATP hydrolysis to move nucleosomes or by chemically modifying histones (NARLIKAR *et al.* 2002). These two mechanisms for chromatin remodeling have been characterized extensively in vitro (ROTH *et al.* 2001; SMITH and PETERSON 2005), but efforts to understand how each functions in the development of metazoa have just begun.

Studies of vulval development in the nematode *Caenorhabditis elegans* could help establish the roles of chromatin remodeling during development. The vulva of the *C. elegans* hermaphrodite is formed by the 22 descendants of three ectodermal blast cells (P5.p, P6.p and P7.p) located along the ventral surface of the animal (SULSTON and HORVITZ 1977). P(5-7).p, three of a set of six equipotent cells P(3-8).p called the vulval equivalence group, are induced to generate vulval cells by an epidermal growth factor (EGF)-like signal from the gonad (SULSTON and WHITE 1980; HILL and STERNBERG 1992). The inductive signal is received and transduced by a conserved receptor tyrosine kinase (RTK)/Ras pathway (KORNFELD 1997). Unlike the other cells of the vulval equivalence group (P3.p, P4.p and P8.p), which divide once and fuse with the nearby hypodermal syncytium (hyp7), P(5-7).p divide three times to generate the cells that form the adult vulva (SULSTON and HORVITZ 1977). Mutations that reduce or eliminate the function of the *let-23* RTK/ *let-60* Ras pathway can result in a vulvaless (Vul) animal in which no cells of the vulval equivalence group express vulval fates; by contrast, mutations that increase the function of this pathway can cause the ectopic adoption of vulval cell fates by P3.p, P4.p and P8.p and result in a multivulva (Muv) animal (BEITEL *et al.* 1990; HAN *et al.* 1990; KATZ *et al.* 1996).

Loss-of-function mutations in the synthetic multivulva (synMuv) genes also can cause a Muv phenotype (HORVITZ and SULSTON 1980; FERGUSON and HORVITZ 1989). These genes have been grouped into three classes, A, B and C

(FERGUSON and HORVITZ 1989; CEOL and HORVITZ 2004). Loss-of-function mutations within any one class do not cause a Muv phenotype, whereas mutations in any two genes within two different classes cause a Muv phenotype (FERGUSON and HORVITZ 1989; CEOL and HORVITZ 2004). The class A synMuv genes encode novel, nuclear components (CLARK *et al.* 1994; HUANG *et al.* 1994; DAVISON *et al.* 2005). Many class B synMuv genes encode homologs of transcriptional repressors and factors that remodel chromatin, including LIN-35 Rb (LU and HORVITZ 1998), the EFL-1/DPL-1 E2F heterodimeric transcription factor (CEOL and HORVITZ 2001), the HDA-1 HDAC1, LET-418 Mi2, LIN-53 RbAp48 NuRD complex (LU and HORVITZ 1998; TONG *et al.* 1998; XUE *et al.* 1998; VON ZELEWSKY *et al.* 2000; UNHAVAITHAYA *et al.* 2002) and HPL-2 Heterochromatin Protein 1 (HP1, (COUTEAU *et al.* 2002). The *Drosophila melanogaster* homologs of some class B synMuv proteins form a complex, identified by two different groups and called Myb-MuvB or dREAM, that is likely to repress the transcription of genes through chromatin remodeling (KORENJAK *et al.* 2004; LEWIS *et al.* 2004). Class C synMuv genes encode homologs of a putative Tip60/NuA4 histone acetyltransferase complex (CEOL and HORVITZ 2004). Because of these homologies, the synMuv genes, which negatively regulate the vulval cell fate, likely by repressing the transcription of genes that promote expression of the vulval cell fates.

In this study, we describe the identification of a *C. elegans* ortholog of *Drosophila ISWI*, called *isw-1*, as a suppressor of the synMuv phenotype. ISWI is an ATP-dependent chromatin-remodeling enzyme identified by homology to *S. cerevisiae* Snf2/Swi2 (ELFRING *et al.* 1994). We show that ISW-1 likely acts as a component of a Nucleosome Remodeling Factor (NURF)-like complex with the *Drosophila* NURF301 ortholog NURF-1 to antagonize the synMuv genes. Our observations reveal the antagonistic functions of a NURF-like chromatin remodeling complex and complexes similar to Myb-MuvB/dREAM, NuRD and TIP60/NuA4 in the determination of multiple cell fates, including the antagonistic regulation of at least one putative target of synMuv transcriptional repression.

MATERIALS AND METHODS

Strains and genetics

C. elegans strains were cultured as described previously and maintained at 20ºC unless otherwise noted (BRENNER 1974). N2 (Bristol) was the wild-type strain. The following mutations and integrants were used:

LGI: *dpy-5(e61)*, *lin-35(n745)*, *lin-53(n833*, *n3368)* (*n3368*, this study), *ccIs4251* (HSIEH *et al.* 1999);

LGII: *unc-4(e120)*, *nurf-1(n4293*, *n4295)* (this study), *dpl-1(n3316)* (CEOL and HORVITZ 2001), *lin-8(n111, n2731)* (THOMAS *et al.* 2003), *lin-56(n2728)* (THOMAS *et al.* 2003), *lin-38(n751)*, *trr-1(n3712)* (CEOL and HORVITZ 2004), *lin-31(n301)*, *let-23(sa62)* (KATZ *et al.* 1996), *rrf-3(pk1426)* (SIMMER *et al.* 2002);

LGIII: *dpy-17(e164)*, *isw-1(n3294*, *n3297*, *n4066)* (this study), *lin-9(n112*, *n942)* (BEITEL *et al.* 2000), *lin-36(n766)* (THOMAS and HORVITZ 1999), *lin-37(n758*, *n2234)* (FERGUSON and HORVITZ 1989; THOMAS *et al.* 2003), *lin-52(n3718)* (THOMAS *et al.* 2003), *lin-13(n387)* (MELENDEZ and GREENWALD 2000), *hpl-2(tm1489)*, *flt-1(tm235)*;

LGIV: *unc-30(e191)*, *pyp-1(n4599)* (this study), *let-60(n1046)* (BEITEL *et al.* 1990; HAN *et al.* 1990), *lin-1(n304*, *e1275)*;

LGV: *unc-46(e177)*, *let-418(n3536*, *n3719)*, *mep-1(q660)*, *lin-54(n3423)*, *hda-1(e1795)* (DUFOURCQ *et al.* 2002), *tam-1(cc567)* (HSIEH *et al.* 1999), *lin-45(ku112)* (SUNDARAM and HAN 1995), *him-5(e1490)*;

LGX: *lin-15A(n767*, *n433)*, *lin-15B(n744)*, *lin-15AB(n765*, *e1763)*, *lin-2(n768)*.

The following reciprocal translocations containing GFP-expressing transgenes integrated at or near the translocation breakpoints were used: *hT2 [qIs48]* LGI; LGIII and *nT1 [qIs51]* LGIV; LGV. *mIn1 [mIs14 dpy-10(e128)]* is a balancer chromosome that expresses GFP. The following mutations were provided by C. Ceol, F. Stegmeier and M. Harrison: *let-418(n3536*, *n3719)*, *lin-54(n3423)*, *mep-1(n3703)*. *flt-1(tm235)* and *hpl-2(tm1489)* were provided by S. Mitani. Those mutant alleles for which no citation is given are described previously (RIDDLE 1997).

RNAi analyses

RNAi by injection was performed as described previously (CEOL and HORVITZ 2004), except single-stranded RNA molecules were annealed by incubation at 85ºC for 15 minutes, then at 37ºC for 30 minutes and slowly cooled to room temperature for one hour. RNAi of *F37A4.6*, the gene predicted to be within an intron of *isw-1*, did not suppress the synMuv phenotype of *lin-53(n833); lin-15A(n767)* mutants (data not shown). The following constructs were used to make dsRNA: for *isw-1*, yk593a10 and yk617c10; for *nurf-1*, yk273g2, yk1151c6, pEA30 (a cDNA encoding the 3' end of *nurf-1b, c, d* and *e*) and pEA147 (a RT-PCR product corresponding to only *nurf-1a*); for *pyp-1*, yk169c6; for *rba-1*, yk117c9; for *H20J04.2*, yk230c2 and yk323f2; for *T26A5.8*, yk471d3; and for*Y53F4B.3*, yk393b2 and yk1412b12. Yuji Kohara kindly provided all yk clones.

Determination of gene structures

For *isw-1*, the sequences of two independent cDNAs, yk593a10 and yk617c10, were determined. 5' rapid amplification of cDNA ends (5' RACE, Invitrogen) was used to determine the 5' end of *isw-1*, and an SL1 splice-leader sequence was detected. For *nurf-1*, the sequences of 15 independent cDNAs were determined: yk62e9 (pEA30), yk98g1, yk172b9, yk374b9, yk381c2, yk480b9, yk565d9, yk752a4, yk765d8, yk879b11, yk1030g7, yk1151c6, yk1288b1, yk1456g11, yk1691d5. Gene-specific primers were used to amplify reverse-transcribed products by PCR to confirm several *nurf-1* transcripts, and a Stratagene *C. elegans* cDNA library also was used for PCR analyses of *nurf-1* gene structures. The 5' ends of *nurf-1b* and *nurf-1c* were identified by SL1 RT-PCR, and the 5' ends of *nurf-1a*, *d* and *e* are from GeneFinder (LIANG *et al.* 2001) predictions.

Isolation of deletion alleles

Genomic DNA pools from EMS-mutagenized animals were screened for deletions using PCR as described previously (CEOL and HORVITZ 2001). Deletion mutant animals were isolated from frozen stocks and backcrossed to the wild type at least twice. *isw-1(n4066)* removes nucleotides 20629 to 21932 of cosmid F37A4. *nurf-1(n4293)* removes 3058 to 3782, and *nurf-1(n4295)* removes 18656

to 19733 of cosmid F26H11. *pyp-1(n4599)* removes nucleotides 26777 to 28936 of cosmid C47E12. *lin-53(n3368)* removes nucleotides 38104 to 38857 of cosmid K07A1.

Scoring of vulval cell fates

For *trr-1(n3712)* and *trr-1(n3712); lin-15B(n744)*, vulval induction was scored during the L4 larval stage using Nomarski optics. If more than three of the six Pn.p cells were induced, the animals were counted as Muv.

Antibody staining

We cloned a full-length *isw-1* cDNA into a vector containing the coding sequence for the maltose-binding protein (MBP). Antisera recognizing ISW-1 were generated by injecting MBP:ISW-1 into two rabbits (Covance). Anti-ISW-1 antibodies were affinity purified using GST (glutathione S-transferase)-tagged ISW-1 as described previously (KOELLE and HORVITZ 1996). Embryos, larvae and adults were fixed as described (FINNEY and RUVKUN). Affinity-purified antibodies were used at a 1:10 dilution for whole-mount staining and at 1:1000 for western blots. Horseradish peroxidase-conjugated secondary antibodies (Jackson ImmunoResearch) were used at 1:3000 for western blots, and Alexfluor 488 (Invitrogen) was used at a 1:200 dilution for detection by whole-mount immunocytochemistry.

Determination of mutant sequences

We used PCR-amplified regions of genomic DNA to determine mutant sequences. For both *isw-1* alleles, all exons and splice junction sequences were determined. All mutations were confirmed using independently derived PCR products. Sequences were determined using an ABI Prism 3100 Genetic Analyzer.

Germline transformation experiments

Germline transformation experiments were performed as described (MELLO *et al.* 1991). For rescue of the *lin-53(n833); isw-1(n3294); lin-15A(n767)* synMuv suppression phenotype, we injected cosmid C28G2 (30 ng/μl). 100 μg/μL of 1 kb DNA ladder (Invitrogen) was used to increase the complexity of the

extrachromosomal arrays, and pTG96 (*sur-5::gfp*) (YOCHEM *et al.* 1998) was used as the coinjection marker at 20 ng/μL.

Suppression of non-vulval defects caused by class B synMuv mutations

Using the same exposure time, GFP expression (Tam phenotype) was quantified for each micrograph within the linear range for signal detection using the Profiler function of the OpenLab software package (Improvision). PGL-1 staining and RNAi sensitivity were scored as described previously (WANG *et al.* 2005). The L1 larval arrest phenotypes of *let-418(n3536)* and *mep-1(n3701)* were scored at 25ºC.

RESULTS

Loss of function of the *C. elegans* homolog of *Drosophila* ISWI causes suppression of the *lin-53; lin-15A* synMuv phenotype

We screened for suppressors of the *lin-53(n833); lin-15A(n767)* synMuv phenotype and identified two mutations, *n3294* and *n3297*, that failed to complement for suppression of the synMuv phenotype (Figure 1A and Table 1). We mapped the synMuv suppressor *n3294* between *sma-3* and *unc-36* on LGIII and obtained transformation rescue of the synMuv suppression phenotype with cosmid C28G4, which contains 16 predicted genes. RNA interference (RNAi) of the gene *F37A4.8* (using either of two cDNA clones; see Materials and methods) caused suppression of the *lin-53; lin-15A* synMuv phenotype. Additionally, expression of an *F37A4.8* cDNA driven by a *dpy-7* promoter (GILLEARD *et al.* 1997) rescued the synMuv suppression phenotype of *n3294* animals (Table 1). We determined that *n3294* and *n3297* harbor two distinct missense mutations in *F37A4.8* (Figs 1B, S1).

Using two independent cDNA clones and one 5' RACE product (see Materials and methods), we determined the sequence of the full-length *F37A4.8* transcript, which included the SL1 *trans*-splice leader sequence found in many *C. elegans* transcripts (BLUMENTHAL 1995), Figure 1B). *F37A4.8* encodes the *C. elegans* homolog of *Drosophila* ISWI, a regulator of transcription and chromatin (ELFRING *et al.* 1994; DEURING *et al.* 2000). We named *F37A4.8 isw-1* (*isw*, ISWI-like).

ISW-1 is 60% identical to *Drosophila* ISWI (ELFRING *et al.* 1994) and 69% identical to human hSNF2h (OKABE *et al.* 1992). ISW-1 contains an AT-hook (REEVES and NISSEN 1990) and two SANT (AASLAND *et al.* 1996) domains; each of these domains can bind DNA. Additionally, ISW-1 contains a domain similar to many helicases (the DEXD/H box) and an ATPase domain. Each are required for chromatin-remodeling activity (CORONA *et al.* 1999). *isw-1(n3294)* is predicted to cause a proline-to-leucine substitution within the DEXD/H domain, implicating

this domain in *isw-1* function. *isw-1(n3297)* is predicted to cause a leucine-to-phenylalanine substitution within a non-conserved region (Figs 1C, S1).

isw-1(n3294) and *isw-1(n3297)* each conferred a fully penetrant recessive synMuv suppression and incompletely penetrant sterile phenotype (Tables 1 and S2). By contrast, RNAi of *isw-1* caused a fully penetrant synMuv suppression and sterile phenotype (Tables 1 and S2). We isolated a deletion allele of *isw-1*, *n4066*, which removes part of the ATPase domain and most of the DEXD/H domain, causing a presumptive null phenotype. The *isw-1(n4066)* deletion allele caused a fully penetrant recessive sterile phenotype (Table S2) but failed to cause strong suppression of the synMuv phenotype (Table 1). Because *isw-1(n4066)* homozygotes are sterile, the animals we studied were descended from *isw-1(n4066)* heterozygotes. Homozygous missense mutants descended from heterozygous mothers also did not have a strong synMuv suppression phenotype (Table 1), so the lack of synMuv suppression observed in *isw-1* homozygotes derived from heterozygous mothers likely was caused by maternally inherited wild-type *isw-1* gene product. *isw-1(n4066)* did perturb the synMuv suppressor function of *isw-1*, because this mutation failed to complement the synMuv suppression phenotype caused by each of the missense alleles (Table 1). *isw-1(n3294)* and *isw-1(n3297)* cause a decrease of *isw-1* function, because each resulted in recessive suppression of the synMuv phenotype and failed to complement the phenotype conferred by a deletion of *isw-1*. Additionally, RNAi of *isw-1* caused a synMuv suppression and sterile phenotype, so the two *isw-1* missense alleles probably cause a partial loss of *isw-1* gene function.

ISW-1 is nuclear, ubiquitously expressed and associated with chromatin

We generated specific antibodies that recognized a protein of the predicted ISW-1 size (~115 kD) by western blot analysis of wild-type but not *isw-1(n4066)* adults (Figure S2A). ISW-1 was present in the nuclei of most, if not all, cells during every stage of *C. elegans* development (Figs S2B, C, D and data not shown). ISW-1 was associated with chromatin, as indicated by colocalization of anti-ISW-1 immunoreactivity with DAPI-stained condensed chromosomes (Figure S2E).

Decreased function of the *C. elegans* homolog of *Drosophila nurf301* suppresses the synMuv phenotype

In *Drosophila*, ISWI acts as the ATPase subunit of several ATP-dependent chromatin-remodeling complexes, including ACF (ITO *et al.* 1997), CHRAC (VARGA-WEISZ *et al.* 1997) and NURF (TSUKIYAMA and WU 1995). We determined whether any of the *C. elegans* genes encoding presumptive components of homologous complexes act similarly to *isw-1* to promote the synMuv phenotype.

Using BLAST (ALTSCHUL *et al.* 1990) and SMART (SONNHAMMER *et al.* 1997) searches, we identified *C. elegans* orthologs of the ACF, CHRAC and NURF complex members. The ACF and CHRAC complexes share one component, ACF1. Deletion of one of the two genes encoding a *C. elegans* ACF1 ortholog (*flt-1*), RNAi of the other ortholog (*H20J04.2*) or both deletion and RNAi together failed to suppress the synMuv phenotype. Furthermore, RNAi of each of the remaining genes encoding CHRAC complex orthologs failed to suppress the synMuv phenotype (Table 2). In these RNAi experiments in which a failure to suppress the synMuv phenotype was observed, it remains possible that the gene plays a role in the antagonism of the synMuv genes, but this role was not seen because the gene was not inactivated sufficiently.

Only RNAi of a *Drosophila* NURF301 ortholog, which we named *nurf-1* (NURF301-like), suppressed the synMuv phenotype (Table 2). The *Drosophila* NURF complex consists of ISWI, NURF301, NURF38 and NURF55 (TSUKIYAMA and WU 1995). RNAi of the sole *C. elegans* NURF38 ortholog, *pyp-1*, or of one of the two NURF55 orthologs, *rba-1*, caused embryonic lethality (data not shown) and thus precluded the scoring of the synMuv suppression phenotype. The other NURF55 ortholog is a class B synMuv gene, *lin-53* (LU and HORVITZ 1998), and was not tested for synMuv suppression for this reason. Additionally, a deletion allele of *pyp-1* caused larval lethality before the third larval stage (data not shown), which precluded scoring of the synMuv suppression phenotype.

Using the sequences determined from 15 independent cDNA clones (see Materials and methods), RT-PCR products and 5' RACE products, we identified five distinct transcripts generated from the *nurf-1* locus (Figure 2A). Each

transcript is predicted to encode a protein with domains similar to some of the domains of *Drosophila* NURF301. However, none of the identified transcripts is predicted to encode a protein with all of the domains contained in full-length NURF301 (Figure 2B).

nurf-1a encodes a protein most similar to the N-terminus of NURF301 and contains domains implicated in binding DNA, including an HMGY/I domain (REEVES and BECKERBAUER 2001), a DDT domain (DOERKS *et al.* 2001) and a PHD finger (SCHINDLER *et al.* 1993; AASLAND *et al.* 1995). *nurf-1b* and *nurf-1c* share two exons with *nurf-1a* and encode proteins with similarity to the C-terminus of NURF301. Unlike *nurf-1b*, which encodes a protein with only a Q-rich domain, *nurf-1c* encodes a protein with two PHD fingers and a bromodomain. The *nurf-1d* and *nurf-1e* transcripts are initiated at different sites but encode the same predicted protein, which shares a C-terminus with NURF-1C. RNAi of *nurf-1a*, but not of the other *nurf-1* transcripts, suppressed the synMuv phenotype of *lin-15AB(n765)* mutants and caused sterility (Figure 2C and data not shown).

To confirm that reduction of the *nurf-1a* transcript was responsible for the suppression of the synMuv phenotype, we isolated two deletion alleles of the *nurf-1* locus, *n4293* and *n4295*. *nurf-1(n4293)* is deleted for part of *nurf-1a* but not of the other *nurf-1* variants. *nurf-1(n4295)* removes part of every *nurf-1* variant except *nurf-1a. nurf-1(n4293)* but not *nurf-1(n4295)* suppressed the synMuv phenotype of *lin-15AB(n765)* mutants and caused sterility, both features of the *isw-1* mutant phenotype (Figure 2C and data not shown). Therefore, *nurf-1a* likely acts with *isw-1* to promote the synMuv phenotype.

The *C. elegans* NURF-like genes *isw-1* and *nurf-1* promote the synMuv phenotypes of all synMuv mutant combinations

The *C. elegans* NURF-like genes might promote the ectopic vulval fates of only specific synMuv mutant combinations, *e.g.* the *lin-53; lin-15A* double mutant. To address this issue, we used RNAi to reduce the function of *isw-1* or *nurf-1* in a variety of synMuv double mutants. Inactivation of *isw-1* or *nurf-1* suppressed not only the synMuv phenotype of *lin-53(n833); lin-15A(n767)* animals but also the

synMuv phenotype of the null double mutant combination *lin-53(n3368); lin-15A(n767)* (Table 3). Additionally, RNAi of *isw-1* or *nurf-1* suppressed other class AB, BC and AC synMuv double mutant combinations (Table 3). Reduction of *isw-1* function suppressed the synMuv phenotype of *lin-53(n833)* in combination with putative null mutations in each of the class A synMuv genes. Additionally, reduction of *isw-1* function suppressed the synMuv phenotype of *lin-15A(n767)* in combination with putative null alleles of all identified class B synMuv genes (Tables 3 and S1).

isw-1 and *nurf-1* promote the multivulva phenotype caused by activation of the Ras pathway

A functional Ras pathway is required for expression of the synMuv phenotype (FERGUSON *et al.* 1987; BEITEL *et al.* 1990; HAN and STERNBERG 1990). Therefore, reduction of *isw-1* function might suppress the synMuv phenotype by reducing the activity of the Ras pathway. If so, *isw-1* might act by promoting the activity of the Ras pathway. However unlike many mutants defective in the Ras pathway, *isw-1* mutants did not have abnormalities in the expression of vulval cell fates.

We tested for a subtle role of *isw-1* in the specification of vulval cells by asking if a weak Vul phenotype conferred by a decrease in Ras pathway activity could be enhanced by an *isw-1* mutation. A *lin-2* partial loss-of-function mutation, *e1453*, causes an incompletely penetrant Vul phenotype (FERGUSON and HORVITZ 1985) and a weak mutation in *lin-45* Raf, *ku112,* does not cause a vulval cell-fate defect (SUNDARAM and HAN 1995). *lin-45(ku112)* has been used to identify mutations that as single mutants do not cause a vulval-fate defect but in combination with *lin-45(ku112)* cause a synthetic vulvaless (synVul) phenotype, implicating the genes defined by such mutations in the generation of vulval cell fates (ROCHELEAU *et al.* 2002). We scored vulval induction in *isw-1; lin-2* and *isw-1; lin-45* double mutants and observed that *isw-1* did not enhance the Vul phenotype caused by *lin-2(e1453)* (42% versus 38%) and did not cause a synVul phenotype in combination with *lin-45(ku112)* (data not shown). These data

suggest that if *isw-1* promotes the activity of the Ras pathway it might act redundantly with other factors.

Gain-of-function mutations in *let-23* RTK or *let-60* Ras cause a Muv phenotype (BEITEL *et al.* 1990; HAN *et al.* 1990; KATZ *et al.* 1996). Reduction of *isw-1* and *nurf-1* function partially suppressed the Muv phenotype caused by increased *let-23* and *let-60* gain-of-function mutations (Table 4). The Ras pathway terminates with the transcription factors LIN-1 ETS and LIN-31 HNF/Forkhead. *lin-1* has a primary role in inhibiting vulval cell fates, such that *lin-1* null mutants have a Muv phenotype (BEITEL *et al.* 1995; TIENSUU *et al.* 2005). LIN-31 when bound to LIN-1 inhibits vulval cell fates, but after phosphorylation by MPK-1 MAPK, LIN-31 promotes vulval cell fates (TAN *et al.* 1998; MILLER *et al.* 2000). *lin-31* mutants can have either a Muv or Vul phenotype, because the vulval cells are unregulated and stochastically adopt a vulval or non-vulval cell fate (MILLER *et al.* 2000). Reduction of *isw-1* and *nurf-1* function suppressed the Muv phenotype caused by a partial loss-of-function *lin-1* mutation and a null *lin-31* mutation but failed to suppress the null *lin-1* mutant phenotype (Table 4). The failure to enhance a sensitized abnormal vulval phenotype and to suppress completely the Muv phenotype caused by an increase in Ras pathway activity suggests either that a greater inhibition of the functions of *isw-1* and *nurf-1* is required to observe complete effects or that other factors act redundantly with the NURF-like genes to promote Ras pathway activity.

Reduction of *isw-1* and *nurf-1* function suppresses non-vulval abnormalities of class B synMuv mutants

Several class B synMuv genes control aspects of a germline-versus-soma cell-fate decisions. Specifically, the somatic cells of some class B synMuv mutants adopt a more germline-like fate, as indicated by the somatic expression of germline genes, such as PGL-1 (KAWASAKI *et al.* 1998); a germline-like appearance of somatic cells in *mep-1* and *let-418* arrested larvae (UNHAVAITHAYA *et al.* 2002); the tandem-array-modifier (Tam) phenotype of increased somatic silencing of expression from repetitive transgenes by a process similar to that

which occurs in the germline (KELLY *et al.* 1997; KELLY and FIRE 1998; HSIEH *et al.* 1999) and enhanced RNAi sensitivity, perhaps caused by ectopic expression of a germline RNA polymerase EGO-1 in the soma producing an increased RNAi effect (WANG *et al.* 2005).

Reduction of *isw-1* and *nurf-1* function suppressed abnormalities associated with defects in the germline-versus-soma cell-fate decision caused by *lin-15B(n744)* and *lin-35(n745)*, including the ectopic somatic expression of the germline-expressed protein PGL-1, the Tam phenotype (quantification in Figure S4) and the RNAi hypersensitivity phenotype (Figs 3A, B, C and data not shown). However, the reduction of *isw-1* or *nurf-1* function did not cause a germline desilencing of expression from repetitive transgenes (data not shown), so both genes might not be required for mechanisms of transcriptional repression in the germline. Additionally, reduction of *isw-1* and *nurf-1* function suppressed the *mep-1* and *let-418* larval-arrest phenotypes (Figure 3D), and somatic cells did not have a germline-like appearance in *isw-1; mep-1* or in *nurf-1; mep-1* double mutants (data not shown). These data indicate that not only are *isw-1* and *nurf-1* required for the synMuv vulval phenotype but also for the ectopic adoption of germline fates in the soma caused by loss of class B synMuv gene function. Therefore the putative synMuv complexes and the NURF-like complex might antagonize the transcription of similar sets of target genes.

DISCUSSION

isw-1 and *nurf-1* antagonize the activities of at least the class B and C synMuv genes in the determination of *C. elegans* cell fates

The synMuv phenotype is caused by mutations in two genes in two different classes, and synMuv single mutants have a wild-type vulval phenotype (HORVITZ and SULSTON 1980; FERGUSON and HORVITZ 1989). The loss of *isw-1* or *nurf-1* function must antagonize a deficit in one or both of the synMuv genes in each suppressed strain to counteract the synMuv phenotype. Because the synMuv phenotypes of class AB, BC and AC double mutants were each suppressed by loss of *isw-1* or *nurf-1* function, the *C. elegans* NURF-like genes must antagonize the functions of at least two classes of synMuv genes. Defects caused by single class B mutants were suppressed by reduction of *isw-1* function (Figure 3), and the vulval phenotype of the class C synMuv mutant *trr-1(n3712)* was suppressed (Table S1). Thus, *isw-1* and *nurf-1* likely antagonize the activities of at least the class B and C synMuv genes. Because a functional Ras pathway is required for the synMuv phenotype, it is possible that the antagonism of the class B and C gene functions caused by reduction of *isw-1* or *nurf-1* function involves a down-regulation of the Ras pathway.

isw-1 and *nurf-1* probably are not targets of synMuv-mediated transcriptional repression, as mRNA levels of each were not increased using semi-quantitative RT-PCR analysis of *lin-53; lin-15A* and *lin-35; lin-15A* mutants compared to the wild type (data not shown). Additionally, ISW-1 levels were not increased noticeably in *lin-53; lin-15A* and *lin-15AB* mutants, based on whole-mount immunofluorescence analysis (data not shown). Therefore, the synMuv genes likely do not act through the NURF-like genes to negatively regulate the vulval cell-fate decision.

ISW-1 and NURF-1 might be components of a NURF-like chromatin-remodeling complex involved in the *C. elegans* vulval cell-fate decision

C. elegans ISW-1 likely acts as part of a NURF-like complex and not as part of a CHRAC-like or ACF-like complex to antagonize the actions of the synMuv proteins, because inhibition of *isw-1* or *nurf-1* but not inhibition of ACF or CHRAC ortholog gene functions suppressed the synMuv phenotype (Table 2). The *Drosophila* NURF complex is composed of four subunits: ISWI, NURF38, NURF55 and NURF301 (TSUKIYAMA and WU 1995). Because loss of the *C. elegans* homolog of NURF38, PYP-1, caused embryonic lethality (data not shown), we have not determined if it functions as a NURF-like complex component to antagonize the actions of the synMuv proteins. *Drosophila* NURF55 is similar to two proteins in *C. elegans*, LIN-53 and RBA-1 (72% and 53% identical, respectively). LIN-53 is a class B synMuv protein and 54% identical to its neighbor RBA-1. Strong reduction-of-function mutations in *lin-53* and *isw-1* cause opposite mutant phenotypes. Therefore, it is unlikely that LIN-53 and ISW-1 always act in the same complex. The LIN-53 homolog NURF55/RbAp48/CAF-1 is present in many chromatin-regulatory complexes, and it is possible that LIN-53 similarly acts in a number of *C. elegans* complexes, possibly both preventing and promoting the synMuv phenotype. If so, the role of LIN-53 in preventing the synMuv phenotype must be predominant, because loss-of-function mutations in *lin-53* cause a synMuv phenotype in combination with mutations in class A genes (LU and HORVITZ 1998). Alternatively, RBA-1 might act with ISW-1 as part of a NURF-like complex. Because *rba-1(*RNAi*)* caused embryonic lethality (data not shown), we have not tested this possibility.

nurf-1, the *C. elegans* homolog of *Drosophila nurf301*, is predicted to encode at least five different proteins, each of which has some similarity to NURF301. Using deletion alleles and RNAi, we found that *nurf-1a* but not *nurf-1b, c, d,* or *e* was required to promote the synMuv phenotype. The region of NURF301 between the DDT domain (DOERKS *et al.* 2001) and the C-terminal PHD fingers (AASLAND *et al.* 1995) interacts with transcription factors required for recruitment of the NURF complex to target gene promoters (XIAO *et al.* 2001). The corresponding regions of NURF-1A, B and C differ in length and could mediate interactions with distinct sets of transcription factors to direct recruitment

of the complex to different promoters. The NURF-1a region that presumably interacts with transcription factors might be responsible for recruitment of the NURF-like complex to promoters of genes required for the vulval cell-fate decision.

The functions of ISW-1 and NURF-1 might be involved in the generation of normal vulval cell fates.

It is possible that the function of the putative *C. elegans* NURF-like complex is required only for the generation of ectopic vulval cell fates, *e.g.* in synMuv mutants, but is not involved in normal vulval development. For example when the inhibitory actions of the synMuv proteins are absent or when the activity of the Ras pathway is increased, the NURF-like complex might promote the specification of ectopic vulval cell fates. However, we observed that *isw-1* is required not only for the Tam phenotype of class B synMuv mutants (Figure 3B) but also for a basal level of repression of expression from the *ccIs4251* GFP reporter (Figure S3). This observation suggests that *isw-1* is required not only in the absence of synMuv activity but also in a wild-type synMuv background to promote expression of genes repressed by the synMuv proteins. By analogy, we propose that the putative NURF-like complex helps promote the normal generation of vulval cell fates in a wild-type synMuv background.

The *C. elegans* NURF-like complex acts antagonistically to complexes similar to Myb-MuvB/dREAM, NuRD and Tip60/NuA4 to control transcription

The *Drosophila* NURF complex slides nucleosomes along the DNA to allow access for transcription factors to bind target sequences in vitro (HAMICHE *et al.* 1999). Both ISWI and NURF301 are required for the transcription of Hox and heat-shock genes in vivo (DEURING *et al.* 2000; BADENHORST *et al.* 2002). Therefore, the NURF complex has been hypothesized to be involved in transcriptional activation. The homologs of many class B synMuv proteins are components of at least two complexes, Myb-MuvB/dREAM and NuRD, involved

in transcriptional repression (TONG *et al.* 1998; XUE *et al.* 1998; KORENJAK *et al.* 2004; LEWIS *et al.* 2004). Studies of *Drosophila* and mammalian cells argue that the NURF complex and the Myb-MuvB/dREAM and NuRD complexes have opposite effects on transcription.

The vulval cell-fate decision in *C. elegans* demonstrates the biological consequences of the opposing effects of the Myb-MuvB/dREAM and NuRD and the NURF chromatin-remodeling activities. We propose that a complex containing both ISW-1 and NURF-1 antagonizes one or more synMuv protein complexes in the transcriptional control of the vulval cell-fate decision. One hypothesis is that loss of transcriptional repression by the synMuv proteins causes a Muv phenotype as a result of the increased transcription of genes that promote the vulval cell-fate decision. The NURF-like complex might be required for this ectopic expression of synMuv target genes. Alternatively, the NURF-like complex might act at targets distinct from those that are misregulated in synMuv mutants, and transcription of these genes would antagonize the activities of the synMuv proteins. The identification of the transcriptional targets of the synMuv proteins and of the NURF-like complex should help differentiate between these two hypotheses. The *Drosophila* Myb-MuvB complex co-purified with sub-stoichiometric amounts of NURF complex members. The actions of and requirements for the NURF complex components for Myb-MuvB function were not investigated (LEWIS *et al.* 2004). Perhaps NURF-like complexes bind Myb-MuvB-like complexes to directly inhibit activities of these complexes.

The antagonism of the *lin-35* Rb and *let-60* Ras mutant phenotypes by partial loss of *isw-1* ISWI function suggests a possible approach to cancer therapy

The functional antagonism between a NURF-like complex and synMuv repressive complexes and/or activation of the Ras pathway could be conserved in humans and important for human cancer. The loss of Rb function is associated with the majority of human carcinomas (ADAMS and KAELIN 1998), and methods to inhibit the defects of Rb-deficient cells should be beneficial as cancer

treatment strategies. Additionally oncogenic forms of human Ras are involved in many cancers, especially cancers of the lung (MINAMOTO *et al.* 2000). Because a reduction of *isw-1* ISWI function can suppress defects associated with a complete loss of *lin-35* Rb or activation of *let-60* Ras in *C. elegans*, inhibition of the human ISW-1 homolog hSNF2h might suppress the effects of Rb loss or of oncogenic Ras in human cells and hence reduce or eliminate the consequences of oncogenic mutations. hSNF2h is a chromatin-remodeling enzyme (OKABE *et al.* 1992; AIHARA *et al.* 1998) and might be a reasonable target for therapeutic intervention.

ACKNOWLEDGMENTS

We thank Beth Castor for DNA sequence determination, Na An for strain management, Andrew Hellman for deletion allele screening, Peter Reddien for use of his microscope, Robyn Tanny and members of the Horvitz laboratory for critical reading of this manuscript, especially Dan Denning, Niels Ringstad and Hillel Schwartz. Strains were provided by the *Caenorhabditis* Genetics Center, which is supported by the NIH National Center for Research Resources and by Shohei Mitani of Tokyo Women's Medical University. We thank Susan Strome for the PGL-1 antisera, Darryl Conte for helpful discussions about PGL-1 staining and Yuji Kohara for EST clones. E.C.A. is an Anna Fuller Cancer Research Fellow and H.R.H. is the David H. Koch Professor of Biology at MIT and an Investigator of the Howard Hughes Medical Institute. This work was supported by NIH grant GM24663.

LITERATURE CITED

AASLAND, R., T. J. GIBSON and A. F. STEWART, 1995 The PHD finger: implications for chromatin-mediated transcriptional regulation. Trends Biochem Sci **20:** 56-59.

AASLAND, R., A. F. STEWART and T. GIBSON, 1996 The SANT domain: a putative DNA-binding domain in the SWI-SNF and ADA complexes, the transcriptional co-repressor N-CoR and TFIIIB. Trends Biochem Sci **21:** 87-88.

ADAMS, P. D., and W. G. KAELIN, JR., 1998 Negative control elements of the cell cycle in human tumors. Curr Opin Cell Biol **10:** 791-797.

AIHARA, T., Y. MIYOSHI, K. KOYAMA, M. SUZUKI, E. TAKAHASHI *et al.*, 1998 Cloning and mapping of SMARCA5 encoding hSNF2H, a novel human homologue of Drosophila ISWI. Cytogenet Cell Genet **81:** 191-193.

ALTSCHUL, S. F., W. GISH, W. MILLER, E. W. MYERS and D. J. LIPMAN, 1990 Basic local alignment search tool. J Mol Biol **215:** 403-410.

BADENHORST, P., M. VOAS, I. REBAY and C. WU, 2002 Biological functions of the ISWI chromatin remodeling complex NURF. Genes Dev **16:** 3186-3198.

BEITEL, G. J., S. G. CLARK and H. R. HORVITZ, 1990 *Caenorhabditis elegans* ras gene *let-60* acts as a switch in the pathway of vulval induction. Nature **348:** 503-509.

BEITEL, G. J., E. J. LAMBIE and H. R. HORVITZ, 2000 The *C. elegans* gene *lin-9*,which acts in an Rb-related pathway, is required for gonadal sheath cell development and encodes a novel protein. Gene **254:** 253-263.

BEITEL, G. J., S. TUCK, I. GREENWALD and H. R. HORVITZ, 1995 The *Caenorhabditis elegans* gene *lin-1* encodes an ETS-domain protein and defines a branch of the vulval induction pathway. Genes Dev **9:** 3149-3162.

BLUMENTHAL, T., 1995 Trans-splicing and polycistronic transcription in Caenorhabditis elegans. Trends Genet **11:** 132-136.

BRENNER, S., 1974 The genetics of *Caenorhabditis elegans*. Genetics **77:** 71-94.

CEOL, C. J., and H. R. HORVITZ, 2001 *dpl-1* DP and *efl-1* E2F act with *lin-35* Rb to antagonize Ras signaling in *C. elegans* vulval development. Mol Cell **7:** 461-473.

CEOL, C. J., and H. R. HORVITZ, 2004 A new class of *C. elegans* synMuv genes implicates a Tip60/NuA4-like HAT complex as a negative regulator of Ras signaling. Dev Cell **6:** 563-576.

CLARK, S. G., X. LU and H. R. HORVITZ, 1994 The *Caenorhabditis elegans* locus *lin-15*, a negative regulator of a tyrosine kinase signaling pathway, encodes two different proteins. Genetics **137:** 987-997.

CORONA, D. F., G. LANGST, C. R. CLAPIER, E. J. BONTE, S. FERRARI *et al.*, 1999 ISWI is an ATP-dependent nucleosome remodeling factor. Mol Cell **3:** 239-245.

COUTEAU, F., F. GUERRY, F. MULLER and F. PALLADINO, 2002 A heterochromatin protein 1 homologue in *Caenorhabditis elegans* acts in germline and vulval development. EMBO Rep **3:** 235-241.

DAVISON, E. M., M. M. HARRISON, A. J. WALHOUT, M. VIDAL and H. R. HORVITZ, 2005 *lin-8*, which antagonizes *C. elegans* Ras-mediated vulval induction, encodes a novel nuclear protein that interacts with the LIN-35 Rb protein. Genetics.

DEURING, R., L. FANTI, J. A. ARMSTRONG, M. SARTE, O. PAPOULAS *et al.*, 2000 The ISWI chromatin-remodeling protein is required for gene expression and the maintenance of higher order chromatin structure in vivo. Mol Cell **5:** 355-365.

DOERKS, T., R. COPLEY and P. BORK, 2001 DDT -- a novel domain in different transcription and chromosome remodeling factors. Trends Biochem Sci **26:** 145-146.

DUFOURCQ, P., M. VICTOR, F. GAY, D. CALVO, J. HODGKIN *et al.*, 2002 Functional requirement for histone deacetylase 1 in *Caenorhabditis elegans* gonadogenesis. Mol Cell Biol **22:** 3024-3034.

ELFRING, L. K., R. DEURING, C. M. MCCALLUM, C. L. PETERSON and J. W. TAMKUN, 1994 Identification and characterization of *Drosophila* relatives of the yeast transcriptional activator SNF2/SWI2. Mol Cell Biol **14:** 2225-2234.

FERGUSON, E. L., and H. R. HORVITZ, 1985 Identification and characterization of 22 genes that affect the vulval cell lineages of the nematode *Caenorhabditis elegans*. Genetics **110:** 17-72.

FERGUSON, E. L., and H. R. HORVITZ, 1989 The multivulva phenotype of certain *Caenorhabditis elegans* mutants results from defects in two functionally redundant pathways. Genetics **123:** 109-121.

FERGUSON, E. L., P. W. STERNBERG and H. R. HORVITZ, 1987 A genetic pathway for the specification of the vulval cell lineages of *Caenorhabditis elegans*. Nature **326:** 259-267.

FINNEY, M., and G. RUVKUN, 1990 The *unc-86* gene product couples cell lineage and cell identity in *C. elegans*. Cell **63:** 895-905.

GILLEARD, J. S., J. D. BARRY and I. L. JOHNSTONE, 1997 *cis* regulatory requirements for hypodermal cell-specific expression of the *Caenorhabditis elegans* cuticle collagen gene *dpy-7*. Mol Cell Biol **17:** 2301-2311.

HAMICHE, A., R. SANDALTZOPOULOS, D. A. GDULA and C. WU, 1999 ATP-dependent histone octamer sliding mediated by the chromatin remodeling complex NURF. Cell **97:** 833-842.

HAN, M., R. V. AROIAN and P. W. STERNBERG, 1990 The *let-60* locus controls the switch between vulval and nonvulval cell fates in *Caenorhabditis elegans*. Genetics **126:** 899-913.

HAN, M., and P. W. STERNBERG, 1990 *let-60*, a gene that specifies cell fates during *C. elegans* vulval induction, encodes a ras protein. Cell **63:** 921-931.

HILL, R. J., and P. W. STERNBERG, 1992 The gene *lin-3* encodes an inductive signal for vulval development in *C. elegans*. Nature **358:** 470-476.

HORVITZ, H. R., and J. E. SULSTON, 1980 Isolation and genetic characterization of cell-lineage mutants of the nematode *Caenorhabditis elegans*. Genetics **96:** 435-454.

HSIEH, J., J. LIU, S. A. KOSTAS, C. CHANG, P. W. STERNBERG *et al.*, 1999 The RING finger/B-box factor TAM-1 and a retinoblastoma-like protein LIN-35

modulate context-dependent gene silencing in *Caenorhabditis elegans*. Genes Dev **13:** 2958-2970.

HUANG, L. S., P. TZOU and P. W. STERNBERG, 1994 The *lin-15* locus encodes two negative regulators of *Caenorhabditis elegans* vulval development. Mol Biol Cell **5:** 395-411.

ITO, T., M. BULGER, M. J. PAZIN, R. KOBAYASHI and J. T. KADONAGA, 1997 ACF, an ISWI-containing and ATP-utilizing chromatin assembly and remodeling factor. Cell **90:** 145-155.

KATZ, W. S., G. M. LESA, D. YANNOUKAKOS, T. R. CLANDININ, J. SCHLESSINGER *et al.*, 1996 A point mutation in the extracellular domain activates LET-23, the *Caenorhabditis elegans* epidermal growth factor receptor homolog. Mol Cell Biol **16:** 529-537.

KAWASAKI, I., Y. H. SHIM, J. KIRCHNER, J. KAMINKER, W. B. WOOD *et al.*, 1998 PGL-1, a predicted RNA-binding component of germ granules, is essential for fertility in *C. elegans*. Cell **94:** 635-645.

KELLY, W. G., and A. FIRE, 1998 Chromatin silencing and the maintenance of a functional germline in *Caenorhabditis elegans*. Development **125:** 2451-2456.

KELLY, W. G., S. XU, M. K. MONTGOMERY and A. FIRE, 1997 Distinct requirements for somatic and germline expression of a generally expressed *Caernorhabditis elegans* gene. Genetics **146:** 227-238.

KOELLE, M. R., and H. R. HORVITZ, 1996 EGL-10 regulates G protein signaling in the *C. elegans* nervous system and shares a conserved domain with many mammalian proteins. Cell **84:** 115-125.

KORENJAK, M., B. TAYLOR-HARDING, U. K. BINNE, J. S. SATTERLEE, O. STEVAUX *et al.*, 2004 Native E2F/RBF complexes contain Myb-interacting proteins and repress transcription of developmentally controlled E2F target genes. Cell **119:** 181-193.

KORNFELD, K., 1997 Vulval development in *Caenorhabditis elegans*. Trends Genet **13:** 55-61.

LEWIS, P. W., E. L. BEALL, T. C. FLEISCHER, D. GEORLETTE, A. J. LINK *et al.*, 2004 Identification of a *Drosophila* Myb-E2F2/RBF transcriptional repressor complex. Genes Dev **18:** 2929-2940.

LIANG, K. Y., Y. F. CHIU and T. H. BEATY, 2001 A robust identity-by-descent procedure using affected sib pairs: multipoint mapping for complex diseases. Hum Hered **51:** 64-78.

LU, X., and H. R. HORVITZ, 1998 *lin-35* and *lin-53*, two genes that antagonize a *C. elegans* Ras pathway, encode proteins similar to Rb and its binding protein RbAp48. Cell **95:** 981-991.

MELENDEZ, A., and I. GREENWALD, 2000 *Caenorhabditis elegans lin-13*, a member of the LIN-35 Rb class of genes involved in vulval development, encodes a protein with zinc fingers and an LXCXE motif. Genetics **155:** 1127-1137.

MELLO, C. C., J. M. KRAMER, D. STINCHCOMB and V. AMBROS, 1991 Efficient gene transfer in *C.elegans*: extrachromosomal maintenance and integration of transforming sequences. Embo J **10:** 3959-3970.

MILLER, L. M., H. A. HESS, D. B. DOROQUEZ and N. M. ANDREWS, 2000 Null mutations in the *lin-31* gene indicate two functions during *Caenorhabditis elegans* vulval development. Genetics **156:** 1595-1602.

MINAMOTO, T., M. MAI and Z. RONAI, 2000 K-ras mutation: early detection in molecular diagnosis and risk assessment of colorectal, pancreas, and lung cancers--a review. Cancer Detect Prev **24:** 1-12.

NARLIKAR, G. J., H. Y. FAN and R. E. KINGSTON, 2002 Cooperation between complexes that regulate chromatin structure and transcription. Cell **108:** 475-487.

OKABE, I., L. C. BAILEY, O. ATTREE, S. SRINIVASAN, J. M. PERKEL *et al.*, 1992 Cloning of human and bovine homologs of SNF2/SWI2: a global activator of transcription in yeast S. cerevisiae. Nucleic Acids Res **20:** 4649-4655.

REEVES, R., and L. BECKERBAUER, 2001 HMGI/Y proteins: flexible regulators of transcription and chromatin structure. Biochim Biophys Acta **1519:** 13-29.

REEVES, R., and M. S. NISSEN, 1990 The A.T-DNA-binding domain of mammalian high mobility group I chromosomal proteins. A novel peptide motif for recognizing DNA structure. J Biol Chem **265:** 8573-8582.

RIDDLE, D. L., BLUMENTHAL T., MEYER, B.J., PRIESS, J.R., 1997 *C. elegans II*. Cold Spring Harbor Laboratory Press, Cold Spring Harbor.

ROCHELEAU, C. E., R. M. HOWARD, A. P. GOLDMAN, M. L. VOLK, L. J. GIRARD *et al.*, 2002 A *lin-45* raf enhancer screen identifies *eor-1*, *eor-2* and unusual alleles of Ras pathway genes in *Caenorhabditis elegans*. Genetics **161:** 121-131.

ROTH, S. Y., J. M. DENU and C. D. ALLIS, 2001 Histone acetyltransferases. Annu Rev Biochem **70:** 81-120.

SCHINDLER, U., H. BECKMANN and A. R. CASHMORE, 1993 HAT3.1, a novel Arabidopsis homeodomain protein containing a conserved cysteine-rich region. Plant J **4:** 137-150.

SIMMER, F., M. TIJSTERMAN, S. PARRISH, S. P. KOUSHIKA, M. L. NONET *et al.*, 2002 Loss of the putative RNA-directed RNA polymerase RRF-3 makes C. elegans hypersensitive to RNAi. Curr Biol **12:** 1317-1319.

SMITH, C. L., and C. L. PETERSON, 2005 ATP-dependent chromatin remodeling. Curr Top Dev Biol **65:** 115-148.

SONNHAMMER, E. L., S. R. EDDY and R. DURBIN, 1997 Pfam: a comprehensive database of protein domain families based on seed alignments. Proteins **28:** 405-420.

SULSTON, J. E., and H. R. HORVITZ, 1977 Post-embryonic cell lineages of the nematode, *Caenorhabditis elegans*. Dev Biol **56:** 110-156.

SULSTON, J. E., and J. G. WHITE, 1980 Regulation and cell autonomy during postembryonic development of *Caenorhabditis elegans*. Dev Biol **78:** 577-597.

SUNDARAM, M., and M. HAN, 1995 The C. elegans ksr-1 gene encodes a novel Raf-related kinase involved in Ras-mediated signal transduction. Cell **83:** 889-901.

TAN, P. B., M. R. LACKNER and S. K. KIM, 1998 MAP kinase signaling specificity mediated by the LIN-1 Ets/LIN-31 WH transcription factor complex during *C. elegans* vulval induction. Cell **93:** 569-580.

THOMAS, J. H., C. J. CEOL, H. T. SCHWARTZ and H. R. HORVITZ, 2003 New genes that interact with *lin-35* Rb to negatively regulate the *let-60* ras pathway in *Caenorhabditis elegans*. Genetics **164:** 135-151.

THOMAS, J. H., and H. R. HORVITZ, 1999 The *C. elegans* gene *lin-36* acts cell autonomously in the *lin-35* Rb pathway. Development **126:** 3449-3459.

TIENSUU, T., M. K. LARSEN, E. VERNERSSON and S. TUCK, 2005 lin-1 has both positive and negative functions in specifying multiple cell fates induced by Ras/MAP kinase signaling in C. elegans. Dev Biol **286:** 338-351.

TONG, J. K., C. A. HASSIG, G. R. SCHNITZLER, R. E. KINGSTON and S. L. SCHREIBER, 1998 Chromatin deacetylation by an ATP-dependent nucleosome remodelling complex. Nature **395:** 917-921.

TSUKIYAMA, T., and C. WU, 1995 Purification and properties of an ATP-dependent nucleosome remodeling factor. Cell **83:** 1011-1020.

UNHAVAITHAYA, Y., T. H. SHIN, N. MILIARAS, J. LEE, T. OYAMA *et al.*, 2002 MEP-1 and a homolog of the NURD complex component Mi-2 act together to maintain germline-soma distinctions in *C. elegans*. Cell **111:** 991-1002.

VARGA-WEISZ, P. D., M. WILM, E. BONTE, K. DUMAS, M. MANN *et al.*, 1997 Chromatin-remodelling factor CHRAC contains the ATPases ISWI and topoisomerase II. Nature **388:** 598-602.

VON ZELEWSKY, T., F. PALLADINO, K. BRUNSCHWIG, H. TOBLER, A. HAJNAL *et al.*, 2000 The *C. elegans* Mi-2 chromatin-remodelling proteins function in vulval cell fate determination. Development **127:** 5277-5284.

WANG, D., S. KENNEDY, D. CONTE, JR., J. K. KIM, H. W. GABEL *et al.*, 2005 Somatic misexpression of germline P granules and enhanced RNA interference in retinoblastoma pathway mutants. Nature **436:** 593-597.

XIAO, H., R. SANDALTZOPOULOS, H. M. WANG, A. HAMICHE, R. RANALLO *et al.*, 2001 Dual functions of largest NURF subunit NURF301 in nucleosome sliding and transcription factor interactions. Mol Cell **8:** 531-543.

XUE, Y., J. WONG, G. T. MORENO, M. K. YOUNG, J. COTE *et al.*, 1998 NURD, a novel complex with both ATP-dependent chromatin-remodeling and histone deacetylase activities. Mol Cell **2:** 851-861.

YOCHEM, J., T. GU and M. HAN, 1998 A new marker for mosaic analysis in *Caenorhabditis elegans* indicates a fusion between hyp6 and hyp7, two major components of the hypodermis. Genetics **149:** 1323-1334.

Table 1. Loss of *isw-1* function suppresses the synMuv phenotype of *lin-53(n833); lin-15A(n767)* mutants

isw-1 genotype in a *lin-53; lin-15A* mutant	% Muv (n)
+/+	100 (319)
n3294 M^{-} [a]	0 (230)
n3294 M^{+} [b]	61 (76)
n3294/+ M^{+} [c]	100 (40)
n3294/+ M^{-} [d]	63 (130)
n3297 M^{-}	0 (121)
n3297 M^{+} [b]	64 (56)
n3297/+ M^{+},[c]	100 (53)
n3297/+ M^{-}, [d]	81 (111)
n3294/*n3297*	0 (103)
n4066 [e] M^{+}	95 (212)
n4066/+ M^{+}	100 (128)
n3294/*n4066*	0 (58)
n3297/*n4066*	0 (38)
isw-1 RNAi	0 (353)
n3294; dpy-7::isw-1(+)	96 (177)

[a] M^{+} or M^{-} denotes the presence (+) or absence (-) of maternal *isw-1* gene product. M^{+} animals were descended from *isw-1* heterozygous mutant hermaphrodites. M^{-} animals were descended from *isw-1* homozygous mutant hermaphrodites.

[b] These animals were the non-GFP-positive offspring of *lin-53(n833); isw-1/qC1 [nIs188]; lin-15A(n767)* hermaphrodites.

[c] These animals were the non-Dpy non-GFP-positive offspring of *dpy-5(e61) lin-53(n833); lin-15A(n767)* hermaphrodites and *lin-53(n833)/ hT2 [qIs48]; isw-1/hT2 [qIs48]; lin-15A(n767)* males.

[d] These animals were the non-Dpy offspring of *dpy-5(e61) lin-53(n833); isw-1; lin-15A(n767)* hermaphrodites and *lin-53(n833); him-5(e1490); lin-15A(n767)* males.

[e] *isw-1(n4066)* caused recessive sterility, so homozygous offspring from heterozygous hermaphrodites were scored. *isw-1(n4066)* was *cis*-marked with *dpy-17(e164)*.

For the dominance, complementation and maternal effect tests with the missense alleles, a *dpy-5(e61) cis*-marked *lin-53(n833)* strain was used.

Table 2. Reduction of NURF-like complex genes but not ACF-like or CHRAC-like genes suppresses the synMuv phenotype

Genotype in addition to *lin-15AB(n765)*	*Drosophila* homolog(s)	*Drosophila* complex(es) in which the homolog is found	% Muv (n)
wild-type	-	-	100 (546)
isw-1(n3294)	ISWI	ACF, CHRAC, NURF	0 (254)
nurf-1(RNAi)	NURF301	NURF	1 (284)
pyp-1(RNAi)	NURF38	NURF	NA[a]
pyp-1(n4599)[b] M^{+}[c]	NURF38	NURF	NA[a]
rba-1(RNAi)	NURF55	NURF	NA[a]
H20J04.2(RNAi)	ACF1	ACF, CHRAC	99 (150)
flt-1(tm235)	ACF1	ACF, CHRAC	100 (158)
flt-1(tm235); H20J04.2(RNAi)	ACF1	ACF, CHRAC	100 (184)
T26A5.8(RNAi)	CHRAC-14	CHRAC	100 (122)
Y53F4B.3(RNAi)	CHRAC-16	CHRAC	100 (210)
Y53F4B.3(RNAi); T26A5.8(RNAi)	CHRAC-14 and CHRAC-16	CHRAC	100 (140)

[a] NA = Not Applicable, because RNAi caused lethality prior to vulval development.

[b] *n4599* caused recessive larval lethality prior to vulval development.

[c] M^{+} denotes that the maternally provided product might be present in these homozygous offspring.

Table 3. Reduction of the *C. elegans* NURF-like genes complex suppresses the synMuv phenotype of multiple synMuv mutant combinations

Genotype	% Muv after control RNAi (n)	% Muv after *isw-1* RNAi (n)	% Muv after *nurf-1a* RNAi (n)
lin-53(n833)[#]*; lin-15A(n767)**	100 (319)	0 (353)	0 (128)
lin-53(n3368); lin-15A(n767)**	100 (95)	2 (155)	0 (86)
*lin-15AB(e1763)**	100 (300)	55 (347)	40 (72)
lin-35(n745); lin-15A(n767)**	100 (143)	14 (70)	8 (62)
lin-37(n758); lin-15A(n433)*[#]	100 (625)	52 (431)	0 (91)
lin-37(n758); lin-15A(n767)**	100 (207)	5 (99)	21 (39)
lin-53(n833)[#]*; lin-8(n2731)**	100 (217)	1 (109)	0 (65)
lin-53(n833)[#]*; lin-56(n2728)**	100 (234)	4 (118)	0 (66)
trr-1(n3712)[M+]*; lin-15A(n767)**	56 (117)	0 (77)	7 (28)
trr-1(n3712)[M+]*; lin-15B(n744)**	49 (59)	3 (75)	23 (22)
lin-8(n111)[#]*; lin-9(n112)*[#]	100 (243)	1 (181)	6 (51)

lin-8, *lin-15A* and *lin-56* are class A synMuv genes. *lin-9*, *lin-15B*, *lin-35*, *lin-37* and *lin-53* are class B synMuv genes. *trr-1* is a class C synMuv gene.

[#] This allele is a partial loss-of-function mutation.

* This allele is a likely complete loss-of-function mutation.

[M+] This allele is a strong loss-of-function mutation, and the mutant phenotype is maternally rescued.

Data concerning the suppression by *isw-1* RNAi of additional synMuv double mutants are found in Table S1.

Table 4. Reduction of *isw-1* or *nurf-1* function suppresses the Muv phenotype of some Ras pathway mutants

Genotype	% Muv after control RNAi (n)	% Muv after *isw-1* RNAi (n)	% Muv after *nurf-1a* RNAi (n)
*let-23(sa62*gf*)*	91 (57)	44 (88)	66 (27)
*let-60(n1046*gf*)*	96 (228)	19 (148)	9 (159)
lin-1(e1275)[#]	87 (100)	22 (107)	2 (103)
*lin-1(n304)**	100 (134)	100 (53)	100 (34)
*lin-31(n301)**	60 (312)	9 (96)	18 (246)

[#] This allele is a partial loss-of-function mutation.

* This allele is a likely complete loss-of-function mutation.

FIGURE DESCRIPTIONS

Figure 1: Loss-of-function mutations in *isw-1* suppress the synMuv phenotype of *lin-53; lin-15A* mutants.

(A) Brightfield micrographs of *C. elegans* 24 hours after the fourth larval stage. Vulvae and psuedovulvae are marked with white triangles and dark triangles, respectively. (Top) The wild-type strain has no pseudovulvae. (Middle) The synMuv mutant *lin-53(n833); lin-15A(n767)* has three pseudovulvae. (Bottom) The *lin-53(n833); isw-1(n3294); lin-15A(n767)* triple mutant has no pseudovulvae. Bacteria, embryos or bubbles were removed from the images. Scale bar, 100 μm.

(B) The genomic structure of *isw-1*. Exons, black boxes. 5' and 3' untranslated regions, white boxes. Predicted translation initiation and termination codons and the polyadenylation site are shown. The locations of the missense mutations and deletion allele are indicated.

(C) A representation of the domain structure of the ISW-1 protein. ISW-1 is similar to *Drosophila* ISWI and other family members, especially in the named domains (see text). The amino acid substitutions of the two missense alleles and the locations of these mutations and the deletion allele are indicated. An alignment of ISW-1 with *S. cerevisiae* SWI2/SNF2 and *Drosophila* ISWI is in Figure S1.

A

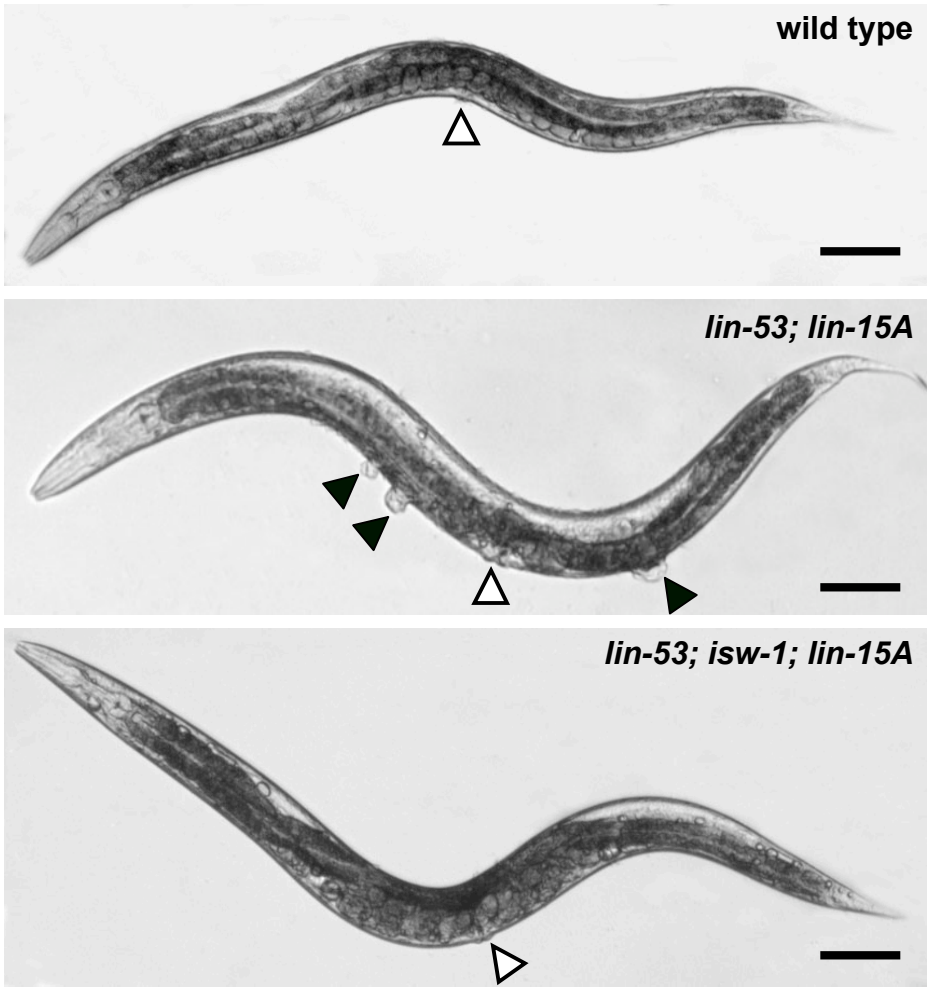
wild type
lin-53; lin-15A
lin-53; isw-1; lin-15A

B

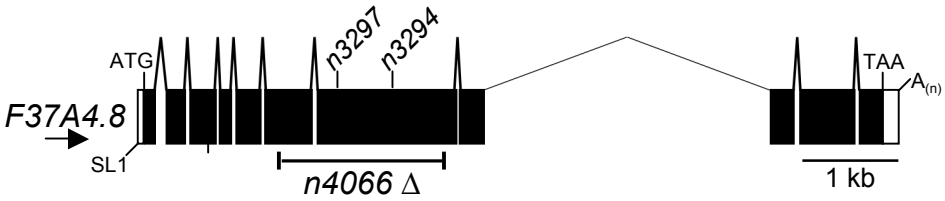
ATG
n3297
n3294
TAA
A(n)
F37A4.8
SL1
n4066 Δ
1 kb

C

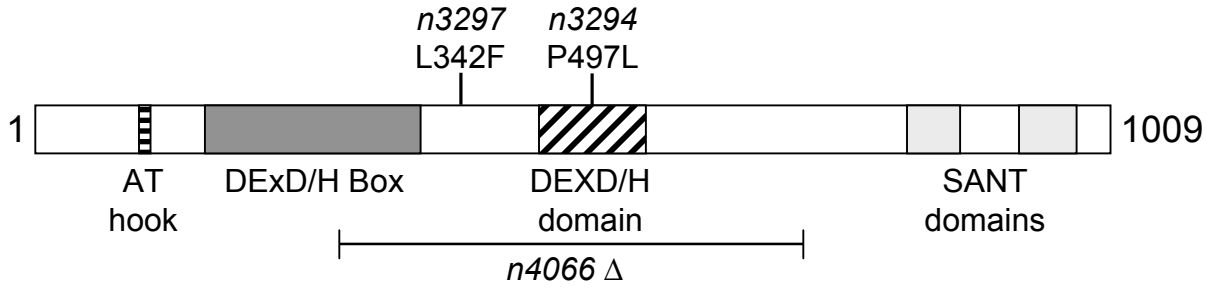
n3297
L342F
n3294
P497L
1
1009
AT
hook
DExD/H Box
DEXD/H
domain
SANT
domains
n4066 Δ

Figure 2: The *nurf-1* locus is predicted to encode multiple proteins. Each protein shares domains with *Drosophila* NURF301. Only the isoform containing the HMGA domain is required for antagonism of the synMuv genes.
(A) Genomic structures of the *nurf-1* isoforms. Exons, black boxes. 5' and 3' untranslated regions, white boxes. The predicted translation initiation and termination codons and the polyadenylation sites are indicated. The locations of the two deletion alleles are shown.
(B) A representation of the NURF-1 protein and domain structure. (Top) The *Drosophila* NURF301 protein (Bottom) The predicted protein products of the *nurf-1* gene. An alignment of the predicted functional domains of NURF-1 with those of *Drosophila* NURF301 is presented in Figure S2.
(C) Reduction of *nurf-1a* function suppresses the synMuv phenotype of *lin-15AB* mutants. RNAi of the *nurf-1a* isoform (pEA147) but not of the *nurf-1b, c, d, e* isoforms (pEA30) caused suppression of the *lin-15AB* synMuv phenotype. Also, deletion of the *nurf-1a* isoform (*n4293*) but not of the *nurf-1b,c,d,e* isoforms (*n4295*) caused suppression of the *lin-15AB* synMuv phenotype. M^+ denotes progeny of heterozygous mutant hermaphrodites, such progeny might retain maternally inherited *nurf-1a* gene products.

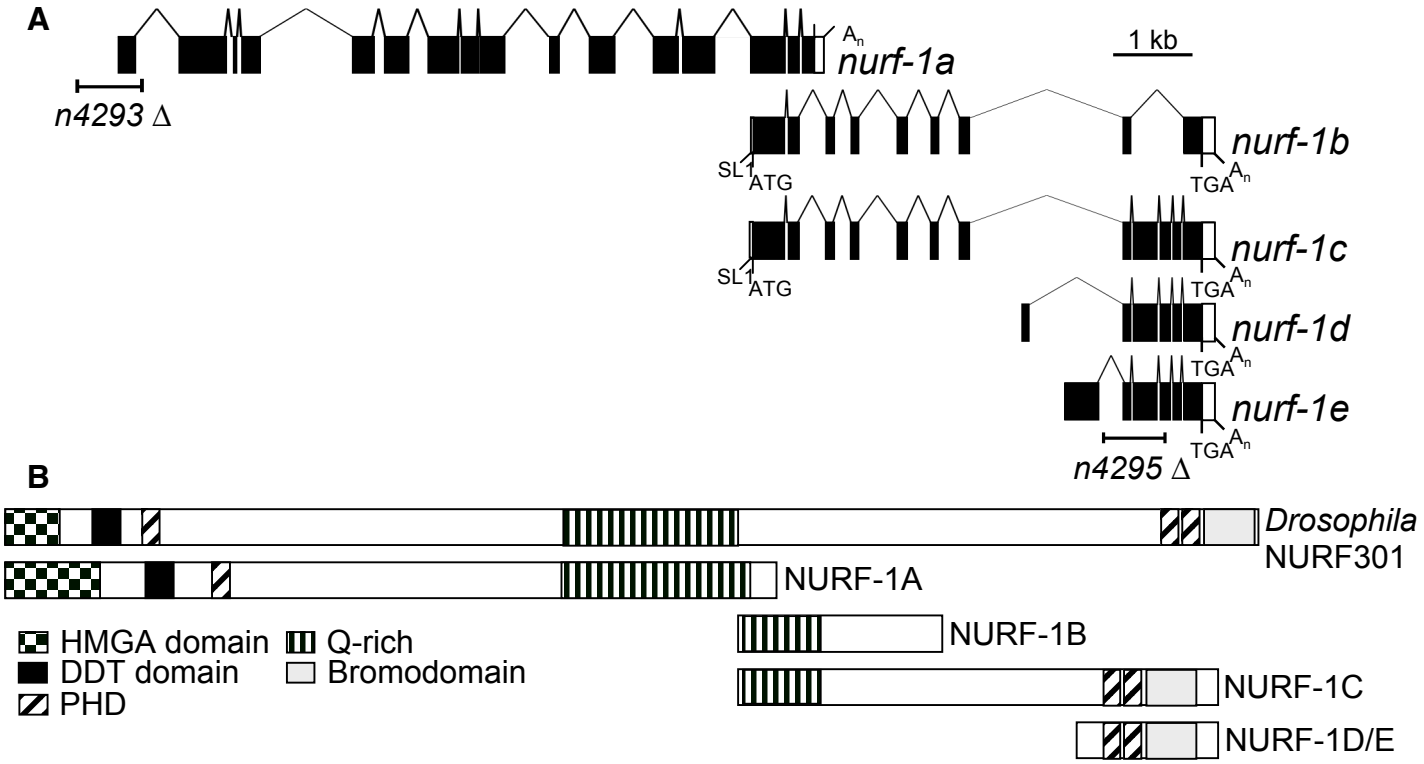

C

Genotype in a *lin-15AB(n765)* mutant background	Percent Muv (n)
nurf-1(+)	100 (546)
nurf-1a RNAi (pEA147)	0 (91)
nurf-1b,c,d,e RNAi (pEA30)	100 (111)
nurf-1a(n4293) M^+	4 (230)
nurf-1b,c,d,e(n4295)	100 (204)

Figure 3: Loss of *isw-1* function suppresses multiple cell-fate defects caused by mutations in class B synMuv genes.

(A) *isw-1(n3294)* suppresses the ectopic expression of PGL-1 in the soma of L1 larvae in the class B synMuv mutant *lin-15B(n744)*. anti-PGL-1 staining is shown in green, and nuclei (4,6-diamidino-2-phenylindole (DAPI) staining) are shown in blue. Scale bars,10 μm.

(B) Loss of *isw-1* function suppresses the Tam phenotype of *lin-15B* animals and represses normal transgene expression. The *ccIs4251* reporter is a simple repetitive transgene that expresses GFP in the nuclei of body-wall muscles. From left to right, *ccIs4251* was expressed in the following backgrounds: wild-type, *isw-1(RNAi)*, *lin-15B(n744)*, *isw-1(RNAi); lin-15B(n744)*. Scale bars,100 μm. A quantification of the Tam experiments is found in Figure S3.

(C) *isw-1* is required for the RNAi sensitivity of the class B synMuv mutant *lin-15B(n744)*. After exposure of animals to *cel-1* RNAi, the number of arrested L2 larvae was scored in at least three independent experiments. The average percent of L2 arrested larvae is shown. Error bars, standard deviations.

(D) The activity of *isw-1* and *nurf-1* are required for the larval-lethal phenotypes of *mep-1(q660)* and *let-418(n3536)* mutants. The percent of sterile adults present at 25ºC reflects the suppression of larval lethality. Error bars, standard deviations.

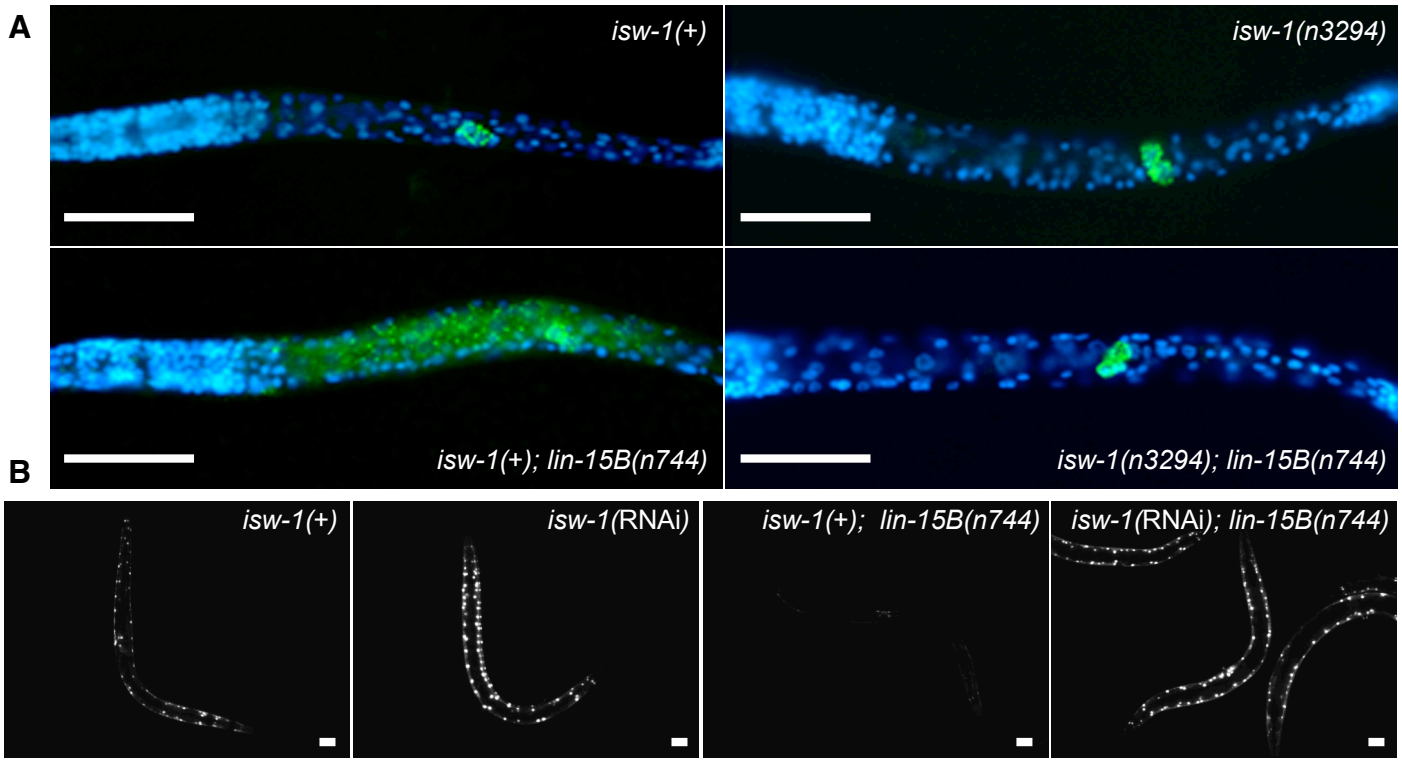
A
isw-1(+)
isw-1(n3294)
isw-1(+); lin-15B(n744)
isw-1(n3294); lin-15B(n744)
B
isw-1(+)
isw-1(RNAi)
isw-1(+); lin-15B(n744)
isw-1(RNAi); lin-15B(n744)

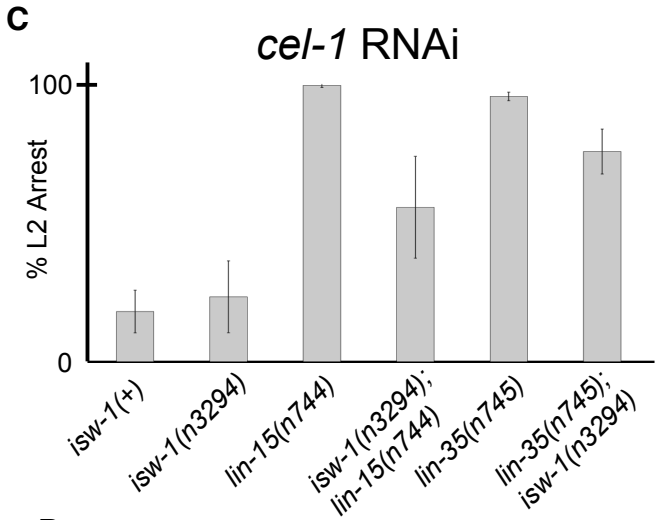
C
cel-1 RNAi
100
0
% L2 Arrest
isw-1(+)
isw-1(n3294)
lin-15(n744)
isw-1(n3294); lin-15(n744)
lin-35(n745)
lin-35(n745); isw-1(n3294)

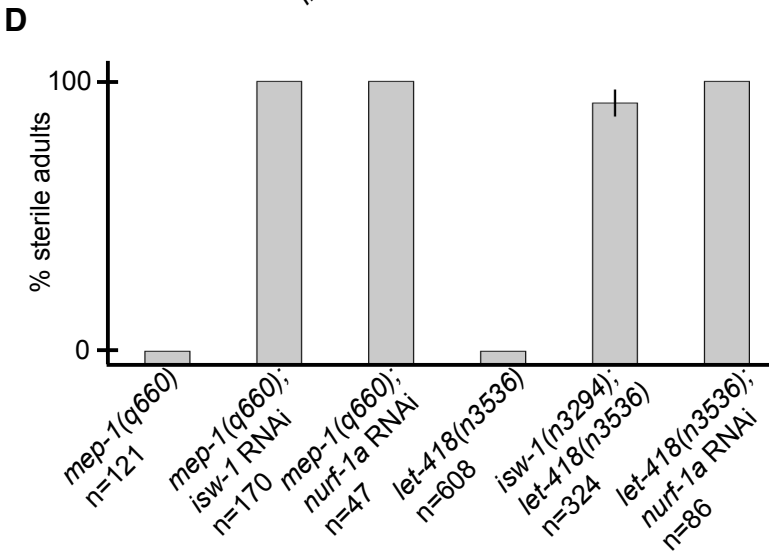
D
100
0
% sterile adults
mep-1(q660) n=121
mep-1(q660); isw-1 RNAi n=170
mep-1(q660); nurf-1a RNAi n=47
let-418(n3536) n=608
isw-1(n3294); let-418(n3536) n=324
let-418(n3536); nurf-1a RNAi n=86

Table S1: *isw-1(*RNAi*)* suppresses the synMuv phenotypes conferred by strong mutations in any class A synMuv gene

Class A synMuv genotype in a *lin-53(n833)* background	% Muv with control RNAi (n)	% Muv with *isw-1* RNAi (n)
lin-8(n2731)	100 (217)	1 (109)
lin-15A(n767)	100 (168)	1 (116)
lin-38(n751)	100 (304)	2 (290)
lin-56(n2728)	100 (234)	4 (118)
*isw-1(*RNAi*)* suppresses the synMuv phenotypes conferred by strong mutations in all class B synMuv genes		
Class B synMuv genotype in a *lin-15A(n767)* background	% Muv with control RNAi (n)	% Muv with *isw-1* RNAi (n)
lin-9(n942)[a] *unc-32(e189)*	99 (147)	47 (302)
lin-13(n387)[a]	96 (110)	7 (160)
lin-15AB(e1763)[b]	100 (300)	55 (347)
lin-35(n745)[b]	100 (143)	14 (70)
lin-36(n766)	100 (311)	1 (214)
lin-37(n758)	99 (381)	5 (99)
lin-52(n3718)[a,b]	100 (20)	5 (20)
lin-53(n3368)[a]	100 (70)	2 (107)
unc-30(e191) lin-54(n3423)[a]	99 (95)	4 (138)
dpl-1(n3316)[a]	99 (191)	2 (246)
efl-1 RNAi[c]	98 (169)	0 (88)
unc-46(e177) tam-1(cc567)[d]	40 (237)	1 (101)
let-418(n3719)[a]	100 (79)	0 (139)
mep-1(n3703)[a]	92 (78)	0 (143)
hda-1(e1795)[a]	59 (96)	12 (51)
hpl-2(tm1489)	100 (348)	0 (269)
*isw-1(*RNAi*)* suppresses the Muv phenotypes conferred by single mutations in class C and class B synMuv genes		
synMuv Genotype	% Muv with control RNAi (n)	% Muv with *isw-1* RNAi (n)
lin-13(n387)[a,d]	19 (77)	0 (55)
hpl-2(tm1489)[d]	71 (110)	0 (109)
trr-1(n3712)[a,]	9 (45)	0 (48)

[a] The animals scored were descended from synMuv mutant heterozygotes.
[b] For these RNAi experiments, the data were derived from RNAi by injection.
[c] *efl-1* was inactivated by RNAi in the control *lin-15A(n767)* and in *isw-1(n3294); lin-15A(n767)* animals
[d] These animals were scored at 25ºC.

Table S2: *isw-1* mutations cause decreased brood sizes and sterility.

isw-1 genotype	Brood size ± s.d.	% Sterile^ (n)
isw-1(+)	279 ± 27	0 (1115)
isw-1(n3294)	76 ± 66	43 (228)
isw-1(n3297)	138 ± 43	5 (554)
*isw-1(n4066)**	NA[#]	100 (89)
*isw-1(*RNAi*)*	NA[#]	100 (266)

^ Sterility was scored viewing live animals with Nomarski optics and fixed animals stained with DAPI using fluorescence microscopy. *isw-1* mutants generated disorganized oocytes that failed to be fertilized. The sterile phenotype of *nurf-1(n4293)* homozygotes was similar to that of *isw-1(n4066)* homozygotes, but the penetrance was lower and some embryos were formed; the animals that hatched from those embryos arrested as early larvae (data not shown).

* These homozygous animals were descended from *isw-1(n4066)* heterozygotes.

[#] Not Applicable, because animals were 100% sterile and therefore had no progeny.

SUPPLEMENTAL FIGURE DESCRIPTIONS

Supplemental Figure 1:

Alignment of ISW-1 with *Drosophila* ISWI and *S. cerevisiae* SWI2/SNF2. Solid boxes indicate two out of three amino acids are identical among ISW-1, ISWI and SWI2/SNF2. Red arrowheads indicate sites of amino acid changes caused by the *isw-1* missense mutations. The *isw-1(n4066)* deletion allele is marked by blue boxes with arrows pointed towards the deleted region. The AT-hook, ATPase, DEAH/D box helicase and SANT domains are indicated by a black and white box, dark grey box, diagonally hatched box and black boxes, respectively.

Supplemental Figure 1

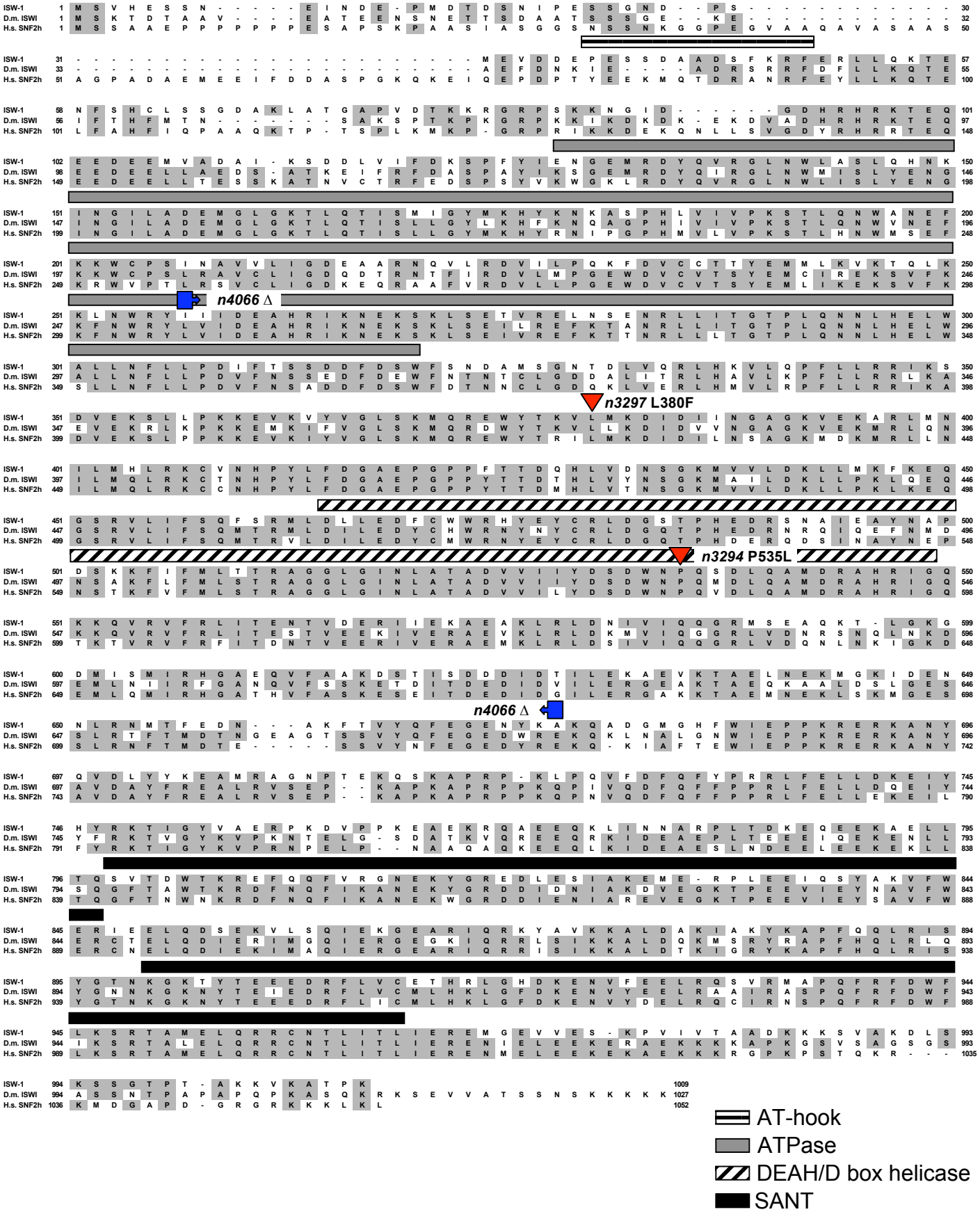

Supplemental Figure 2:

Alignment of the predicted domains of NURF-1 and *Drosophila* NURF301. Solid boxes indicate identity between NURF-1 and NURF301. The domains are shown from N-terminus to C-terminus and correspond to the domains shown in Figure 2B: (A) AT-hook motifs of the HMGA domain; (B) DDT domains; (C) PHD fingers; (D) bromodomains.

Supplemental Figure 3

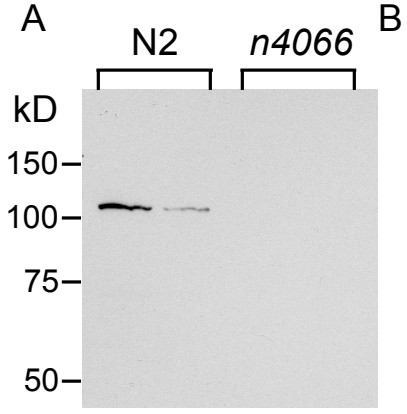

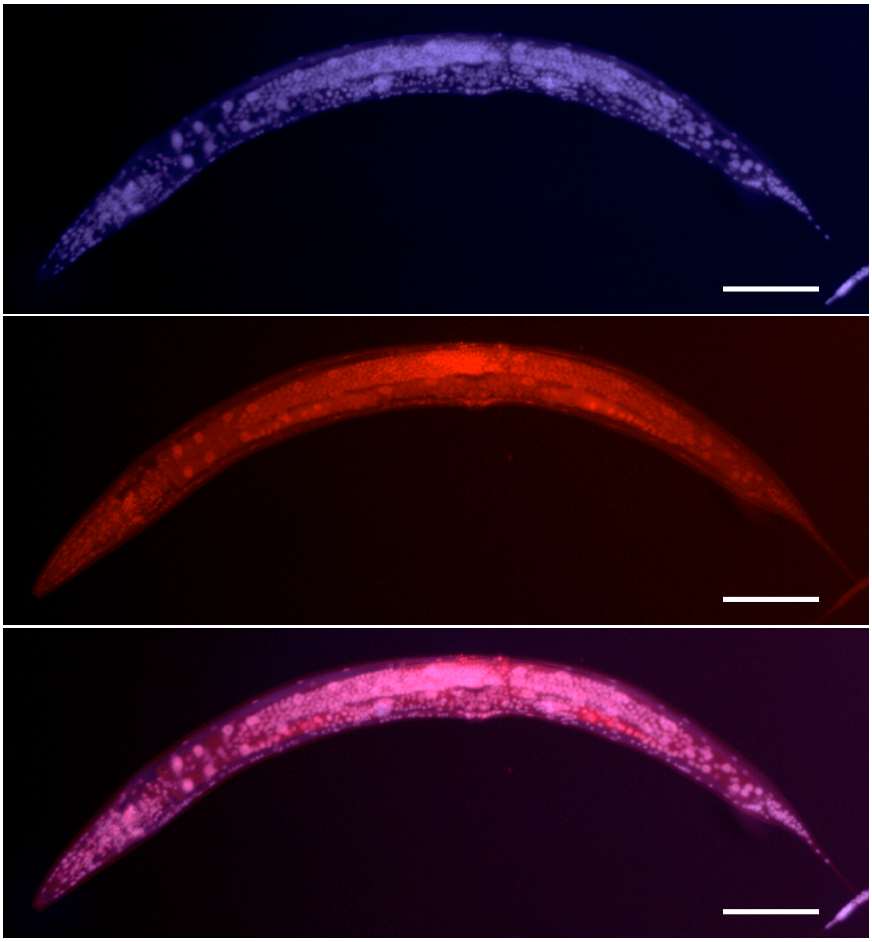

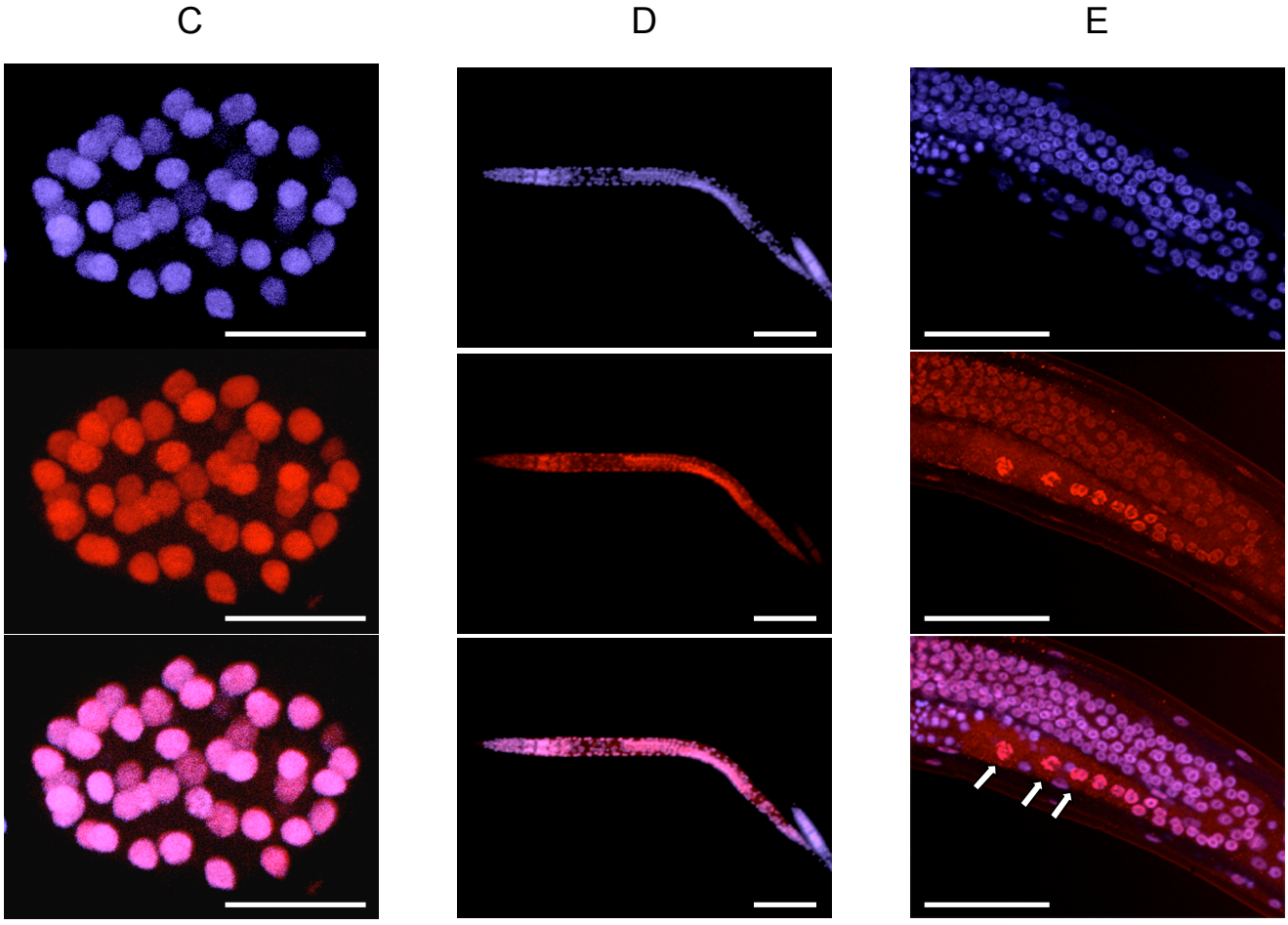

Supplemental Figure 3:

ISW-1 is broadly expressed in the nuclei of most if not all cells throughout development.

(A) Anti-ISW-1 antisera are specific for ISW-1. A western blot showing the specificity of the ISW-1 antisera by the presence of a ~110 kD band in the wild-type protein samples from 50 and 25 animals (lanes 1 and 2) but not in the *isw-1(n4066)* mutant protein samples from 50 and 25 animals (lanes 3 and 4). For B-E, red is anti-ISW-1 staining, and blue is DAPI. The colocalization appears as purple. From top to bottom, DAPI, anti-ISW-1 and merge.

(B) ISW-1 expression in a young adult. Scale bar, 100 μm.

(C) ISW-1 expression in a ~64-cell embryo. Scale bar, 10 μm.

(D) ISW-1 expression in third stage larva. Scale bar, 100 μm.

(E) ISW-1 expression in an adult germline. Note the high level of ISW-1 staining in the oocytes (white arrows). Scale bar, 50 μm.

Supplemental Figure 2

Supplemental Figure 4:

Shown are the mean levels of GFP expression from the *ccIs4251* transgene reporter in the experiments shown in Figure 4D, as measured by number of pixels in a defined region of interest from at least 10 animals in each genetic background. The fluorescence from the vulva to the posterior end was quantified within the linear range of detection (see Materials and Methods). Error bars, standard deviations.

Supplemental Figure 4

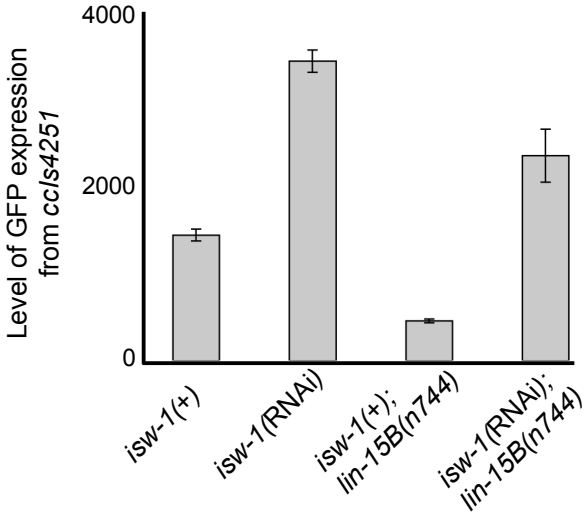

CHAPTER FOUR ADDENDUM

isw-1 is required for the ectopic expression of *lin-3* EGF in *lin-15AB(n765)* mutants

Recently, *lin-3* EGF was identified as a transcriptional target of the synMuv genes (CUI *et al.* 2006). The authors reported that class AB synMuv mutants but not class A or B single mutants have increased *lin-3* EGF transcription. Because *lin-3* encodes the ligand for the Ras pathway (HILL and STERNBERG 1992), ectopic expression causes increased Ras pathway activity, which leads to ectopic vulval cell fates and a Muv phenotype (KATZ *et al.* 1995).

We identified *isw-1* as a suppressor of the synMuv phenotype (ANDERSEN *et al.* 2006), and it encodes a homolog of an ATP-dependent chromatin-regulatory protein. I hypothesized that because in class AB synMuv double mutants the loss of transcriptional repression causes an increase in *lin-3* transcription, perhaps ISW-1 as a part of the NURF-like complex with the *C. elegans* NURF301 homolog NURF-1 promotes that ectopic *lin-3* transcription. This hypothesis would explain why loss of *isw-1* suppresses the synMuv phenotype, because *lin-3* can not longer be ectopically expressed, and why single *isw-1* mutants do not have abnormal vulval development, because *isw-1* is required only for the increased expression of *lin-3* EGF and not for normal *lin-3* expression. Therefore, *isw-1(n3294)* synMuv suppressed animals should have wild-type levels of *lin-3* EGF.

We used real-time reverse-transcriptase PCR assays (see Chapter Two) to measure levels of *lin-3* expression in wild-type animals, *lin-15AB* synMuv mutants and the *isw-1(n3294); lin-15AB* synMuv suppressed strain (Addendum Figure 1). Our preliminary results showed that *lin-15AB* caused increased expression of *lin-3*, and that increased expression of *lin-3* required *isw-1*. These results confirm that in synMuv mutants transcriptional repression of *lin-3* is decreased and *lin-3* transcription is increased. The *isw-1(n3294); lin-15AB(n765)* synMuv suppressed mutants had lower levels of *lin-3* expression than the

synMuv strain *lin-15AB(n765)*. Therefore, the increase in *lin-3* expression in class AB synMuv mutants requires the ATP-dependent chromatin-remodeling activities of the NURF-like complex to ectopically express *lin-3*. Without these chromatin-remodeling activities, *lin-3* transcription is not increased, and a wild-type vulval phenotype is expressed.

***isw-1* is required for the class A double mutant synMuv phenotype**

The NURF-like complex opposes the actions of the synMuv genes in the control of multiple cell fates. We found that loss of *isw-1* suppressed the synMuv phenotype of all class AB double mutants tested (see above). Additionally, RNAi of *isw-1* suppressed the Muv phenotypes and the germline-versus-soma cell-fate defects of single class B mutants (see above). Taken together these results suggest that *isw-1* likely acts downstream of or in parallel to at least the class B synMuv genes. Recently, Adam Saffer found that some class AA synMuv double mutants have Muv phenotypes at high temperatures (A. Saffer and H. R. Horvitz, unpublished results). We tested whether inactivation of *isw-1* could suppress the class A double mutant synMuv phenotypes of *lin-38(n751); lin-15A(n767)* and *n4441; lin-15A(n767)* (Addendum Table 1). We found that in both strains the synMuv phenotype was suppressed after RNAi of *isw-1*. Therefore, *isw-1* likely acts downstream of or in parallel to both the class A and the class B genes in the control of vulval cell fates.

ADDENDUM LITERATURE CITED

ANDERSEN, E. C., X. LU and H. R. HORVITZ, 2006 *C. elegans* ISWI and NURF301 antagonize an Rb-like pathway in the determination of multiple cell fates. Development **133:** 2695-2704.

CUI, M., J. CHEN, T. R. MYERS, B. J. HWANG, P. W. STERNBERG, I. GREENWALD and M. HAN, 2006 SynMuv genes redundantly inhibit *lin-3*/EGF expression to prevent inappropriate vulval induction in *C. elegans*. Dev Cell **10:** 667-672.

HILL, R. J., and P. W. STERNBERG, 1992 The gene *lin-3* encodes an inductive signal for vulval development in *C. elegans*. Nature **358:** 470-476.

KATZ, W. S., R. J. HILL, T. R. CLANDININ and P. W. STERNBERG, 1995 Different levels of the *C. elegans* growth factor LIN-3 promote distinct vulval precursor fates. Cell **82:** 297-307.

Addendum Table 1: Reduction of *isw-1* suppresses the synMuv phenotype of class A synMuv double mutants at 25ºC

Genotype	% Muv after control RNAi (n)	% Muv after *isw-1* RNAi (n)
lin-38(n751); lin-15A(n767)	28 (169)	0 (132)
n4441; lin-15A(n767)	45 (40)	0 (86)

FIGURE DESCRIPTIONS

Addendum Figure 1: *isw-1(n3294)* suppresses the increased level of *lin-3* expression in the class AB double mutant *lin-15AB(n765)*

Real-time RT-PCR experiments were performed using RNA samples from the genotypes indicated. Each real-time PCR experiment was performed in triplicate on RNA samples from three different culture growths. Mean ΔΔCt values were used to calculate relative changes in *lin-3* expression normalized to levels of *rpl-26*. The normalized change of *lin-3* is shown with the range determined from the standard deviation.

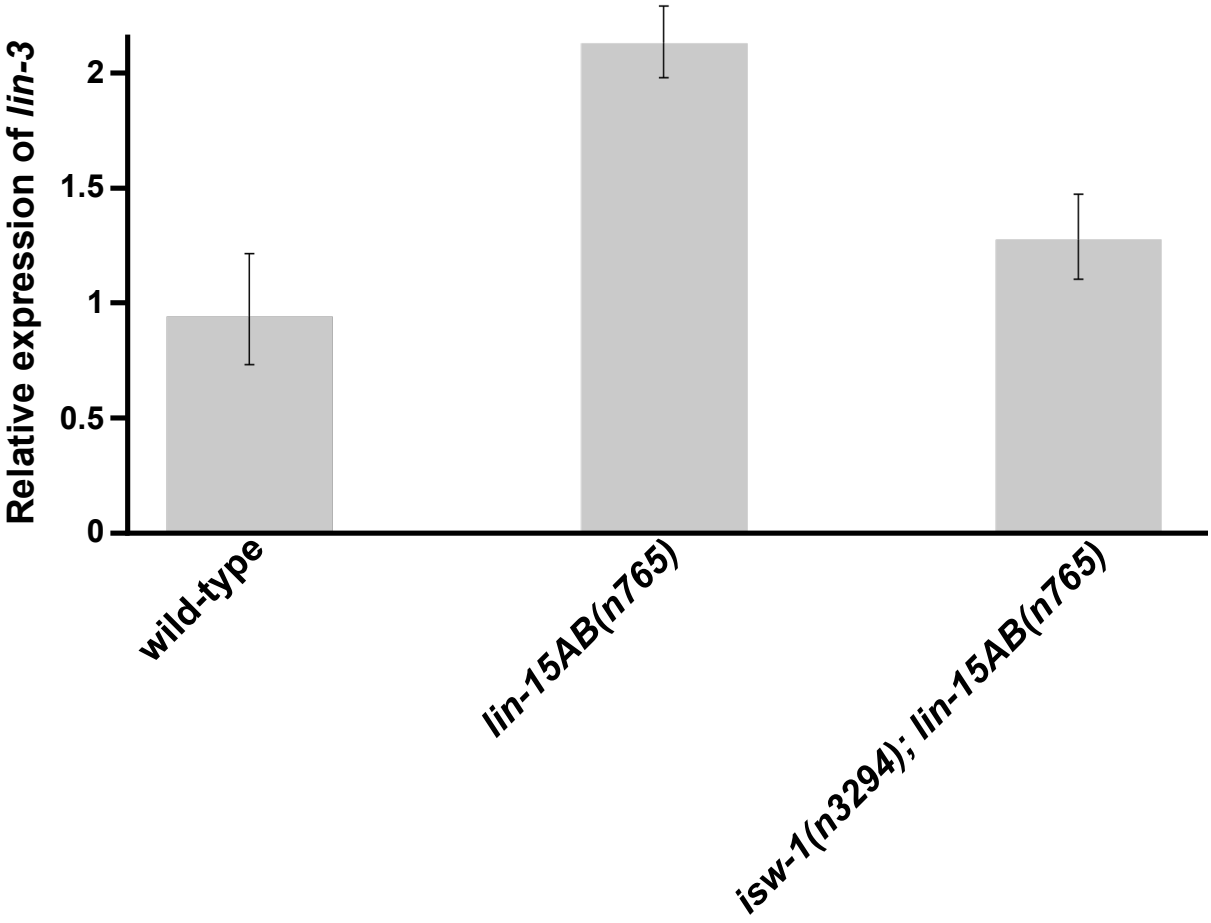
Relative expression of lin-3
2
1.5
1
0.5
0
wild-type
lin-15AB(n765)
isw-1(n3294); lin-15AB(n765)

CHAPTER FIVE

lst-3, the *C. elegans* CARP-1 homolog, inhibits vulval cell fates by the transcriptional repression of *lin-3* EGF

Erik C. Andersen, Scott Clark[1], Melanie Worley[2] and H. Robert Horvitz

[1] *Present address:* Skirball Institute Program of Molecular Neurobiology, NYU School of Medicine, 540 First Avenue, New York, NY 10016

[2] *Present address:* University of California, Berkeley, Department of Molecular and Cell Biology, 142 LSA #3200, Berkeley, CA 94720

Graduate student Scott Clark identified *n2070* in a *lin-15AB* synMuv suppressor screen. He determined that the mutant phenotype was dominant and mapped the responsible mutation to chromosome IV. I mapped the mutation further, cloned the gene (*lst-3*) and performed the characterization described here. Undergraduate student Melanie Worley made the *lst-3a* cDNA construct under my supervision.

This manuscript is being prepared for publication.

SUMMARY

Conserved Ras and Notch cell-signaling pathways promote *Caenorhabditis elegans* vulval cell fates. Ras pathway activity promotes the 1º vulval fate and inhibits the 2º vulval fate, and Notch pathway activity promotes the 2º vulval fate and inhibits the 1º vulval fate. Vulval cell fates are inhibited by the parallel-acting synthetic multivulva (synMuv) genes, which are grouped into either class A or B genes. We identified a mutation that suppresses the synMuv phenotype and found that this mutation is a gain-of-function allele of the gene *lst-3*. *lst-3* is activated by the Notch pathway to inhibit the Ras pathway in presumptive 2º vulval cells to ensure low levels of Ras pathway activity and proper 2º vulval fate specification. We found that *lst-3* encodes a homolog of human CARP-1, a cell-cycle and apoptosis regulatory protein and putative transcription factor. Our findings indicate that *lst-3* might inhibit the Ras pathway by repressing the transcription of the Ras pathway ligand *lin-3* EGF. By analogy, we suggest that CARP-1 might act as a tumor suppressor by inhibiting the expression of growth factor signals.

INTRODUCTION

Peptide growth factors regulate cell proliferation, growth and differentiation (DEUEL 1987). The expression of these growth factors is tightly controlled. In humans, a failure to properly control growth factor expression can lead to excess cell proliferation and cancer. The signals from growth factors are transduced through a small number of conserved intercellular signaling pathways during development. These signaling pathways control cell proliferation, growth and differentiation by regulating the transcription of genes important for cell-fate determination (SUNDARAM 2005; STERNBERG 2006).

The development of the vulva of the *Caenorhabditis elegans* hermaphrodite provides an example of cell-fate determination controlled by growth factor-mediated cell-signaling pathways (STERNBERG 2006). The vulva is formed by the 22 descendants of three ectodermal blast cells (P5.p, P6.p and P7.p) located on the ventral surface of the animal (SULSTON and HORVITZ 1977). These three cells are specified to become vulval cells from a set of six equipotent cells (P3.p through P8.p), called the vulval equivalence group. An EGF-like ligand expressed in the gonadal anchor cell (AC) near the vulval equivalence group induces P5.p, P6.p and P7.p to adopt vulval cell fates (SULSTON and WHITE 1980; KIMBLE 1981) through activation of a conserved receptor tyrosine kinase (RTK)/Ras proto-oncogene cell-signaling cascade (KORNFELD 1997). P6.p adopts the 1º vulval fate, dividing three more times to generate eight descendants. P5.p and P7.p adopt 2º vulval cell fates with each cell generating seven descendants. The remaining three cells of the vulval equivalence group, P3.p, P4.p and P8.p, adopt non-vulval cell fates, typically dividing once and fusing with the nieghboring syncytial hypoderm (STERNBERG and HORVITZ 1986).

The three cells of the vulval equivalence group induced to become vulval cells adopt either the 1º or the 2º vulval cell fate. The decision to become a 1º or 2º cell is determined by the level of Ras or Notch pathway activity in that cell (SUNDARAM 2005). The induced cell with the most Ras pathway activation

becomes a 1º vulval cell and expresses LIN-12 Notch receptor ligands, which signal to the neighboring cells to become 2º vulval cells (CHEN and GREENWALD 2004). The 1º cell also down-regulate expression and membrane localization of LIN-12 Notch, reinforcing the 1º vulval cell-fate decision (SHAYE and GREENWALD 2005). Vulval cells adopting the 2º cell fate express genes that are the targets of the LIN-12/LAG-1 transcription factors to reinforce the 2º vulval cell fate and repress the 1º vulval cell fate (YOO *et al.* 2004). This combination of positive and negative feedback creates the pattern of cell fates generated during vulval development, 2º - 1º - 2º, which ultimately gives rise to a wild-type vulva (SULSTON and HORVITZ 1977; STERNBERG and HORVITZ 1986).

Genetic screens have identified many mutants defective in the adoption of vulval cell fates (KORNFELD 1997). These mutants have either of two phenotypes: no cells of the vulval equivalence group adopt vulval fates (called vulvaless or Vul) or more than three cells of the vulval equivalence group adopt vulval cell fates (called multivulva or Muv). Along with genetic studies of the *Drosophila* eye (SIMON 1994) and biochemical studies of mammalian cells (MALUMBRES and BARBACID 2003), Vul and Muv mutants helped define the Ras and Notch cell-signaling pathways (KORNFELD 1997). Genetic studies of vulval development have also identified negative regulators of the Ras pathway, which are required for attenuation of this proto-oncogene mediated cell-signaling pathway (MOGHAL and STERNBERG 2003). These genes, which were identified as mutations able to suppress the Vul phenotypes caused by Ras pathway loss-of-function mutations, include *gap-1*, a Ras GTPase activating protein (HAJNAL *et al.* 1997), *sli-1*, a c-Cbl homolog (JONGEWARD *et al.* 1995; YOON *et al.* 1995), *unc-101*, an AP47 homolog (LEE *et al.* 1994) and the uncloned gene *sli-3* (GUPTA *et al.* 2006). Transcriptional targets of LIN-12/LAG-1 in 2º vulval cells include the Ras pathway negative regulators *lip-1*, a MAPK phosphatase (BERSET *et al.* 2001), *ark-1*, an Ack-related non-receptor tyrosine kinase (HOPPER *et al.* 2000) and a group of *lateral signal target* (*lst*) genes (YOO *et al.* 2004).

The synthetic multivulva (synMuv) genes define other pathways that inhibit vulval cell fates (HORVITZ and SULSTON 1980; FERGUSON and HORVITZ 1989). The synMuv genes are grouped into two classes: A and B (FERGUSON and HORVITZ 1989 and Chapter 3). Most loss-of-function mutations within one class do not cause a Muv phenotype, but mutations of genes in any two classes cause a highly penetrant Muv phenotype. The class A synMuv genes encode novel nuclear proteins, and most have putative DNA-binding domains (CLARK *et al.* 1994; HUANG *et al.* 1994; DAVISON *et al.* 2005; A.M. Saffer, E.M. Davison and H.R.H., unpublished results). The class B synMuv genes encode homologs of transcriptional repressors and proteins that remodel chromatin (LU and HORVITZ 1998; VON ZELEWSKY *et al.* 2000; CEOL and HORVITZ 2001; COUTEAU *et al.* 2002; DUFOURCQ *et al.* 2002; UNHAVAITHAYA *et al.* 2002; CEOL and HORVITZ 2004; CEOL *et al.* 2006). These homologies suggest that the synMuv genes might negatively regulate vulval cell fates through the transcriptional repression of genes that promote the vulval fate. Recently, several synMuv genes likely regulate the transcriptional repression of the *lin-3* EGF ligand (CUI *et al.* 2006a); it has been reported that synMuv mutants have increased expression of this Ras pathway ligand, which causes the ectopic adoption of vulval cell fates.

MATERIALS AND METHODS

Strains and genetics:

C. elegans was cultured at 20ºC with *Escherichia coli* OP50 as described (BRENNER 1974), unless otherwise indicated. The wild-type strain used was N2 (Bristol). For mapping using single-nucleotide polymorphisms, we used the wild-type strain CB4856 (Hawaiian). All mutations are described previously (RIDDLE 1997), unless from this work or noted otherwise:

LGI: *lin-35(n745)*, *lin-61(n3809)* (HARRISON *et al.* 2007), *lst-1(ok814)*,

LGII: *lin-8(n111, n2731)* (DAVISON *et al.* 2005), *lin-31(n301)* (MILLER *et al.* 2000), *dep-1(zh34)* (BERSET *et al.* 2005), *dpl-1(n2994)* (CEOL and HORVITZ 2001), *let-23(sa62*, *sy1*, *sy97)* (AROIAN *et al.* 1990; KATZ *et al.* 1996), *lin-56(n2728)* (THOMAS *et al.* 2003), *lin-38(n751)*, *syIs12 [hs::lin-3]* (KATZ *et al.* 1995),

LGIII: *lin-37(n4903)* (ANDERSEN *et al.* 2006), *lin-9(n112)*, *lin-12(n137*, *n460*, *n941)* (GREENWALD *et al.* 1983), *unc-101(sy108)* (LEE *et al.* 1994),

LGIV: *lin-1(e1275)* (BEITEL *et al.* 1995), *lip-1(zh15)* (BERSET *et al.* 2001), *lin-3(n378)*, *let-60(n1876*, *n1046)*, *ark-1(sy247)* (HOPPER *et al.* 2000), *lst-3(n2070*, *gk433*, *n4590*, *n4565*, *n4566*, *n4575)* (this work),

LGV: *mys-1(n3681)* (CEOL and HORVITZ 2004)

LGX: *sli-1(sy143)* (JONGEWARD *et al.* 1995), *gap-1(ga133)* (HAJNAL *et al.* 1997), *lin-15B(n2993, n744)*, *lin-15A(n433*, *n767)*, *lin-15AB(n765*, *n309)*, *nIs202 [lst-3::yfp]*, *syIs50 [cdh-3::gfp]* (PETTITT *et al.* 1996), *syIs59 [egl-17::cfp]* (INOUE *et al.* 2002).

The LGIV duplication *yDp1* and deficiency *sDf23* were used for studies of gene dosage. The following reciprocal translocations with GFP-expressing transgenes integrated at or near the translocation breakpoints were used: *hT2 [qIs48]* LGI; LGIII, *eT1 [nIs266]* LGIII; LGV, *nT1 [qIs51]* LGIV; LGV. *mIn1 [mIs14 dpy-10(e128)]* (EDGLEY and RIDDLE 2001) and *qC1 [nIs189]* (ANDERSEN *et al.* 2006) are balancer chromosomes that express GFP. *lst-1(ok814)* was kindly provided by the *C. elegans* Knockout Consortium.

Linked double mutants with *lst-3* alleles were constructed by combining single mutations with mutations causing a visible mutant phenotype in *cis*. The two *cis*-marked mutations were crossed to generate heterozygous males and then those males were mated to a strain with both *cis*-marker mutations. Selecting wild-type progeny from that cross isolated recombinants. For example to construct a *lin-1(e1275) lst-3(gk433)* double mutant, we mated males of the genotype *dpy-13(e184) + lst-3(gk433) + / + lin-1(e1275) + unc-30(e191)* with *dpy-13(e184) unc-30(e191)* hermaphrodites and selected non-Unc non-Dpy cross progeny. These animals had recombined *lin-1(e1275)* and *lst-3(gk433)* in *trans* to *dpy-13(e184) unc-30(e191)*.

The *lst-3* transcriptional reporter expressing *yfp*, *arEx460* (YOO *et al.* 2004), was kindly provided by Iva Greenwald. We wanted to determine the expression pattern of *lst-3*, so we generated an integrated transgenic reporter using *arEx460* using the following protocol. We irradiated L4 hermaphrodites using a cobalt-60 gamma ray source for one hour (4800 Rads). Five irradiated P_0 animals were distributed onto 50-mm Petri plates. The progeny were allowed to consume all the bacteria on the plates and transferred on a segment of agar from the original plate to a fresh 20-mm Petri plate with new bacteria. This procedure was done three times. From the last transfer, four YFP+ animals were distributed singly to 50-mm Petri plates, and their progeny were scored for the presence of YFP. Cultures in which all animals expressed YFP were kept, backcrossed two times to the wild type and mapped to linkage groups using visible markers (BRENNER 1974). The integrant *nIs202* was used in subsequent analyses, because *nIs202* mapped to LGX and had high YFP expression as compared to other integrated lines.

Isolation of *n2070* and *cis*-dominant suppressor isolates:
Suppressors of the *lin-15AB(n765)* synMuv phenotype were isolated after mutagenesis using ethyl methanesulfonate (EMS) (BRENNER 1974). Five mutagenized P_0 synMuv mutants were transferred to a single 50-mm Petri plate

and grown at 22.5ºC. Progeny were screened for animals that lacked the synMuv phenotype. The progeny of 38,000 F_1 animals were screened in this way. The synMuv suppressor *n2070* was identified in this screen.

Linked suppressors of the *n2070* dominant synMuv suppression phenotype were identified after mutagenesis of *lst-3(n2070)/nT1[qIs51]; lin-15AB(n765)* L4 hermaphrodites as described (BRENNER 1974). We allowed these animals to recover for one hour and then transferred 20 to 25 to 100-mm Petri plates. We screened for Muv animals after 3-5 days at 20ºC. Roughly 10,000 haploid genomes were screened.

Isolation of deletion alleles:

Genomic DNA pools from trimethyl psoralen-mutagenized animals exposed to ultraviolet light were screened for deletions using PCR as described (LIU *et al.* 1999). Deletion mutants were isolated from frozen stocks and backcrossed to the wild type at least six times. The *lst-3(n4590)* deletion allele begins with the sequence CGAGATATTATGGCA and ends with the sequence TGGGGCGCCGCGCCG. The *lst-3(gk433)* deletion allele begins with the sequence ATCATTCATTCGTGTA and ends with the sequence ATTCAGCTTCTCAACGCG corresponding to sequence found in the *C. elegans* wild-type genomic clone Y37A1.

Genetic mapping:

Ten of 14 Unc non-Dpy progeny and five of 17 were Dpy non-Unc progeny from the + *n2070* + / *unc-30* + *dpy-4; lin-15AB(n765)* three-point mapping cross carried *n2070*. *unc-30 n2070 dpy-4; lin-15AB(n765)* mutant animals were constructed for polymorphism mapping using CB4856. Recombinants were generated from animals heterozygous for LGIV between CB4856 and N2: *unc-30 n2070 dpy-4 / + + +* (CB4856)*; lin-15AB(n765)*. We isolated 17 recombinants. One recombinant broke right of *pkP4092* and to the left of *n2070*, and four recombinants broke left of snp_F20H6[1] and to the right of *n2070*. The region

defined by the polymorphism mapping experiments contains 46 predicted open reading frames.

Determination of allele sequences:

We used PCR-amplified regions of genomic DNA to determine mutant and wild-type allele sequences. All exon, intron and splice-junction sequences were determined in *lst-3(n2070)* and the linked suppressors *lst-3(n4565*, *n4566*, *n4575)*. All mutations were confirmed using independently derived PCR products. An ABI Prism 3100 Genetic Analyzer was used to determine the sequences. The resulting sequence reads were analyzed using Sequencher software (GeneCodes).

Construction of single and double unlinked *lst-3* strains:

lst-3(gk433), *lst-3(n4590)* and *lst-3(n2070)* were balanced in *trans* by the double-mutant combination *unc-30(e191) dpy-4(e1166)* and by the reciprocal translocation *nT1[qIs51]*. In some cases, the deletion alleles *lst-3(gk433* and *n4590)* were followed using PCR assays to detect deletion and wild-type sequences. In all constructions where PCR was used to follow a deletion allele at least two independent genomic DNA preparations and PCR assays were performed. An allele-specific PCR assay was developed to follow *lst-3(n2070)* and the wild-type *lst-3* sequence. This type of PCR assay is called SNAP (single-nucleotide amplified polymorphisms) (DRENKARD *et al.* 2000), and we optimized it for use with *lst-3*. Like strain constructions using PCR to follow *lst-3* deletion alleles, two independent genomic DNA preparations and PCR assays were performed for all constructions using PCR to follow *lst-3(n2070)*.

***lst-3* gain-of-function phenocopy suppression of the synMuv phenotype**

Germline transformation experiments were done as described (MELLO *et al.* 1991). Platinum High-Fidelity Taq Polymerase (Invitrogen) was used to amplify the *lst-3* genomic region and two kb of DNA at both the 5' and 3' end of the gene.

The PCR product was injected into *lin-15AB(n765)* synMuv mutants with pTG96 (*sur-5::gfp*) (YOCHEM *et al.* 1998) as a co-injection marker at 20 ng/μL. Only F_1 transformants were obtained, and the synMuv phenotype of each transformant was suppressed.

Scoring the vulval cell fate

For strains in which the Muv phenotype was to be compared to the Muv phenotype of other strains, the percent of Muv animals was counted in three independently grown cultures. The mean and standard deviation of the Muv phenotype was calculated. In some cases, vulval induction was scored during the L4 larval stage using Nomarski optics.

RNA-mediated interference assays

The Ahringer library for RNAi by feeding (FRASER *et al.* 2000; KAMATH *et al.* 2003) was used. NGM agar with 25 μg/mL mM carbenicillin and 1 mM IPTG was aliquoted into each well of a 24-well culture dish. Bacterial strains expressing dsRNAs corresponding to each gene were grown overnight in 96-deep-well plates with 700 μL of Luria broth supplemented with 25 μg/mL mM carbenicillin. 15 μL of each overnight culture was distributed onto each of four wells of the 24-well culture dish so that each culture dish contained RNAi clones for six genes. An independent RNAi by injection experiment was performed using dsRNA produced from the cDNA clone yk338g10 (kindly provided by Yuji Kohara) and as described previously (ANDERSEN *et al.* 2006).

Molecular biology

To define the *lst-3* gene structures, we determined the sequences of three independent cDNAs, yk338g10, yk1045d10 and yk1079d11. We used 5' rapid amplification of cDNA ends (5' RACE, Invitrogen) to determine the 5' end of *lst-3*, and we detected an SL1 splice-leader sequence. We constructed a full-length *lst-3* cDNA using the 5' RACE clone and the cDNA yk338g11. The two sequences

were combined using the yeast-mediated ligation system described previously (OLDENBURG *et al.* 1997) and using the Gateway recombinase system (Invitrogen) transferred to make clone pEA202.

Microscopy and image processing

We used an upright compound microscope Axioskop 2 (Zeiss) microscope equipped with Nomarski optics, YFP, CFP and GFP filter sets (Chroma). All images were collected using OpenLabs software and processed using Adobe Photoshop.

Quantitative real-time reverse-transcriptase polymerase chain reactions (real-time RT-PCRs)

Synchronized wild-type and mutant animals were grown and larvae were harvested at or near the L2/L3 larval transition, when vulval induction occurs. For the wild type, this larval transition occurs around 33 hours post-L1 arrest. Total RNA was extracted using Trizol (Invitrogen). First-strand cDNA was prepared from 1 μg total RNA by using the SuperScript III First-strand Synthesis Supermix for qRT-PCR (Invitrogen). Each real-time reverse-transcriptase (RT)-PCR mix contained 10 ng of RT products, 25 μL of 2X SYBR Green PCR Master Mix (Applied Biosystems) and 0.4 μM of each primer. The real-time PCR was performed using triplicate samples in a DNA Engine Opticon System (BioRad). Three independent samples of each genotype were prepared, and levels of *lin-3* and *rpl-26* were quantified from each biological replicate. The ΔC_T values for *lin-3* were determined using *rpl-26* as the internal reference, and the $\Delta\Delta C_T$ values were calculated for each genotype compared to the wild type (as described in the Applied Biosystems real-time PCR manual). All changes were normalized to the wild type. The error shown are the ranges of relative *lin-3*/*rpl-26* ratios for three trials determined from the standard deviations of the $\Delta\Delta C_T$ values.

RESULTS

n2070 suppresses the synMuv phenotypes of non-null *lin-15AB* alleles

n2070 could affect a process downstream of or in parallel to the class A genes, the class B genes or both pathways to cause synMuv suppression. Alternatively it could cause an increase in the normal function of a gene that opposed the synMuv phenotype specifically of *lin-15AB(n765)* mutants, acting as an allele-specific suppressor. To determine the specificity of the *n2070* synMuv suppression phenotype, we combined *n2070* with different loss-of-function alleles of the *lin-15AB* operon (Table 1). *n2070* did not suppress the synMuv phenotype caused by the *lin-15AB* null allele *n309* but did suppress the incompletely penetrant synMuv phenotype caused by *lin-15AB(n2993 n433)*. These results show that *n2070* is not an allele-specific suppressor of the synMuv phenotype.

We combined *n2070* with a different synMuv class AB double mutant *dpl-1(n2994) lin-56(n2728). n2070* failed to suppress the synMuv phenotype of this strain. Failure to suppress the *dpl-1 lin-56* synMuv phenotype might be caused by the strength of *n2070* as a synMuv suppressor. Alternatively, *n2070* could be a gene-specific suppressor of *lin-15A* or *lin-15B*. To distinguish these two possibilities, we plan to combine *n2070* with less penetrant and expressive synMuv mutant combinations.

n2070 suppresses a unique group of synMuv pleiotropies

Genes that specifically oppose the synMuv pathways have been identified in two different screens (ANDERSEN *et al.* 2006; CUI *et al.* 2006b). Previously, we reported that a putative NURF-like complex encoded by two synMuv suppressor genes, *isw-1* and *nurf-1*, oppose the synMuv pathways (ANDERSEN *et al.* 2006). Additionally, we found that *isw-1* opposes other aspects of the class B mutant phenotype, including the germline-versus-soma cell-fate distinction (UNHAVAITHAYA *et al.* 2002). The ectopic activation of germline processes in the soma of class B synMuv mutants causes an enhanced sensitivity to RNAi (WANG

et al. 2005; LEHNER *et al.* 2006) and silencing of repetitive transgenes (HSIEH *et al.* 1999).

n2070 did not suppress the enhanced RNAi sensitivity or the silencing of repetitive transgenes found in class B mutants (data not shown). Therefore, the gene mutated in *n2070* is likely not a regulator of the germline-versus-soma cell-fate decision. Some class B synMuv genes inhibit the expression of transgenes, specifically the *lag-2::gfp* reporter transgene (DUFOURCQ *et al.* 2002; POULIN *et al.* 2005). *n2070* did not suppress the ectopic expression of *lag-2::gfp* caused by a class B synMuv mutant (data not shown), suggesting that the gene mutated in *n2070* does not promote *lag-2* expression. Together, these results show that *n2070* likely is different that known synMuv suppressors such as *isw-1* and therefore might represent a novel synMuv regulatory mechanism. These observations and the dominant synMuv suppressor phenotype motivated us to identify the gene mutated in *n2070* animals.

n2070 causes a gain-of-function phenotype by increasing the normal function of *Y37A1B.1*

n2070 causes a completely penetrant dominant synMuv suppression phenotype: *n2070 / +* heterozygotes have a vulval phenotype identical to that of *n2070* homozygotes (Table 2). We mapped *n2070* between *unc-30* and *dpy-4* on chromosome IV (see Materials and Methods). We performed gene-dosage studies to determine how *n2070* affects gene function, *i.e.* whether it causes loss-of-function or gain-of-function. The deficiency *sDf23* lacks the region between *unc-30* and *dpy-4* and did not cause a synMuv suppression phenotype by haploinsufficiency (Table 2). Because the synMuv suppression phenotype is dominant and not haploinsufficient, *n2070* likely causes a gain-of-function. Additionally, the synMuv suppression phenotype was not caused by an increase of one gene dose, as determined by using the duplication of that region, *yDp1*. The *n2070* synMuv suppression phenotype also was not altered by an increase or decrease of one gene dose using *yDp1* and *sDf23*, respectively. Together,

these results suggest that the *n2070* mutation causes either an increase in the wild-type function or an altered function of the gene.

Using single-nucleotide polymorphisms, we mapped the *n2070* mutation to a 46-gene interval. Because the *n2070* phenotype was caused by a gain-of-function, we used RNA-mediated interference (RNAi, FIRE *et al.* 1998) to inactivate the 46 genes in this interval. RNAi of *Y37A1B.1* but not any of the other 45 genes in this region eliminated the *n2070* synMuv suppression phenotype (Table 2). We determined the sequence of *Y37A1B.1* in *n2070*. *n2070* is a missense mutation resulting in a presumptive proline-to-leucine substitution at amino-acid position 151 of the predicted protein sequence (Figures 1a and 2).

Because *n2070* causes a gain-of-function phenotype, loss-of-function mutations of the gene mutated in this strain might suppress the gain-of-function phenotype by eliminating the increased or altered function of that gene. Therefore, we sought intragenic revertants of the *n2070* dominant synMuv suppression phenotype (see Materials and Methods) and identified three linked revertants that eliminated the *n2070* phenotype (see *n4565*, *n4566* and *n4575* in Table 2). The revertant alleles each have nonsense mutations of *Y37A1B.1*.

If *n2070* causes an increase or altered function of *Y37A1B.1*, then loss-of-function mutations like *n4565*, *n4566* and *n4575* should only eliminate the synMuv suppression phenotype in *cis* to *n2070*. A *Y37A1B.1* null allele, *gk433*, did not eliminate the synMuv suppression phenotype caused by *n2070* in *trans*, proving that *n2070* affects *Y37A1B.1* function and not a neighboring gene (Table 2). Although the duplication *yDp1* did not phenocopy *n2070*, transgenes generated with additional copies of *Y37A1B.1* suppressed the synMuv phenotype of *lin-15AB(n765)* mutants. These results suggest that *n2070* causes increased *Y37A1B.1* wild-type activity, which inhibits vulval cell fates.

Y37A1B.1 is *lst-3*, which encodes the human cell-cycle and apoptosis regulatory protein CARP-1

Y37A1B.1 was identified by Yoo *et al.* (2004) as a putative downstream transcriptional target of the *lin-12* Notch lateral-signaling cascade named *lst-3*, for (*lst*, *lateral signal target*). Predicted transcriptional targets of LAG-1, a Notch pathway transcriptional cofactor, include many genes that negatively regulate the Ras pathway, such as *lip-1*, a phosphatase that dephosphorylates MAPK in cells adopting the 2º vulval cell fate leading to its inactivation (BERSET *et al.* 2001), *ark-1*, an Ack-related non-receptor tyrosine kinase homolog that might inhibit LET-23 EGFR activity (HOPPER *et al.* 2000) and a group of *lst* genes (YOO *et al.* 2004). Inactivation of *lst-2*, *lst-3*, *lst-4* and *ark-1* by RNAi in a sensitized mutant background causes ectopic vulval induction and persistent expression of a 1º vulval cell fate marker, *egl-17::cfp*. These results suggest that the LIN-12-mediated lateral signal inactivates the Ras pathway in the cells fated to become 2º vulval cells. Therefore, the suppression of the synMuv phenotype by *lst-3(n2070)* might be through inhibition of the Ras pathway.

We found that *lst-3* has two splice variants and is SL1 *trans*-spliced (Figure 1a). Using BLAST database searches (ALTSCHUL *et al.* 1990), we determined that *lst-3* encodes the *C. elegans* homolog of human CARP-1. LST-3 and CARP-1 have OB-fold and SAP domains (Figures 1b and 2). The OB-fold domain binds oligonucleotides and oligosaccharides (THEOBALD *et al.* 2003). Recently, the OB-fold domain has been reported to be structurally similar to the cold-shock domain important for transcription antitermination (NAKAMINAMI *et al.* 2006). The SAP domain is a DNA-binding domain found in many transcription factors (ARAVIND and KOONIN 2000). Because of this homology to CARP-1, a transcriptional regulator of cell cycle and apoptosis, and conservation of two putative DNA-binding domains, LST-3 might inhibit the vulval cell fate by repressing the transcription of genes in the Ras pathway.

lst-3 is expressed broadly throughout development

Using the endogenous promoter of *lst-3* fused to *yfp*, we determined the expression pattern of *lst-3* (Figure 3). Reporter expression was first detected starting at roughly the 300-cell stage of embryogenesis and continuing throughout adulthood. YFP under the control of the *lst-3* promoter was seen in all major tissues of the animal throughout development. We analyzed a time-course of expression during vulval development starting at the late L2 larval stage (Figure 4). Expression was observed throughout vulval development in P3.p through P8.p and their descendants. Rarely, we noted decreased expression of YFP in the 1º vulva cell lineage starting after the second division of P6.p (data not shown). However, the majority of animals scored expressed YFP highly in all vulval cells throughout vulval development. LST-3 is expressed more broadly than some members of the Ras pathway (TAN *et al.* 1998; MILLER *et al.* 2000); this ubiquitous expression pattern is similar to that observed for many synMuv proteins (VON ZELEWSKY *et al.* 2000; CEOL and HORVITZ 2001; UNHAVAITHAYA *et al.* 2002; CEOL and HORVITZ 2004; HARRISON *et al.* 2006).

lst-3 is a new class B synMuv gene

Using two independent presumptive null mutations of *lst-3*, we determined that *lst-3* loss-of-function caused a synMuv phenotype (Table 3). Single mutants with either *lst-3* null allele were not Muv, but a synMuv phenotype resulted when each was combined with the class A mutation *lin-15A(n433)*. We used *lst-3(gk433)* for all subsequent *lst-3* loss-of-function analyses. This null mutation combined with mutations of each class A synMuv gene caused incompletely penetrant Muv phenotypes at 20ºC. When combined in double mutants with null mutations of several class B synMuv genes, *lst-3(gk433)* did not cause a Muv phenotype. At high temperatures, *lst-3* was required redundantly for viability with *lin-15B*, *lin-35* and *lin-37*. In *lst-3(n2070)* gain-of-function mutants, there is an increase in the inhibition of vulval cell fates causing synMuv suppression. By contrast in *lst-3(gk433)* null mutants, there is a decrease in the inhibition of vulval cell fates

causing a synMuv phenotype when combined with class A mutations. Therefore, these results suggest that *lst-3* normally inhibits the adoption of vulval cell fates and is required for viability in class B mutant backgrounds.

***lst-3* inhibits the Ras pathway in a manner similar to the synMuv genes**

Mutations of negative regulators increase Ras pathway signaling. Single mutants of these negative regulators do not have obvious vulval defects, but in combination with mutations of other negative regulators, these mutations cause a Muv phenotype. Genes that inhibit vulval fates have been identified in several genetic screens (FERGUSON and HORVITZ 1985; FERGUSON and HORVITZ 1989; JONGEWARD *et al.* 1995; THOMAS *et al.* 2003; BERSET *et al.* 2005; CEOL *et al.* 2006; GUPTA *et al.* 2006). Thus far, these negative regulators can be divided into two classes, those that inhibit the Ras pathway upstream of *let-23* EGFR (CEOL *et al.* 2006), perhaps through transcriptional repression of *lin-3* EGF (CUI *et al.* 2006a), or those that act downstream of *let-23* EGFR (JONGEWARD *et al.* 1995; GUPTA *et al.* 2006). The synMuv genes might inhibit vulval fates by repressing transcription of *lin-3* EGF, and genes like *ark-1*, *dep-1*, *gap-1*, *lip-1*, *sli-1*, *sli-3* and *unc-101* might inhibit vulval fates through negatively regulating LET-23 EGFR activity or the activities of downstream pathway members (LEE *et al.* 1994; JONGEWARD *et al.* 1995; HAJNAL *et al.* 1997; HOPPER *et al.* 2000; BERSET *et al.* 2001; BERSET *et al.* 2005; GUPTA *et al.* 2006).

To determine whether *lst-3* inhibits vulval cell fates like the synMuv genes or like other negative regulators of the Ras pathway, we determined whether *lst-3* inhibits the Ras pathway through *let-23* EGFR. The *let-23(sy97)* mutation eliminates the function of *let-23* during vulval development (AROIAN *et al.* 1990). We combined the *lst-3(gk433)* null mutation with *let-23(sy97)* and scored the Vul phenotype. *lst-3(gk433)* failed to suppress the Vul phenotype of *let-23(sy97)* (100% (n=26) for *let-23(sy97); lst-3(gk433)* vs 100% (n=77) for *let-23(sy97)*). Therefore, like the class B synMuv genes, *lst-3* acts upstream of or in parallel to *let-23* to inhibit vulval fates.

Next, we determined whether *lst-3* inhibits the Ras pathway in parallel to other negative regulators. Some of these negative regulators caused a synMuv phenotype in combination with the class A mutation *lin-15A(n767)* (Table 4). Mutations of *ark-1*, a Ras pathway negative regulator, cause a synMuv phenotype with class A synMuv, *gap-1* or *sli-1* mutations but failed to suppress the Vul phenotype of *let-23(sy97)* mutants (HOPPER *et al.* 2000). Additionally, *ark-1* was identified as a putative transcriptional target of the Notch pathway like *lst-3*. We determined that *lst-3* did not have attributes of the vulval phenotype shared with *ark-1* in the inhibition of vulval fates, because loss of *lst-3* did not cause a Muv phenotype in *gap-1* or *sli-1* null mutant backgrounds (Table 5). For this reason, *lst-3* might be a different class of Ras pathway negative regulator from *ark-1*.

Next, we combined *lst-3* gain-of-function and loss-of-function mutations with mutations that increase or decrease Ras pathway signaling to determine epistatic relationships (Table 6). If *lst-3* acts downstream of or in parallel to a particular Ras pathway gene, the Muv phenotypes caused by an increase in Ras pathway signaling upstream of that gene would be suppressed by *lst-3(n2070)* and enhanced by *lst-3(gk433).* Consistent with this hypothesis, *lst-3* mutations modified the Muv phenotypes caused by overexpression of *lin-3* EGF or gain-of-function mutations of *let-23* EGFR and *let-60* Ras. The Muv phenotypes caused by strong or null loss-of-function mutations of *lin-1* or *lin-31*, respectively, were not modified by a loss or gain of *lst-3* function. Therefore *lst-3* likely acts downstream of or in parallel to *let-60* Ras and upstream of or in parallel to *lin-1* and *lin-31*.

To characterize how *lst-3* inhibits vulval cell fates, we combined loss-of-function and gain-of-function *lst-3* mutations with vulval cell-fate reporters (Figure 5). We found that *lst-3* did not affect the anchor cell fate, observed using a *cdh-3* GFP reporter (PETTITT *et al.* 1996). Many negative regulators of the Ras pathway cause persistent expression of the 1º vulval cell fate marker, *egl-17::gfp*, in the 2º vulval cell lineages (YOO *et al.* 2004). We did not observe persistent expression

of GFP under control of the *egl-17* reporter, suggesting that *lst-3* is different from previously described negative regulators of the Ras pathway acting downstream of *let-23* EGFR.

lst-3 CARP-1 might repress the transcription of genes that promote vulval fates

LST-3 and CARP-1 share OB-fold and SAP putative DNA-binding domains. Because it has these two DNA-interaction domains, LST-3 might be a transcriptional regulator. Using genetic epistasis analysis, we determined that *lst-3* is acting upstream of or in parallel to *let-23* EGFR and upstream of or in parallel to the Ras pathway transcription factors *lin-1* and *lin-31*. Genes acting at either of these two steps regulate transcription: the synMuv genes regulate *lin-3* EGF levels upstream of *let-23* EGFR and some Ras pathway regulators regulate Ras pathway target genes with the *lin-1* and *lin-31* transcription factors.

We tested whether *lst-3* could affect transcriptional repression of the gene *mat-3*, which is involved in promoting vulval fates (GARBE *et al.* 2004). Some class B synMuv genes suppress the vulval defects of a partial loss-of-function mutation in the promoter of *mat-3*. This mutation reduces *mat-3* function specifically in the vulval cells. The suppression of *mat-3* vulval defects by some class B synMuv mutations is caused by increased transcription of *mat-3*, which bypasses the effect of the promoter mutation on the vulval cell cycle. Loss of *lst-3* function suppressed the *mat-3* vulval defect from 61% to 32%, suggesting that *lst-3* represses transcription of *mat-3* in vulval cells.

The synMuv genes likely repress the transcription of the Ras pathway ligand *lin-3* EGF (CUI *et al.* 2006a). In synMuv mutants, loss of transcriptional repression leads to increased expression of *lin-3*, which induces ectopic vulval cell fates. We quantified expression of *lin-3* EGF in *lst-3* gain-of-function and loss-of-function mutants (Figure 6). Unlike the class B synMuv genes tested so far, loss of *lst-3* did not cause ectopic expression of *lin-3*, even in the *lin-15A* class A synMuv mutant background. However, the gain-of-function allele *lst-*

3(n2070) suppressed the ectopic expression of *lin-3* EGF in *lin-15AB(n765)* synMuv mutants. These results suggest that LST-3 might repress the transcription of *lin-3* EGF, and the suppression of the synMuv phenotype might occur through increased transcriptional repression of *lin-3* EGF by LST-3(n2070).

DISCUSSION AND FUTURE DIRECTIONS

From the isolation of an allele with a dominant synMuv suppression phenotype caused by the increased function of *lst-3*, we identified a new class B synMuv gene. *lst-3* has been reported to be transcriptionally controlled by the Notch pathway to inhibit Ras pathway activity in cells specified to become 2º vulval cells. The inhibition of the Ras pathway might be through the transcriptional repression of the Ras pathway ligand *lin-3* EGF. Because *lst-3* encodes a homolog of the human protein CARP-1, a known regulator of cell-cycle progression and apoptosis, these studies could describe a novel mode of tumor suppression.

lst-3(n2070) is likely a vulval-specific suppressor of the synMuv phenotype

The *C. elegans* NURF-like complex opposes the functions of the synMuv genes in the control of at least two different cell-fate decisions: vulval fates and germline-versus-soma fates (ANDERSEN *et al.* 2006). *lst-3(n2070)* opposed the functions of the synMuv genes only in the control of vulval fates. Loss of the NURF-like complex generally antagonizes the synMuv genes: the synMuv phenotype of nearly every synMuv double mutant combination tested is suppressed. *lst-3(n2070)* is either a much weaker synMuv suppressor or specifically antagonizes partial *lin-15AB* loss-of-function synMuv phenotypes. Future studies of the gene-specificity of synMuv suppression by *lst-3(n2070)* are required. Given the phenotypic differences between NURF-like complex loss-of-function mutants and the gain-of-function mutant *lst-3(n2070)*, there are at least two ways to oppose synMuv gene functions: generally in all tissue types, like *isw-1* and *nurf-1*, or specifically in the vulval lineage, like *lst-3(n2070)*.

How does *lst-3* negatively regulate the Ras pathway?

Some synMuv genes encode proteins that are predicted to repress the transcription of *lin-3* EGF in tissues near the vulval cells (CUI *et al.* 2006a). Not

surprisingly given this role in the regulation of the Ras pathway ligand *lin-3* EGF, some of the synMuv genes act upstream of or in parallel to *let-23* EGFR in genetic epistasis tests (CEOL *et al.* 2006). We found that *lst-3* acts upstream of or in parallel to *let-23* EGFR and might repress transcription of *lin-3* EGF. However, we also found that *lst-3* is epistatic to some Ras pathway genes downstream of *let-23* EGFR, notably *let-60(n1046)*, but not epistatic to the null phenotypes of the Ras pathway transcription factors *lin-1* and *lin-31*. These results suggest that *lst-3* inhibits the Ras pathway at two different points, that upstream members of the Ras pathway are sensitive to levels of the ligand *lin-3* EGF or both hypotheses. Future investigations of the genetic relationships between Ras pathway components and *lst-3* are required.

Given the epistatic relationship between *lin-1* or *lin-31* mutant phenotypes and *lst-3*, LST-3 could act with the LIN-1/LIN-31 complex to inhibit vulval fates. The LIN-1/LIN-31 transcriptional repressor complex inhibits transcription of genes that promote vulval cell-fate specification in all vulval cells prior to vulval induction (TAN *et al.* 1998). After vulval induction mediated by the Ras pathway, MPK-1 phosphorylates LIN-1 and LIN-31 causing the complex to disassociate in cells specified to adopt 1º or 2º vulval cell fates. Subsequently, each protein separately promotes the 1º vulval cell fate (MILLER *et al.* 2000; TIENSUU *et al.* 2005). Notch pathway activity ensures that the cells neighboring the 1º cell adopt 2º cell fates. Part of the negative regulation of the Ras pathway mediated by the Notch pathway in 2º vulval cells could use *lst-3*. LST-3 could act with the LIN-1/LIN-31 repressor complex to inhibit the adoption of 1º vulval cell fates by repressing the transcription of genes that promote that vulval cell fate. The LIN-1/LIN-31/LST-3 complex could inhibit Ras pathway activity by inhibiting expression of the Ras pathway ligand *lin-3* EGF. Autocrine signaling through the expression of LIN-3 and then binding to the LET-23 EGFR receptors on the same cell or paracrine signaling through secretion of LIN-3 or expression of membrane-bound LIN-3 (DUTT *et al.* 2004) could promote adoption of 1º vulval cell fates. The LIN-1/LIN-

31/LST-3 complex would be required to inhibit this autocrine and/or paracrine LIN-3 EGF signaling to prevent ectopic 1° vulval cell fates.

A novel gain-of-function mutation in the OB-fold domain of the *C. elegans* CARP-1 homolog might increase transcriptional repression

lst-3(n2070) likely increases wild-type *lst-3* function, which inhibits vulval cell fates. The missense change found in this mutant corresponds to a putative proline-to-leucine amino-acid change in the oligomer binding (OB)-fold domain. The OB-fold domain has been shown to bind oligonucleotides or oligosaccharides (THEOBALD *et al.* 2003). The specificity of the oligonucleotide binding is limited to single-stranded DNA or RNA molecules. The OB-fold domain is similar to cold-shock domains, which act as transcriptional antiterminators or melt secondary structures in RNA (NAKAMINAMI *et al.* 2006). Because the *lst-3(n2070)* mutation is in the OB-fold domain, this domain might function in transcriptional repression, perhaps together with the SAP DNA-binding domain (ARAVIND and KOONIN 2000). Many OB-fold domains and cold-shock domains have been characterized structurally (THEOBALD *et al.* 2003). The amino-acid sequences are not well conserved across these structurally similar proteins. For this reason, we were unable to hypothesize how the proline-to-leucine amino-acid change would affect the OB-fold domain structure. Structural studies of LST-3 might reveal how this missense change increases the normal function of LST-3 and how the conserved residue in CARP-1 might control cell-cycle progression and apoptosis.

The human LST-3 homolog, CARP-1, might inhibit cell-cycle progression through transcriptional repression of EGF receptor ligands

Human CARP-1 was identified as a gene required for cell-cycle arrest and apoptosis in breast cancer cell lines exposed to the retinoid CD437 (RISHI *et al.* 2003). Overexpression of CARP-1 caused increased levels of $p21^{CIP1}$ and apoptosis. Additionally, CARP-1 promotes apoptosis by activation of caspase 9

and phosphorylation of p38 MAPK after treatment with the EGF receptor antagonist Iressa (RISHI *et al.* 2006). Given our data concerning *lin-3* EGF, CARP-1 could inhibit cell-cycle progression by repressing transcription of genes that encode EGF. Without persistent expression of growth factors like EGF, cells will stop growth and die. Transcriptional repression of growth-factor signals is a hallmark of tumor suppression (HANAHAN and WEINBERG 2000). Perhaps humans with defective CARP-1 transcriptional repression have increased expression of EGF leading uncontrolled growth. Understanding more about how LST-3 functions to inhibit *lin-3* EGF expression might teach us much about how CARP-1 acts as a tumor-suppressor protein.

Future Directions

LST-3 is similar to mammalian CARP-1, and both proteins have putative DNA-binding domains, including the OB-fold and SAP domains. To understand how *lst-3* inhibits vulval fates, we should determine if LST-3 binds DNA and its binding site. To determine if LST-3 binds DNA, *C. elegans* genomic DNA could be distributed onto nitrocellulose filters and recombinant LST-3 can be applied to the filters. If LST-3 binds DNA, then it might be detected bound to the spots where genomic DNA has been distributed. To determine the site where LST-3 binds DNA, two approaches can be tried. First, expression analysis on microarrays comparing gain-of-function and loss-of-function *lst-3* mutants to the wild type might show genes that are oppositely regulated. The promoters from there genes can be scanned for common motifs. Second, systematic evolution of ligands by exponential enrichment (SELEX) can be tried to determine the binding sites of LST-3. Hopefully these methods can determine the sites of DNA binding by LST-3, which will lead to a better understanding of LST-3 transcriptional target genes.

Similar analyses to those performed in Chapter Three should be done using *lst-3* mutations to look for shared or separate molecular functions from other class B synMuv genes. These analyses might determine how *lst-3* acts to

inhibit vulval fates by including it with a molecular function that has been previously described, such as the shared *efl-1/dpl-1* activity. In addition to these genetic analyses, the binding partners of LST-3 should be determined. Over the past seven years, we have created a comprehensive collection of class A and B synMuv genes in the Gateway recombinase system, allowing for rapid construction of expression plasmids (E.C.A., C.J. Ceol, A.M. Saffer and H.R.H., unpublished results). Directed yeast-two hybrid assays between LST-3 and all synMuv proteins should be done. Additionally, I have produced antisera that might specifically recognize LST-3. After determination of specificity, immunoprecipitation assays followed by mass spectroscopic analyses of interacting peptides can be performed. Chromatin immunoprecipitations using antisera specific to LST-3 could determine where LST-3 binds in the *lin-3* genomic region. Using genetics and biochemistry, these complementary approaches should identify the genes and proteins that act with *lst-3* to control *lin-3* transcription important for the inhibition of vulval fates.

lst-3 has been reported to be a presumptive downstream transcriptional target of the Notch pathway. Because RNAi of *lst-3* caused a Muv phenotype in a *gap-1* mutant background but not on its own, *lst-3* is thought to be a negative regulator of the Ras pathway. To more conclusively show that *lst-3* is a transcriptional target of the Notch pathway, quantitative measures of *lst-3* expression should be performed in *lin-12* Notch gain-of-function and loss-of-function mutants. Additionally using cell ablation experiments, we can quickly determine whether *lst-3* causes an increase in *lin-3* expression in the AC or in other tissues. If the operated animals still express the synMuv phenotype, then that phenotype is not dependent on the AC. This result also suggests that *lin-3* might be expressed from other tissue(s).

ACKNOWLEDGMENTS

We thank Na An for strain management, Beth Castor for DNA sequence determination, Andrew Hellman for deletion allele identification, and Niels Ringstad and Adam Saffer for their critical reading of this manuscript. Strains were provided by the *Caenorhabditis* Genetics Center, which is supported by the NIH National Center for Research Resources. We thank Iva Greenwald for providing the *arEx460* strain and Yuji Kohara for EST clones. E.C.A. is an Anna Fuller Cancer Research Fellow, and H.R.H. is the David H. Koch Professor of Biology at MIT and an Investigator of the Howard Hughes Medical Institute. This work was supported by NIH grant GM24663.

LITERATURE CITED

ALTSCHUL, S. F., W. GISH, W. MILLER, E. W. MYERS and D. J. LIPMAN, 1990 Basic local alignment search tool. J Mol Biol **215:** 403-410.

ANDERSEN, E. C., X. LU and H. R. HORVITZ, 2006 *C. elegans* ISWI and NURF301 antagonize an Rb-like pathway in the determination of multiple cell fates. Development **133:** 2695-2704.

ARAVIND, L., and E. V. KOONIN, 2000 SAP - a putative DNA-binding motif involved in chromosomal organization. Trends Biochem Sci **25:** 112-114.

AROIAN, R. V., M. KOGA, J. E. MENDEL, Y. OHSHIMA and P. W. STERNBERG, 1990 The *let-23* gene necessary for *Caenorhabditis elegans* vulval induction encodes a tyrosine kinase of the EGF receptor subfamily. Nature **348:** 693-699.

BEITEL, G. J., S. TUCK, I. GREENWALD and H. R. HORVITZ, 1995 The *Caenorhabditis elegans* gene *lin-1* encodes an ETS-domain protein and defines a branch of the vulval induction pathway. Genes Dev **9:** 3149-3162.

BERSET, T., E. F. HOIER, G. BATTU, S. CANEVASCINI and A. HAJNAL, 2001 Notch inhibition of RAS signaling through MAP kinase phosphatase LIP-1 during *C. elegans* vulval development. Science **291:** 1055-1058.

BERSET, T. A., E. F. HOIER and A. HAJNAL, 2005 The *C. elegans* homolog of the mammalian tumor suppressor Dep-1/Scc1 inhibits EGFR signaling to regulate binary cell fate decisions. Genes Dev **19:** 1328-1340.

BRENNER, S., 1974 The genetics of *Caenorhabditis elegans*. Genetics **77:** 71-94.

CEOL, C. J., and H. R. HORVITZ, 2001 *dpl-1* DP and *efl-1* E2F act with *lin-35* Rb to antagonize Ras signaling in *C. elegans* vulval development. Mol Cell **7:** 461-473.

CEOL, C. J., and H. R. HORVITZ, 2004 A new class of *C. elegans* synMuv genes implicates a Tip60/NuA4-like HAT complex as a negative regulator of Ras signaling. Dev Cell **6:** 563-576.

CEOL, C. J., F. STEGMEIER, M. M. HARRISON and H. R. HORVITZ, 2006 Identification and classification of genes that act antagonistically to *let-60* Ras signaling in *Caenorhabditis elegans* vulval development. Genetics **173:** 709-726.

CHEN, N., and I. GREENWALD, 2004 The lateral signal for LIN-12/Notch in *C. elegans* vulval development comprises redundant secreted and transmembrane DSL proteins. Dev Cell **6:** 183-192.

CLARK, S. G., X. LU and H. R. HORVITZ, 1994 The *Caenorhabditis elegans* locus *lin-15*, a negative regulator of a tyrosine kinase signaling pathway, encodes two different proteins. Genetics **137:** 987-997.

COUTEAU, F., F. GUERRY, F. MULLER and F. PALLADINO, 2002 A heterochromatin protein 1 homologue in *Caenorhabditis elegans* acts in germline and vulval development. EMBO Rep **3:** 235-241.

CUI, M., J. CHEN, T. R. MYERS, B. J. HWANG, P. W. STERNBERG, I. GREENWALD and M. HAN, 2006a SynMuv genes redundantly inhibit *lin-3*/EGF expression to prevent inappropriate vulval induction in *C. elegans*. Dev Cell **10:** 667-672.

CUI, M., E. B. KIM and M. HAN, 2006b Diverse chromatin remodeling genes antagonize the Rb-involved SynMuv pathways in *C. elegans*. PLoS Genet **2:** e74.

DAVISON, E. M., M. M. HARRISON, A. J. WALHOUT, M. VIDAL and H. R. HORVITZ, 2005 *lin-8*, which antagonizes *C. elegans* Ras-mediated vulval induction, encodes a novel nuclear protein that interacts with the LIN-35 Rb protein. Genetics.

DEUEL, T. F., 1987 Polypeptide growth factors: roles in normal and abnormal cell growth. Annu Rev Cell Biol **3:** 443-492.

DRENKARD, E., B. G. RICHTER, S. ROZEN, L. M. STUTIUS, N. A. ANGELL, M. MINDRINOS, R. J. CHO, P. J. OEFNER, R. W. DAVIS and F. M. AUSUBEL, 2000 A simple procedure for the analysis of single nucleotide polymorphisms facilitates map-based cloning in *Arabidopsis*. Plant Physiol **124:** 1483-1492.

DUFOURCQ, P., M. VICTOR, F. GAY, D. CALVO, J. HODGKIN and Y. SHI, 2002 Functional requirement for histone deacetylase 1 in *Caenorhabditis elegans* gonadogenesis. Mol Cell Biol **22:** 3024-3034.

DUTT, A., S. CANEVASCINI, E. FROEHLI-HOIER and A. HAJNAL, 2004 EGF signal propagation during *C. elegans* vulval development mediated by ROM-1 rhomboid. PLoS Biol **2:** e334.

EDGLEY, M. L., and D. L. RIDDLE, 2001 LG II balancer chromosomes in *Caenorhabditis elegans*: *mT1(II;III)* and the *mIn1* set of dominantly and recessively marked inversions. Mol Genet Genomics **266:** 385-395.

FERGUSON, E. L., and H. R. HORVITZ, 1985 Identification and characterization of 22 genes that affect the vulval cell lineages of the nematode *Caenorhabditis elegans*. Genetics **110:** 17-72.

FERGUSON, E. L., and H. R. HORVITZ, 1989 The multivulva phenotype of certain *Caenorhabditis elegans* mutants results from defects in two functionally redundant pathways. Genetics **123:** 109-121.

FIRE, A., S. XU, M. K. MONTGOMERY, S. A. KOSTAS, S. E. DRIVER and C. C. MELLO, 1998 Potent and specific genetic interference by double-stranded RNA in *Caenorhabditis elegans*. Nature **391:** 806-811.

FRASER, A. G., R. S. KAMATH, P. ZIPPERLEN, M. MARTINEZ-CAMPOS, M. SOHRMANN and J. AHRINGER, 2000 Functional genomic analysis of *C. elegans* chromosome I by systematic RNA interference. Nature **408:** 325-330.

GARBE, D., J. B. DOTO and M. V. SUNDARAM, 2004 *Caenorhabditis elegans lin-35*/Rb, *efl-1*/E2F and other synthetic multivulva genes negatively regulate the anaphase-promoting complex gene *mat-3*/APC8. Genetics **167:** 663-672.

GREENWALD, I. S., P. W. STERNBERG and H. R. HORVITZ, 1983 The *lin-12* locus specifies cell fates in *Caenorhabditis elegans*. Cell **34:** 435-444.

GUPTA, B. P., J. LIU, B. J. HWANG, N. MOGHAL and P. W. STERNBERG, 2006 *sli-3* negatively regulates the LET-23/epidermal growth factor receptor-

mediated vulval induction pathway in *Caenorhabditis elegans*. Genetics **174:** 1315-1326.

HAJNAL, A., C. W. WHITFIELD and S. K. KIM, 1997 Inhibition of *Caenorhabditis elegans* vulval induction by *gap-1* and by *let-23* receptor tyrosine kinase. Genes Dev **11:** 2715-2728.

HANAHAN, D., and R. A. WEINBERG, 2000 The hallmarks of cancer. Cell **100:** 57-70.

HARRISON, M. M., C. J. CEOL, X. LU and H. R. HORVITZ, 2006 Some *C. elegans* class B synthetic multivulva proteins encode a conserved LIN-35 Rb-containing complex distinct from a NuRD-like complex. Proc Natl Acad Sci U S A **103:** 16782-16787.

HARRISON, M. M., X. LU and H. R. HORVITZ, 2007 LIN-61, one of two *Caenorhabditis elegans* MBT-repeat-containing proteins, acts with the DRM and NuRD-like protein complexes in vulval development but not in certain other biological processes. Genetics.

HOPPER, N. A., J. LEE and P. W. STERNBERG, 2000 ARK-1 inhibits EGFR signaling in *C. elegans*. Mol Cell **6:** 65-75.

HORVITZ, H. R., and J. E. SULSTON, 1980 Isolation and genetic characterization of cell-lineage mutants of the nematode *Caenorhabditis elegans*. Genetics **96:** 435-454.

HSIEH, J., J. LIU, S. A. KOSTAS, C. CHANG, P. W. STERNBERG and A. FIRE, 1999 The RING finger/B-box factor TAM-1 and a retinoblastoma-like protein

LIN-35 modulate context-dependent gene silencing in *Caenorhabditis elegans*. Genes Dev **13:** 2958-2970.

HUANG, L. S., P. TZOU and P. W. STERNBERG, 1994 The *lin-15* locus encodes two negative regulators of *Caenorhabditis elegans* vulval development. Mol Biol Cell **5:** 395-411.

INOUE, T., D. R. SHERWOOD, G. ASPOCK, J. A. BUTLER, B. P. GUPTA, M. KIROUAC, M. WANG, P. Y. LEE, J. M. KRAMER, I. HOPE, T. R. BURGLIN and P. W. STERNBERG, 2002 Gene expression markers for *Caenorhabditis elegans* vulval cells. Gene Expr Patterns **2:** 235-241.

JONGEWARD, G. D., T. R. CLANDININ and P. W. STERNBERG, 1995 *sli-1*, a negative regulator of *let-23*-mediated signaling in *C. elegans*. Genetics **139:** 1553-1566.

KAMATH, R. S., A. G. FRASER, Y. DONG, G. POULIN, R. DURBIN, M. GOTTA, A. KANAPIN, N. LE BOT, S. MORENO, M. SOHRMANN, D. P. WELCHMAN, P. ZIPPERLEN and J. AHRINGER, 2003 Systematic functional analysis of the *Caenorhabditis elegans* genome using RNAi. Nature **421:** 231-237.

KATZ, W. S., R. J. HILL, T. R. CLANDININ and P. W. STERNBERG, 1995 Different levels of the *C. elegans* growth factor LIN-3 promote distinct vulval precursor fates. Cell **82:** 297-307.

KATZ, W. S., G. M. LESA, D. YANNOUKAKOS, T. R. CLANDININ, J. SCHLESSINGER and P. W. STERNBERG, 1996 A point mutation in the extracellular domain activates LET-23, the *Caenorhabditis elegans* epidermal growth factor receptor homolog. Mol Cell Biol **16:** 529-537.

KIMBLE, J., 1981 Alterations in cell lineage following laser ablation of cells in the somatic gonad of *Caenorhabditis elegans*. Dev Biol **87:** 286-300.

KORNFELD, K., 1997 Vulval development in *Caenorhabditis elegans*. Trends Genet **13:** 55-61.

LEE, J., G. D. JONGEWARD and P. W. STERNBERG, 1994 *unc-101*, a gene required for many aspects of *Caenorhabditis elegans* development and behavior, encodes a clathrin-associated protein. Genes Dev **8:** 60-73.

LEHNER, B., A. CALIXTO, C. CROMBIE, J. TISCHLER, A. FORTUNATO, M. CHALFIE and A. G. FRASER, 2006 Loss of LIN-35, the *Caenorhabditis elegans* ortholog of the tumor suppressor p105Rb, results in enhanced RNA interference. Genome Biol **7:** R4.

LIU, L. X., J. M. SPOERKE, E. L. MULLIGAN, J. CHEN, B. REARDON, B. WESTLUND, L. SUN, K. ABEL, B. ARMSTRONG, G. HARDIMAN, J. KING, L. MCCAGUE, M. BASSON, R. CLOVER and C. D. JOHNSON, 1999 High-throughput isolation of *Caenorhabditis elegans* deletion mutants. Genome Res **9:** 859-867.

LU, X., and H. R. HORVITZ, 1998 *lin-35* and *lin-53*, two genes that antagonize a *C. elegans* Ras pathway, encode proteins similar to Rb and its binding protein RbAp48. Cell **95:** 981-991.

MALUMBRES, M., and M. BARBACID, 2003 RAS oncogenes: the first 30 years. Nat Rev Cancer **3:** 459-465.

MELLO, C. C., J. M. KRAMER, D. STINCHCOMB and V. AMBROS, 1991 Efficient gene transfer in *C.elegans*: extrachromosomal maintenance and integration of transforming sequences. Embo J **10:** 3959-3970.

MILLER, L. M., H. A. HESS, D. B. DOROQUEZ and N. M. ANDREWS, 2000 Null mutations in the *lin-31* gene indicate two functions during *Caenorhabditis elegans* vulval development. Genetics **156:** 1595-1602.

MOGHAL, N., and P. W. STERNBERG, 2003 The epidermal growth factor system in *Caenorhabditis elegans*. Exp Cell Res **284:** 150-159.

NAKAMINAMI, K., D. T. KARLSON and R. IMAI, 2006 Functional conservation of cold shock domains in bacteria and higher plants. Proc Natl Acad Sci U S A **103:** 10122-10127.

OLDENBURG, K. R., K. T. VO, S. MICHAELIS and C. PADDON, 1997 Recombination-mediated PCR-directed plasmid construction *in vivo* in yeast. Nucleic Acids Res **25:** 451-452.

PETTITT, J., W. B. WOOD and R. H. PLASTERK, 1996 *cdh-3*, a gene encoding a member of the cadherin superfamily, functions in epithelial cell morphogenesis in *Caenorhabditis elegans*. Development **122:** 4149-4157.

POULIN, G., Y. DONG, A. G. FRASER, N. A. HOPPER and J. AHRINGER, 2005 Chromatin regulation and sumoylation in the inhibition of Ras-induced vulval development in *Caenorhabditis elegans*. Embo J **24:** 2613-2623.

RIDDLE, D. L., BLUMENTHAL T., MEYER, B.J., PRIESS, J.R., 1997 *C. elegans II*. Cold Spring Harbor Laboratory Press, Cold Spring Harbor.

RISHI, A. K., L. ZHANG, M. BOYANAPALLI, A. WALI, R. M. MOHAMMAD, Y. YU, J. A. FONTANA, J. S. HATFIELD, M. I. DAWSON, A. P. MAJUMDAR and U. REICHERT, 2003 Identification and characterization of a cell cycle and apoptosis

regulatory protein-1 as a novel mediator of apoptosis signaling by retinoid CD437. J Biol Chem **278:** 33422-33435.

RISHI, A. K., L. ZHANG, Y. YU, Y. JIANG, J. NAUTIYAL, A. WALI, J. A. FONTANA, E. LEVI and A. P. MAJUMDAR, 2006 Cell cycle- and apoptosis-regulatory protein-1 is involved in apoptosis signaling by epidermal growth factor receptor. J Biol Chem **281:** 13188-13198.

SHAYE, D. D., and I. GREENWALD, 2005 LIN-12/Notch trafficking and regulation of DSL ligand activity during vulval induction in *Caenorhabditis elegans*. Development **132:** 5081-5092.

SIMON, M. A., 1994 Signal transduction during the development of the *Drosophila* R7 photoreceptor. Dev Biol **166:** 431-442.

STERNBERG, P. W., 2006 Pathway to RAS. Genetics **172:** 727-731.

STERNBERG, P. W., and H. R. HORVITZ, 1986 Pattern formation during vulval development in *C. elegans*. Cell **44:** 761-772.

SULSTON, J. E., and H. R. HORVITZ, 1977 Post-embryonic cell lineages of the nematode, *Caenorhabditis elegans*. Dev Biol **56:** 110-156.

SULSTON, J. E., and J. G. WHITE, 1980 Regulation and cell autonomy during postembryonic development of *Caenorhabditis elegans*. Dev Biol **78:** 577-597.

SUNDARAM, M. V., 2005 The love-hate relationship between Ras and Notch. Genes Dev **19:** 1825-1839.

TAN, P. B., M. R. LACKNER and S. K. KIM, 1998 MAP kinase signaling specificity mediated by the LIN-1 Ets/LIN-31 WH transcription factor complex during *C. elegans* vulval induction. Cell **93:** 569-580.

THEOBALD, D. L., R. M. MITTON-FRY and D. S. WUTTKE, 2003 Nucleic acid recognition by OB-fold proteins. Annu Rev Biophys Biomol Struct **32:** 115-133.

THOMAS, J. H., C. J. CEOL, H. T. SCHWARTZ and H. R. HORVITZ, 2003 New genes that interact with *lin-35* Rb to negatively regulate the *let-60* ras pathway in *Caenorhabditis elegans*. Genetics **164:** 135-151.

TIENSUU, T., M. K. LARSEN, E. VERNERSSON and S. TUCK, 2005 *lin-1* has both positive and negative functions in specifying multiple cell fates induced by Ras/MAP kinase signaling in *C. elegans*. Dev Biol **286:** 338-351.

UNHAVAITHAYA, Y., T. H. SHIN, N. MILIARAS, J. LEE, T. OYAMA and C. C. MELLO, 2002 MEP-1 and a homolog of the NURD complex component Mi-2 act together to maintain germline-soma distinctions in *C. elegans*. Cell **111:** 991-1002.

VON ZELEWSKY, T., F. PALLADINO, K. BRUNSCHWIG, H. TOBLER, A. HAJNAL and F. MULLER, 2000 The *C. elegans* Mi-2 chromatin-remodelling proteins function in vulval cell fate determination. Development **127:** 5277-5284.

WANG, D., S. KENNEDY, D. CONTE, JR., J. K. KIM, H. W. GABEL, R. S. KAMATH, C. C. MELLO and G. RUVKUN, 2005 Somatic misexpression of germline P granules and enhanced RNA interference in retinoblastoma pathway mutants. Nature **436:** 593-597.

YOCHEM, J., T. GU and M. HAN, 1998 A new marker for mosaic analysis in *Caenorhabditis elegans* indicates a fusion between hyp6 and hyp7, two major components of the hypodermis. Genetics **149:** 1323-1334.

YOO, A. S., C. BAIS and I. GREENWALD, 2004 Crosstalk between the EGFR and LIN-12/Notch pathways in *C. elegans* vulval development. Science **303:** 663-666.

YOON, C. H., J. LEE, G. D. JONGEWARD and P. W. STERNBERG, 1995 Similarity of *sli-1*, a regulator of vulval development in *C. elegans*, to the mammalian proto-oncogene c-cbl. Science **269:** 1102-1105.

Table 1: *n2070* might be a gene-specific suppressor of the *lin-15AB* synMuv phenotype

genotype	% multivulva (n)	
	+	*n2070*
lin-15AB(n765)	100 (486)	0 (307)
lin-15AB(n2993 n433)	66 (112)	0 (187)
lin-15AB(n309)	100 (139)	100 (103)
dpl-1(n2994) lin-56(n2728)	100 (92)	100 (61)
lin-61(n3809); lin-15A(n767)	42 (425)	45 (464)

Table 2: *n2070* causes a gain-of-function synMuv suppression phenotype

genotype[a]	% multivulva (n)
+	100 (961)
n2070 / +	0 (129)
n2070	0 (307)
+; yDp1	100 (147)
+ / sDf23	100 (47)
n2070 / +; yDp1	0 (40)
n2070 / sDf23	0 (24)
n2070 n4565 / +	100 (116)
n2070 n4566 / +	100 (179)
n2070 n4575 / +	100 (136)
n2070 / gk433	0 (39)
n2070 and *Y37A1B.1* RNAi	100 (203)
Y37A1B.1(+++)[b]	0 (26)

[a] All strains contained the synMuv mutation *lin-15AB(n765)*.

[b] This strain contained an extrachromosomal array composed of many wild-type copies of the *Y37A1B.1* locus.

Table 3: *lst-3* is a class B synMuv gene			
genotype	% multivulva ± s.d.		
	20ºC	22.5ºC	25ºC
+	0 ± 0	0 ± 0	0 ± 0
lst-3(gk433)	0 ± 0	0 ± 0	0 ± 0
lst-3(n4590)	0 ± 0	0 ± 0	0 ± 0
lst-3(gk433); lin-15A(n433)	0 ± 0	20 ± 7	85 ± 6
lst-3(n4590); lin-15A(n433)	0 ± 0	35 ± 24	79 ± 4
lst-3(gk433); lin-15A(n767)	31 ± 4	88 ± 5	99 ± 1
lin-8(n2731); lst-3(gk433)	41 ± 19	86 ± 5	93 ± 1
lin-38(n751); lst-3(gk433)	16 ± 1	65 ± 6	100 ± 0
lin-56(n2728); lst-3(gk433)	45 ± 2	96 ± 2	97 ± 6
lst-3(gk433); lin-15B(n744)	0 ± 0	0 ± 0	Lvl
lin-35(n745); lst-3(gk433)	0 ± 0	0 ± 0	Lvl
lin-37(n4903); lst-3(gk433)	0 ± 0	0 ± 0	Lvl

lin-8, *lin-15A*, *lin-38* and *lin-56* are class A synMuv genes, and *lin-15B*, *lin-35* and *lin-37* are class B synMuv genes.

Table 4: *lst-3* and some other negative regulators of the Ras pathway act redundantly with the class A gene *lin-15A* to inhibit vulval cell fates

genotype[a]	% multivulva (n)	
	20ºC	25ºC
+	0 (285)	0 (332)
lst-3(gk433)	31 (143)	99 (227)
lst-1(ok814)	0 (145)	15 (144)
dep-1(zh34)	0 (82)	0 (125)
sli-3(sy341)	0 (130)	0 (88)
unc-101(sy108)	0 (140)	0 (150)
lip-1(zh15)	0 (125)	0 (39)
ark-1(sy247)	96 (268)	100 (168)
sli-1(sy143)	96 (489)	100 (366)
gap-1(ga133)	16 (208)	94 (191)

[a] All strains carry the class A mutation *lin-15A(n767)*.

ND, not determined yet

Table 5: Negative regulators of the Ras pathway do not act redundantly with *lst-3* to inhibit vulval cell fates

genotype[a]	20ºC	25ºC
+	0 (256)	0 (282)
lst-1(ok814)	0 (128)	0 (62)
dep-1(zh34)	0 (85)	0 (58)
sli-3(sy341)	0 (121)	Lvl
unc-101(sy108)	Lvl	Lvl
lip-1(zh15)	0 (115)	0 (110)
ark-1(sy247)	ND	ND
sli-1(sy143)	0 (84)	Lvl
gap-1(ga133)	1 (282)	0 (55)

[a] All strains carry the *lst-3* null allele *lst-3(gk433)*.

ND, not determined yet

Table 6: *lst-3* acts upstream of or in parallel to the *lin-1* and *lin-31* Ras pathway transcription factor genes.

genotype	% multivulva in *lst-3* background ± s.d.		
	+	*gk433* (lf)	*n2070* (gf)
syIs12	69 ± 2	84 ± 3	0 ± 0
let-23(sa62)	93 ± 8	Lvl	16 ± 1
let-60(n1046)[a]	86 ± 0	99 ± 0	ND
lin-31(n301)	80 ± 3	80 ± 7	75 ± 5
lin-1(e1275)[a]	54 ± 10	46 ± 13	ND

ND, not determined

[a] These vulval phenotypes were scored at 17.5ºC.

FIGURE DESCRIPTIONS

Figure 1. *Y37A1B.1* gene structures and predicted protein structure.
(A) The mRNA structure of *Y37A1B.1a* and *Y37A1B.1b* are indicated. Exons are indicated by black boxes; 5' and 3' untranslated regions are indicated by white boxes. The locations of the three nonsense alleles, the gain-of-function allele *n2070* and the two deletion alleles are labeled.
(B) A representation of the domain structure of the Y37A1B.1a protein. Y37A1B.1a and Y37A1B.1b are both similar to human CARP-1, especially in the named domains (see text). The amino-acid substitution of the gain-of-function allele *n2070* is indicated (yellow arrow head).

Figure 1

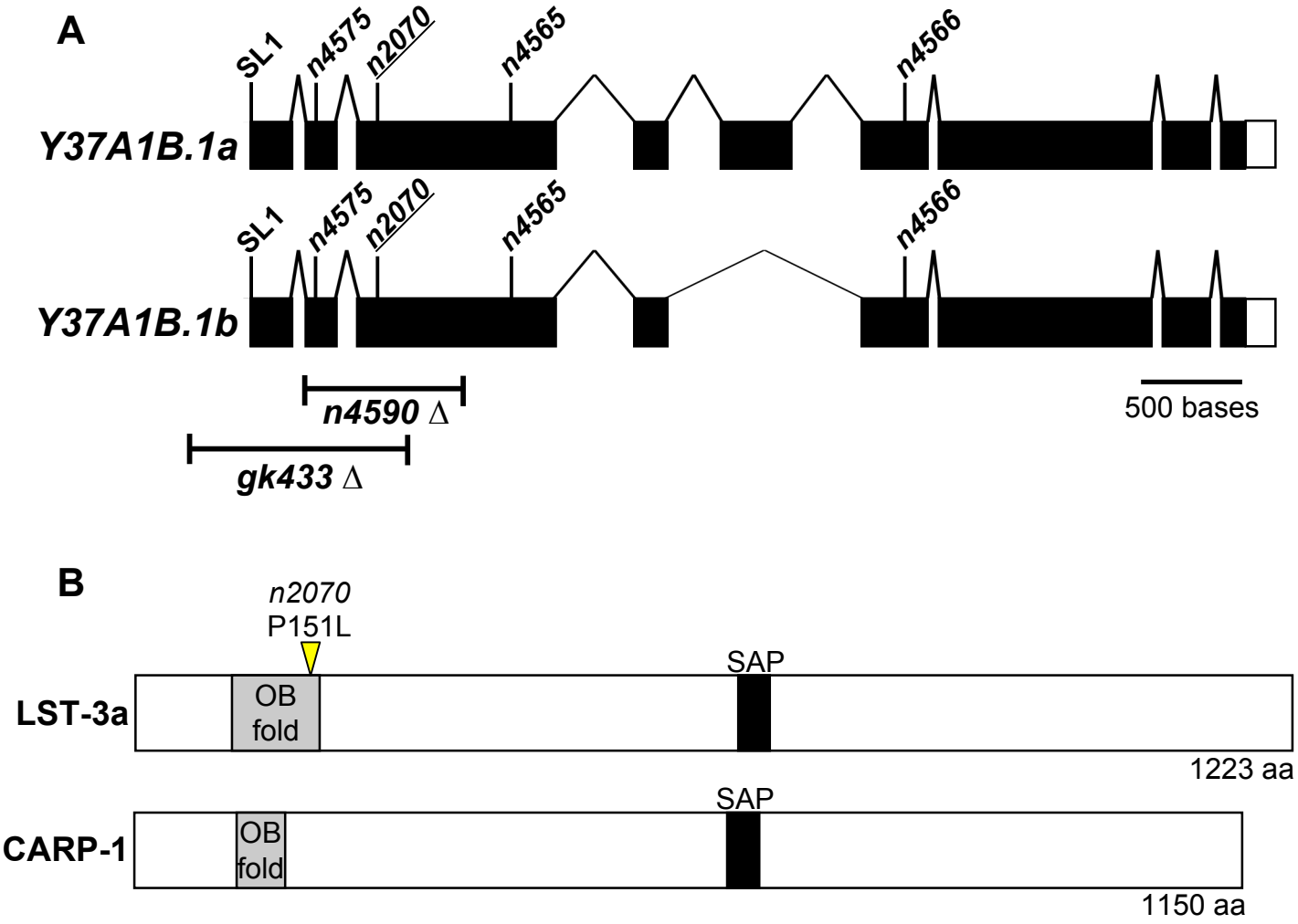
A
SL1
n4575
n2070
n4565
n4566
Y37A1B.1a
SL1
n4575
n2070
n4565
n4566
Y37A1B.1b
n4590 Δ
gk433 Δ
500 bases
B
n2070
P151L
SAP
LST-3a
OB fold
1223 aa
SAP
CARP-1
OB fold
1150 aa

Figure 2. Alignment of LST-3 with human CARP-1. Solid boxes indicate identity between LST-3 and CARP-1. Red arrowheads indicate the sites of nonsense mutations of the intragenic revertants. The yellow arrowhead indicates the site of the *n2070* amino-acid substitution. The grey bar above the amino-acid sequence indicates the predicted OB-fold domain, and the checkered bar indicates the predicted SAP domain.

Figure 2

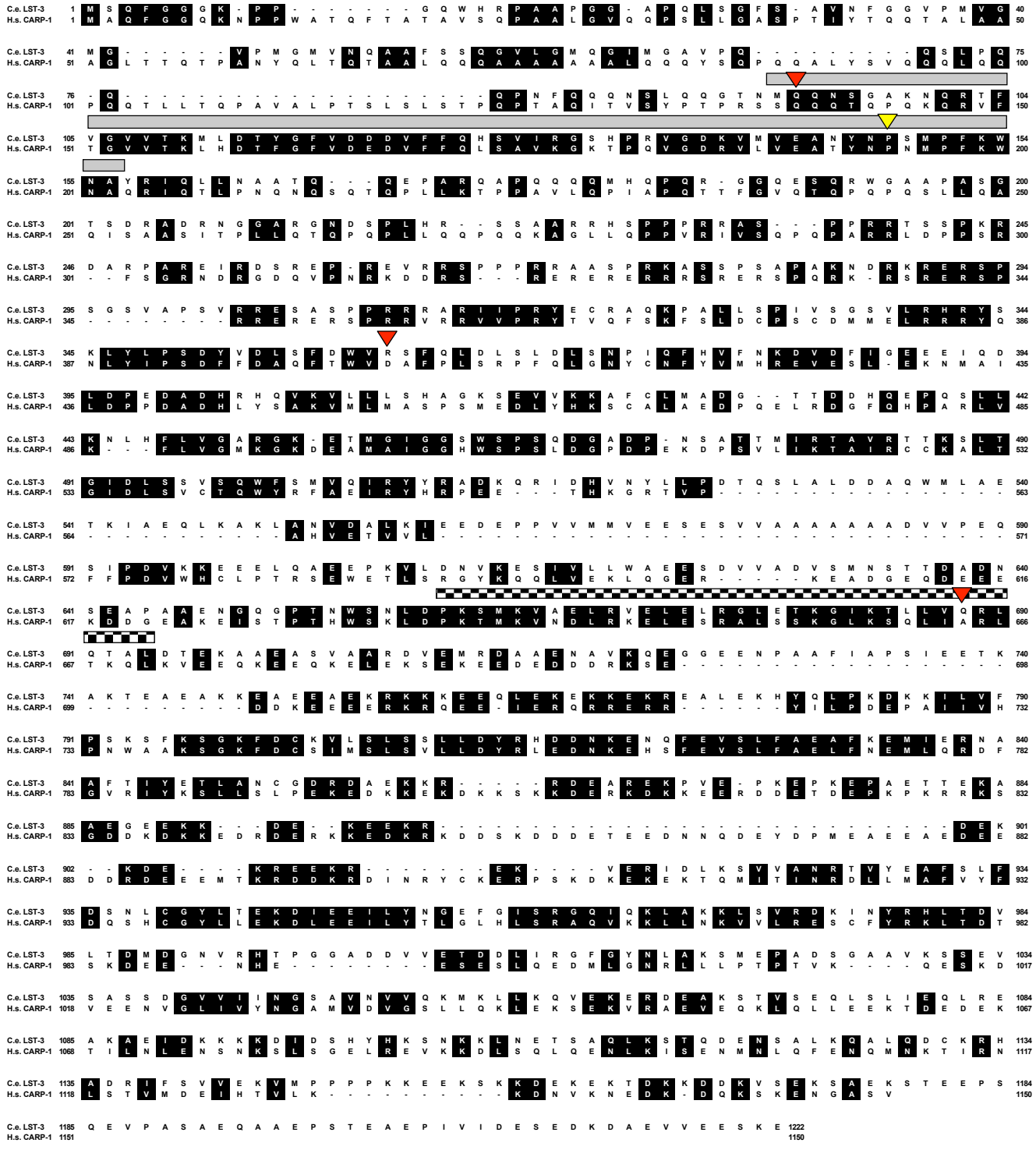

Figure 3. Expression of yellow fluorescent protein (YFP) under the control of the *lst-3* promoter in wild-type animals.

(A) A comma-stage embryo with YFP expression in most if not all cells of the embryo. Scale bar: 10 μm.

(B) An L1 larval stage animal with YFP expression in many cells throughout the animal, including strong expression in head neurons, tail neurons and hypodermal cells. Scale bar: 10 μm.

(C) An L4 larval stage animal with YFP expression in many cells throughout the animal, including strong expression in head neurons and vulval cells. Scale bar: 50 μm.

(D) A one-day old adult animal with YFP expression in many cells throughout the animals, including strong expression in head neurons, hypodermal cells and tail neurons. Scale bar: 50 μm.

Figure 3

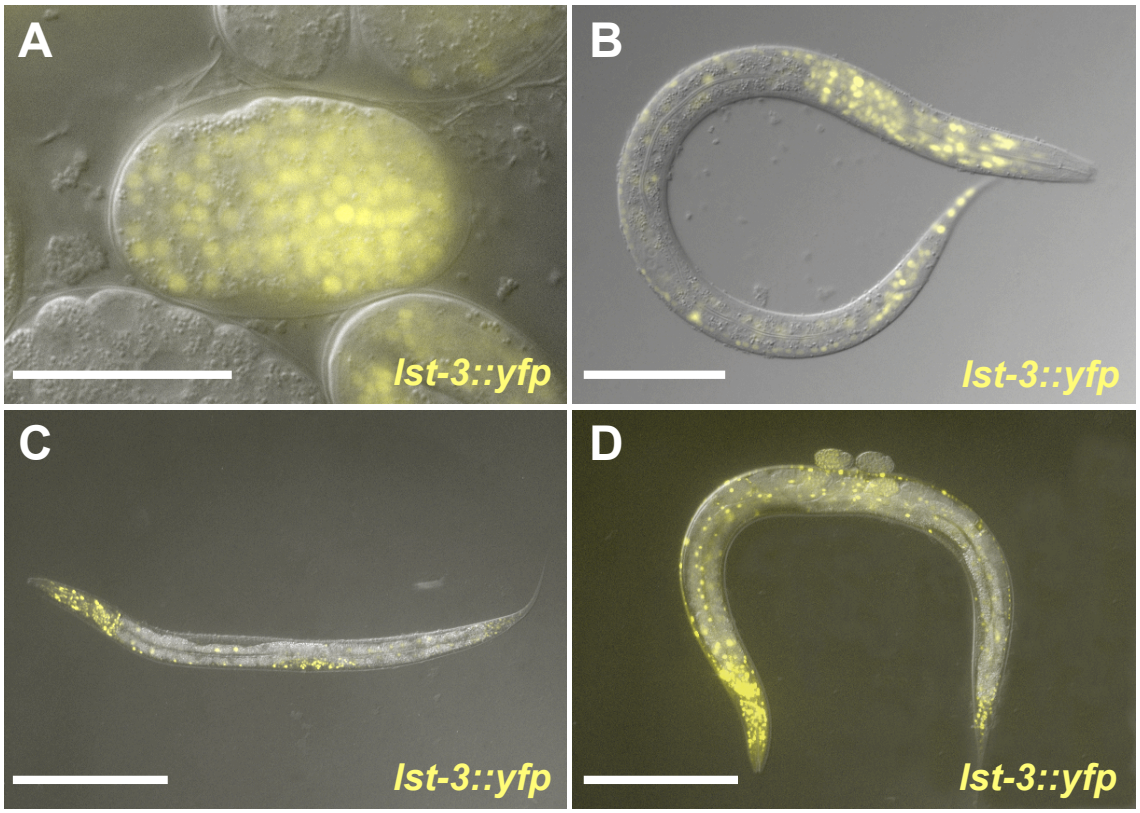

Figure 4. Expression of yellow fluorescent protein (YFP) under the control of the *lst-3* promoter in wild-type animals during vulval development.
The mid-body of wild-type animals at time-points throughout vulval development. All scale bars are 10 μm.
(A) An L2 larval stage animal expressing YFP strongly in the nucleus of the AC (blue arrowhead) and weakly in the nuclei of the P5.p and P6.p cells (white arrowheads).
(B) A larva near the L2/L3 larval transition with expression of YFP strongest in the nuclei of the AC and the daughters of P5.p, P6.p and P7.p (white arrowheads).
(C-D) L3 larvae with expression of YFP observed in the nuclei of P5.p, P6.p and P7.p descendants (white brackets).
(E-G) L3 larvae with expression of YFP observed in the nuclei of P5.p, P6.p and P7.p descendants. The vulval invagination is indicated with a white arrowhead.
(H) The same animal as in (G) except a different focal plane is shown to indicate that the 1° vulva cell descendants of P6.p express YFP (white arrow heads).

Figure 4

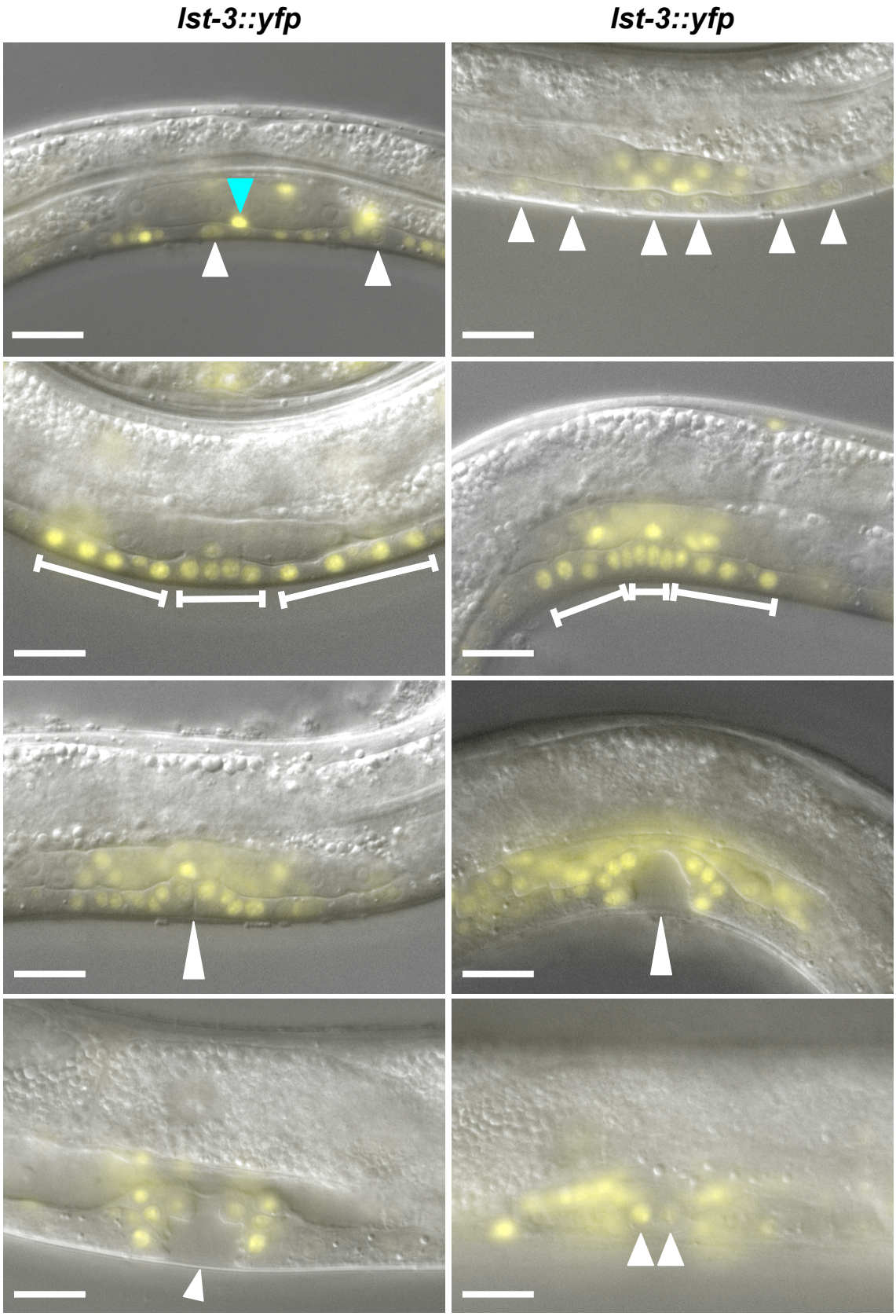

Figure 5. Expression of two vulval cell-fate reporters, *cdh-3::gfp* and *egl-17::cfp*, are not affected by an increase or an absence of *lst-3* activity.
(Top row) The *cdh-3* promoter drives expression of GFP in the anchor cell and 2º vulval cells. GFP expression is identical in wild-type (left), *lst-3(gk433)* (middle) and *lst-3(n2070)* (right) animals. Scale bars: 10 μm.
(Bottom row) The *egl-17* promoter drives expression of CFP in the 1º vulval cells during the early L3 larval stage. CFP expression is identical in wild-type (left), *lst-3(gk433)* (middle) and *lst-3(n2070)* (right) animals. Scale bars: 10 μm.

Figure 5

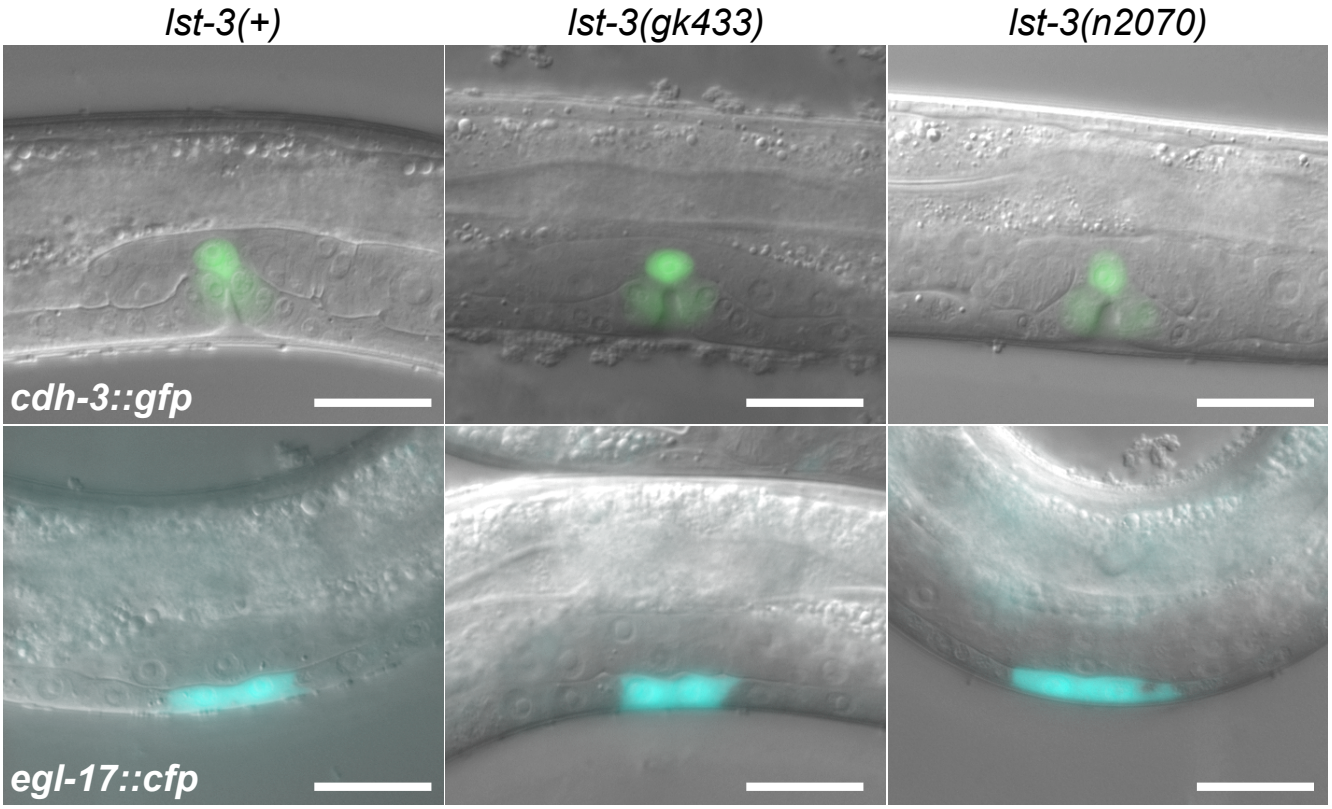

Figure 6. *lst-3(n2070)* suppresses the increased level of *lin-3* expression found in the class AB double mutant *lin-15AB(n765)*

Real-time RT-PCR experiments were performed using RNA samples from animals of the genotypes shown. Mean $\Delta\Delta C_T$ values were used to calculate relative changes in *lin-3* expression normalized to levels of *rpl-26* (see Materials and Methods). Mean values and ranges of relative *lin-3*/*rpl-26* ratios for three trials are shown.

Figure 6

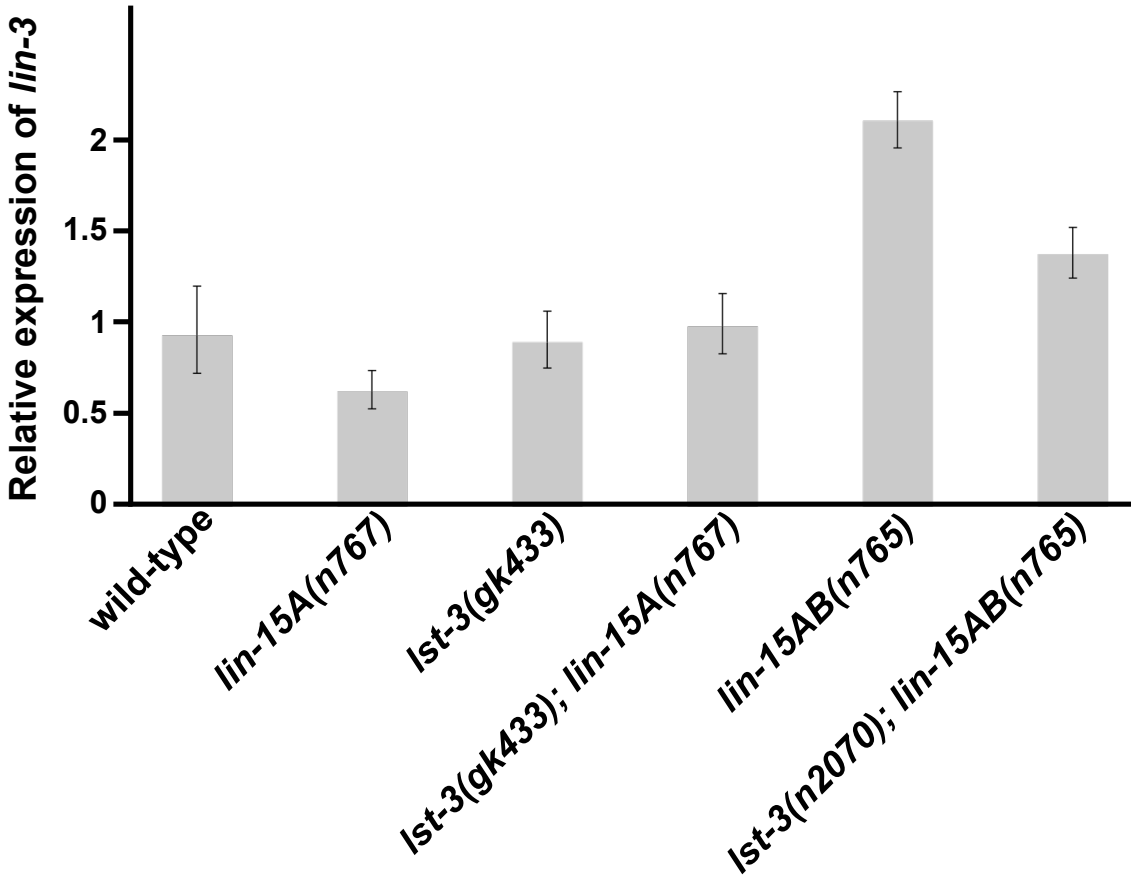
Relative expression of lin-3
0
0.5
1
1.5
2
wild-type
lin-15A(n767)
lst-3(gk433)
lst-3(gk433); lin-15A(n767)
lin-15AB(n765)
lst-3(n2070); lin-15AB(n765)

CHAPTER SIX

DPL-1 DP, LIN-35 Rb, and EFL-1 E2F act with the MCD-1 Zinc-finger protein to promote programmed cell death in *C. elegans*

Peter W. Reddien[*], Erik C. Andersen, Michael C. Huang[†] and H. Robert Horvitz

[*] *Present address:* Department of Biology, Massachusetts Institute of Technology, Whitehead Institute, 9 Cambridge Center, Cambridge, MA 02142, USA

[†] *Present address:* Department of Neurosurgery, Pasquerilla Healthcare Center, Seventh Floor, Georgetown University Hospital, 3800 Reservoir Road, NW, Washington, DC 20007

My contribution to this manuscript includes Table 5 and the addendum. Peter Reddien and I wrote the manuscript.

This chapter is published as Reddien *et al.* (2007) Genetics 175(4):1719-1733

SUMMARY

The genes *egl-1*, *ced-9*, *ced-4*, and *ced-3* play major roles in programmed cell death in *C. elegans*. To identify genes that have more subtle activities, we sought mutations that confer strong cell-death defects in a genetically sensitized mutant background. Specifically, we screened for mutations that enhance the cell-death defects caused by a partial loss-of-function allele of the *ced-3* caspase gene. We identified mutations in two genes not previously known to affect cell death, *dpl-1* and *mcd-1* (modifier of cell death). *dpl-1* encodes the *C. elegans* homolog of DP, the human E2F-heterodimerization partner. By testing genes known to interact with *dpl-1*, we identified roles in cell death for four additional genes: *efl-1* E2F, *lin-35* Rb, *lin-37* Mip40, and *lin-52* dLin52. *mcd-1* encodes a novel protein that contains one zinc finger and that is synthetically required with *lin-35* Rb for animal viability. *dpl-1* and *mcd-1* act with *efl-1* E2F and *lin-35* Rb to promote programmed cell death and do so by regulating the killing process rather than by affecting the decision between survival and death. We propose that the DPL-1 DP, MCD-1 Zinc finger, EFL-1 E2F, LIN-35 Rb, LIN-37 Mip40, and LIN-52 dLin52 proteins act together in transcriptional regulation to promote programmed cell death.

INTRODUCTION

Programmed cell death is important for many aspects of animal development, including morphogenesis, homeostasis, and neuronal refinement (GLÜCKSMANN 1951; JACOBSON *et al.* 1997; SAUNDERS 1966). Studies of the mechanisms of programmed cell death in the nematode *Caenorhabditis elegans* have identified a pathway that is largely conserved in other organisms, including humans (METZSTEIN *et al.* 1998). Four genes -- *egl-1, ced-9, ced-4,* and *ced-3* -- regulate essentially all somatic programmed cell death and define the core metazoan cell-death execution machinery. EGL-1, which promotes cell death, is a BH3-only protein that binds to and inhibits the CED-9 protein (CONRADT and HORVITZ 1998). CED-9, which inhibits cell death (HENGARTNER *et al.* 1992), is similar to the human proto-oncoprotein BCL-2 (HENGARTNER and HORVITZ 1994b; YAN *et al.* 2005) and localizes to mitochondria (CHEN *et al.* 2000). CED-9 binds CED-4 (SPECTOR *et al.* 1997), which localizes to mitochondria in a CED-9-dependent manner (CHEN *et al.* 2000), promotes cell death (ELLIS and HORVITZ 1986), and is similar to the human pro-apoptotic protein APAF-1 (YUAN and HORVITZ 1992; ZOU *et al.* 1997). The expression of *egl-1* or the loss of *ced-9* function can trigger cell death and result in a change in the localization of CED-4 from mitochondria to the perinuclear region (CHEN *et al.* 2000). CED-4 activates CED-3 (SHAHAM and HORVITZ 1996b), which promotes cell death (ELLIS and HORVITZ 1986) and is a defining member of a family of cysteine proteases termed caspases (YUAN *et al.* 1993). CED-4 can interact directly with the CED-3 procaspase (WU *et al.* 1997) and facilitate the processing of proCED-3 into active CED-3 (CHINNAIYAN *et al.* 1997; YANG *et al.* 1998).

Other *C. elegans* genes appear to promote cell death more subtly. For example, the gene *ced-8* XK affects the timing of programmed cell deaths in *C. elegans* and has a minor role in cell killing (STANFIELD and HORVITZ 2000). The gene *ced-9*, which inhibits programmed cell death, also can promote cell death (HENGARTNER and HORVITZ 1994a). The gene *cps-6* encodes a mitochondrial

endonuclease G protein that likely promotes cell death (PARRISH *et al.* 2001). The process of the engulfment of dying cells also promotes cell death (HOEPPNER *et al.* 2001; REDDIEN *et al.* 2001). Additional genes that affect programmed cell death in *C. elegans*, such as those encoding proteins that mediate the ability of engulfment to promote cell death, that mediate the cell-killing activities of *ced-8* or *ced-9*, or that act downstream of CED-3 remain to be identified. We reasoned that genes with subtle contributing roles in programmed cell death might be identified by screening for mutations that further decrease cell death in a genetic background in which cell death is partially impaired. Here we report the identification and characterization of genes we identified using this approach and present evidence that these genes control activities that promote programmed cell death.

MATERIALS AND METHODS

Strains: *C. elegans* was cultured at 20°C on NGM agar with *E. coli* OP50 as described (BRENNER 1974). In general, the wild-type strain was N2. For mapping with polymorphisms, the wild-type strain RC301 was used. All mutations used have been described (RIDDLE *et al.* 1997), unless from this work or otherwise noted. The following mutations were used:

LGI; *lin-61(n3446), dpy-5(e61), lin-35(n745), lin-35(n2239, n2242)* (LU and HORVITZ 1998), *unc-13(e1091), unc-29(e1072), lin-53(n833)* (LU and HORVITZ 1998), *unc-75(e950), ced-1(e1735, n3390, n3402)* (HEDGECOCK *et al.* 1983), *hT2 [qIs48]* (MATHIES *et al.* 2003), *nIs128* (H. Schwartz and H.R.H., unpublished observations)

LGII; *lin-8(n111)*, *lin-8(n2731)* (THOMAS *et al.* 2003), *eT1, dpy-10(e128), egl-27(n170), lin-56(n2728)* (THOMAS *et al.* 2003), *rol-6(e187), dpl-1(n2994, n3316, n3380)* (CEOL and HORVITZ 2001), *unc-4(e120), rol-1(e91), lin-38(n751), mcd-1(n3376, n4005)* (this work), *unc-52(e444), mIn1 [dpy-10(e128) mIs14]* (EDGLEY and RIDDLE 2001), *mnC1 [dpy-10 unc-52]*

LGIII; *qC1, unc-79(e1068), ced-4(n1162, n2273), dpy-17(e164), lin-37(n758), lin-36(n766), lin-9(n112), lin-13(n770)*, *unc-32(e189), unc-16(e109), lin-52(n771), lin-52(n3718)* (THOMAS *et al.* 2003), *ced-7(n3370, n3373, n3378, n3383, n3401, n3408, n3394)* (this work), *unc-69(e587), unc-50(e306), ced-9(n2812, n1950 n2161, n1653, n3377, n3400, n3407)* (DESAI *et al.* 1988; HENGARTNER *et al.* 1992; HENGARTNER and HORVITZ 1994b), *ced-4(n3379, n3392*) (this work), *hT2 [qIs48]* (MATHIES *et al.* 2003)

LGIV; *ced-2(n3387)* (this work), *dpy-20(e1282), unc-30(e191), let-60(n1876), ced-3(n2427, n2447, n2452, n3374, n3375, n3384, n3403, n3406, n3411)* (SHAHAM *et al.* 1999), *dpy-4(e1166), nT1 [qIs51]* (MATHIES *et al.* 2003)

LGV; *eT1, lin-40(s1593)* (SOLARI *et al.* 1999), *tam-1(cc567)* (HSIEH *et al.* 1999), *unc-46(e177), let-418(s1617), dpy-11(e224), mys-1(n3681)* (CEOL and HORVITZ

2004)*, egl-1(n1084 n3082)* (CONRADT and HORVITZ 1998)*, hda-1(e1795)* (DUFOURCQ *et al.* 2002), *unc-76(e911), nIs96* (REDDIEN *et al.* 2001) LGX; *unc-20(e112), ced-8(n1891), lin-15(n433, n744, n767), chd-3(eh4)* (VON ZELEWSKY *et al.* 2000)*, nIs106* (REDDIEN *et al.* 2001)

Isolation of *n4005*: *mcd-1(n4005)* was isolated by screening a library of UV-trimethylpsoralen-induced deletions using PCR as described previously (JANSEN *et al.* 1997). The *mcd-1(n4005)* deletion begins at base 1228 after the A of ATG within the second intron and extends through base 2325 within the third exon. If the *mcd-1* mRNA in *n4005* animals is spliced from the second to the fourth exon, the product is predicted to be out-of-frame and could generate a protein of 92 amino acids.

Genetic mapping: Four of 52 *n3376/n3376* progeny from *n3376+/+unc-52* heterozygous animals were heterozygous for *unc-52*. 0/15 Rol-1 non-Dpy-10 animals from *dpy-10 rol-1+/++n3376* carried *n3376.* 20/21 Rol-1 non-Unc-52 recombinants between *rol-1* and *unc-52* from *rol-1+unc-52/+n3376+* animals carried *n3376*, and 1/21 did not. 0/93 F2 animals from *n3380+/+rol-6* heterozygous animals recombined between *n3380* and *rol-6*. From 18 recombinants selected between *dpy-10+rol-1/+n3380+* animals, 5/18 were between *dpy-10* and *n3380* and 13/18 were between *n3380* and *rol-1*. From 22 recombinants selected between *dpy-10+unc-4/+n3380+* animals, 9/22 were between *dpy-10* and *n3380* and 13/22 were between *n3380* and *unc-4*.

Polymorphism identification and mapping: PCR-size polymorphisms on LGIIR between RC301 and N2 were identified by PCR-amplifying approximately 1 kb fragments from intergenic regions and analyzing fragment sizes by electrophoresis. *nP89* is located in the region of the genome represented in cosmid F08G2; the RC301 PCR product amplified with primers PWR.G1 5'-GCCGAAGAAGCGATACTGAATG -3' and PWR.G2 5'-

AAGCCCCCTTGAAAAATGAGC -3' is approximately 1.1 kb; N2,1.0 kb. *nP90* is located in the region of the genome represented in YAC Y51H1A; the RC301 PCR product amplified with primers PWR.G11 5'- GTCATTGTGCGTTGATGGGAG -3' and PWR.G12 5'- TTACCGAGTGCGTTCTGTGAATC -3' is approximately 1.3 kb; N2, 1.2 kb. *nP91* is located in the region of the genome represented in cosmid W02B8; the RC301 PCR product amplified with primers PWR.G21 5'- CCATCATTTGTCATTGGAGCG -3' and PWR.G22 5'- AGGGTAGGGGCACGGTAGATAAAG -3' is approximately 1.2 kb; N2, 1.1 kb. *nP92* is located in the region of the genome represented in cosmid W07G1; the RC301 PCR product amplified with primers PWR.G31 5'- CATTGGTAGTTGTCGGCTTCCTG -3' and PWR.G32 5'- CCTTTTCATTTTTGCGGTGTCC -3' is approximately 1.5 kb; N2, 1.2 kb. Recombinants were generated from animals heterozygous for LGII between RC301 and N2: *rol-1 n3376 unc-52* (N2)*/+++* (RC301); *ced-3(n2427); nIs106* animals. We isolated 20 Rol-1 non-Unc-52 recombinants and generated homozygous recombinant strains. Two recombinants were found to the right of *nP89* and the left of *n3376*, and one recombinant was found to the left of *nP91* and the right of *n3376*.

Molecular Biology: The *mcd-1* cDNA was excised from the phage clone yk464e11 (Y. Kohara, personal communication). To determine the 5' end of *mcd-1* messages we used a 5'-rapid amplification of cDNA ends (RACE) system (Gibco). DNA sequences were determined using an automated ABI 373A DNA sequencer (Applied Biosystems). RNAi was performed by microinjection or feeding, as previously described (FIRE *et al.* 1998; TIMMONS *et al.* 2001). RNAi of *efl-1, efl-2,* and *lin-35* was performed using *efl-1, efl-2,* and *lin-35* cDNAs previously described (CEOL and HORVITZ 2001; LU and HORVITZ 1998). RNAi of *mcd-1* was performed from a template isolated by PCR amplification of a region of the third exon of *mcd-1* (see Figure 3) using primers carrying the T7 promoter, I.9, 5'- GATCGATAATACGACTCACTATAGGGCGGAAAATCCGCCAAAAAAAATCGG -

3', and I.10, 5'-GATCGATAATACGACTCACTATAGGGGATCACAGAGTCGATCCATTACAGG-3'. Similar methods were used to amplify and generate RNA from *F08G2.7, Y51H1A.1, Y51H1A.2, Y51H1A.4*, and *Y51H1A.5*.

RESULTS

Defects in programmed cell death in *C. elegans* have been efficiently quantified using two assays. First, a P_{lin-11} *gfp* reporter allows the deaths of specific cells in the ventral cord to be assessed (REDDIEN *et al.* 2001). The P_{lin-11} *gfp* reporter is expressed in the six VC motor neurons, P3-8.aap (P, P blast cell; a, anterior daughter; p, posterior daughter), of the ventral cord (Figure 1A). The cells W.ap (W, W blast cell), P1-2.aap, and P9-12.aap, which die in the wild type, survive in animals with defects in programmed cell death and express P_{lin-11} *gfp* (REDDIEN *et al.* 2001). Five of these cells, P2.aap and P9-12.aap can be reliably and easily scored for cell survival using a fluorescence stereomicroscope.

A second assay for programmed cell death uses Nomarski optics to determine the number of cell nuclei in another specific region of the animal, the anterior pharynx (HENGARTNER *et al.* 1992; SHAHAM *et al.* 1999). Animals carrying strong loss-of-function alleles of the killer gene *ced-3* have about 12-13 extra cells in this region, whereas animals carrying weak alleles of *ced-3* (for example, *n2427)* have about 1-2 extra cells in this region (SHAHAM *et al.* 1999). We observed that the degree of the cell-death defect conferred by the weak loss-of-function allele *ced-3(n2427)* as determined by counting the number of extra cells in anterior pharynges did not substantially vary with genetic background (Table S1), suggesting that mutations that caused alterations in cell number in *ced-3(n2427)* animals would reflect specific effects on cell death rather than non-specific effects on animal health.

A genetic screen for enhancers of *ced-3(n2427)*:

Using the P_{lin-11} *gfp* assay described above, we observed that *ced-3(n2427)* results in 4% of animals having all five VC-like cells (P2.aap and P9-12.aap, n=50). We previously showed that mutations in engulfment genes enhance the cell-death defects conferred by *ced-3(n2427)* as assayed with P_{lin-11} *gfp* (REDDIEN *et al.* 2001). For example, 88% of *ced-1(e1735); ced-3(n2427)* animals had all five

extra VC-like cells present (n=50), whereas 0% of *ced-1(e1735)* animals (n=50) had all five extra VC-like cells present (REDDIEN *et al.* 2001). *ced-1* is necessary for engulfment and encodes a cell-corpse receptor (HEDGECOCK *et al.* 1983; ZHOU *et al.* 2001). We therefore concluded that the P_{lin-11} *gfp* assay could be used for isolating mutations that enhance *ced-3(n2427)*.

We mutagenized *ced-3(n2427);* P_{lin-11} *gfp* animals, selected individual F2 progeny with five extra VC-like cells, and determined if these animals generated progeny with enhanced cell-death defects (Figure 1B). We expected to obtain alleles in the cell-death execution genes *ced-3, ced-4*, and *egl-1*. Because loss-of-function mutations in the *ced-9* gene enhance the cell-death defect caused by weak alleles of *ced-3* (HENGARTNER and HORVITZ 1994a), we anticipated that mutations in *ced-9* would also be isolated. We isolated six strains that likely carry mutations in *ced-3*, two in *ced-4*, and three in *ced-9* (Figure 1C). Because mutations in engulfment genes can enhance the cell-death defect caused by *ced-3(n2427)*, we also expected to isolate alleles of engulfment genes. At least 10 of the strains we isolated have defects in the engulfment of dying cells. We determined, using complementation tests, that two of these strains carry a mutation in *ced-1*, seven in *ced-7*, and one in *ced-2* (Figure 1C). Many alleles of *ced-7* might have been isolated because loss of *ced-7* function strongly enhances weak cell-death defects (Reddien et al. 2001). Two mutations, *n3376* and *n3380*, define new cell-death genes, as described below.

The mutations *n3376* and *n3380* define two new cell-death genes:
Animals carrying the mutations *n3376* and *n3380* had defects in cell death (Figure 1D, E). Genetic mapping established that *n3376* and *n3380* reside at different locations on LGII (Figure 1F). Because no previously characterized *C. elegans* cell-death gene is located on LGII, these mutations define new cell-death genes. The gene defined by *n3380* is a previously known gene, *dpl-1* (Figure 1G, see below for details). We named the gene defined by *n3376*, *mcd-1* (*mcd*, modifier of cell death). More than 60% of double mutant animals carrying *mcd-1(n3376)* or

dpl-1(n3380) with *ced-3(n2427)* had all five extra VC-1-like cells in their ventral cords, whereas only 4% of *ced-3(n2427)* single mutant animals had all five extra VC-1-like cells present (Figure 1D). *mcd-1(n3376)* and *dpl-1(n3380)* also enhanced cell-death defects conferred by *ced-3(n2427)* in the anterior pharynx (Table 1), indicating that these mutations affect programmed cell death broadly rather than specifically in the ventral cord. Furthermore, *mcd-1(n3376)* and *dpl-1(n3380)* enhanced the cell-death defect associated not only with the CED-3 G474R substitution caused by the *n2427* allele but also with the S446L substitution caused by the *n2447* allele (Figure S2A). Therefore, *mcd-1(n3376)* and *dpl-1(n3380)* are not allele-specific enhancers of *ced-3* and likely generally affect the ability of cells to die if programmed cell death is slightly impaired. We generated animals homozygous for *mcd-1(n3376)* and *dpl-1(n3380)* in a wild-type *ced-3* background. These animals were viable with no obvious morphological abnormalities. *mcd-1(n3376)* and *dpl-1(n3380)* each conferred a weak block in programmed cell death in the presence of an intact core cell-death execution pathway, indicating *mcd-1* and *dpl-1* have normal roles in promoting cell death (Figure 1E).

***n3380* is an allele of *dpl-1* DP:**

We mapped *n3380* between *unc-4* and *dpy-10* on LGII (Figure 1F, Materials and methods). We found that existing mutations in a gene in this region, *dpl-1*, enhanced the cell-death defect conferred by *ced-3(n2427)* (Table 1). *dpl-1* encodes the *C. elegans* ortholog of the mammalian E2F-heterodimerization partner DP (CEOL and HORVITZ 2001). We performed complementation tests and determined that the *dpl-1*(*n3316)* mutation (CEOL and HORVITZ 2001) failed to complement *n3380* for the enhancement of *ced-3(n2427)* (Table 1 and data not shown). *dpl-1* is a class B synthetic multivulva (synMuv) gene (CEOL and HORVITZ 2001). The synMuv genes fall into three classes, A, B, and C. Animals carrying mutations in any two genes from different classes undergo ectopic vulval development, the result of normally non-vulval cells adopting a vulval fate; the

resulting phenotype is termed multivulva (Muv) (CEOL and HORVITZ 2004; FERGUSON and HORVITZ 1989; HORVITZ and SULSTON 1980). We found that *dpl-1(n3380); lin-15A(n767)* animals were Muv (*n767* is a class A synMuv mutation; (FERGUSON and HORVITZ 1989), indicating that *dpl-1(n3380)* acts as a class B synMuv mutation, like other mutations in *dpl-1.* We determined the sequence of the *dpl-1* open reading frame in *dpl-1(n3380)* animals and found a C-to-T mutation predicted to result in a Q486stop (TAA) alteration in the 595-amino acid DPL-1 protein (Figure 1G). Together these results indicate that *n3380* is an allele of the gene *dpl-1*. Because *dpl-1* null alleles confer a sterile phenotype (CEOL and HORVITZ 2001), *dpl-1(n3380)* is not a null allele of *dpl-1*. *dpl-1(n3380)* conferred cell-death defects similar to those of the *dpl-1* allele *n2994* and the *dpl-1* null allele *n3316* (Table 1).

***n3376* is an allele of a gene predicted to encode a novel zinc-finger protein:** We mapped the mutation *n3376* to a region of approximately 75 kilobase pairs containing 13 predicted genes (Figure 1F, see Materials and methods). We inhibited the function of candidate genes in this region by RNAi (RNA-mediated genetic interference; (FIRE *et al.* 1998) and found that inhibition of *Y51H1A.6*, but not of *F08G2.7*, *Y51H1A.1, Y51H1A.2, Y51H1A.4,* or *Y51H1A.5*, caused enhancement of the cell-death defect of *ced-3(n2427)* animals (Table 1). We defined the structure of the *Y51H1A.6* genomic locus by determining the sequence of a cDNA clone, yk464e11 (kindly provided by Y. Kohara) (Figure 1H). We determined the 5' end of the *Y51H1A.6* transcript using 5' RACE (Rapid Amplification of cDNA Ends) and found *Y51H1A.6* transcripts to carry the SL1 *trans*-spliced leader sequence, which is commonly found on *C. elegans* mRNAs (KRAUSE and HIRSH 1987). We identified a C-to-T mutation predicted to cause an H277Y substitution in the Y51H1A.6 protein in *mcd-1(n3376)* animals (Figure 1H). We isolated a deletion allele of *Y51H1A.6*, *n4005* (Figure 1H, Materials and methods) and found that *n4005* resulted in a phenotype similar to that of *mcd-1(n3376)* and failed to complement *mcd-1(n3376)* for the enhancement of *ced-3*

(Table 1). *n4005* appears to be a strong loss-of-function allele of *mcd-1*. Together these findings indicate that *Y51H1A.6* is the gene defined by *n3376*.

The *mcd-1* gene is predicted to encode a highly acidic novel protein containing one candidate C2H2 zinc finger and has no other significant homology to known genes (Figures 1H, S1). This C2H2 zinc finger (FKCAECGDGFPVMDRLCDHMIKQH) is an exact match to canonical zinc-finger domains (Y/F-X-C-X2-4-C-X3-F-X5-L-X2-H-X3-5-H, (WOLFE *et al.* 2000). The *mcd-1(n3376)* missense mutation changes the first C2H2 histidine to a tyrosine (Figure 1H), indicating the MCD-1 zinc finger is important for the MCD-1 cell-death function. Zinc-finger domains can interact with DNA (WOLFE *et al.* 2000) and mediate protein-protein interactions (MACKAY and CROSSLEY 1998).

***efl-1* E2F and *lin-35* Rb promote cell death:**

Given that *dpl-1* acts in *C. elegans* development with the E2F-like gene *efl-1* and the Rb-like gene *lin-35* (CEOL and HORVITZ 2001; LU and HORVITZ 1998; PAGE *et al.* 2001), we asked whether these and other *dpl-1*-interacting genes also affect programmed cell death. DP-1 from mammals can bind to and promote DNA-binding by E2F-1 (GIRLING *et al.* 1993; HELIN *et al.* 1993). E2F proteins can affect DNA replication, cell-cycle progression, and development in mammals (BRACKEN *et al.* 2004)(HELIN 1998) and can interact with the tumor-suppressor protein pRb (DYSON 1998). E2F proteins can promote programmed cell death (HARBOUR and DEAN 2000b). We found that, like *dpl-1 DP*, *efl-1 E2F* and *lin-35 Rb* promoted programmed cell death (Table 2A, Figure S2B, C). Because mutations in *efl-1* confer sterility, we studied the role of *efl-1* E2F in programmed cell death using RNAi. RNAi of *efl-1* enhanced the weak cell-death defects conferred by *ced-3(n2427)*. Perturbation of a second *C. elegans* E2F-like gene, *efl-2*, caused no observed cell-death defects (data not shown). We studied the role of *lin-35* Rb in programmed cell death using the putative null allele *n745*. Enhancement of a weak cell-death defect was caused by *lin-35(n745)* (Table 2A), as well as by RNAi of *lin-35* and by other putative *lin-35* null alleles (Figure S2C and data not shown). Our

data suggest *dpl-1*, *lin-35*, and *efl-1* act together in programmed cell death as they do in vulval development. The cell-death defects of *dpl-1* mutants were stronger than those of *efl-1(RNAi)* animals or of animals carrying a putative *lin-35* null allele, *n745* (LU and HORVITZ 1998), for unknown reasons. Disruption of the class B synMuv genes *lin-37* and *lin-52* also enhanced *ced-3(n2427)* (Table 2A, Figure S2D). *lin-52(n771)* more strongly enhanced the cell-death defect conferred by *ced-3(n2427)* in the anterior pharynx than in the ventral cord (Table 2A, Figure S2D). *lin-37* encodes a protein similar to the Myb-interacting Mip40 protein (KORENJAK *et al.* 2004) and can physically interact with LIN-53 RbAP48, an Rb-interacting protein (WALHOUT *et al.* 2000). *lin-52* encodes a novel protein with similarity to proteins of unknown function in humans and *Drosophila* (THOMAS *et al.* 2003).

Disruption of class B synMuv genes - *lin-9, lin-15B, lin-36,* or *lin-53* -or any of the class A synMuv genes *lin-8, lin-15A, lin-38,* or *lin-56* did not enhance *ced-3(n2427)* (Table 2B). Therefore, the synMuv genes likely do not control a single process that affects both vulval cell fate and cell death. Rb-associated proteins have been found in multiple complexes, including a nucleosome-remodeling and histone-deacetylase complex (NuRD; (XUE *et al.* 1998) and two complexes from *Drosophila* containing the transcription factor Myb and multiple class B synMuv-like proteins (Myb-MuvB and dREAM; (LEWIS *et al.* 2004). We failed to detect a cell-death role for candidate *C. elegans* components of a NuRD complex (Table 2B): *hda-1* (LU and HORVITZ 1998), *let-418* (VON ZELEWSKY *et al.* 2000), *chd-3* (VON ZELEWSKY *et al.* 2000), *lin-40 (egr-1)* (CHEN and HAN 2001b; SOLARI *et al.* 1999), and *egl-27* (SOLARI *et al.* 1999). We also failed to detect a cell-death role for *lin-9,* which encodes a protein similar to a component of the Myb-MuvB and dREAM complexes (Table 2B). Together, our results suggest DPL-1 DP, EFL-1 E2F, LIN-35 Rb, LIN-52 and LIN-37 Mip40 define a novel association of class B synMuv proteins that act to promote programmed cell death. Because of lethality associated with strong loss-of-function alleles of multiple *C. elegans* genes encoding candidate NuRD, Myb-MuvB, and dREAM complex components, we examined animals with incomplete loss of function for some genes (Table 2B).

Roles for essential candidate NuRD, Myb-MuvB, and dREAM complex components in programmed cell death therefore remain possible.

Because the synMuv genes act antagonistically to *let-60* Ras in vulval development (BEITEL *et al.* 1990; FERGUSON *et al.* 1987; HAN and STERNBERG 1990; STERNBERG and HAN 1998), we asked whether the *dpl-1* gene acts antagonistically to *let-60* Ras in cell death. Null alleles of *let-60* confer maternally rescued larval lethality and zygotically suppress the synMuv phenotype conferred by *dpl-1* mutants (CEOL and HORVITZ 2001). We examined homozygous *let-60(n1876)* animals from heterozygous mothers. *let-60(n1876)* did not significantly affect the cell-death phenotype of *ced-3(n2427)* animals and did not suppress the enhanced cell-death defect of *dpl-1(n3380); ced-3(n2427)* animals (Figure S2E). These observations indicate that *dpl-1* does not promote cell death by antagonizing Ras signaling.

dpl-1 and _mcd-1_ might act together and with _lin-35_ Rb and _efl-1_ E2F to promote cell death:

To ask whether *dpl-1* and *mcd-1* act together or separately with one another and with *lin-35* and *efl-1* to promote cell death, we assayed the number of extra cells conferred by *ced-3(n2427)* in the anterior pharynges of appropriate double and triple mutant animals. *dpl-1, mcd-1*, *lin-35*, and *efl-1* did not appear to act additively (Tables 3B, S2B). *dpl-1(n3380) mcd-1(n3376)* animals had slightly more extra cells in their ventral cords than did *dpl-1(n3380)* or *mcd-1(n3376)* single mutant animals (Figure S2F) but not in their anterior pharynges (Table S2B). Furthermore, *dpl-1(n3380) mcd-1(n3376); ced-3(n2427)* and *dpl-1(n3380) mcd-1(n4005); ced-3(n2427)* animals did not have more extra cells in their anterior pharynges than did *dpl-1(n3380); ced-3(n2427)* and *mcd-1(n3376); ced-3(n2427)* or *mcd-1(n4005); ced-3(n2427)* animals (Table 3B). That *dpl-1(n3380)* and *mcd-1(n3376)* or *mcd-1(n4005)* can confer additive defects with other mutations that caused similar levels of cell-death defects (*ced-1, ced-8, ced-9*, see below, Table 3C) indicates that changes in cell-killing efficiency are within the detectable range

of this assay. Thus, *dpl-1*, *mcd-1*, *lin-35*, and *efl-1* might act together to promote cell death.

***dpl-1* and *mcd-1* promote cell death in a manner independent of *ced-1* and *ced-8*:**

We asked whether *dpl-1* and *mcd-1* act together with other subtle cell-death regulators. Mutations in engulfment genes (e.g., *ced-1)* can decrease cell killing (REDDIEN *et al.* 2001). Mutations in *ced-8* cause a delay in cell death, enhance weak alleles of *ced-3,* and cause very weak defects in cell killing on their own (STANFIELD and HORVITZ 2000). We observed that mutations in *mcd-1* and *dpl-1* enhanced cell-killing defects conferred by *ced-1(e1735)* or *ced-8(n1891)* (Table 3C). Because *ced-1(e1735)* and *ced-8(n1891)* are both null or strong loss-of-function alleles (STANFIELD and HORVITZ 2000; ZHOU *et al.* 2001), our data indicate *mcd-1* and *dpl-1* act independently from *ced-8* and *ced-1*. Furthermore, we examined doubly mutant strains carrying a wild-type *ced-3* locus and observed enhanced cell-death defects: *ced-1(e1735); dpl-1(n3380)* animals, *ced-1(e1735); mcd-1(n3376)* animals, *dpl-1(n3380); ced-8(n1891)* animals, and *mcd-1(n3376); ced-8(n1891)* animals had defects in cell killing greater than those seen in the single mutants (Table S2C, Figure S2F). In addition, *n3376* and *n3380* did not cause defects in engulfment. These results indicate that *dpl-1* and *mcd-1* control one of multiple parallel processes that redundantly and significantly contribute to cell death.

***dpl-1* and *mcd-1* do not promote cell death through regulation of *ced-9*:**

The *egl-1* gene is required for essentially all programmed cell death in *C. elegans* and can be transcriptionally up-regulated to promote programmed cell death (CONRADT and HORVITZ 1998; CONRADT and HORVITZ 1999). Because DP, Rb, and E2F can act in transcriptional regulation and *mcd-1* has a zinc-finger domain, we sought to determine whether these genes might affect *egl-1* expression. *egl-1* acts upstream of *ced-9* (CONRADT and HORVITZ 1998). To determine whether *dpl-1* and

mcd-1 act downstream or upstream of the death-inhibiting role of *ced-9*, we asked whether mutations in these genes could enhance *ced-3(n2427)* in the absence of *ced-9* function using the *ced-9* null allele *n2812* (Table 3C). *ced-9* has both a death-inhibiting and a death-promoting role (HENGARTNER and HORVITZ 1994a). We found that *ced-3(n2427)* animals had on average 1.8 extra cells in their anterior pharynges, while *ced-9(n2812); ced-3(n2427)* animals had 6.3 extra cells (Table 3A). Triple mutant animals with *ced-9(n2812)*; *ced-3(n2427)* in addition to *mcd-1(n3376)* or *dpl-1(n3380)* had an enhanced number of extra cells (9.4 and 10.6, respectively, Table 3C). By contrast, null alleles of *egl-1* do not enhance the cell-killing defects of *ced-9(n2812)*; *ced-3(n2427)* double mutants (CONRADT and HORVITZ 1998). These results indicate that *dpl-1* and *mcd-1* have cell-death promoting activity downstream of or independent of the cell-death protective activity of *ced-9*. In addition, the data indicate *dpl-1* and *mcd-1* act independently from the cell-death promoting activity of *ced-9*. Because *egl-1* acts to inhibit *ced-9*, *dpl-1* and *mcd-1* likely do not promote death by regulating *egl-1* transcription.

dpl-1 and _mcd-1_ can affect cells fated to live:

Embryos lacking maternal and zygotic *ced-9* undergo excessive programmed cell death and die, i. e., in such embryos cells that are normally fated to live instead die (HENGARTNER *et al.* 1992). This lethality can be suppressed by mutations in the killer genes *ced-3* and *ced-4* (HENGARTNER *et al.* 1992). To determine if perturbation of *dpl-1* and *mcd-1* can affect the ectopic programmed cell death of cells that normally live, we utilized the observation that animals carrying both the *ced-9(n1653)* temperature-sensitive allele and the *ced-4(n2273)* mutation confer a synthetic maternal-effect lethality caused by excessive programmed cell death (SHAHAM and HORVITZ 1996a). The *ced-4(n2273)* mutation affects *ced-4* splicing and affects production of the minor cell-death inhibitory CED-4L product; therefore, *ced-9(n1653) ced-4(n2273)* animals might confer synthetic lethality as a result of a reduction of both *ced-9* death-inhibitory function and *ced-4L* death-inhibitory function (SHAHAM and HORVITZ 1996a). *ced-9(n1653) ced-4(n2273)* synthetic

maternal-effect lethality can be suppressed by mutations that otherwise cause a very weak cell-death defect (E. Speliotes and H. R. H., unpublished results), suggesting that cells that normally live are poised between life and death in these animals. We found that either *dpl-1(n3380)* or *mcd-1(n3376)* partially suppressed the synthetic lethality conferred by *ced-9(n1653) ced-4(n2273)* (Table 4). *dpl-1(n3380)* or *mcd-1(4005)* also partially suppressed the maternal-effect lethality conferred by the *ced-9* partial loss-of-function mutant *ced-9(n1950 n2161)* (Table 4). Therefore, *dpl-1* and *mcd-1* likely are active in cells that normally live and can promote the ability of such cells to die when cell-death inhibitory activity is reduced. Cell deaths in *C. elegans* are normally invariant among individuals (SULSTON and HORVITZ 1977). Our observations indicate that *dpl-1* and *mcd-1* likely do not act to mediate the effects of lineage-regulated factors that specify cell death, because these genes can affect the ability of any cell to die. This hypothesis is supported by our direct observation of the cell-death process in *mcd-1* and *dpl-1* mutants using Nomarski optics (see below).

Cells can initiate the death process and recover in *dpl-1(n3380)* and *mcd-1(n4005)* animals: We directly observed cell death within the P9, P10, and P11 neuroblast lineages in *dpl-1(n3380)* and *mcd-1(n4005)* animals. Animals also carried the $P_{lin\text{-}11}$ *gfp* reporter, allowing us to determine whether any Pn.aap cell ultimately survived and differentiated. We observed no defect in cell division patterns (*dpl-1(n3380)*, n=8 and *mcd-1(n4005)*, n=6). We observed that the cell-death process could initiate and be followed by episodic changes in the morphology of the dying cells (Figure 2A, B). Some cells ultimately survived following these episodic morphological changes. Specifically, four of 24 Pn.aap cells failed to die in the time period observed in *dpl-1(n3380);* $P_{lin\text{-}11}$ *gfp* animals, and all four of these cells expressed GFP. Four of 18 Pn.aap cells failed to die in the time period observed in *mcd-1(n4005);* $P_{lin\text{-}11}$ *gfp* animals, and three of these cells expressed GFP. The initiation of cell condensation during cell death requires the CED-3 caspase (REDDIEN *et al.* 2001). Therefore, we suggest that cells lacking

normal *dpl-1* or *mcd-1* function can occasionally recover following the activation of CED-3 and the initiation of morphological changes associated with the cell-death process (Figure 2C).

***dpl-1* and *mcd-1* do not affect CED-3 caspase-independent death:**

Strong loss-of-function alleles of *ced-3*, including a deletion allele that completely lacks the CED-3 protease-encoding region, *ced-3(n2452),* do not completely block programmed cell death (SHAHAM *et al.* 1999). For example, *ced-1(e1735); ced-3(n2452)* animals generated a few apparent cell corpses: 7 of 50 animals had two or more corpses in the heads of L1 larvae, suggesting that a low level of cell death can occur independently of the *ced-3* caspase. *mcd-1* and *dpl-1* had no effect on these *ced-3*-independent deaths: 8 of 50 L1 larvae had two or more corpses, and 6 of 50 animals had two or more corpses in *ced-1(e1735); mcd-1(n3376); ced-3(n2452)* and *ced-1(e1735); dpl-1(n3380); ced-3(n2452)* animals, respectively). We therefore suggest that *dpl-1* and *mcd-1* promote cell death by affecting a process controlled by the CED-3 caspase rather than by acting independently from and parallel to CED-3 activity.

Loss of *mcd-1* function confers synthetic lethality with mutations in *lin-35* Rb and other class B synMuv genes:

Reduction of *mcd-1* function by deletion or RNAi did not cause noticeable growth defects as compared to the wild type. However, perturbation of *mcd-1* function in combination with mutations in some class B synMuv genes conferred synthetic lethality (larval arrest) or slow growth (Table 5A). Specifically, RNAi of *mcd-1* and *mcd-1(n4005)* synthetically caused 100% arrest during the first larval stage of *lin-9(n112), lin-15B(n744), lin-35(n745), lin-37(n758),* and *lin-54(n2231)* animals, slow larval growth of *lin-53(n833)* animals, and slow growth and some larval arrest of animals carrying mutations in *dpl-1* and *lin-13*. *mcd-1(n4005)* also synthetically caused slow larval growth in animals carrying a mutation in the class C synMuv gene *mys-1* (Table 5A). Additionally, an L1-arrest phenotype was observed in

mcd-1(n4005) animals when the class B synMuv genes *lin-54*, *dpl-1*, *lin-9*, or *lin-37* were inactivated by RNAi. *mcd-1(n4005)* and RNAi of *mcd-1* did not cause synthetic lethality with the class B synMuv mutations *tam-1(cc567), lin-36(n766),* or *lin-52(n771)* (Table 5B) or with the class A synMuv mutations *lin-8(n2731)*, *lin-15A(n767), lin-38(n751),* or *lin-56(n2728)* (Table 5C). *lin-36(n766)* and *lin-52(n771)* are non-null alleles (THOMAS *et al.* 2003). RNAi of *mcd-1* did not cause a synMuv phenotype in combination with the class B mutations *lin-36(n766)* and *lin-52(n771)*. These results indicate that *mcd-1* acts redundantly with most but not all class B synMuv genes for growth and viability.

DISCUSSION

From a screen for mutations that enhanced the cell-death defect caused by a weak *ced-3* allele we identified two new positive regulators of programmed cell death in *C. elegans, mcd-1* and *dpl-1*. *mcd-1* encodes a novel zinc-finger protein that acts together with the *dpl-1 DP* gene. Because DP is the dimerization partner for the E2F transcription factor in mammals (GIRLING *et al.* 1993; HELIN *et al.* 1993), these genes likely affect *C. elegans* cell death via transcription. DP and E2F can act together with Rb and a number of chromatin regulators in transcriptional repression (HARBOUR and DEAN 2000a). A large number of genes encoding proteins implicated in chromatin remodeling have been identified in *C. elegans* that act together with *dpl-1* DP in regulating vulval development. These genes, called "synMuv" for their synthetic multivulva loss-of-function phenotype (FERGUSON and HORVITZ 1989), number at least 27. We found that a few of these genes promote cell death; these genes encode an E2F-like protein (EFL-1), an Rb-like protein (LIN-35), a Mip40-like protein (LIN-37), and one novel protein with similarity to proteins in humans and *Drosophila* (LIN-52). Therefore, a DP/E2F-like heterodimeric transcription factor probably acts together with an Rb-like protein, the MCD-1 zinc-finger protein, a Mip40-like protein, and the LIN-52 protein to promote cell death in *C. elegans* via transcriptional regulation.

E2F and Rb proteins have roles in cancer and effects on cell death in mammals (HARBOUR and DEAN 2000b; SHERR and MCCORMICK 2002). Similar to the case in *C. elegans*, loss of function of E2F-1 in mice leads to reduced cell death (FIELD *et al.* 1996; YAMASAKI *et al.* 1996). However, in contrast to *C. elegans*, in the mouse loss of Rb function leads to increased cell death (MACLEOD *et al.* 1996; MORGENBESSER *et al.* 1994). It is possible that Rb-like genes promote cell death in mammals but that this defect is obscured by cell-cycle abnormalities; cell-cycle abnormalities are known to trigger cell death in mammals (EVAN and LITTLEWOOD 1998). In *C. elegans*, an E2F-like and an Rb-like protein act together, rather than antagonistically, to regulate vulval development (CEOL and HORVITZ

2001), the cell cycle (BOXEM and VAN DEN HEUVEL 2002), and cell death (this work). Because E2F-4 and E2F-5 are known to act together with Rb to mediate transcriptional repression in mammals (FROLOV and DYSON 2004), some of the mammalian Rb and E2F genes might act together to promote cell death, as observed in *C. elegans*.

How might *dpl-1*, *mcd-1*, *lin-35*, *efl-1*, *lin-37*, and *lin-52* affect *C. elegans* cell death?

Rb and E2F/DP are cell-cycle regulators, and a misregulated cell cycle can trigger cell death in mammals (EVAN and LITTLEWOOD 1998). However, our data are inconsistent with the hypothesis that cell-cycle abnormalities account for the enhanced cell-death defects we observed. For example, the P9-11 neuroblast lineages in *dpl-1* and *mcd-1* mutants were grossly normal (i. e., no cell cycle arrest or aberrant division patterns were observed, *dpl-1(n3380); nIs106*, n=8; *mcd-1(n4005); nIs106*, n=6). Furthermore, cell-cycle roles have been identified in *C. elegans* for a subset of synMuv genes, including *lin-35* Rb, *dpl-1* DP, *efl-1 E2F, lin-9 ALY, lin-15B,* and *lin-36* (BOXEM and VAN DEN HEUVEL 2001; BOXEM and VAN DEN HEUVEL 2002), but this subset does not match the subset of synMuv genes that affects cell death. Specifically, not all synMuv genes that affect the cell cycle affect cell death (*lin-9, lin-15, lin-36)*, and a synMuv gene that does not affect the cell cycle can affect cell death (*lin-37*). Many class B synMuv genes probably have multiple functions in development, such as regulation of the cell cycle and regulation of cell fate. For example, many synMuv genes have no observed effect on the cell cycle and act together with synMuv genes like *dpl-1*, *lin-35,* and *efl-1* to regulate vulval cell fates. We propose that *dpl-1*, *mcd-1, efl-1*, *lin-35*, *lin-37,* and *lin-52* act together to regulate cell death via transcriptional regulation of specific targets that affect the cell-death process rather than act non-specifically to affect cell death as a consequence of effects on the cell cycle. Mammalian Rb and E2F-like proteins probably also have non-cell cycle roles (FROLOV and DYSON 2004; LANDSBERG *et al.* 2003).

There are multiple mammalian candidate E2F/DP transcriptional targets that could interface with the cell-death pathway. For example, E2F can trigger cell death via transcriptional activation of the p53 tumor-suppressor gene (HARBOUR and DEAN 2000b). However, we observed that a putative null allele of the *C. elegans* P53-like gene *cep-1* (DERRY *et al.* 2001; SCHUMACHER *et al.* 2001) failed to cause enhancement of the cell-death defects in *ced-3(n2427)* animals (data not shown). E2F genes can also regulate transcription of caspase (MULLER *et al.* 2001) and the *Apaf-1* (MORONI *et al.* 2001) genes. No clear candidate EFL-1 binding sites are readily apparent in *ced-3* or *ced-4* regulatory regions that are evolutionarily conserved with the related species *C. briggsae*. The initiation of cell death in *C. elegans* is known to involve transcription (CONRADT and HORVITZ 1999; METZSTEIN *et al.* 1996; METZSTEIN and HORVITZ 1998; THELLMANN *et al.* 2003), raising the possibility that *dpl-1, mcd-1*, and interacting genes regulate the transcription of *egl-1* to promote cell-death initiation. However, multiple lines of evidence are inconsistent with this hypothesis. First, *egl-1* acts upstream of the cell-death inhibitory *ced-9* gene (CONRADT and HORVITZ 1998), and *dpl-1* and *mcd-1* do not. Second, *dpl-1* and *mcd-1* do not act only in cells fated to die. Third, cells that fail to die in *dpl-1* and *mcd-1* mutants display morphological changes reflecting attempts at cell death rather than a complete failure to initiate cell death. *dpl-1* and *mcd-1* therefore likely control the death process rather than the life vs. death decision-making process. We do not know whether *dpl-1* and *mcd-1* act to control the activity of the core cell death-execution pathway (CED-9, CED-4, CED-3) or act independently. Our data indicate *dpl-1* and *mcd-1* do not mediate the effects of engulfment on cell death and do not act together with *ced-8*; engulfment and *ced-8* are other known cell-death contributing factors. Because loss-of-function of *mcd-1* and *dpl-1* did not perturb the low level of cell death that occurs independently of the CED-3 caspase, these genes likely function in a pathway with CED-3.

MCD-1 is a novel regulator of cell death and is synthetically required for viability with the LIN-35 Rb tumor suppressor:

MCD-1 has a single C2H2 zinc finger and no obvious homology to other domains or proteins in existing databases. Because caspases execute the death process, modulators of cell death are candidate caspase targets for proteolysis. However, MCD-1 does not contain candidate CED-3 cleavage sites conserved in the related species *C. briggsae*. Many uncharacterized zinc-finger proteins exist in mammals, one or more of which could share functional similarities with MCD-1. Given known functions for C2H2 zinc fingers, MCD-1 could be a DNA-binding protein or be involved in protein-protein interactions. *mcd-1* acts with a number of synMuv genes to regulate cell death. Because *mcd-1* is synthetically required for viability with *lin-35 Rb* and many other class B synMuv genes, *mcd-1* must act redundantly with these genes in some developmental processes. This might be because different assemblages of transcriptional regulatory factors control distinct developmental events (see below). Because Rb is a known tumor-suppressor gene, *mcd-1* and potential interacting genes could define an uncharacterized complex that acts redundantly with Rb as a tumor suppressor in mammals.

Subsets of synMuv genes control diverse aspects of biology:

Our finding that a subset of synMuv genes affects cell death and that a different subset of synMuv genes is synthetically required for animal viability add to an increasing number of functional categorizations of synMuv genes. Subsets of synMuv genes control at least 14 diverse biological processes in *C. elegans* (BENDER *et al.* 2004; BOXEM and VAN DEN HEUVEL 2001; BOXEM and VAN DEN HEUVEL 2002; CEOL and HORVITZ 2004; CHEN and HAN 2001a; CUI *et al.* 2004; DUFOURCQ *et al.* 2002; FAY *et al.* 2002; FAY *et al.* 2003; FAY *et al.* 2004; FERGUSON and HORVITZ 1989; GARBE *et al.* 2004; PAGE *et al.* 2001; REDDY and VILLENEUVE 2004; UNHAVAITHAYA *et al.* 2002; WANG *et al.* 2005). The set of synMuv genes that affects one process is often distinct from the set affecting others. Therefore, the

diverse functions of LIN-35 Rb and associated synMuv proteins could be mediated by different assemblages of co-regulators of transcription. Many of the class B synMuv genes encode proteins similar to those found in several chromatin-remodeling complexes in other organisms, including the NuRD, Myb-MuvB, and dREAM transcriptional repression complexes (KORENJAK *et al.* 2004; LEWIS *et al.* 2004; XUE *et al.* 1998). Our studies define a new candidate assemblage of synMuv proteins, containing DPL-1, EFL-1, LIN-35, MCD-1, LIN-37, and LIN-52 and regulating programmed cell death.

Our results with *mcd-1* highlight the complex manner in which synMuv genes are utilized. For example, mutations in some of the class B synMuv genes that cause synthetic lethality with loss of *mcd-1* cause no detectable defect in cell death (e. g., *lin-9* and *lin-15B*), whereas others do cause defects in cell death (e. g., *lin-35*). By contrast, one class B synMuv mutation that causes a defect in cell death, *lin-52(n771)*, is homozygous viable with *mcd-1(n4005)*. The process that is affected by *mcd-1* and synthetically required for viability with some class B synMuv genes is likely distinct from the process affected by *mcd-1* during cell death, because different gene sets associate with these aspects of the *mcd-1* loss-of-function phenotype. The hypothesis that *mcd-1* acts in at least two processes might explain the observation that *mcd-1* appears to act redundantly with *lin-35 Rb, dpl-1 DP*, and other class B synMuv genes for growth and viability but not for cell death. Continued genetic studies in *C. elegans* should allow for the systematic dissection of the functional associations among the synMuv genes. Given that some synMuv genes are similar to human tumor-suppressor proteins (e.g., *lin-35 Rb*), an understanding of these associations could have important implications for our understanding of genes regulating human cancer.

A candidate transcriptional-regulatory complex controls one of multiple redundant activities that promote programmed cell death in *C. elegans*:
We have identified six new *C. elegans* cell-death genes: *mcd-1*, *dpl-1*, *efl-1*, *lin-35*, *lin-37*, and *lin-52*. These genes are not needed for most cell death; rather, they

have contributing roles. The primary cell-death pathway components remain *egl-1, ced-9*, *ced-4,* and *ced-3*. When animals contain mutations in multiple genes that control independent, cell-death contributing activities, robust cell-death defects are observed. For example, every animal we observed with mutations in *dpl-1* and the cell-corpse engulfment gene *ced-1* had abnormal cell death in the ventral cord. Therefore, together, cell-death modifiers have very significant roles in the cell-death process. Other independent cell death-promoting activities might exist and be identified using the strategy presented in this manuscript. An understanding of cell death, a process important for disease and development, must account for the many partially redundant and largely unexplained activities that have been identified (Figure 2D). The genes described in this manuscript are candidates to define components of a transcriptional regulatory complex that contains DP, E2F, Rb, MCD-1, LIN-52, and LIN-37 proteins and that promotes programmed cell death. Given the involvement of misregulated programmed cell death in cancer and neurodegenerative disorders, we have identified a new category of genes as potential therapeutic targets for the manipulation of cell death to treat human disease.

ACKNOWLEDGMENTS

We thank Yamini Jagganath for assistance with screening. We thank Rajesh Ranganthan for co-coordinating the design and construction of the deletion library, members of the Horvitz laboratory for efforts in deletion library construction, and Beth Castor for deletion library screening. We thank Na An for maintaining the Horvitz laboratory strain collection. We thank Brendan Galvin and Hillel Schwartz for comments concerning this manuscript. P.W.R. was supported by a National Science Foundation predoctoral fellowship. E.C.A. is an Anna Fuller Graduate Fellow. H.R.H. is the David H. Koch Professor of Biology at M.I.T. and an Investigator of the Howard Hughes Medical Institute. This work was supported by National Institutes of Health grant GM24663 to H.R.H. and by the Howard Hughes Medical Institute.

LITERATURE CITED

BEITEL, G. J., S. G. CLARK and H. R. HORVITZ, 1990 *Caenorhabditis elegans ras* gene *let-60* acts as a switch in the pathway of vulval induction. Nature **348:** 503-509.

BENDER, A. M., O. WELLS and D. S. FAY, 2004 *lin-35*/Rb and *xnp-1*/ATR-X function redundantly to control somatic gonad development in *C. elegans*. Dev Biol **273:** 335-349.

BOXEM, M., and S. VAN DEN HEUVEL, 2001 *lin-35* Rb and *cki-1* Cip/Kip cooperate in developmental regulation of G1 progression in *C. elegans*. Development **128:** 4349-4359.

BOXEM, M., and S. VAN DEN HEUVEL, 2002 *C. elegans* class B synthetic multivulva genes act in G(1) regulation. Curr. Biol. **12:** 906-911.

BRACKEN, A. P., M. CIRO, A. COCITO and K. HELIN, 2004 E2F target genes: unraveling the biology. Trends Biochem Sci **29:** 409-417.

BRENNER, S., 1974 The genetics of *Caenorhabditis elegans*. Genetics **77:** 71-94.

CEOL, C. J., and H. R. HORVITZ, 2001 *dpl-1* DP and *efl-1* E2F act with *lin-35* Rb to antagonize Ras signaling in *C. elegans* vulval development. Mol Cell **7:** 461-473.

CEOL, C. J., and H. R. HORVITZ, 2004 A new class of *C. elegans* synMuv genes implicates a Tip60/NuA4-like HAT complex as a negative regulator of Ras signaling. Dev. Cell **6:** 563-576.

CHEN, F., B. M. HERSH, B. CONRADT, Z. ZHOU, D. RIEMER *et al.*, 2000 Translocation of *C. elegans* CED-4 to nuclear membranes during programmed cell death. Science **287:** 1485-1489.

CHEN, Z., and M. HAN, 2001a *C. elegans* Rb, NuRD, and Ras regulate *lin-39*-mediated cell fusion during vulval fate specification. Curr Biol **11:** 1874-1879.

CHEN, Z., and M. HAN, 2001b Role of *C. elegans lin-40* MTA in vulval fate specification and morphogenesis. Development **128:** 4911-4921.

CHINNAIYAN, A. M., D. CHAUDHARY, K. O'ROURKE, E. V. KOONIN and V. M. DIXIT, 1997 Role of CED-4 in the activation of CED-3. Nature **388:** 728-729.

CONRADT, B., and H. R. HORVITZ, 1998 The *C. elegans* protein EGL-1 is required for programmed cell death and interacts with the Bcl-2-like protein CED-9. Cell **93:** 519-529.

CONRADT, B., and H. R. HORVITZ, 1999 The TRA-1A sex determination protein of *C. elegans* regulates sexually dimorphic cell deaths by repressing the *egl-1* cell death activator gene. Cell **98:** 317-327.

CUI, M., D. S. FAY and M. HAN, 2004 *lin-35*/Rb cooperates with the SWI/SNF complex to control *Caenorhabditis elegans* larval development. Genetics **167:** 1177-1185.

DERRY, W. B., A. P. PUTZKE and J. H. ROTHMAN, 2001 *Caenorhabditis elegans* p53: Role in Apoptosis, Meiosis, and Stress Resistance. Science **294:** 591-595.

DESAI, C., G. GARRIGA, S. L. MCINTIRE and H. R. HORVITZ, 1988 A genetic pathway for the development of the *Caenorhabditis elegans* HSN motor neurons. Nature **336:** 638-646.

DUFOURCQ, P., M. VICTOR, F. GAY, D. CALVO, J. HODGKIN *et al.*, 2002 Functional requirement for histone deacetylase 1 in *Caenorhabditis elegans* gonadogenesis. Mol. Cell Biol. **22:** 3024-3034.

DYSON, N., 1998 The regulation of E2F by pRB-family proteins. Genes Dev **12:** 2245-2262.

EDGLEY, M. L., and D. L. RIDDLE, 2001 LG II balancer chromosomes in *Caenorhabditis elegans*: *mT1*(II;III) and the *mIn1* set of dominantly and recessively marked inversions. Mol Genet Genomics **266:** 385-395.

ELLIS, H. M., and H. R. HORVITZ, 1986 Genetic control of programmed cell death in the nematode *C. elegans*. Cell **44:** 817-829.

EVAN, G., and T. LITTLEWOOD, 1998 A matter of life and cell death. Science **281:** 1317-1322.

FAY, D. S., S. KEENAN and M. HAN, 2002 *fzr-1* and *lin-35/Rb* function redundantly to control cell proliferation in *C. elegans* as revealed by a nonbiased synthetic screen. Genes Dev. **16:** 503-517.

FAY, D. S., E. LARGE, M. HAN and M. DARLAND, 2003 *lin-35*/Rb and *ubc-18*, an E2 ubiquitin-conjugating enzyme, function redundantly to control pharyngeal morphogenesis in *C. elegans*. Development **130:** 3319-3330.

FAY, D. S., X. QIU, E. LARGE, C. P. SMITH, S. MANGO *et al.*, 2004 The coordinate regulation of pharyngeal development in *C. elegans* by *lin-35*/Rb, *pha-1*, and *ubc-18*. Dev. Biol. **271:** 11-25.

FERGUSON, E. L., and H. R. HORVITZ, 1989 The multivulva phenotype of certain *Caenorhabditis elegans* mutants results from defects in two functionally redundant pathways. Genetics **123:** 109-121.

FERGUSON, E. L., P. W. STERNBERG and H. R. HORVITZ, 1987 A genetic pathway for the specification of the vulval cell lineages of *Caenorhabditis elegans*. Nature **326:** 259-267.

FIELD, S. J., F. Y. TSAI, F. KUO, A. M. ZUBIAGA, W. G. KAELIN, JR. *et al.*, 1996 E2F-1 functions in mice to promote apoptosis and suppress proliferation. Cell **85:** 549-561.

FIRE, A., S. XU, M. K. MONTGOMERY, S. A. KOSTAS, S. E. DRIVER *et al.*, 1998 Potent and specific genetic interference by double-stranded RNA in *Caenorhabditis elegans*. Nature **391:** 806-811.

FROLOV, M. V., and N. J. DYSON, 2004 Molecular mechanisms of E2F-dependent activation and pRB-mediated repression. J Cell Sci **117:** 2173-2181.

GARBE, D., J. B. DOTO and M. V. SUNDARAM, 2004 *Caenorhabditis elegans lin-35*/Rb, *efl-1*/E2F and other synthetic multivulva genes negatively regulate

the anaphase-promoting complex gene *mat-3*/APC8. Genetics **167:** 663-672.

GIRLING, R., J. F. PARTRIDGE, L. R. BANDARA, N. BURDEN, N. F. TOTTY *et al.*, 1993 A new component of the transcription factor DRTF1/E2F. Nature **362:** 83-87.

GLÜCKSMANN, A., 1951 Cell deaths in normal vertebrate ontogeny. Biol. Rev. **26:** 59-86.

HAN, M., and P. W. STERNBERG, 1990 *let-60*, a gene that specifies cell fates during *C. elegans* vulval induction, encodes a ras protein. Cell **63:** 921-931.

HARBOUR, J. W., and D. C. DEAN, 2000a Chromatin remodeling and Rb activity. Curr Opin Cell Biol **12:** 685-689.

HARBOUR, J. W., and D. C. DEAN, 2000b The Rb/E2F pathway: expanding roles and emerging paradigms. Genes Dev **14:** 2393-2409.

HEDGECOCK, E. M., J. E. SULSTON and J. N. THOMSON, 1983 Mutations affecting programmed cell deaths in the nematode *Caenorhabditis elegans*. Science **220:** 1277-1279.

HELIN, K., 1998 Regulation of cell proliferation by the E2F transcription factors. Curr Opin Genet Dev **8:** 28-35.

HELIN, K., C. L. WU, A. R. FATTAEY, J. A. LEES, B. D. DYNLACHT *et al.*, 1993 Heterodimerization of the transcription factors E2F-1 and DP-1 leads to cooperative trans-activation. Genes Dev **7:** 1850-1861.

HENGARTNER, M. O., R. E. ELLIS and H. R. HORVITZ, 1992 *Caenorhabditis elegans* gene *ced-9* protects cells from programmed cell death. Nature **356:** 494-499.

HENGARTNER, M. O., and H. R. HORVITZ, 1994a Activation of *C. elegans* cell death protein CED-9 by an amino-acid substitution in a domain conserved in Bcl-2. Nature **369:** 318-320.

HENGARTNER, M. O., and H. R. HORVITZ, 1994b *C. elegans* cell survival gene *ced-9* encodes a functional homolog of the mammalian proto-oncogene bcl-2. Cell **76:** 665-676.

HOEPPNER, D. J., M. O. HENGARTNER and R. SCHNABEL, 2001 Engulfment genes cooperate with *ced-3* to promote cell death in *Caenorhabditis elegans*. Nature **412:** 202-206.

HORVITZ, H. R., and J. E. SULSTON, 1980 Isolation and genetic characterization of cell-lineage mutants of the nematode *Caenorhabditis elegans*. Genetics **96:** 435-454.

HSIEH, J., J. LIU, S. A. KOSTAS, C. CHANG, P. W. STERNBERG *et al.*, 1999 The RING finger/B-box factor TAM-1 and a retinoblastoma-like protein LIN-35 modulate context-dependent gene silencing in *Caenorhabditis elegans*. Genes Dev. **13:** 2958-2970.

JACOBSON, M. D., M. WEIL and M. C. RAFF, 1997 Programmed cell death in animal development. Cell **88:** 347-354.

JANSEN, G., E. HAZENDONK, K. L. THIJSSEN and R. H. PLASTERK, 1997 Reverse genetics by chemical mutagenesis in *Caenorhabditis elegans*. Nat. Genet. **17:** 119-121.

KORENJAK, M., B. TAYLOR-HARDING, U. K. BINNE, J. S. SATTERLEE, O. STEVAUX *et al.*, 2004 Native E2F/RBF complexes contain Myb-interacting proteins and repress transcription of developmentally controlled E2F target genes. Cell **119:** 181-193.

KRAUSE, M., and D. HIRSH, 1987 A trans-spliced leader sequence on actin mRNA in *C. elegans*. Cell **49:** 753-761.

LANDSBERG, R. L., J. E. SERO, P. S. DANIELIAN, T. L. YUAN, E. Y. LEE *et al.*, 2003 The role of E2F4 in adipogenesis is independent of its cell cycle regulatory activity. Proc. Natl. Acad. Sci. **100:** 2456-2461.

LEWIS, P. W., E. L. BEALL, T. C. FLEISCHER, D. GEORLETTE, A. J. LINK *et al.*, 2004 Identification of a *Drosophila* Myb-E2F2/RBF transcriptional repressor complex. Genes Dev **18:** 2929-2940.

LU, X., and H. R. HORVITZ, 1998 *lin-35* and *lin-53*, two genes that antagonize a *C. elegans* Ras pathway, encode proteins similar to Rb and its binding protein RbAp48. Cell **95:** 981-991.

MACKAY, J. P., and M. CROSSLEY, 1998 Zinc fingers are sticking together. Trends Biochem Sci **23:** 1-4.

MACLEOD, K. F., Y. HU and T. JACKS, 1996 Loss of Rb activates both p53-dependent and independent cell death pathways in the developing mouse nervous system. EMBO J **15:** 6178-6188.

MATHIES, L. D., S. T. HENDERSON and J. KIMBLE, 2003 The *C. elegans* Hand gene controls embryogenesis and early gonadogenesis. Development **130:** 2881-2892.

METZSTEIN, M. M., M. O. HENGARTNER, N. TSUNG, R. E. ELLIS and H. R. HORVITZ, 1996 Transcriptional regulator of programmed cell death encoded by *Caenorhabditis elegans* gene *ces-2*. Nature **382:** 545-547.

METZSTEIN, M. M., and H. R. HORVITZ, 1998 The *C. elegans* cell-death specification gene *ces-1* encodes a Snail-family zinc-finger protein. Mol. Cell **4:** 309-319.

METZSTEIN, M. M., G. M. STANFIELD and H. R. HORVITZ, 1998 Genetics of programmed cell death in *C. elegans*: Past, present and future. Trends Genet. **14:** 410-416.

MORGENBESSER, S. D., B. O. WILLIAMS, T. JACKS and R. A. DEPINHO, 1994 p53-dependent apoptosis produced by Rb-deficiency in the developing mouse lens. Nature **371:** 72-74.

MORONI, M. C., E. S. HICKMAN, E. L. DENCHI, G. CAPRARA, E. COLLI *et al.*, 2001 Apaf-1 is a transcriptional target for E2F and p53. Nat Cell Biol **3:** 552-558.

MULLER, H., A. P. BRACKEN, R. VERNELL, M. C. MORONI, F. CHRISTIANS *et al.*, 2001 E2Fs regulate the expression of genes involved in differentiation, development, proliferation, and apoptosis. Genes Dev **15:** 267-285.

PAGE, B. D., S. GUEDES, D. WARING and J. R. PRIESS, 2001 The *C. elegans* E2F- and DP-related proteins are required for embryonic asymmetry and negatively regulate Ras/MAPK signaling. Mol Cell **7:** 451-460.

PARRISH, J., L. LI, K. KLOTZ, D. LEDWICH, X. WANG *et al.*, 2001 Mitochondrial endonuclease G is important for apoptosis in *C. elegans*. Nature **412:** 90-94.

REDDIEN, P. W., S. CAMERON and H. R. HORVITZ, 2001 Phagocytosis promotes programmed cell death in *C. elegans*. Nature **412:** 198-202.

REDDY, K. C., and A. M. VILLENEUVE, 2004 *C. elegans* HIM-17 links chromatin modification and competence for initiation of meiotic recombination. Cell **118:** 439-452.

RIDDLE, D. L., T. BLUMENTHAL, B. J. MEYER and J. R. PRIESS (Editors), 1997 *C. elegans II*. Cold Spring Harbor Laboratory Press, Cold Spring Harbor, NY.

SAUNDERS, J., 1966 Death in embryonic systems. Science **154:** 604-612.

SCHUMACHER, B., K. HOFMANN, S. BOULTON and A. GARTNER, 2001 The *C. elegans* homolog of the p53 tumor suppressor is required for DNA damage-induced apoptosis. Curr Biol **11:** 1722-1727.

SHAHAM, S., and H. R. HORVITZ, 1996a An alternatively spliced *C. elegans ced-4* RNA encodes a novel cell death inhibitor. Cell **86:** 201-208.

SHAHAM, S., and H. R. HORVITZ, 1996b Developing *Caenorhabditis elegans* neurons may contain both cell-death protective and killer activities. Genes Dev. **10:** 578-591.

SHAHAM, S., P. W. REDDIEN, B. DAVIES and H. R. HORVITZ, 1999 Mutational analysis of the *Caenorhabditis elegans* cell-death gene *ced-3*. Genetics **153:** 1655-1671.

SHERR, C. J., and F. MCCORMICK, 2002 The RB and p53 pathways in cancer. Cancer Cell **2:** 103-112.

SOLARI, F., A. BATEMAN and J. AHRINGER, 1999 The *Caenorhabditis elegans* genes *egl-27* and *egr-1* are similar to MTA1, a member of a chromatin regulatory complex, and are redundantly required for embryonic patterning. Development **126:** 2483-2494.

SPECTOR, M. S., S. DESNOYERS, D. J. HOEPPNER and M. O. HENGARTNER, 1997 Interaction between the *C. elegans* cell-death regulators CED-9 and CED-4. Nature **385:** 653-656.

STANFIELD, G. M., and H. R. HORVITZ, 2000 The *ced-8* gene controls the timing of programmed cell deaths in *C. elegans*. Mol. Cell **5:** 423-433.

STERNBERG, P. W., and M. HAN, 1998 Genetics of RAS signaling in *C. elegans*. Trends Genet **14:** 466-472.

SULSTON, J. E., and H. R. HORVITZ, 1977 Post-embryonic cell lineages of the nematode, *Caenorhabditis elegans.* Dev. Biol. **56:** 110-156.

THELLMANN, M., J. HATZOLD and B. CONRADT, 2003 The Snail-like CES-1 protein of *C. elegans* can block the expression of the BH3-only cell-death activator gene *egl-1* by antagonizing the function of bHLH proteins. Development **130:** 4057-4071.

THOMAS, J. H., C. J. CEOL, H. T. SCHWARTZ and H. R. HORVITZ, 2003 New genes that interact with *lin-35* Rb to negatively regulate the *let-60 ras* pathway in *Caenorhabditis elegans*. Genetics **164:** 135-151.

TIMMONS, L., D. L. COURT and A. FIRE, 2001 Ingestion of bacterially expressed dsRNAs can produce specific and potent genetic interference in *Caenorhabditis elegans*. Gene **263:** 103-112.

UNHAVAITHAYA, Y., T. H. SHIN, N. MILIARAS, J. LEE, T. OYAMA *et al.*, 2002 MEP-1 and a homolog of the NURD complex component Mi-2 act together to maintain germline-soma distinctions in *C. elegans*. Cell **111:** 991-1002.

VON ZELEWSKY, T., F. PALLADINO, K. BRUNSCHWIG, H. TOBLER, A. HAJNAL *et al.*, 2000 The *C. elegans* Mi-2 chromatin-remodelling proteins function in vulval cell fate determination. Development **127:** 5277-5284.

WALHOUT, A. J., R. SORDELLA, X. LU, J. L. HARTLEY, G. F. TEMPLE *et al.*, 2000 Protein interaction mapping in *C. elegans* using proteins involved in vulval development. Science **287:** 116-122.

WANG, D., S. KENNEDY, D. CONTE, JR., J. K. KIM, H. W. GABEL *et al.*, 2005 Somatic misexpression of germline P granules and enhanced RNA interference in retinoblastoma pathway mutants. Nature **436:** 593-597.

WOLFE, S. A., L. NEKLUDOVA and C. O. PABO, 2000 DNA recognition by Cys2His2 zinc finger proteins. Annu Rev Biophys Biomol Struct **29:** 183-212.

WU, D., H. D. WALLEN, N. INOHARA and G. NUNEZ, 1997 Interaction of the *Caenorhabditis elegans* death protease CED-3 by CED-4 and CED-9. J. Biol. Chem. **272:** 21449-21454.

XUE, Y., J. WONG, G. T. MORENO, M. K. YOUNG, J. COTE *et al.*, 1998 NURD, a novel complex with both ATP-dependent chromatin-remodeling and histone deacetylase activities. Mol. Cell **2:** 851-861.

YAMASAKI, L., T. JACKS, R. BRONSON, E. GOILLOT, E. HARLOW *et al.*, 1996 Tumor induction and tissue atrophy in mice lacking E2F-1. Cell **85:** 537-548.

YAN, N., J. CHAI, E. S. LEE, L. GU, Q. LIU *et al.*, 2005 Structure of the CED-4-CED-9 complex provides insights into programmed cell death in *Caenorhabditis elegans*. Nature **437:** 831-837.

YANG, X., H. Y. CHANG and D. BALTIMORE, 1998 Essential role of CED-4 oligomerization in CED-3 activation and apoptosis. Science **281:** 1355-1357.

YUAN, J., and H. R. HORVITZ, 1992 The *Caenorhabditis elegans* cell death gene *ced-4* encodes a novel protein and is expressed during the period of extensive programmed cell death. Development **116:** 309-320.

YUAN, J., S. SHAHAM, S. LEDOUX, H. M. ELLIS and H. R. HORVITZ, 1993 The *C. elegans* cell death gene *ced-3* encodes a protein similar to mammalian interleukin-1 beta-converting enzyme. Cell **75:** 641-652.

ZHOU, Z., E. HARTWIEG and H. R. HORVITZ, 2001 CED-1 Is a transmembrane receptor that mediates cell corpse engulfment in *C. elegans*. Cell **104:** 43-56.

ZOU, H., W. J. HENZEL, X. LIU, A. LUTSCHG and X. WANG, 1997 Apaf-1, a human protein homologous to *C. elegans* CED-4, participates in cytochrome c-dependent activation of caspase-3. Cell **90:** 405-413.

Table 1. *n3376* and *n3380* affect many programmed cell deaths and are mutations in *Y51H1A.6* and *dpl-1,* respectively

genotype	Number extra cells (anterior pharynx)[a]
wild-type	0.1 ± 0.1 (n=20)
ced-3(n2452)	11.0 ± 0.4 (n=20)
ced-3(n2427)[b]	1.8 ± 0.2 (n=40)
dpl-1(n3380); ced-3(n2427)[b]	6.1 ± 0.4 (n=20)
mcd-1(n3376); ced-3(n2427)[b]	5.9 ± 0.4 (n=20)
dpl-1(n3380)[b]	0.2 ± 0.1 (n=20)
mcd-1(n3376)[b]	0.6 ± 0.2 (n=30)
dpl-1(n2994); ced-3(n2427)[b]	6.1 ± 0.4 (n=20)
dpl-1(n3316 (M+)*); ced-3(n2427)*[b, c, d]	3.7 ± 0.7 (n=9)
dpl-1(n3316 (M*n3316/n3380*)*); ced-3(n2427)*[b, c, e]	7.3 ± 0.7 (n=10)
Y51H1A.6(RNAi); ced-3(n2427)[b]	6.3 ± 0.5 (n=15)
mcd-1(n4005)[b]	1.0 ± 0.2 (n=20)
mcd-1(n4005); ced-3(n2427)	5.9 ± 0.3 (n=40)
mcd-1(n3376/n4005); ced-3(n2427)[b]	6.5 ± 0.7 (n=6)

[a] the number of extra cells in the anterior pharynx of L3 larvae were determined using Nomarski optics (Hengartner et al. 1992; Shaham et al. 1999). In the wild type, 16 cells undergo programmed cell death in this region. Data are means ± standard errors of the means.

[b] this strain was also homozygous for *nIs106.*

[c] this strain was also homozygous for *dpy-10(e128).*

[d] (M+) indicates that the parental genotype of these animals was heterozygous for the mutation.

[e] (M*n3316/n3380*) indicates the parental genotype of these *n3316/n3316* animals was *n3316/n3380*.

Table 2. *efl-1* E2F and *lin-35* Rb promote cell death	
Genotype	**No. Extra Cells (anterior pharynx)[a]**
A. Loss of function of *efl-1*, *lin-35*, *lin-37*, and *lin-52* decreases cell death	
ced-3(n2427)[b]	1.8 ± 0.2 (n=40)
ced-3(n2427); efl-1(RNAi)[b]	4.8 ± 0.3 (n=30)
lin-35(n745); ced-3(n2427)[b, c]	5.1 ± 0.4 (n=20)
lin-37(n758); ced-3(n2427)[b]	5.5 ± 0.5 (n=15)
lin-52(n771); ced-3(n2427)[b, d]	4.5 ± 0.3 (n=35)
B. Loss of function of many synMuv genes and putative NuRD complex-encoding genes does not perturb cell death	
ced-3(n2427)[b]	1.8 ± 0.2 (n=40)
lin-8(n111); lin-9(n112); ced-3(n2427)[b]	1.3 ± 0.3 (n=20)
ced-3(n2427); lin-15(n767)[e]	1.6 ± 0.3 (n=20)
lin-38(n751); lin-9(n112); ced-3(n2427)[b, f]	2.3 ± 0.3 (n=14)
lin-56(2728); ced-3(n2427); lin-15(n744)	1.8 ± 0.2 (n=20)
lin-8(n111); lin-36(n766); ced-3(n2427)[b, d]	1.1 ± 0.3 (n=20)
lin-53(n833); ced-3(n2427)[g, h]	2.7 ± 0.4 (n=20)
hda-1(e1795 M+*); ced-3(n2427)*[b, i]	2.0 ± 0.4 (n=20)
ced-3(n2427); let-418(s1617 M+*)*[b, i, j]	1.5 ± 0.3 (n=29)
ced-3(n2427); chd-3(eh4)	2.3 ± 0.4 (n=20)
ced-3(n2427); lin-40(s1593 M+*)*[b, i, j]	0.7 ± 0.2 (n=15)
egl-27(n170); ced-3(n2427)[b, k]	1.0 ± 0.2 (n=20)

[a]the number of extra cells were determined as described in Table 1.

[b] this strain was also homozygous for *nIs106.*

[c] this strain was also homozygous for *unc-13(e1091).*

[d] this strain was also homozygous for *unc-32(e189).*

[e] this strain was also homozygous for *lin-61(n3446).*

[f] this strain was also homozygous for *unc-52(e444).*

[g] this strain was also homozygous for *dpy-5(e61).*

[h] this strain was also heterozygous for *nIs106.*

[i] (M+) is described in Table 1.

[j] this strain was also homozygous for *unc-46(e177).*

[k] this strain was also homozygous for *unc-4(e120).*

Table 3. *dpl-1* DP, *mcd-1*, *efl-1* E2F, and *lin-35* Rb define a new class of cell-death promoting genes that act together and that do not inhibit *ced-9* or act together with *ced-1* or *ced-8*

Genotype	Number extra cells (anterior pharynx)[a]
A. Mutations that enhance cell death defects caused by *ced-3(n2427)*	
ced-3(n2427)[b]	1.8 ± 0.2 (n=40)
dpl-1(n3380); ced-3(n2427)[b]	6.1 ± 0.4 (n=20)
mcd-1(n3376); ced-3(n2427)[b]	5.9 ± 0.4 (n=20)
mcd-1(n4005); ced-3(n2427)[b]	5.9 ± 0.3 (n=40)
efl-1(RNAi); ced-3(n2427)[b, c]	4.9 ± 0.5 (n=20)
lin-35(n745); ced-3(n2427)[b, d]	5.1 ± 0.4 (n=20)
ced-1(e1735); ced-3(n2427)[b]	5.9 ± 0.4 (n=30)
ced-3(n2427); ced-8(n1891)	5.7 ± 0.3 (n=45)
ced-9(n2812); ced-3(n2427)[e]	6.3 ± 0.5 (n=30)
B. Combinations of mutations that do not cause additive defects	
dpl-1(n3380) mcd-1(n3376); ced-3(n2427)[b, f, g]	5.9 ± 0.2 (n=67)
dpl-1(n3380) mcd-1(n4005); ced-3(n2427)[b, f]	5.4 ± 0.3 (n=25)
dpl-1(n3380); efl-1(RNAi); ced-3(n2427)[b, c]	6.6 ± 0.4 (n=20)
mcd-1(n3376); efl-1(RNAi); ced-3(n2427)[b, c]	6.2 ± 0.4 (n=20)
lin-35(n745); dpl-1(n3380); ced-3(n2427)[b, d]	6.5 ± 0.4 (n=20)
lin-35(n745); mcd-1(n3376); ced-3(n2427)[b]	6.4 ± 0.4 (n=20)
C. Combinations of mutations that cause additive defects	
ced-1(e1735); dpl-1(n3380); ced-3(n2427)[b, f]	9.6 ± 0.3 (n=20)
ced-1(e1735); mcd-1(n3376); ced-3(n2427)[b]	8.8 ± 0.3 (n=40)
dpl-1(n3380); ced-3(n2427); ced-8(n1891)	8.5 ± 0.4 (n=25)
mcd-1(n3376); ced-3(n2427); ced-8(n1891)	9.0 ± 0.5 (n=20)
dpl-1(n3380); ced-9(n2812); ced-3(n2427)[b]	10.6 ± 0.3 (n=45)
mcd-1(n3376); ced-9(n2812); ced-3(n2427)[b, e]	9.4 ± 0.4 (n=45)

[a]the number of extra cells were determined as described in Table 1.

[b] this strain was also homozygous for *nIs106.*

[c] the gene *efl-2* was also inhibited by RNAi in this strain. Because two *E2F*-like genes have been identified in *C. elegans* (Ceol and Horvitz 2001) it is possible that *efl-1* and *efl-2* act partially redundantly for some processes; we therefore inhibited both genes.

[d] this strain was also homozygous for *unc-13(e1091).*

[e] this strain was also homozygous for *unc-30(e191)*.

[f] this strain was also homozygous for *unc-4(e120).*

[g] this strain was also homozygous for *rol-1(e91).*

Table 4. *mcd-1(n3376)* and *dpl-1(n3380)* suppress *ced-4(n2273) ced-9(n1653)* and *ced-9(n1950 n2161)* maternal-effect lethality

Maternal genotype	Genotype[a]	Number of viable progeny (n)[b]
ced-4(n2273) ced-9(n1653)/qC1	*ced-4(n2273) ced-9(n1653)*	0 (many)
mcd-1(n3376); ced-4(n2273) ced-9(n1653)/qC1	*mcd-1(n3376); ced-4(n2273) ced-9(n1653)*	4.9 ± 3.1 (n=20)
dpl-1(n3380); ced-4(n2273) ced-9(n1653)/qC1	*dpl-1(n3380); ced-4(n2273) ced-9(n1653)*	18.5 ± 12.1 (n=15)
		Number of hatched progeny (n)[c]
unc-69(e587) ced-9(n1950 n2161)/qC1	*unc-69(e587) ced-9(n1950 n2161)*	0.0 ± 0.0 (n=6)
dpl-1(3380); unc-69(e587) ced-9(n1950 n2161)/qC1	*dpl-1(3380); unc-69(e587) ced-9(n1950 n2161)*	29.4 ± 14.0 (n=12)
mcd-1(n4005); unc-69(e587) ced-9(n1950 n2161)/qC1	*mcd-1(n4005); unc-69(e587) ced-9(n1950 n2161)*	18.1 ± 11.0 (n=12)

All animals were homozygous for *nIs106*.

[a] *ced-4(n2273) ced-9(n1653)/ced-4(n2273) ced-9(n1653)* animals were recognized by the fact that they had extra VC-like cells in the ventral cord (data not shown). Animals with four or five extra VC-like cells were picked as *ced-4(n2273) ced-9(n1653)/ced-4(n2273) ced-9(n1653)* animals. *unc-69(e587) ced-9(n1950 n2161)* homozygous animals were recognized by their Unc-69 phenotype. The *dpl-1(n3380); unc-69(e587) ced-9(n1950 n2161)/qC1* strain was also homozygous for *unc-30(e191)*.

[b] The number of progeny were determined by counting larval stage 3 (L3) or older animals on plates four days after young adults were placed onto petri plates. Data are means ± standard deviation.

[c] *dpl-1(3380); unc-69(e587) ced-9(n1950 n2161)* and *mcd-1(n4005); unc-69(e587) ced-9(n1950 n2161)* animals arrested as larvae approximately the size of L1 larvae. We therefore quantified the number of larvae present. Data are means ± standard deviations.

Table 5. *mcd-1* loss-of-function causes synthetic lethality with some class B synMuv mutations	
Genotype	**Growth phenotype[a]**
A. Some class B and C synMuv mutations cause synthetic growth and viability defects with *mcd-1(n4005)*	
mcd-1(n4005)	viable[b]
lin-53(n833); mcd-1(n4005)[d]	slow growth[e]
mcd-1(n4005); lin-13(n770)	slow growth[e]
mcd-1(n4005); lin-54(n2231)	slow growth[e]
dpl-1(n3380) mcd-1(n4005)[f]	slow growth[e, g]
mcd-1(n4005); lin-9(n112)	L1 arrest[h]
lin-35(n745); mcd-1(n4005)	L1 arrest[h]
mcd-1(n4005); lin-37(n758)	L1 arrest[i]
mcd-1(n4005); mys-1(n3681)	slow growth[e]
B. Some class B synMuv mutations do not cause synthetic lethality with *mcd-1(n4005)*	
mcd-1(n4005); lin-36(n766)	viable
mcd-1(n4005); lin-52(n771)	viable
mcd-1(n4005); tam-1(cc567)[c]	viable
C. Class A synMuv mutations do not cause synthetic lethality with *mcd-1(n4005)*	
lin-8(n2731) mcd-1(n4005)	viable
mcd-1(n4005); lin-15A(n767)	viable
lin-38(n751) mcd-1(n4005)	viable
lin-56(n2728) mcd-1(n4005)	viable

[a] The growth phenotype was assayed at 20ºC and 25ºC by picking L4 larvae and quantifying the time until greater than 50% of the next generation reached the L4 larval stage.

[b] Viable strains can be maintained and have a growth phenotype of between 3 and 3.5 days.

[c] strain also contained *unc-46(e177)*

[d] strain also contained *dpy-5(e61)*

[e] The development of this strain was delayed two days as compared to the *mcd-1* single mutant strain or the respective class B synMuv mutant strain at 20ºC.

[f] strain also contains *unc-4(e120)*

[g] *dpl-1(n3380) unc-4 mcd-1(n4005)* animals were homozygous viable and slow-growing at 20ºC. At 25ºC the strain could not be maintained after 24 days with infertile adults, sick slow-growing larvae and some arrested larvae.

[h] 100% of the animals arrested as larvae in size similar to L1 larvae, whereas the *mcd-1* single mutant and the respective class B synMuv mutant strains do not.

[i] At 20ºC animals were either small, infertile Muv adults, sick slow-growing larvae, or arrested larvae. At 22.5ºC and 25ºC, 100% of the animals arrested as larvae in size similar to L1 larvae.

FIGURE DESCRIPTIONS

Figure 1: The *mcd-1* Zn finger and *dpl-1* DP genes were identified as cell death-promoting genes from a genetic screen

(A) Ventral cord cell lineage diagrams. W, W blast cell. P, P blast cell. Arrow, cell that fails to die and that expresses P_{lin-11} *gfp*. In the wild type, P3-8.aap (a, anterior daughter; p, posterior daughter) survive and express P_{lin-11} *gfp*. W.ap, P1-2.aap, and P9-12.aap normally die (SULSTON and HORVITZ 1977). In *ced-3(lf)* animals, no cell death occurs and W.ap, P1-2.aap, and P9-12.aap survive and express P_{lin-11} *gfp* (REDDIEN *et al.* 2001). The large green midbody region reflects GFP expression in the vulva from the *lin-11* promoter.

(B) Schematic of the *ced-3(n2427)* enhancer screen (see Materials and methods for details).

(C) Results from the *ced-3* enhancer screen. From approximately 13,000 mutagenized haploid genomes, 37 mutations were isolated.

(D, E) Distribution of percentages of animals with 0-5 extra cells in the ventral cord. The five cells P2.aap and P9-12.aap were scored using the assay described in Figure 1. At least 50 young adult animals of each genotype were scored. *nIs106,* P_{lin-11} *gfp* reporter (REDDIEN *et al.* 2001).

(F) *n3380* is located in the region on LGII between the genes *rol-6* and *unc-4*. *n3376* is located between two polymorphisms, *nP89* and *nP91*, on LGII, a region of approximately 75 kilobases. See Materials and methods for details.

(G) Protein structure of DPL-1 DP. The blue box indicates the putative DNA binding region of DPL-1 and the yellow box the putative E2F binding region, as previously described (CEOL and HORVITZ 2001). The *n3316* mutation is a deletion following the third codon, and *n2994* is a splice-site mutation predicted to alter protein structure following amino acid 227 (CEOL and HORVITZ 2001). *n3380* is a C-to-T nonsense mutation that at Q486.

(H) The gene *Y51H1A.6* is *mcd-1* (see text for details). The 5' end carries a SL1 *trans*-spliced leader sequence (see text), and the 3'UTR is approximately 750 bp.

We isolated a deletion allele, *n4005*, that removes part of intron two and part of exon three of *Y51H1A.6* (see Materials and methods). The red line labeled "Zn" depicts the zinc finger-encoding region of *mcd-1*. The MCD-1 zinc-finger region amino acid sequence is shown below the gene structure diagram. Red stars indicate the residues that define the C2H2 domain, and blue stars indicate other residues conserved with the canonical C2H2 zinc finger. *n3376* is a C-to-T mutation resulting in an H277Y substitution in the MCD-1 protein and is indicated by a red arrowhead.

Figure 1

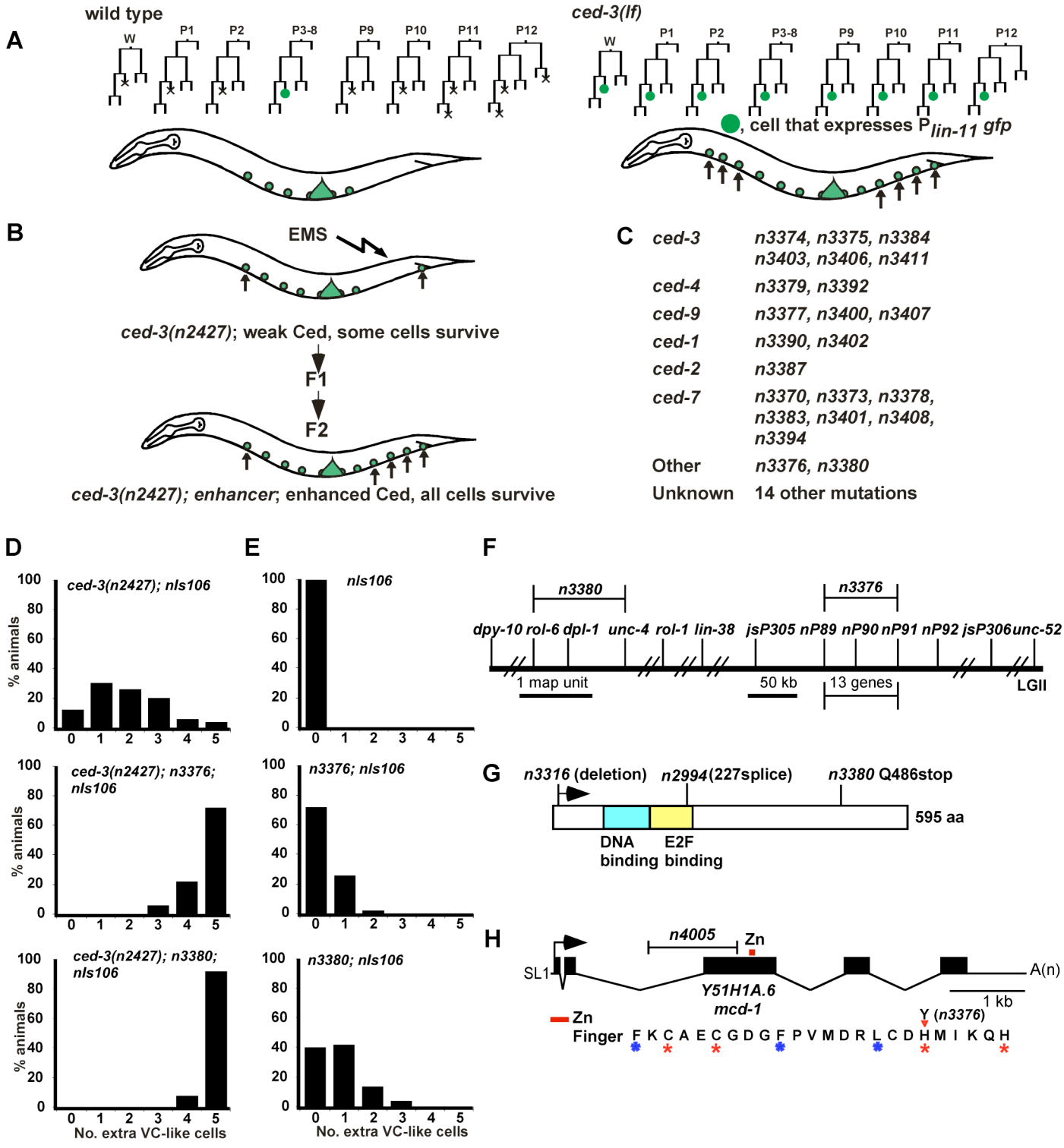
A
wild type
ced-3(lf)
W
P1
P2
P3-8
P9
P10
P11
P12
, cell that expresses P lin-11 gfp
B
EMS
ced-3(n2427); weak Ced, some cells survive
F1
F2
ced-3(n2427); enhancer; enhanced Ced, all cells survive
C
ced-3 n3374, n3375, n3384 n3403, n3406, n3411
ced-4 n3379, n3392
ced-9 n3377, n3400, n3407
ced-1 n3390, n3402
ced-2 n3387
ced-7 n3370, n3373, n3378, n3383, n3401, n3408, n3394
Other n3376, n3380
Unknown 14 other mutations
D
ced-3(n2427); nls106
ced-3(n2427); n3376; nls106
ced-3(n2427); n3380; nls106
% animals
No. extra VC-like cells
E
nls106
n3376; nls106
n3380; nls106
No. extra VC-like cells
F
n3380
n3376
dpy-10 rol-6 dpl-1 unc-4 rol-1 lin-38 jsP305 nP89 nP90 nP91 nP92 jsP306 unc-52
1 map unit
50 kb
13 genes
LGII
G
n3316 (deletion)
n2994 (227splice)
n3380 Q486stop
595 aa
DNA binding
E2F binding
H
n4005
Zn
SL1
A(n)
Y51H1A.6
mcd-1
1 kb
Zn Finger
Y (n3376)
F K C A E C G D G F P V M D R L C D H M I K Q H

Figure 2: Abnormalities in the cell-death process in *dpl-1(n3380)* and *mcd-1(n4005)* animals

(A) P9.aap in a *dpl-1(n3380); nIs106* animal was condensed 2 hours 10 minutes after its generation. By 4 hours 10 minutes after its generation, P9.aap had recovered and appeared morphologically normal. 36 hours later, P9.aap expressed $P_{lin\text{-}11}gfp$. P9.aap is indicated by an arrow. Anterior, left. Posterior, right. Dorsal, top. Ventral, down. In the 4 hour 10 minute image anterior is right and posterior is left.

(B) P11.aap in an *mcd-1(n4005); nIs106* animal condensed 3 hours 22 minutes after its generation. This cell had first displayed attributes of a dying cell one hour 35 minutes after its generation. 3 hours 27 minutes after generation P11.aap recovered, and P11.aaap had normal nuclear morphology. 3 hours 42 minutes after generation, P11.aap condensed, and P11.aaap was condensed as well. 3 hours 47 minutes after generation, P11.aap recovered. P11.aap was observed until 5 hours 25 minutes after generation without any further obvious attempts at death. 36 hours later, no GFP fluorescence was detected in the P11 region, indicating this cell either failed to express *lin-11* or ultimately died. P11.aap is indicated by a black arrow and P11.aaap is indicated by a red arrow. Anterior, left. Posterior, right. Dorsal, down. Ventral, top.

(C) Model for the effects of *dpl-1* and *mcd-1* on cell killing. Top, in a cell specified to die in wild-type animals, the CED-3 caspase is activated and the MCD-1 Zn finger, DPL-1 DP, LIN-35 Rb, EFL-1 E2F, LIN-37 Mip40, and LIN-52 dLin52 proteins mediate transcriptional regulation of unknown targets to allow cell death to occur. Middle, in the absence of the CED-3 caspase, cells fail to display the morphological alterations characteristic of cell death. In the absence of *mcd-1* or *dpl-1*, CED-3 is still activated and initiates the cell-death process. The execution of cell death occasionally fails, and cells can survive and differentiate.

(D) Multiple activities function independently and additively to promote cell death.

The MCD-1 Zn finger, DPL-1 DP, LIN-35 Rb, EFL-1 E2F, LIN-37 Mip40, and LIN-52 dLin52 proteins define a transcriptional regulatory activity that promotes cell death. This activity functions in an additive manner with the cell-killing activity of the CED-9 Bcl-2 and CED-8 XK proteins, as well as with the genes that control the process of engulfment to promote cell death. Multiple other activities could exist and act in a similar additive manner to control cell-death execution.

Figure 2

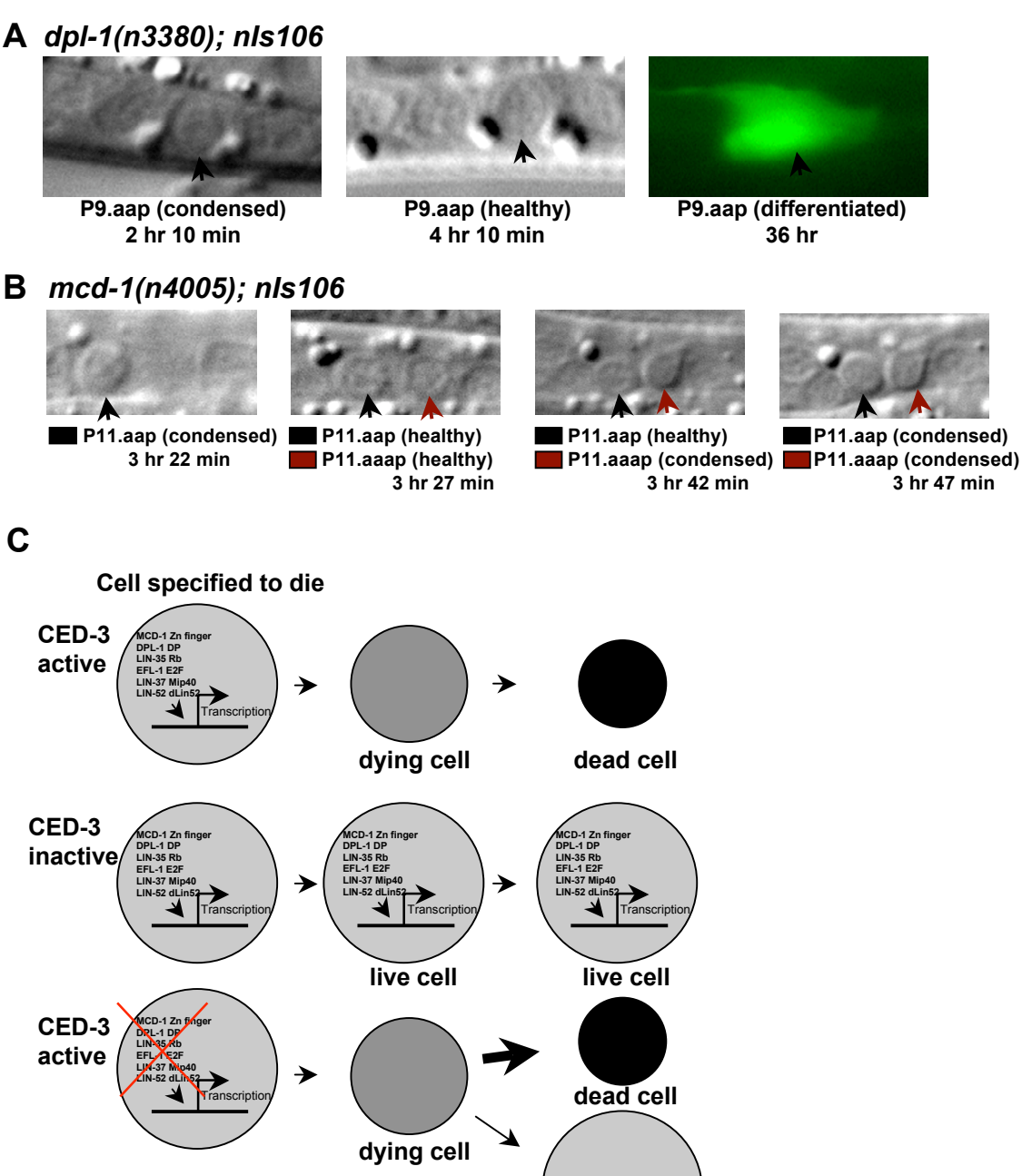
A dpl-1(n3380); nls106
P9.aap (condensed)
2 hr 10 min
P9.aap (healthy)
4 hr 10 min
P9.aap (differentiated)
36 hr
B mcd-1(n4005); nls106
P11.aap (condensed)
3 hr 22 min
P11.aap (healthy)
P11.aaap (healthy)
3 hr 27 min
P11.aap (healthy)
P11.aaap (condensed)
3 hr 42 min
P11.aap (condensed)
P11.aaap (condensed)
3 hr 47 min
C
Cell specified to die
CED-3 active
MCD-1 Zn finger
DPL-1 DP
LIN-35 Rb
EFL-1 E2F
LIN-37 Mip40
LIN-52 dLin52
Transcription
dying cell
dead cell
CED-3 inactive
live cell
live cell
CED-3 active
dead cell
dying cell
live cell
D
MCD-1 Zn finger
DPL-1 DP
LIN-35 Rb
EFL-1 E2F
LIN-37 Mip40
LIN-52 dLin52
CED-9 Bcl-2 (killing function)
CED-8 XK
engulfment
others?
programmed cell death

Table S1. Cell-death defects conferred by *ced-3(n2427)* do not vary substantially with genetic background

genotype	No. Extra Cells (anterior pharynx)[a]
wild type	0.1 ± 0.0
ced-3(n2427)[b]	1.8 ± 0.2
unc-29; ced-3(n2427)	1.7 ± 0.2
unc-16 unc-50; ced-3(n2427)[b]	1.6 ± 0.4
dpy-17 unc-32; ced-3(n2427)[b]	1.1 ± 0.3
dpy-20 ced-3(n2427)	1.9 ± 0.4
unc-79 dpy-17; ced-3(n2427)	1.0 ± 0.3
unc-30 ced-3(n2427); dpy-11; unc-20[b]	1.7 ± 0.4
unc-30 ced-3(n2427) dpy-4[b]	2.1 ± 0.3
dpy-5 unc-75; ced-3(n2427)[b]	1.2 ± 0.3
dpy-5; rol-6; unc-32; ced-3(n2427)[b]	1.3 ± 0.3

[a]the number of extra cells in the anterior pharynx of L3 larvae were determined using Nomarski optics. In the wild type 16 cells undergo programmed cell death in this region. At least 15 animals were scored of each genotype. Data are means ± standard error of the means.

[b] this strain was also homozygous for *nIs106.*

Table S2. Supplemental supporting data for Table 3.	
Genotype	**Number extra cells (anterior pharynx)[a]**
A. Single cell-death mutants alone or in combination with *ced-3(n2427)*	
ced-3(n2427)[b]	1.8 ± 0.2 (n=40)
dpl-1(n3380)[b]	0.2 ± 0.1 (n=20)
mcd-1(n3376)[b]	0.6 ± 0.2 (n=30)
mcd-1(n4005)[b]	1.0 ± 0.2 (n=20)
ced-8(n1891)	1.1 ± 0.2 (n=30)
mcd-1(n3376); ced-3(n2427)[b]	5.9 ± 0.4 (n=20)
mcd-1(n4005); ced-3(n2427)[b]	5.9 ± 0.3 (n=40)
lin-35(n745); ced-3(n2427)[b, c]	5.1 ± 0.4 (n=20)
ced-1(e1735); ced-3(n2427)[b]	5.9 ± 0.4 (n=30)
ced-9(n2812); ced-3(n2427)[d]	6.3 ± 0.5 (n=30)
B. Combinations of mutations that do not cause additive defects	
dpl-1(n3380) mcd-1(n3376)[b, d, e, f]	0.8 ± 0.1 (n=20)
dpl-1(n3380) mcd-1(n4005)[b, e]	0.6 ± 0.2 (n=20)
lin-35(RNAi); mcd-1(n3376); ced-3(n2427)[b]	5.7 ± 0.7 (n=15)
lin-35(n2242); mcd-1(n3376); ced-3(n2427)[b]	5.7 ± 0.5 (n=20)
C. Combinations of mutations that cause additive defects	
dpl-1(n3380); ced-8(n1891)	2.5 ± 0.4 (n=20)
mcd-1(n3376); ced-8(n1891)	2.4 ± 0.3 (n=20)
ced-1(e1735); mcd-1(n4005); ced-3(n2427)[b]	9.8 ± 0.5 (n=20)
ced-1(e1735) lin-35(n745); ced-3(n2427)[b, c]	8.7 ± 0.5 (n=20)
mcd-1(n4005); ced-9(n2812); ced-3(n2427)[b, g]	8.9 ± 0.4 (n=25)

[a]the number of extra cells were determined as described in Table 1.

[b] this strain was also homozygous for *nIs106.*

[c] this strain was also homozygous for *unc-13(e1091).*

[d] this strain was also homozygous for *unc-30(e191)*.

[e] this strain was also homozygous for *unc-4(e120).*

[f] this strain was also homozygous for *rol-1(e91).*

[g] this strain was also homozygous for *dpy-17(e164)*.

Figure S1

Y51H1A.6 predicted protein sequence, as determined from the *Y51H1A.6* cDNA sequence described in Fig. 3. The black box indicates the putative Zn finger domain of Y51H1A.6. Red stars indicate the residues that define the C2H2 domain, and blue stars indicate other residues conserved with the canonical C2H2 zinc finger (Wolfe et al. 2000). *n3376* is a C-to-T mutation resulting in a H277Y substitution in the Y51H1A.6 protein and is indicated by a red arrowhead.

Figure S1

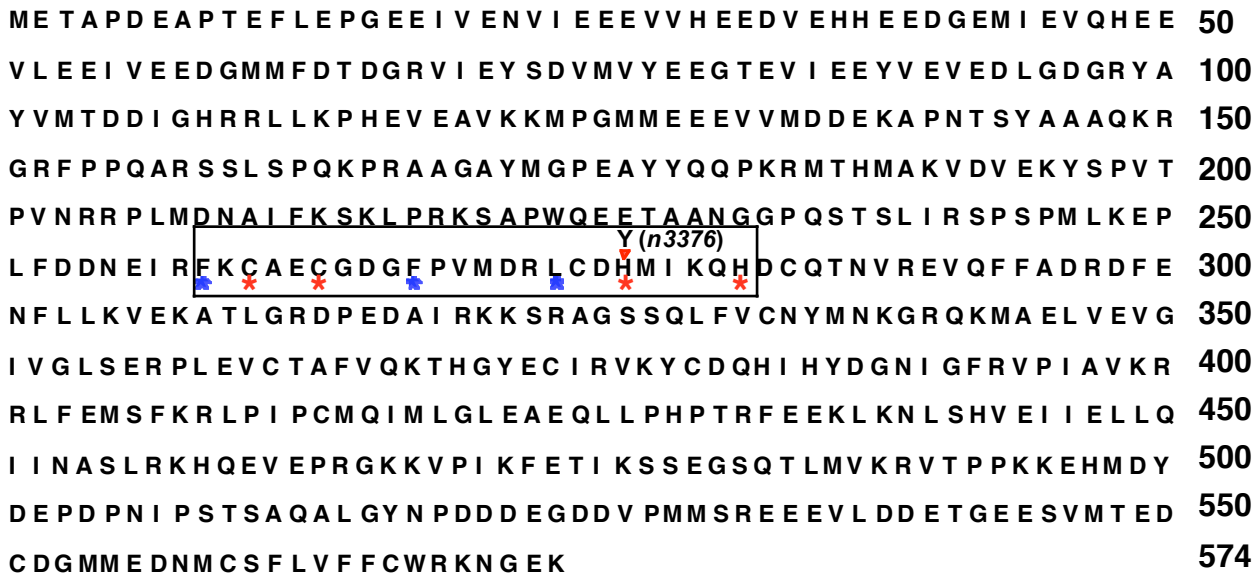
ME TA PD EA PT EF LE PG EE I V EN V I EE EV V H EE DV EH H E E D G EM I EV Q H E E 50
V L E E I V E E D G M M F D T D G R V I EY S D V M V Y E E G T E V I E E Y V E V E D L G D G R Y A 100
Y V M T D D I G H R R L L K P H E V E A V K K M P G M M E E E V V M D D E K A P N T S Y A A A Q K R 150
G R F P P Q A R S S L S P Q K P R A A G A Y M G P E A Y Y Q Q P K R M T H M A K V D V E K Y S P V T 200
P V N R R P L M D N A I F K S K L P R K S A P W Q E E T A A N G G P Q S T S L I R S P S P M L K E P 250
Y (n3376)
L F D D N E I R F K C A E C G D G F P V M D R L C D H M I K Q H D C Q T N V R E V Q F F A D R D F E 300
N F L L K V E K A T L G R D P E D A I R K K S R A G S S Q L F V C N Y M N K G R Q K M A E L V E V G 350
I V G L S E R P L E V C T A F V Q K T H G Y E C I R V K Y C D Q H I H Y D G N I G F R V P I A V K R 400
R L F E M S F K R L P I P C M Q I M L G L E A E Q L L P H P T R F E E K L K N L S H V E I I E L L Q 450
I I N A S L R K H Q E V E P R G K K V P I K F E T I K S S E G S Q T L M V K R V T P P K K E H M D Y 500
D E P D P N I P S T S A Q A L G Y N P D D D E G D D V P M M S R E E E V L D D E T G E E S V M T E D 550
C D G M M E D N M C S F L V F F C W R K N G E K 574

Figure S2

Supplemental ventral cord cell-death data.

(A-F) Distribution of percentages of animals with 0-5 extra cells in the ventral cord. The five cells P2.aap and P9-12.aap were scored using the assay described in Fig. 1. At least 50 young adult animals of each genotype were scored. *nIs96* and *nIs106,* $P_{lin\text{-}11}$ *gfp* reporters (Reddien et al. 2001).

(A) *mcd-1(n3376)* and *dpl-1(n3380)* enhance a second allele (*n2447*) of *ced-3.*

(B-D) Some class B synMuv mutations enhance cell-death defects conferred by *ced-3(n2427)*.

(E) A mutation in *let-60 ras* fails to suppress the cell-death defect caused by *dpl-1(n3380).*

(F) *ced-1(e1735)* causes a partially additive defect in cell death with *n3376* and *n3380*.

Figure S2

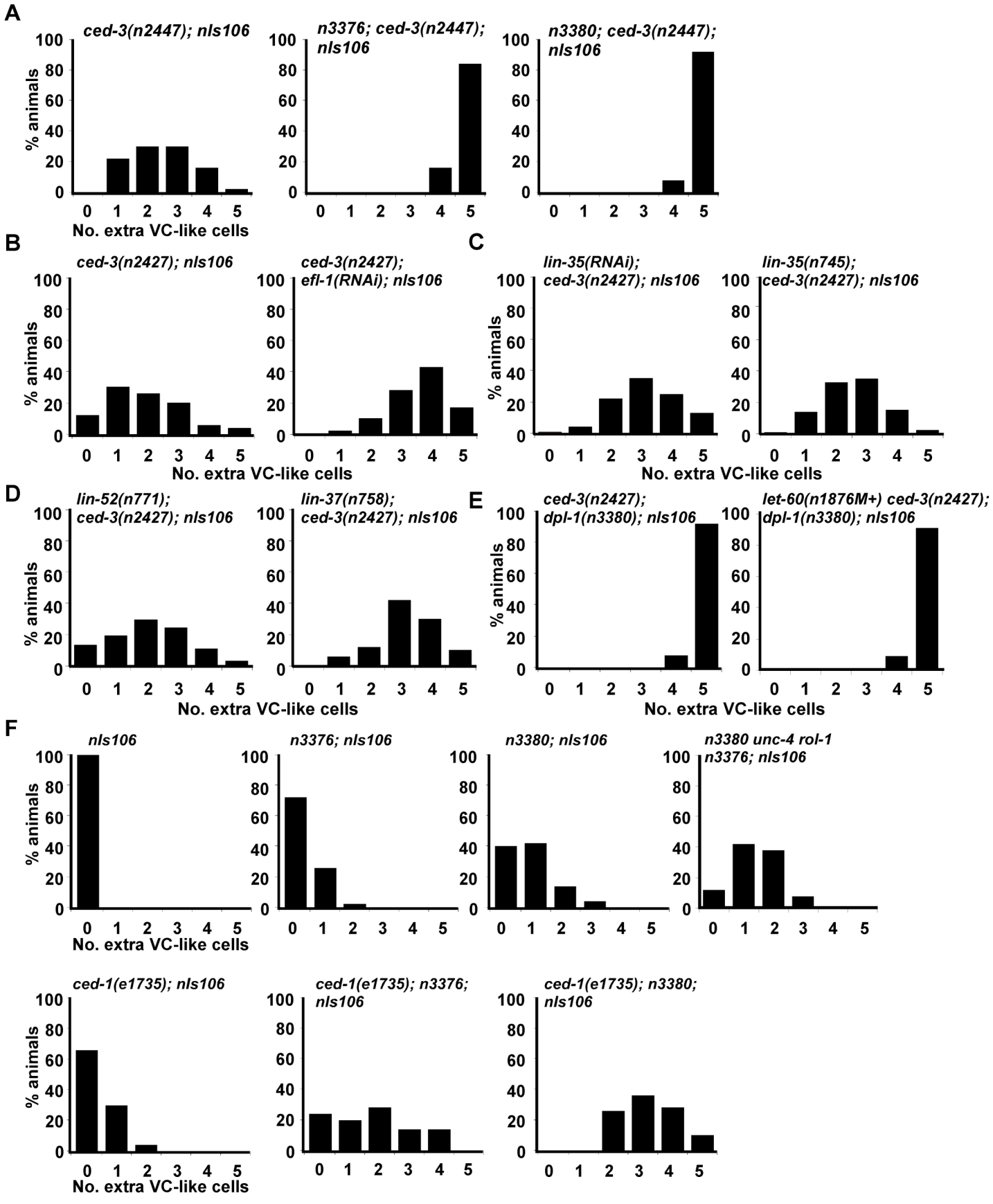
A
ced-3(n2447); nls106
n3376; ced-3(n2447); nls106
n3380; ced-3(n2447); nls106
B
ced-3(n2427); nls106
ced-3(n2427); efl-1(RNAi); nls106
C
lin-35(RNAi); ced-3(n2427); nls106
lin-35(n745); ced-3(n2427); nls106
D
lin-52(n771); ced-3(n2427); nls106
lin-37(n758); ced-3(n2427); nls106
E
ced-3(n2427); dpl-1(n3380); nls106
let-60(n1876M+) ced-3(n2427); dpl-1(n3380); nls106
F
nls106
n3376; nls106
n3380; nls106
n3380 unc-4 rol-1 n3376; nls106
ced-1(e1735); nls106
ced-1(e1735); n3376; nls106
ced-1(e1735); n3380; nls106
% animals
No. extra VC-like cells

CHAPTER SIX ADDENDUM

During strain constructions to make a *mcd-1; lin-36* double mutant, we found that the deletion allele *mcd-1(n4005)* caused a class A synMuv phenotype. Subsequently, we combined *mcd-1(n4005)* and an independently isolated deletion allele, *mcd-1(n4140)*, with mutations in class A and B synMuv genes (Addendum Table 1). We found neither *mcd-1* single mutant had a Muv phenotype at any temperature. However, when *mcd-1(n4005)* was combined with mutations in class A and B synMuv genes, a Muv phenotype was observed. *mcd-1(n4005)* did not cause a Muv phenotype when combined with the class A null mutations *lin-8(n2731)* and *lin-56(n2728)* but did when combined with *lin-15A(n767)* and *lin-38(n751)*. The synMuv phenotype with the class A mutation *lin-15A(n767)* was also observed after RNAi of *lin-15A* (data not shown), suggesting the phenotype is caused by a loss of *lin-15A* function. The phenotypes of class AA double mutants with *mcd-1* are less penetrant than those of class AA double mutants without *mcd-1* (Chapter Three). The analyses of redundancy within the class A synMuv genes (Chapter Three) should be performed on *mcd-1* to characterize the class A function of *mcd-1*. We also combined *mcd-1(n4005)* with strong or null class B synMuv mutations. *mcd-1(n4005)* caused a synMuv defect in all double mutant combinations with class B genes, indicating that *mcd-1* might be a new class A synMuv gene.

Howerver, RNAi of *mcd-1* did not cause a synMuv phenotype in class A or B mutant strains (data not shown). Additionally, rescue experiments using clones containing the entire *mcd-1* coding region or heterologous expression constructs (like *dpy-7* and *lin-31*) could not rescue the synMuv phenotype of *mcd-1(n4005); lin-36(n766)*. Therefore, we were concerned that *mcd-1(n4005)* and *mcd-1(n4140)* might not cause a loss of *mcd-1* function. The two deletion alleles remove the beginning of exon three and might be bypassed by splicing, as splice acceptor sites are present just 3' to the end of the two deletion alleles (data not shown). RNAi of *mcd-1* caused the synMuv phenotype of *mcd-1(n4005); lin-*

52(n771) to decrease from 89% (n=101) to 46% (n=46) at 25ºC. Analyses of definitive *mcd-1* null alleles and rescue experiments should define the role of *mcd-1* in the inhibition of vulval cell fates.

Addendum Table 1: *mcd-1(n4005)* causes a class A synMuv phenotype

genotype[a]	% multivulva (n)[b] 20°C	22.5°C	25°C
+	0 (147)	0 (534)	0 (478)
lin-8(n2731)	0 (143)	0 (172)	1 (194)
lin-15A(n767)	0 (213)	1 (248)	30 (144)
lin-38(n751)	1 (186)	1 (425)	1 (282)
lin-56(n2728)	0 (362)	0 (391)	0 (216)
lin-9(n112 M^+*)*[c]	64 (61)	99 (140)	100 (120)[d]
lin-13(n770)	1 (280)	24 (334)	72 (167)
lin-35(n745 M^+*)*[c]	40 (124)	71 (92)	95 (81)
lin-36(n766)	5 (326)	54 (421)	99 (288)
lin-36(n766)[e]	3 (325)	18 (796)	72 (629)
lin-37(n758 M^+*)*[c]	20 (81)	50 (109)	85 (46)
lin-52(n771)	1 (203)	20 (81)	50 (56)[d, f]
lin-53(n833)[g]	0 (341)	23 (507)	72 (65)
lin-54(n2231)	57 (136)	88 (51)	88 (34)[d]
dpl-1(n3380)[h]	17 (354)	36 (291)	NA[i]
tam-1(cc567)[j]	0 (305)	0 (284)	5 (269)

NA = Not applicable

[a] Every strain carried the *mcd-1(n4005)* mutation, unless otherwise noted.

[b] The vulval phenotypes of at least 200 animals were scored at least 24 hours post-L4 larval stage at either 20ºC, 22.5ºC or 25ºC. Single mutants of the class B synMuv genes were not multivulva at any temperature: *lin-9(n112), lin-13(n770), lin-35(n745)*, *lin-36(n766)*, *lin-37(n758), lin-52(n771)*, *lin-53(n833)*, *lin-54(n2231), dpl-1(n2994), tam-1(cc567)*. The class A synMuv mutant *lin-15A(n767)* is weakly multivulva (4%) at 25ºC and the class A synMuv mutants *lin-8(n2731), lin-38(n751),* and *lin-56(n2728)* are not multivulva at any temperature.

[c] M^+ indicates the animals were derived from hermaphrodites heterozygous for the class B synMuv gene and thus have wild-type class B synMuv maternal products. The class B synMuv mutations in these double mutants caused synthetic lethality with *mcd-1(n4005)*. See chapter text for details.

[d] Gene inactivation of this class B synMuv gene by RNAi caused a synMuv phenotype in the *mcd-1(n4005)* strain.

[e] This strain contained the *mcd-1(n4140)* deletion allele.

[f] The null *lin-52* allele *n3718* in combination with *mcd-1(n4005)* has an enhanced synMuv defect.

[g] strain also contains *dpy-5(e61)*

[h] strain also contains *unc-4(e120)*

[i] The Muv phenotype was not scored because these animals die prior to vulval development.

[j] strain also contains *unc-46(e177)*

CHAPTER SEVEN

Where do we go from here?
(a.k.a. Future Directions)

Nearly all synMuv genes have been cloned during the tenure of my doctoral studies, and many genes encode proteins homologous to tumor suppressors and/or regulators of chromatin. In this chapter, I will discuss what I think should be done in future experiments to understand more about how the synMuv genes control cell-fate specification through chromatin remodeling. These ideas focus upon one major issue: We must understand more about the molecular mechanisms mediated by the synMuv genes. This chapter is organized as a priority list with the most pressing experiments explained first.

Characterization of *lin-3* EGF as a target of the synMuv genes

Do all synMuv genes regulate *lin-3* EGF transcription?

Cui *et al.* (2006a) reported that the Ras pathway ligand *lin-3* EGF is a presumptive target of the following class A and B synMuv proteins, LIN-8, LIN-15A, LIN-15B, LIN-35 and LIN-36. In these class A or B single mutants, the authors found that *lin-3* expression levels are not significantly different from levels in the wild type. Only in class AB double mutants are levels of *lin-3* transcription increased, because of the loss of the transcriptional repression mediated by the synMuv genes. The authors also hypothesized that the source of the ectopic expression of *lin-3* is the hyp7 hypodermal syncytium neighboring the vulval cells. However, Adam Saffer has shown that the expression constructs used to test the cell-type specificity in Cui *et al.* (2006a) are not specific for hyp7 (A. M. Saffer and H.R.H., unpublished results). Therefore, we do not yet know the site of LIN-3 inductive ligand ectopic expression in synMuv mutants. Regardless, these results suggest that *lin-3* is the presumptive target of at least some of the synMuv proteins.

To date, five class A synMuv genes and 26 class B synMuv genes have been identified (Chapter One, Table 1). Levels of *lin-3* expression have been quantitatively analyzed only in a small number of synMuv mutants. All of the synMuv genes should be tested in synMuv single and double mutants for effects

on *lin-3* transcription. Some class B synMuv genes are likely not transcriptional repressors of *lin-3*. For example, *gap-1*, the RasGAP, and *ark-1*, the Ack-related kinase homolog, inhibit the Ras pathway through promoting the GTPase activity of Ras and inhibiting LET-23 EGFR, respectively. These genes likely act directly on Ras pathway members and not upstream at the level of *lin-3* transcription. Through a comprehensive analysis, we might determine which class A and B synMuv genes are repressing the transcription of *lin-3* or acting on downstream members of the Ras pathway.

As described in Chapter Three, I found that many of the genes within a synMuv class act in parallel. With the increasingly growing set of class AA and BB double mutants that have Muv phenotypes, quantitative assays of *lin-3* transcription levels should be performed on these strains. These assays will show whether the class A or class B genes act alone to repress *lin-3* transcription. Additionally, these experiments might reveal a relationship between the penetrance of the Muv phenotype and *lin-3* transcription levels. For example, do stains with the most penetrant Muv phenotypes also have the highest levels of *lin-3* transcription? Equally important to test are those class B synMuv single mutants that have Muv phenotypes, like *hda-1*, *hpl-2* and *trr-1*. Given many of the hypotheses of how the synMuv genes might act in transcriptional repression discussed below, these data would greatly aid our understanding of the functions of the synMuv proteins in the repression of transcription.

Do the synMuv genes directly repress *lin-3* transcription?

Our laboratory and others have produced antisera that specifically recognizes most of the class A and B synMuv proteins. Using chromatin-immunoprecipitation (ChIP) experiments, we should determine which synMuv proteins bind directly to the *lin-3* promoter and/or genomic region. These experiments will aid our understanding of which synMuv proteins act directly in transcriptional repression. Because many of the class B genes encode proteins that are conserved but not associated with chromatin remodeling, regulation of

transcription and/or tumor suppression, the identification of which proteins interact specifically with the *lin-3* promoter will focus us our efforts for the experiments described in the section below.

Do the synMuv proteins that act directly on *lin-3* remodel chromatin?

The most important direction for the future analysis of the synMuv genes and their functions during vulval development is to understand the chromatin structure and modification state of the *lin-3* promoter. First, I would like to consider the source of RNA, DNA or protein for subsequent analyses. Then, I will discuss the assays most needed to understand how these genes control chromatin remodeling and transcription in the regulation of vulval fates.

At the time of vulval cell-fate specification during the L2-to-L3 larval transition, there are six cells with the capacity to adopt vulval cell fates. The gonadal anchor cell (AC) expresses LIN-3 and induces three of those cells to adopt vulval cell fates. Therefore, only one cell in the wild-type animal likely expresses LIN-3 important for vulval induction. Perhaps in class AB synMuv mutants, nuclei throughout the animal express *lin-3* ectopically. With an increase in the number of cells with activated *lin-3* transcription, differences in *lin-3* expression levels and nucleosome position might be detectable. Two techniques could be applied to enrich for cells that might ectopically express *lin-3*. The first is laser capture microdissection, in which plastic is adhered to cells using a focused laser beam. The second technique is the sorting of nuclei from a specific tissue using GFP. There are promoters that drive expression in hyp7. The GFP-expressing nuclei of hyp7 could be collected from large populations of synchronized wild-type and synMuv mutant animals. Using either of these techniques, homogeneous cell (or nuclei) populations could be collected and probed for differences in *lin-3* expression, in chromatin structure of the *lin-3* promoter or in protein composition.

Regardless of whether homogeneous cell populations can be collected, the nucleosome positions within the *lin-3* promoter should be determined in wild-

type and synMuv mutant animals. This locus includes roughly 5 kb of promoter and 6 kb of coding and intronic sequence. Once the chromatin structure of the *lin-3* genomic region has been determined from wild-type animals, the modification states of the histones within this region should be determined. Given the work I presented in Chapter Two, the most useful modification states to determine would be trimethylation of histone H3K4, H3K9, H3K27 and H3K36 and acetylation of histone H3K9, because we have quantitative western blot data in which to compare. Subsequently, methylation of histone H4K20, mono- or dimethylation of histone H3 residues and acetylation of histone H4 residues can be determined. These data would create a detailed map of the locations of the nucleosomes within the *lin-3* genomic locus and their modification states.

Why use vulval cell-fate mutants to look at chromatin remodeling and transcription? The *C. elegans* vulva is a paradigm of cell-fate determination, organogenesis, inter- and intracellular signaling. We have a large collection of loss-of-function and gain-of-function mutants that are deficient in this cell-fate decision. Using this massive collection of mutants, we can determine which chromatin states (either nucleosome positioning or histone modification state or both) are dependent on which genes. Subsequent genetic screens can be designed to detect specific chromatin-remodeling effects. These analyses of how chromatin and transcription regulate cell-fate decisions in specific cells are more addressable in genetically tractable organisms, like *Drosophila* and *C. elegans*. Studies in *C. elegans* allow for analyses to be done more quickly (than *Drosophila)* and for determination of how those processes or genes affect the fates of single cells (more difficult in *Drosophila*).

After the determination of nucleosome positioning and chromatin modification states within the *lin-3* locus in wild-type animals during vulval development, synMuv single and double mutants should be assayed. It can quickly be determined which nucleosome positions and/or histone modification states are dependent on which genes. These studies can reveal novel roles for

conserved but uncharacterized genes in specific chromatin-remodeling biochemical activities.

I found that *met-1* and *met-2* are required for wild-type levels of both histone H3K9 and H3K36 trimethylation (Chapter Two). There are defects in both of these methylation marks in single *met-1* or *met-2* mutants from embryonic protein extracts. Additionally, *met-1* or *met-2* double mutants with *lin-15A* had increased levels of *lin-3* transcription, indicating that each regulates the repression of *lin-3* transcription. The nucleosome positioning and chromatin modification state should be determined in *met-1* and *met-2* single mutants. As proposed in Chapter Two, perhaps H3K36 trimethylation creates a binding site for the NuRD-like complex, which deacetylates H3K9, MET-2 then methylates H3K9 and HP1 binds. If this hypothesis is correct, then the coding region of *lin-3* would have less H3K9 trimethylation in *met-1* mutants. *met-2* mutants likely would have decreased levels of H3K9 trimethylation in the promoter and coding regions of the *lin-3* genomic locus. Importantly, because both *met-1* and *met-2* are proposed to act in the inhibition of transcription, levels of H3K4 trimethylation should be increased in the promoter and coding region of *lin-3*. Using HPL-1 and HPL-2 specific antisera (COUSTHAM *et al.* 2006; SCHOTT *et al.* 2006), the distribution of the HP1 homologs should be determined within the *lin-3* locus. These analyses of H3K9, H3K36 or HP1 homolog localization within the *lin-3* locus should be expanded to include other class A and B synMuv mutants. In this way, we can determine if novel or uncharacterized chromatin factors control these specific chromatin-regulatory events.

In Chapter Four, I proposed that the *C. elegans* NURF-like complex might allow transcriptional activators to bind the *lin-3* promoter. Because loss-of-function mutations in *isw-1* not only suppress the synMuv phenotype but also suppress the ectopic activation of *lin-3* transcription in synMuv mutants (Chapter Four Addendum), the NURF-like complex might be required for the ectopic activation of *lin-3* only when the repressive activities of the synMuv proteins are lost. To determine how the NURF-like complex promotes the ectopic transcription

of *lin-3* in synMuv mutants, a detailed comparison of the *lin-3* promoter nucleosome positioning in the wild type, class AB double mutants and the suppressed class AB double mutant with *isw-1(n3294)* should be performed. These assays might determine whether *isw-1* causes nucleosome positioning associated with ectopic *lin-3* transcription in synMuv mutants or in a wild-type synMuv background. Additionally, the DNA sites not occluded by nucleosomes might identify sequences bound by factors required to promote *lin-3* transcription.

The MES-2/MES-3/MES-6 complex has been shown to have H3K27 histone methyltransferase activity (BENDER *et al.* 2004), and MES-4 has been reported to have H3K36 histone methyltransferase activity (BENDER *et al.* 2006). These *mes* genes are also required for expression of the synMuv phenotype of *lin-15AB(n765)* mutants (Chapter Two). First, *lin-3* transcription levels should be assayed in suppressed synMuv strains with *mes* mutations. If *lin-3* transcription levels are unaffected, then the *mes* genes are not promoting *lin-3* transcription. Otherwise, *lin-3* modifications states should be assayed. Both *met-1* and *mes-4* are thought to mediate H3K36 methylation, but these genes have opposing roles in the control of vulval fates. Perhaps an investigation of chromatin-modification state within the *lin-3* promoter in these two mutant strains will resolve this issue.

Using antisera specific to different synMuv proteins, the order of recruitment of these chromatin-remodeling activities can be determined. The transcriptional control of HO endonuclease expression in *S. cerevisiae* (COSMA *et al.* 1999) is regulated by chromatin-remodeling activities that bind this promoter in an ordered stepwise manner. Similarly, transcriptional repression of *lin-3* might be mediated by a stepwise cascade, including gene-specific transcriptional repressors like LIN-35 Rb, the DRM complex and/or the NuRD-like complex, the histone methyltransferases MET-1 and MET-2 and the HP1 homologs.

The molecular analyses described in this section might allow us to use the large collection of vulval mutants to describe more fully how many conserved but uncharacterized chromatin-remodeling factors and transcriptional modulators

regulate transcription important for cell-fate determination or tumor suppression in humans.

Where is *lin-3* expressed normally and where is it expressed in synMuv mutants?

All of synMuv proteins studied thus far are expressed in the nuclei of all cells, but *lin-3* is expressed only in the AC. Where do the synMuv genes regulate *lin-3* transcription, in all cells or only in a subset? Assays to measure *lin-3* transcription levels are done on whole animals, and the developmental stage of these animals is likely not homogeneous. An assay to measure the amount of *lin-3* expression in single cells within an intact animal would circumvent these issues. Perhaps one way to address this issue is to use homologous recombination (BARRETT *et al.* 2004; BEREZIKOV *et al.* 2004; ROBERT and BESSEREAU 2007) to add a six amino-acid tetracysteine peptide to LIN-3. Membrane permeante biarsenical compounds that are fluorescent bind this small peptide sequence (CHEN and TING 2005). The LIN-3::tetracysteine fusion might allow for LIN-3 levels to be measured and localization determined in the developing animal. Alternatively, homologous recombination can be used to add a FLAG or other protein tag to LIN-3. Fixed animals of different stages can be assayed for levels of LIN-3 expression and localization. Some major issues to consider (and overcome, if possible) are that *lin-3* is expressed at very low levels in few cells, some LIN-3 is membrane-bound and LIN-3 is a diffusible ligand, so focused expression might not be present. If these assays are sufficiently robust and high-throughput, then genetic screens should be designed to identify mutants defective in LIN-3 protein expression or localization.

Many synMuv genes and suppressors might prevent the ectopic initiation of *lin-3* transcription downstream of the promoter

I have proposed a model to explain the actions of many class B synMuv genes, integrating findings from my studies with those involving other organisms.

In *S. cerevisiae*, actively transcribed genes are correlated with histone H3K4 trimethylation and H3K9 acetylation in the promoter region and H3K36 trimethylation throughout the promoter and coding regions. The trimethylation of H3K4 and H3K9 acetylation are required to recruit ATP-dependent chromatin-remodeling enzymes to open chromatin in the promoter region necessary for transcriptional initiation. Set2, the yeast H3K36 HMT binds the elongating RNA polymerase II, phosphorylated on serine five of the carboxyl-terminal domain (CTD). Eaf3, a chromodomain-containing protein, which recruits the Rpd3S histone deacetylase complex to deacetylate H3K9 within the coding sequence downstream of the promoter, binds the methylation of H3K36. In mutants for many of these genes, ectopic transcription initiation is observed downstream in the coding region. In mammalian cells, the region downstream of the promoter is enriched for H3K9 trimethylation and HP1gamma, but whether either mark functions in the inhibition of ectopic transcriptional initiation is not known.

My studies of *met-1* and *met-2* during *C. elegans* vulval development made connections between H3K9 trimethylation and H3K36 trimethylation in the inhibition of transcriptional initiation downstream of the promoter (Chapter Two). MET-1 might be required for the recruitment of the NuRD-like complex to genomic regions downstream of the promoter region through the trimethylation of H3K36. The NuRD-like complex would then deacetylate H3K9. Subsequently, MET-2 would trimethylate H3K9, which would create a binding site for the *C. elegans* HP1 homologs HPL-1 and HPL-2. In yeast, the trimethylation of H3K36 also interacts with the NuA4 complex, which acetylates histone H4 tail lysines to inhibit ectopic transcriptional initiation. A similar interaction might exist in the control of *lin-3* transcription, as the NuA4 complex is composed of class C synMuv protein homologs. MET-1, MET-2, the NuRD-like complex, the NuA4-like complex and the HP1 homologs could act together in the inhibition of *C. elegans* vulval cell fates by preventing inappropriate transcriptional initiation of *lin-3* downstream of its promoter.

Unlike most other class B synMuv mutations, mutations in each of these genes cause a Muv phenotype in the absence of class A mutations. This result was first observed for *let-418* Mi-2 mutants, which have the class C synMuv defect of ectopic induction of P8.p. In Chapter Two, synMuv phenotypes were described using *met-1*, *met-2*, *hpl-1* and *hpl-2* multiple mutants. Additionally, the genes that encode members of the presumptive NuRD-like and NuA4-like complexes all cause Muv phenotypes as single mutants. Perhaps loss of any of these mechanisms is sufficient to cause increased transcriptional initiation of *lin-3* and a Muv phenotype. Assays to score levels of *lin-3* transcription in these single mutants might support this hypothesis.

In yeast, the kinases that phosphorylate the CTD of RNA polymerase II are required for subsequent methylation steps. Cdk9 mediates phosphorylation of serine five of the CTD, and in *C. elegans* the Tousled-like kinase (TLK-1) mediates some of this phosphorylation (HAN *et al.* 2003). Inhibition of transcriptional elongation using 6-azauracil caused lethality at high concentrations but not a synMuv phenotype with class A or B mutations (E.C.A. and H.R.H., unpublished results). Therefore just inhibiting elongation is not sufficient to cause a synMuv defect. Perhaps specific inhibition of *tlk-1* or the *C. elegans* Cdk9 homolog would cause a class B synMuv defect. Additionally, none of the synMuv genes are similar to yeast Eaf3. *C. elegans* MRG-1 is the closest homolog of Eaf3 (FUJITA *et al.* 2002; TAKASAKI *et al.* 2007).

One exciting hypothesis is that the trimethylation of H3K36 is bound by the chromodomain of LET-418 and not an Eaf3 homolog. This possibility can be assayed using affinity pull-downs with H3K36 trimethylated peptides and the chromodomain of LET-418. Given that *let-418* causes a class C defect and LET-418 has been shown to be a part of the NuRD-like complex, it might be a member of both the NuRD-like complex and the NuA4-like complex. This hypothesis is supported by the observation that none of the of class C genes encode an ATP-dependent chromatin-remodeling enzyme. Although SSL-1 was proposed to provide this function, mutations in this gene do not cause canonical

class C defects like those caused by *let-418* mutations. LET-418 is possibly at the nexus of control of both the deacetylation of H3K9 and the acetylation of H4K8 important for the prevention of ectopic transcriptional initiation.

Studies of the inhibition of the *C. elegans* vulval cell-fate decision could inform directly on the inhibition of ectopic transcriptional initiation. Using genetic studies of *C. elegans* vulval development paired with the molecular analyses described above, we have the opportunity to investigate and connect a canonical transcriptional repression cascade (the NuRD-like complex, MET-2 and HP1 homologs) to H3K36 trimethylation mediated transcriptional initiation repression.

Direct and quantitative measurements of Ras pathway activity are required to more specifically measure pathway levels important for vulval cell-fate specification

To date, we have only the indirect measures of Ras pathway activity associated with levels of *lin-3* transcription or the vulval phenotype. Measurements of transcription of the Ras pathway ligand might not directly correlate with the level of Ras pathway activity. To understand better how the Ras pathway promotes and the synMuv genes inhibit vulval cell-fate specification, quantitative measures of Ras pathway activity are needed.

One assay of Ras pathway activity that could be adapted to a quantitative metric is the phosphorylation of the *C. elegans* mitogen-activated protein kinase (MAPK), MPK-1, which is a hallmark or Ras pathway activation. Using quantitative western blots (Chapter Two), levels of phosphorylated MPK-1 can be assayed and normalized to levels of total MPK-1. In this way, we might be able to more directly measure Ras pathway activation in the wild type and compare it to a variety of synMuv mutant strains. We might also determine how the levels of *lin-3* transcription correlate with levels of MPK-1 phosphorylation and how both correlate with the induction of vulval cell fates.

Another assay of Ras pathway activity that could be adapted to a quantitative metric is the dimerization of LET-23 EGFR receptors on the cell

membrane or association of SEM-5 Grb2 with the autophosphorylated LET-23 receptor. Both of these measures should use fluorescence resonance energy transfer (FRET) between molecules labeled with different fluorophores. Recently, this technique has been applied to EGFR dimerization in the cell membrane after EGF ligand binding (LIU *et al.* 2007). A similar technique could be used to observe membrane FRET between LET-23 receptors labeled with two different fluorophores. Likewise, the SH2 domains of SEM-5 are thought to bind an activated and phosphorylated LET-23, so labeled SEM-5 and LET-23 might allow for detection of Ras pathway activation. Other downstream components could be adapted in similar ways. For example, the association of the LIN-1/LIN-31 transcription factor heterodimer might be detected by FRET. After activation of the Ras pathway, LIN-1 and LIN-31 are phosphorylated by MPK-1, and the heterodimer disassociates. In this assay, the loss of FRET signal would show Ras pathway activation. These assays might indicate the Ras pathway activity at the single-cell level, which will be especially useful for determining the threshold level of Ras pathway activity required for an induced vulval cell fate.

These assays would allow for direct measurement of Ras pathway activation levels. If successful and large numbers of animals can be quantitatively scored, then these methods should be used in genetic screens. Many mutants have been identified in which the mutant vulval phenotype was too subtle to map or score. These mutants might be addressable using these quantitative assays. Because these types of quantitative measures have not been applied to large-scale screens for vulval mutants, new genetic screens could be performed to identify genes that either promote or inhibit vulval cell fates.

The synMuv proteins inhibit the transcription of other target genes that control diverse aspects of *C. elegans* biology

Some class B synMuv genes repress the transcription of other target genes, including the Hox gene *lin-39* (CHEN and HAN 2001), the Notch ligand *lag-2* (DUFOURCQ *et al.* 2002; POULIN *et al.* 2005), and the germline genes *pgl-1*, *glh-*

2 and *glh-3* (UNHAVAITHAYA *et al.* 2002). Understanding the nucleosome positioning and chromatin modification states within the genomic regions of these different genes might allow for comparative studies of how different synMuv genes control the transcription of diverse target genes.

These types of comparative studies would be aided by the identification of all synMuv target genes. Gene expression analyses of synMuv mutants compared to the wild type have not been reported. Comparisons between class AB double mutants and the wild type might yield more significant differences than comparisons to single synMuv mutants. Preliminary gene expression analyses comparing *lin-35; lin-15A* synMuv double mutants to the wild type showed increased levels of many germline genes, including *gpd-1*, *pgl-1* and *pgl-3* (E.C.A. and H.R.H., unpublished results). If the synMuv genes are studied comprehensively, expression profile signatures might be detected. These expression profile signatures could also be used as a method to categorize the synMuv genes.

Two additional methods could be used to identify the synMuv target genes utilizing microarrays that contain sequences for the entire *C. elegans* genome. These arrays combined with methods to enrich for sequences in which synMuv proteins bind might help to identify synMuv target genes. Chromatin immunoprecipitation (ChIP) experiments and DNA adenine methyltransferase identification (DamID) assays could be used. These techniques have been used on *Drosophila* and mammalian cells in culture but not yet on whole developing animals. Comparing the promoters of these putative direct synMuv targets might also allow for identification of DNA-binding sites. Through these analyses, we might determine a more complete set of synMuv target genes.

Some class B synMuv mutants have phenotypic defects other than vulval cell-fate specification defects. These other defects are likely caused by ectopic gene expression. In the majority of these pleiotropic synMuv defects, a comprehensive study of all synMuv mutations causing the defect has not been described. Pleiotropies to be analyzed include synthetic lethality with *mcd-1*, *psa-*

1, *pha-1*, *fzr-1*, *ubc-18* and *xnp-1*, cell-cycle defects, maintenance of the germline/soma cell-fate distinction, sex determination, programmed cell death and meiotic recombination. These different pleiotropic defects might allow for the parsing of the synMuv genes into groups that control different aspects of *C. elegans* biology. These synMuv groups can also be analyzed for overlapping sets of co-regulated genes to determine the transcriptional targets controlling each pleiotropy.

Future genetic analyses of the synMuv genes and their suppressors

To date, we do not know the transcription factors that promote or inhibit the expression of *lin-3* or the sites where they bind. One site in an intron of *lin-3* is required for the expression of *lin-3* from the AC (HWANG and STERNBERG 2004) and is bound by HLH-2, a Daughterless homolog transcription factor. Adam Saffer identified a site in the promoter region of *lin-3* that is likely required for transcriptional repression mediated by the class A proteins (A.M. Saffer and H.R.H., unpublished results). He identified this site in a genetic screen for class A mutants. Because this sequence is thought to have mutated a class A protein binding site for transcriptional repression, *lin-3* is over-expressed, and a dominant class A synMuv phenotype results. A screen for mutations that cause a dominant class B synMuv phenotype might identify a similar sequence where class B proteins bind. Such a screen should be performed in a way to identify mutations on linkage group IV (the location of *lin-3*) first, because haploinsufficient class B synMuv mutations are numerous (E.C.A. and H.R.H., unpublished observations).

Within the collection of 120 synMuv suppressors (see Appendix One for a fuller description) might be an isolate with a mutation in a site required for promoting the expression of *lin-3*. The sequence of the *lin-3* locus should be determined for those synMuv suppressors that map to a genetic interval containing *lin-3.* Some of these isolates might have promoter mutations or mutations in sites where positively acting transcription factors bind.

Both the genetic screens for *lin-3* mutations causing dominant class B synMuv phenotypes and *lin-3* promoter mutations should be combined with assays that remove parts of the *lin-3* promoter and look for causality in the synMuv phenotype and synMuv suppression phenotype. A deletion that removes a binding site for a positive regulator of *lin-3* transcription might suppress the synMuv phenotype, and a deletion that removes a binding site for a negative regulator might cause a class A or B synMuv phenotype. These genetic analyses will complement the molecular analyses mentioned above to help determine more about the control of *lin-3* transcription important for vulval cell-fate determination.

In Appendix One, I describe how the isolates from two synMuv suppressor screens might be parsed into chromatin and non-chromatin classes. These experiments could allow the rapid identification of isolates that will be important to molecularly identify and characterize. Given that an RNAi screen for synMuv suppressors has been performed (CUI *et al.* 2006b), efforts should be taken to quickly identify whether new genes exist within our collection of 120 synMuv suppressors. I constructed polymorphic synMuv strains to quickly map synMuv suppressors to genetic intervals. Once these intervals are determined, they should be searched for known synMuv suppressor genes. The identification of alleles of known synMuv suppressors will allow for molecular analyses to be performed with laborious RNAi procedures. More importantly, new synMuv suppressors can be identified if the intervals lack known suppressor genes.

The recent identification of a histone demethylase that removes methyl groups from both trimethylated H3K9 and H3K36 (KLOSE *et al.* 2006) suggests a shared mechanism between HMTs that mediate both H3K9 and H3K36 trimethylation. Perhaps mutations in the JHDM3A homolog in *C. elegans* would suppress the defects associated with loss of *met-1* and *met-2* as levels of H3K9 and H3K36 trimethylation might be sufficient to prevent ectopic *lin-3* transcription. Additionally, inhibition of the elongating polymerase might suppress the synMuv phenotype because the increased level of *lin-3* transcription would be inhibited.

Because some of the *mes* genes cause synMuv suppression (Chapter Two), there are likely histone demethylases that when mutated will cause a synMuv defect. Using RNAi or deletion analyses and 6-azauracil, these hypotheses can be tested simply and quickly.

An unbiased biochemical purification of synMuv proteins should be done to identify new synMuv proteins and novel synMuv protein interactions

To date, an unbiased biochemical purification of the synMuv proteins has not been performed. Such purification might identify new synMuv proteins that have been missed by genetic screens because mutations in these genes cause lethality or are redundant with other genes. Additionally, many synMuv proteins are conserved but uncharacterized in other organisms. An unbiased purification might identify novel synMuv protein interactions conserved in other organisms, including humans.

Over the past ten years, the Horvitz laboratory and others have created antisera specific for many class A and B synMuv proteins. These antisera can be used to follow synMuv proteins through purification schemes that ultimately end in protein identification by mass spectrometry. Assays could also be designed to follow specific biochemical activities through a protein purification scheme, including histone deacetylase activity (HDA-1), ATP-dependent chromatin-remodeling activity (LET-418), histone acetyltransferase activity (MYS-1) and histone H3K9 or H3K36 trimethylation assays (MET-1 and MET-2). RNAi or deletion of the genes encoding these protein interactors can be assayed for synMuv or synMuv suppressor activity.

Many synMuv proteins are predicted to be DNA-binding transcription factors. These include members of the DRM complex (EFL-1, DPL-1 and LIN-54), the THAP domain containing proteins LIN-15B and LIN-36 and the presumptive heteromer LIN-15A/LIN-56. Recent studies have shown that HP1 can bind DNA independently of histone methylation or even histones, so other canonical chromatin regulators recruited by DNA-binding factors might bind

independently. Many of these proteins bind DNA and could recruit separable, redundant transcriptional repression mechanisms. Also, because many synMuv mutants have distinct sets of pleiotropies, different synMuv proteins might act at different target genes to repress transcription. Much is left to be determined about which synMuv proteins bind DNA, at what sites and to what effect.

Concluding remarks

A molecular understanding of how the synMuv genes control chromatin structure, modification state and transcription might allow the power of *C. elegans* genetics to be applied these topics in the control of cell-fate specification. Given that one of the most significant and long-standing problems in epigenetics is how chromatin states are inherited from one cell to the next through development, *C. elegans* with its well characterized lineage could provide a platform to address this issue.

ACKNOWLEDGMENTS

I thank Adam Saffer and Kostantinos Boulias for their insightful edits and comments on this chapter.

LITERATURE CITED

BARRETT, P. L., J. T. FLEMING and V. GOBEL, 2004 Targeted gene alteration in *Caenorhabditis elegans* by gene conversion. Nat Genet **36:** 1231-1237.

BENDER, L. B., R. CAO, Y. ZHANG and S. STROME, 2004 The MES-2/MES-3/MES-6 complex and regulation of histone H3 methylation in *C. elegans*. Curr Biol **14:** 1639-1643.

BENDER, L. B., J. SUH, C. R. CARROLL, Y. FONG, I. M. FINGERMAN, S. D. BRIGGS, R. CAO, Y. ZHANG, V. REINKE and S. STROME, 2006 MES-4: an autosome-associated histone methyltransferase that participates in silencing the X chromosomes in the *C. elegans* germ line. Development **133:** 3907-3917.

BEREZIKOV, E., C. I. BARGMANN and R. H. PLASTERK, 2004 Homologous gene targeting in *Caenorhabditis elegans* by biolistic transformation. Nucleic Acids Res **32:** e40.

CHEN, I., and A. Y. TING, 2005 Site-specific labeling of proteins with small molecules in live cells. Curr Opin Biotechnol **16:** 35-40.

CHEN, Z., and M. HAN, 2001 *C. elegans* Rb, NuRD, and Ras regulate *lin-39*-mediated cell fusion during vulval fate specification. Curr Biol **11:** 1874-1879.

COSMA, M. P., T. TANAKA and K. NASMYTH, 1999 Ordered recruitment of transcription and chromatin remodeling factors to a cell cycle- and developmentally regulated promoter. Cell **97:** 299-311.

COUSTHAM, V., C. BEDET, K. MONIER, S. SCHOTT, M. KARALI and F. PALLADINO, 2006 The *C. elegans* HP1 homologue HPL-2 and the LIN-13 zinc finger protein form a complex implicated in vulval development. Dev Biol **297:** 308-322.

CUI, M., J. CHEN, T. R. MYERS, B. J. HWANG, P. W. STERNBERG, I. GREENWALD and M. HAN, 2006a SynMuv genes redundantly inhibit *lin-3*/EGF expression to prevent inappropriate vulval induction in *C. elegans*. Dev Cell **10:** 667-672.

CUI, M., E. B. KIM and M. HAN, 2006b Diverse chromatin remodeling genes antagonize the Rb-involved SynMuv pathways in *C. elegans*. PLoS Genet **2:** e74.

DUFOURCQ, P., M. VICTOR, F. GAY, D. CALVO, J. HODGKIN and Y. SHI, 2002 Functional requirement for histone deacetylase 1 in *Caenorhabditis elegans* gonadogenesis. Mol Cell Biol **22:** 3024-3034.

FUJITA, M., T. TAKASAKI, N. NAKAJIMA, T. KAWANO, Y. SHIMURA and H. SAKAMOTO, 2002 MRG-1, a mortality factor-related chromodomain protein, is required maternally for primordial germ cells to initiate mitotic proliferation in *C. elegans*. Mech Dev **114:** 61-69.

HAN, Z., J. R. SAAM, H. P. ADAMS, S. E. MANGO and J. M. SCHUMACHER, 2003 The *C. elegans* Tousled-like kinase (TLK-1) has an essential role in transcription. Curr Biol **13:** 1921-1929.

HWANG, B. J., and P. W. STERNBERG, 2004 A cell-specific enhancer that specifies *lin-3* expression in the *C. elegans* anchor cell for vulval development. Development **131:** 143-151.

KLOSE, R. J., K. YAMANE, Y. BAE, D. ZHANG, H. ERDJUMENT-BROMAGE, P. TEMPST, J. WONG and Y. ZHANG, 2006 The transcriptional repressor JHDM3A demethylates trimethyl histone H3 lysine 9 and lysine 36. Nature **442:** 312-316.

LIU, P., T. SUDHAHARAN, R. M. KOH, L. C. HWANG, S. AHMED, I. N. MARUYAMA and T. WOHLAND, 2007 Investigation of the dimerization of proteins from the epidermal growth factor receptor family by single wavelength fluorescence cross-correlation spectroscopy. Biophys J.

POULIN, G., Y. DONG, A. G. FRASER, N. A. HOPPER and J. AHRINGER, 2005 Chromatin regulation and sumoylation in the inhibition of Ras-induced vulval development in *Caenorhabditis elegans*. Embo J **24:** 2613-2623.

ROBERT, V., and J. L. BESSEREAU, 2007 Targeted engineering of the *Caenorhabditis elegans* genome following *Mos1*-triggered chromosomal breaks. Embo J **26:** 170-183.

SCHOTT, S., V. COUSTHAM, T. SIMONET, C. BEDET and F. PALLADINO, 2006 Unique and redundant functions of *C. elegans* HP1 proteins in post-embryonic development. Dev Biol **298:** 176-187.

TAKASAKI, T., Z. LIU, Y. HABARA, K. NISHIWAKI, J. NAKAYAMA, K. INOUE, H. SAKAMOTO and S. STROME, 2007 MRG-1, an autosome-associated protein, silences X-linked genes and protects germline immortality in *Caenorhabditis elegans*. Development **134:** 757-767.

UNHAVAITHAYA, Y., T. H. SHIN, N. MILIARAS, J. LEE, T. OYAMA and C. C. MELLO, 2002 MEP-1 and a homolog of the NURD complex component Mi-2 act

together to maintain germline-soma distinctions in *C. elegans*. Cell **111:** 991-1002.

APPENDIX ONE

Separation of the synMuv suppressors into putative chromatin and non-chromatin classes

I wanted to identify other genes that might encode chromatin regulators involved in antagonizing the synMuv genes, like *isw-1*. The 120 synMuv suppressor isolates can be grouped into putative chromatin or non-chromatin classes based upon two criteria: (1) Loss of *isw-1* suppresses other aspects of the class B synMuv phenotype not associated with vulval development, and other chromatin suppressors might do the same. (2) The *lin-15AB(n765)* mutation might affect the transcriptional termination of the *lin-15AB* operon, and some non-chromatin suppressors could be *lin-15AB(n765)*-specific suppressors if they affect transcriptional termination.

BACKGROUND AND SIGNIFICANCE

Isolation of suppressors of the synthetic multivulva (synMuv) phenotype likely will identify genes that antagonize the synMuv genes. Because many synMuv genes encode regulators of transcription and chromatin structure, suppressor mutations might cause reduction or elimination of function of transcriptional target genes of the synMuv proteins. One suppressor of the synMuv phenotype has been identified as *isw-1* and characterized as a general synMuv suppressor gene (Chapter Four and CUI *et al.* 2006). Identification of new synMuv suppressor genes could aid our understanding of how chromatin modulators regulate vulval cell fates.

Two previous graduate students in the Horvitz laboratory, Scott Clark and Xiaowei Lu, performed synMuv suppressor screens (CLARK 1992 and X. Lu, unpublished results). Scott Clark screened for suppressors of the *lin-15AB(n765)* synMuv phenotype and isolated 166 mutations. His suppressor strains were grouped into two general classes. One class suppressed the synMuv phenotype to a Vul phenotype. Isolates of this class characterized by Scott Clark and others led to the identification and characterization of many genes in the RTK/Ras pathway and the Hox gene *lin-39* (CLARK *et al.* 1992a; CLARK *et al.* 1992b; KORNFELD *et al.* 1995a; KORNFELD *et al.* 1995b). The other class, which contains 80 isolates, was named the “wild-type” suppressor class. These suppressor strains suppressed the synMuv phenotype to a “wild-type” vulval phenotype. “Wild-type” is in quotes, because the vulval phenotypes of many suppressed animals vary from protruding vulvae to weakly Muv. Scott’s initial characterization was an analysis of the temperature sensitivity and maternal effects of the synMuv suppression phenotypes of some synMuv suppressor isolates. Despite these studies, we understand little about the regulation of the *lin-15AB* operon, which contains the class A gene, *lin-15A*, and the class B gene, *lin-15B* (CLARK *et al.* 1994; HUANG *et al.* 1994). A recent finding from the Han laboratory determined that the molecular lesion in the *lin-15AB(n765)* strain is an insertion into *lin-15B*

causing a complete loss of *lin-15B* function (M. Cui and M. Han, unpublished results), the first gene transcribed in the *lin-15AB* operon (CLARK *et al.* 1994; HUANG *et al.* 1994). This insertion contains a putative transcriptional-termination sequence, which might cause a partial loss of *lin-15A* function by inappropriate termination of transcription of the *lin-15AB* operon. Therefore some of the "wild-type" suppressors might be *lin-15AB(n765)*-specific synMuv suppressors that restore expression of *lin-15A* by partially inhibiting transcriptional termination.

The Vidal laboratory identified a putative interaction between LIN-53 and LIN-37, two class B synMuv proteins, using yeast two-hybrid assays (WALHOUT *et al.* 2000). Additionally, this interaction was abrogated by the missense mutation *lin-53(n833)*, suggesting the possible importance of that residue for the LIN-37 interaction *in vivo*. Xiaowei Lu performed a screen for suppressors of the *lin-53(n833); lin-15A(n767)* synMuv phenotype with the hope of identifying interactional suppressor mutations in *lin-37* that restored the interaction of LIN-37 with LIN-53(n833) (X. Lu and H. R. Horvitz, unpublished results). Xiaowei isolated 43 suppressors of the synMuv phenotype, of which two caused a Vul phenotype. Many of the other suppressor isolates were mapped to linkage groups and assigned to complementation groups by Xiaowei (Table 1). She focused on isolates that mapped to linkage group III near *lin-37* and cloned *isw-1*, the *C. elegans* homolog of *Drosophila* ISWI (Chapter Four, ANDERSEN *et al.* 2006).

From among 120 suppressors of the synMuv phenotype in our strain collection, I wanted to identify other chromatin regulators that would antagonize the synMuv genes in the determination of vulval cell fates, like *isw-1*. I performed two assays to parse these suppressor isolates. The first assay was designed to identify suppressors that antagonize the synMuv genes in the regulation of non-vulval cell-fate decisions. Many of the class B synMuv genes are required for the germline-versus-soma cell-fate decision (UNHAVAITHAYA *et al.* 2002; WANG *et al.* 2005; LEHNER *et al.* 2006). Mutations in some class B synMuv genes cause somatic cells to become more like germline cells. This cell-fate transformation can be readily scored using the tandem-array modifier (Tam) phenotype (HSIEH

et al. 1999). The Tam phenotype is observed when a repetitive transgene normally expressed in the soma is silenced ectopically in the soma of mutant animals by a mechanism that normally occurs only in the germline (WANG *et al.* 2005). I found that loss of *isw-1* function suppresses the Tam phenotype of some class B synMuv genes, including *lin-15B* (ANDERSEN *et al.* 2006). This assay will help to identify genes that generally anatagonize the synMuv genes in tissues other than the vulva. The second assay was designed to determine whether the suppressor could be *lin-15AB(n765)*-specific by using RNAi of *lin-15A*. If these suppressors specifically perturbed the transcriptional termination of the *lin-15AB* operon caused by the *lin-15AB(n765)* mutation, then the reduction of *lin-15A* function should restore the synMuv phenotype.

MATERIALS AND METHODS

Determination of the Tam phenotype

Each suppressor isolate was combined with the *myo-3::gfp* reporter *ccIs4251* in the *lin-15AB(n765)* background. I picked hermaphrodites during the fourth larval stage to 25ºC. After four days, I scored the progeny of these animals for body-wall muscle expression of GFP using a fluorescence dissecting microscope. Animals with the Tam phenotype had decreased GFP expressing in the body-wall muscle as compared to the *ccIs4251* control strain. This decreased GFP expression was both in the intensity of GFP in body-wall muscle nuclei and also in the number of body-wall muscle nuclei expressing GFP. For example, fewer nuclei expressed less GFP than the control strain. Animals with suppression of the Tam phenotype had greater GFP expression than the *ccIs4251; lin-15AB(n765)* control strain. The criteria for scoring greater GFP expression are the reciprocal as the decreased GFP expression criteria.

RNAi analyses

I performed RNAi feeding as described previously (KAMATH *et al.* 2003), except the *lin-15A* feeding construct was made using the Gateway recombinase system (Invitrogen) of a full-length *lin-15A* cDNA (E. M. Davison and H. R. Horvitz, unpublished results). RNAi injection was performed as described previously (ANDERSEN *et al.* 2006), using clone pEA147 for *nurf-1*.

RESULTS

Some synMuv suppressor isolates suppress the Tam phenotype caused by *lin-15AB(n765)*

The Tam phenotype might be caused by a transformation of somatic cells into a more germline-like cell fate (HSIEH *et al.* 1999). This cell-fate transformation could cause proteins that normally repress transcription from repetitive transgenes in the germline to function ectopically in the soma. Repetitive transgenes such as the *myo-3::gfp* reporter *ccIs4251* are silenced ectopically in the soma of some class B synMuv mutants. I tested for suppression of the *lin-15AB(n765)* Tam phenotype caused by eleven synMuv suppressor mutants. Previously, I determined that loss of *isw-1* and *nurf-1* suppress the Tam phenotype of *lin-15B* mutations (ANDERSEN *et al.* 2006), and I determined using the null allele *bn73* and Cui *et al.* confirmed using RNAi that *mes-4* suppressed the Tam phenotype of *lin-15AB(n765)* (Table 3, (CUI *et al.* 2006). The dominant synMuv suppressor allele *lst-3(n2070)* failed to suppress the Tam phenotype of *lin-15AB(n765)*. Similarly, six other synMuv suppressors, *n1481*, *n1521*, *n1831*, *n2054*, *n2073* and *n2130*, failed to suppress the Tam phenotype caused by *lin-15AB(n765)*. One uncharacterized synMuv suppressor, *n2125*, suppressed the Tam phenotype. Clearly, many more synMuv suppressor isolates remain to be tested.

Some synMuv suppressor isolates might be *lin-15AB(n765)*-specific synMuv suppressors defective in transcriptional termination

The *lin-15AB(n765)* mutation causes a complete loss of *lin-15B* function and a partial loss-of-function of *lin-15A*. *lin-15AB(n765)* contains an insertion into the *lin-15B* gene of a large sequence containing a transcription termination signal (M. Cui and M. Han, unpublished results). Therefore, the complete loss of *lin-15B* likely is caused by this insertion, and the partial loss of *lin-15A* is caused by incomplete transcription of *lin-15A* from the *lin-15AB* operon. Mutations that suppress the *lin-15AB(n765)* synMuv phenotype could be in genes required for

the proper termination of transcription. If the termination of transcription is deficient, then the *lin-15AB(n765)* lesion is bypassed and *lin-15A* is transcribed causing a wild-type vulval phenotype and synMuv suppression. To determine which suppressors affect this putative function, I inactivated *lin-15A* in the eleven suppressor strains previously tested for Tam suppression (Table 4). The RNAi of *lin-15A* should cause a synMuv phenotype in suppressors in which *lin-15A* transcription has been restored by the suppressor mutation. RNAi of *lin-15A* caused the synMuv phenotype in the following suppressor mutant backgrounds: *lst-3(n2070)*, *n1481*, *n1521*, *n1831*, *n2073* and *n2130* (Table 3). *n2125* and *isw-1(n3294)* caused suppression of the synMuv phenotype even in the presence of a reduction of *lin-15A* function.

DISCUSSION AND FUTURE DIRECTIONS

The two assays used to parse the synMuv suppressor isolates into different groups gave promising preliminary results. From our analyses, I determined that *n2125* acts similarly to *isw-1*, *nurf-1* and *mes-4* to suppress the Tam phenotype and the synMuv phenotype of *lin-15AB(n765)* in the presence of *lin-15A* RNAi. These results suggest that *n2125* might harbor a mutation in a chromatin-regulatory gene and should be cloned and characterized.

The synMuv suppressor allele *lst-3(n2070)* did not suppress the Tam phenotype and the synMuv phenotype in the presence of *lin-15A* RNAi. I believe that *lst-3* antagonizes the synMuv phenotype by decreasing activity of the Ras pathway (Chapter Five) and not by regulating transcriptional termination. The inability of *lst-3(n2070)* to suppress the synMuv phenotype in the presence of *lin-15A* RNAi might be because this hypermorphic allele of *lst-3* weakly suppresses the synMuv phenotype.

These analyses allow the 120 synMuv suppressor isolates to be parsed into two general classes: a chromatin-regulatory class like *isw-1*, *nurf-1* and *mes-4* and a non-chromatin class. These two synMuv suppressor classes should be genetically characterized similarly to confirm the initial classification and to learn more about how these genes effect cell-fate determination.

The future studies of new synMuv suppressor should be similar to and expand upon the studies described in Chapters Four and Five. In short, one should determine the null phenotype of the synMuv suppressor gene and use the strongest loss-of-function mutation in all future analyses, determine the gene and allele specificity of the synMuv suppressor, score suppression of other class AB synMuv double mutants, including class AB double mutants not on linkage group X, score suppression of Muv phenotypes not caused by loss of the synMuv genes and score suppression of non-vulval mutant phenotypes, including PGL-1 expression in the soma (UNHAVAITHAYA *et al.* 2002; WANG *et al.* 2005), male tail

cell-fate determination and synthetic lethality with a variety of mutations (FAY *et al.* 2002; FAY *et al.* 2003; CUI *et al.* 2004; FAY *et al.* 2004; REDDIEN *et al.* 2007).

Suppressors that fail to suppress the synMuv phenotype after RNAi of *lin-15A* could be either regulators of transcriptional termination or weak suppressors of the synMuv phenotype. Suppressors that fail to suppress the Tam phenotype caused by *lin-15AB(n765)* could be vulval-specific or weak suppressors. Strong and/or general suppressors of the vulval cell fate, like *isw-1* and perhaps *n2125*, might also antagonize the synMuv genes in other tissues. Suppressors that antagonize the synMuv phenotype of *lin-15AB(n765) lin-15A(*RNAi*)* and the Tam phenotype of *lin-15AB(n765)* might represent a class of chromatin regulators similar to *isw-1*, *nurf-1* and *mes-4* required for all aspects of the synMuv phenotype.

ACKNOWLEDGMENTS

I would like to thank Robyn Tanny and Ezequiel Alvarez-Saavedra for critical reading of this appendix.

LITERATURE CITED

ANDERSEN, E. C., X. LU and H. R. HORVITZ, 2006 *C. elegans* ISWI and NURF301 antagonize an Rb-like pathway in the determination of multiple cell fates. Development **133:** 2695-2704.

CLARK, S. G., 1992 Intercellular signalling and homeotic genes required during vulval development in *C. elegans*. Ph. D. Thesis, Massachusetts Institute of Technology.

CLARK, S. G., X. LU and H. R. HORVITZ, 1994 The *Caenorhabditis elegans* locus *lin-15*, a negative regulator of a tyrosine kinase signaling pathway, encodes two different proteins. Genetics **137:** 987-997.

CLARK, S. G., M. J. STERN and H. R. HORVITZ, 1992a *C. elegans* cell-signalling gene *sem-5* encodes a protein with SH2 and SH3 domains. Nature **356:** 340-344.

CLARK, S. G., M. J. STERN and H. R. HORVITZ, 1992b Genes involved in two *Caenorhabditis elegans* cell-signaling pathways. Cold Spring Harb Symp Quant Biol **57:** 363-373.

CUI, M., D. S. FAY and M. HAN, 2004 *lin-35*/Rb cooperates with the SWI/SNF complex to control *Caenorhabditis elegans* larval development. Genetics **167:** 1177-1185.

CUI, M., E. B. KIM and M. HAN, 2006 Diverse chromatin remodeling genes antagonize the Rb-involved SynMuv pathways in *C. elegans*. PLoS Genet **2:** e74.

FAY, D. S., S. KEENAN and M. HAN, 2002 *fzr-1* and *lin-35*/Rb function redundantly to control cell proliferation in *C. elegans* as revealed by a nonbiased synthetic screen. Genes Dev **16:** 503-517.

FAY, D. S., E. LARGE, M. HAN and M. DARLAND, 2003 *lin-35*/Rb and *ubc-18*, an E2 ubiquitin-conjugating enzyme, function redundantly to control pharyngeal morphogenesis in *C. elegans*. Development **130:** 3319-3330.

FAY, D. S., X. QIU, E. LARGE, C. P. SMITH, S. MANGO and B. L. JOHANSON, 2004 The coordinate regulation of pharyngeal development in *C. elegans* by *lin-35*/Rb, *pha-1*, and *ubc-18*. Dev Biol **271:** 11-25.

HSIEH, J., J. LIU, S. A. KOSTAS, C. CHANG, P. W. STERNBERG and A. FIRE, 1999 The RING finger/B-box factor TAM-1 and a retinoblastoma-like protein LIN-35 modulate context-dependent gene silencing in *Caenorhabditis elegans*. Genes Dev **13:** 2958-2970.

HUANG, L. S., P. TZOU and P. W. STERNBERG, 1994 The *lin-15* locus encodes two negative regulators of *Caenorhabditis elegans* vulval development. Mol Biol Cell **5:** 395-411.

KAMATH, R. S., A. G. FRASER, Y. DONG, G. POULIN, R. DURBIN, M. GOTTA, A. KANAPIN, N. LE BOT, S. MORENO, M. SOHRMANN, D. P. WELCHMAN, P. ZIPPERLEN and J. AHRINGER, 2003 Systematic functional analysis of the *Caenorhabditis elegans* genome using RNAi. Nature **421:** 231-237.

KORNFELD, K., K. L. GUAN and H. R. HORVITZ, 1995a The *Caenorhabditis elegans* gene *mek-2* is required for vulval induction and encodes a protein similar to the protein kinase MEK. Genes Dev **9:** 756-768.

KORNFELD, K., D. B. HOM and H. R. HORVITZ, 1995b The *ksr-1* gene encodes a novel protein kinase involved in Ras-mediated signaling in *C. elegans*. Cell **83:** 903-913.

LEHNER, B., A. CALIXTO, C. CROMBIE, J. TISCHLER, A. FORTUNATO, M. CHALFIE and A. G. FRASER, 2006 Loss of LIN-35, the *Caenorhabditis elegans* ortholog of the tumor suppressor p105Rb, results in enhanced RNA interference. Genome Biol **7:** R4.

REDDIEN, P. W., E. C. ANDERSEN, M. C. HUANG and H. R. HORVITZ, 2007 DPL-1 DP, LIN-35 Rb and EFL-1 E2F Act With the MCD-1 Zinc-Finger Protein to Promote Programmed Cell Death in *Caenorhabditis elegans*. Genetics **175:** 1719-1733.

UNHAVAITHAYA, Y., T. H. SHIN, N. MILIARAS, J. LEE, T. OYAMA and C. C. MELLO, 2002 MEP-1 and a homolog of the NURD complex component Mi-2 act together to maintain germline-soma distinctions in *C. elegans*. Cell **111:** 991-1002.

WALHOUT, A. J., R. SORDELLA, X. LU, J. L. HARTLEY, G. F. TEMPLE, M. A. BRASCH, N. THIERRY-MIEG and M. VIDAL, 2000 Protein interaction mapping in *C. elegans* using proteins involved in vulval development. Science **287:** 116-122.

WANG, D., S. KENNEDY, D. CONTE, JR., J. K. KIM, H. W. GABEL, R. S. KAMATH, C. C. MELLO and G. RUVKUN, 2005 Somatic misexpression of germline P granules and enhanced RNA interference in retinoblastoma pathway mutants. Nature **436:** 593-597.

Table 1: Isolates from Xiaowei Lu's *lin-53(n833); lin-15A(n767)* synMuv suppressor screen

complementation group	linkage group	alleles	mapping data
lin(3220)	II	*n3214*, *n3215*, *n3217*, *n3220*, *n3279*, *n3284*, *n3285*, *n3286*, *n3287*, *n3288*, *n3290*, *n3295*, *n3296*, *n3300*, *n3301*, *n3305*, *n3306*, *n3308*, *n3309*	13/63 Rol non-Unc were *n3220* / +
isw-1	III	*n3289*, *n3294*, *n3297*	cloned
lin(3216)	IV	*n3216*	linked to *bli-6* (0/20)
lin(n3283)	IV	*n3283*	linked to *bli-6* (0/20)
lin(3218)	V	*n3218*	*dpy-11* (6/73) *n3218* (67/73) *unc-76*
lin(n3219)	X	*n3219*	4/20 *n3219* were Unc-3 non-Unc-84, 16/20 *n3219* were non-Unc-3 non-Unc-84
lin(n3222)	X	*n3222*	none
not assigned	not assigned	*n3221*, *n3280*, *n3281*, *n3282*, *n3291*, *n3292*, *n3293*, *n3298*, *n3299*, *n3302*, *n3303*, *n3304*, *n3305*, *n3309*,	none
not assigned, Vul	not assigned, Vul	*n3223*, *n3307*	none

All of these alleles were isolated and mapped previously (X. Lu and H.R. Horvitz, unpublished results).

Table 2: Some synMuv mutations cause ectopic silencing of repetitive transgenes in the soma, or the Tam phenotype.

genotype	Tam?
lin-8(n2731)	No
lin-15A(n767)	No
lin-38(n751)	No
lin-56(n2728) [a]	No
lin-9(n112)	Yes
lin-13(n770)	Yes
lin-15B(n744)	Yes
lin-35(n745)	Yes
lin-36(n766) [b]	No
lin-37(n4903)	Yes
lin-52(n771)	Yes
lin-53(n833)	Yes
lin-54(n2231)	Yes
dpl-1(n2994)	Yes
tam-1(cc567)	Yes
hda-1(e1795)	Yes
*efl-1(*RNAi*)*	Yes
hpl-2(tm1489) [b]	No
met-1(n4337)	No
met-2(n4256)	No
ark-1(n3701)	No
gap-1(n3535)	No
sli-1(n3538)	No
lst-3(gk433)	No
lin-61(n3809) [b]	No
let-418(n3719)	Yes

The first four genes are class A synMuv genes, and the second group are class B synMuv genes.

[a] *lin-56(n3355)*, another *lin-56* null allele, did not cause the Tam phenotype, so I believe that loss of *lin-56* does not cause the Tam phenotype.

[b] Other putative null alleles (*lin-36(n3096)*, *hpl-2(n4274)* and *lin-61(n3442)*) did not cause a Tam phenotype, so I believe these mutants do not cause the Tam phenotype.

Table 3: Some synMuv suppressors are required for the Tam phenotype caused by *lin-15AB(n765)*

genotype*	Tam?
+	Yes
isw-1(n3294)	No
*nurf-1(*RNAi*)*	No
mes-4(bn73)	No
lst-3(n2070) / +	Yes
n1481	Yes
n1521	Yes
n1831	Yes
n2054	Yes
n2073	Yes
n2125	No
n2130	Yes

* Every strain contained *ccIs4251; lin-15AB(n765)*.

Table 4: Some synMuv suppressors might suppress the transcriptional termination defect caused by *lin-15AB(n765)*

genotype*	Muv after *lin-15A* RNAi?
+	Yes
isw-1(n3294)	No
*nurf-1(*RNAi*)*	No
mes-4(bn73)	No
lst-3(n2070) / +	Yes
n1481	Yes
n1521	Yes
n1831	Yes
n2054	No
n2073	Yes
n2125	No
n2130	Yes

* Every strain contained *ccIs4251; lin-15AB(n765)*.

APPENDIX TWO

Identification of suppressors of the *let-418(n3536)* larval-lethal phenotype

These screens were carried out by rotation graduate students Sebastian Treusch, Divya Mathur and myself. I constructed the *let-418* strain for the genetic screens and managed isolates after the rotations.

BACKGROUND AND SIGNIFICANCE

Several screens for suppressors of the synMuv vulval phenotype have been performed (Chapters Four and Five, Appendix One, CUI *et al.* 2006). The genes identified in these screens have helped us to understand how chromatin-regulatory complexes antagonize the synMuv proteins to control the vulval cell-fate decision. The proteins encoded by suppressors like *isw-1* and *nurf-1* might form an ATP-dependent chromatin-regulatory complex that opposes the synMuv proteins and promotes the RTK/Ras pathway (ANDERSEN *et al.* 2006). Similarly *mes-2*, *mes-3*, *mes-4* and *mes-6* might act together to oppose the synMuv genes (Chapter Two, CUI *et al.* 2006). In addition to causing a vulval cell-fate defect, many synMuv mutants (especially class B synMuv mutants) have defects in other aspects of *C. elegans* development, including germline maintenance, the germline/soma cell-fate decision and redundant requirements for viability (MELENDEZ and GREENWALD 2000; CEOL and HORVITZ 2001; COUTEAU *et al.* 2002; FAY *et al.* 2002; UNHAVAITHAYA *et al.* 2002; FAY *et al.* 2003; CEOL and HORVITZ 2004; CUI *et al.* 2004; FAY *et al.* 2004; REDDY and VILLENEUVE 2004; CARDOSO *et al.* 2005; WANG *et al.* 2005; COUSTHAM *et al.* 2006; LEHNER *et al.* 2006). To our knowledge, no screens for suppressors of non-vulval aspects of the synMuv loss-of-function phenotype have been performed. For this reason, we sought suppressors of the larval-lethal phenotype of *let-418(n3536)*.

let-418 encodes the *C. elegans* homolog of the human Mi-2 protein (VON ZELEWSKY *et al.* 2000). Mi-2 was identified as the autoantigen of the human disease dermatomyositis (SEELIG *et al.* 1995). Like Mi-2, the class B synMuv protein LET-418 contains ATPase and helicase domains (required in Mi-2 for sliding nucleosomes along the DNA; (BOUAZOUNE *et al.* 2002), two PHD fingers and two chromodomains for binding to modified N-terminal histone tails (NIELSEN *et al.* 2002; PALACIOS *et al.* 2006) and a DNA-binding domain. LET-418 associates with three other class B synMuv proteins, HDA-1, LIN-53 and MEP-1, to form a *C. elegans* Nucleosome Remodeling and Deacetylase (NuRD)-like

complex (UNHAVAITHAYA *et al.* 2002). In mammals and *Xenopus laevis*, the NuRD complex slides nucleosomes and deacetylates lysines on the N-terminal histone tail to repress transcription (XUE *et al.* 1998; ZHANG *et al.* 1998). Null mutations of *let-418* cause a recessive sterile and vulval cell-fate specification defect. Single *let-418* mutants have an incompletely penetrant ectopic induction of P8.p that is enhanced by loss of class A and B synMuv genes, similar to class C mutants (VON ZELEWSKY *et al.* 2000). RNAi of *let-418* causes larval lethality with some somatic cells being transformed into germline-like cells (UNHAVAITHAYA *et al.* 2002). Therefore, *let-418* is thought to regulate the germline-to-soma cell-fate decision.

MATERIALS AND METHODS

Scoring the larval-lethal phenotype

We distributed five to ten *let-418(n3536)* hermaphrodites during the late L4 larval stage to one of three temperatures: 20ºC, 22.5ºC and 25ºC. We scored the progeny of these animals at each temperature for vulval, germline and viability phenotypes.

Isolation of mutant alleles

We mutagenized *let-418(n3536)* hermaphrodites with ethyl methanesulfonate (EMS) as described previously (BRENNER 1974). We allowed the animals to recover for one hour and then transferred 30-35 P_0 larvae in the late L4 larval stage to 100-mm Petri plates at 20ºC. After four days, the resulting F_1 progeny from each plate of P_0 animals were treated with hypochlorite in separate 15-mL conical tubes until dissolved as described previously (WOOD 1988) to isolated synchronized embryos. The undissolved embryos remained in solution. From each culture of F_1 animals, 8,000 F_2 embryos were distributed onto a single 100-mm Petri plate and cultured at 25ºC. We screened these F_2 animals for viability beyond the first larval stage.

RESULTS

First, we characterized the phenotype of the temperature-sensitive partial loss-of-function allele *let-418(n3536)*, which was isolated in a class B synMuv screen and not characterized further (CEOL *et al.* 2006). Single *let-418(n3536)* mutants have no obvious phenotypic abnormalities at 20ºC, weak ectopic vulval cell fates and incompletely penetrant sterility at 22.5ºC and a completely penetrant larval-lethal phenotype at 25ºC (Table 1). The arrest larvae from 25ºC are slightly larger than wild-type L1 larvae. A genetic selection should help us to understand more about how *let-418* regulates the germline-to-soma cell-fate decision and, perhaps, how the synMuv genes regulate the vulval cell-fate decision. This temperature-sensitive larval-lethal phenotype allowed us to perform a genetic selection for mutants that could survive at 25ºC (described in Materials and Methods).

We screened the progeny of roughly 100,000 F_1 animals at 25ºC for suppressors of the *let-418(n3536)* larval-lethal phenotype. We identified ten independent suppressor isolates (Table 2). Although two-point mapping strains were constructed, we did not characterize these isolates further.

DISCUSSION AND FUTURE DIRECTIONS

We screened the progeny of 100,000 F_1 *let-418(n3536)* animals at 25ºC, which represents 200,000 haploid genomes. From these screens, we identified ten independent suppressor isolates. We learned several important considerations for mapping, characterization and additional screens. First, the temperature at which the strains are grown must be well controlled. Slight perturbations of 0.5ºC can cause complete viability of the parent strain (if slightly less than 25ºC) or complete lethality in suppressor strain (if slightly higher than 25ºC) (data not shown). Second, suppressors that allow the parent strain to survive at 25ºC might have an incompletely penetrant or expressive suppression phenotype. Animals initially selected as suppressors might have failed the retest for this reason.

To address these issues, several steps should be applied to future work on this topic. First, each isolate and the parental strain should be retested for viability at half-degree increments from 24ºC to 26ºC. This temperature-response curve will help to us to understand more about the larval-lethal phenotype and its suppression. Perhaps a more suitable temperature to increase the rate of suppressor recovery can be discovered and applied to future selections. Complementation tests should be performed among the existing isolates to determine how many genes have mutated to cause this phenotype of the suppression of larval lethality. If all isolates fall into one or a few complementation groups, then the selection for EMS-inducible independent mutations might be saturated. If so, different mutagens including ionizing radiation could be tried to possibly give a wider range of mutant alleles.

These suppressors might represent a class of synMuv suppressors not identified by previous synMuv vulval suppressor screens. After mapping and complementation tests, each suppressor should be tested for suppression of the *mep-1*(RNAi*)* larval-lethal phenotype, because *let-418* and *mep-1* are thought to

act together and mutations in each cause larval lethality. General suppressors of the germline-to-soma cell-fate decision might suppress both mutant phenotypes, so suppression of other aspects of the germline-to-soma cell-fate defect should be scored, including the Tam phenotype (HSIEH *et al.* 1999) and RNAi hypersensitivity (WANG *et al.* 2005; LEHNER *et al.* 2006). Also, these isolates should be tested for suppression of the synMuv vulval phenotype. Hopefully, these assays will allow for the classification of synMuv suppressors obtained from this selection and from other screens to allow a better analysis of genes that antagonize defects associated with loss of the synMuv genes.

ACKNOWLEDGMENTS

I would like to thank Robyn Tanny and Ezequiel Alvarez-Saavedra for critical reading of this appendix.

LITERATURE CITED

ANDERSEN, E. C., X. LU and H. R. HORVITZ, 2006 *C. elegans* ISWI and NURF301 antagonize an Rb-like pathway in the determination of multiple cell fates. Development **133:** 2695-2704.

BOUAZOUNE, K., A. MITTERWEGER, G. LANGST, A. IMHOF, A. AKHTAR, P. B. BECKER and A. BREHM, 2002 The dMi-2 chromodomains are DNA binding modules important for ATP-dependent nucleosome mobilization. Embo J **21:** 2430-2440.

BRENNER, S., 1974 The genetics of *Caenorhabditis elegans*. Genetics **77:** 71-94.

CARDOSO, C., C. COUILLAULT, C. MIGNON-RAVIX, A. MILLET, J. J. EWBANK, M. FONTES and N. PUJOL, 2005 XNP-1/ATR-X acts with RB, HP1 and the NuRD complex during larval development in *C. elegans*. Dev Biol **278:** 49-59.

CEOL, C. J., and H. R. HORVITZ, 2001 *dpl-1* DP and *efl-1* E2F act with *lin-35* Rb to antagonize Ras signaling in *C. elegans* vulval development. Mol Cell **7:** 461-473.

CEOL, C. J., and H. R. HORVITZ, 2004 A new class of *C. elegans* synMuv genes implicates a Tip60/NuA4-like HAT complex as a negative regulator of Ras signaling. Dev Cell **6:** 563-576.

CEOL, C. J., F. STEGMEIER, M. M. HARRISON and H. R. HORVITZ, 2006 Identification and classification of genes that act antagonistically to *let-60*

Ras signaling in *Caenorhabditis elegans* vulval development. Genetics **173:** 709-726.

COUSTHAM, V., C. BEDET, K. MONIER, S. SCHOTT, M. KARALI and F. PALLADINO, 2006 The *C. elegan*s HP1 homologue HPL-2 and the LIN-13 zinc finger protein form a complex implicated in vulval development. Dev Biol **297:** 308-322.

COUTEAU, F., F. GUERRY, F. MULLER and F. PALLADINO, 2002 A heterochromatin protein 1 homologue in *Caenorhabditis elegans* acts in germline and vulval development. EMBO Rep **3:** 235-241.

CUI, M., D. S. FAY and M. HAN, 2004 *lin-35*/Rb cooperates with the SWI/SNF complex to control *Caenorhabditis elegans* larval development. Genetics **167:** 1177-1185.

CUI, M., E. B. KIM and M. HAN, 2006 Diverse chromatin remodeling genes antagonize the Rb-involved SynMuv pathways in *C. elegans*. PLoS Genet **2:** e74.

FAY, D. S., S. KEENAN and M. HAN, 2002 *fzr-1* and *lin-35*/Rb function redundantly to control cell proliferation in *C. elegans* as revealed by a nonbiased synthetic screen. Genes Dev **16:** 503-517.

FAY, D. S., E. LARGE, M. HAN and M. DARLAND, 2003 *lin-35*/Rb and *ubc-18*, an E2 ubiquitin-conjugating enzyme, function redundantly to control pharyngeal morphogenesis in *C. elegans*. Development **130:** 3319-3330.

FAY, D. S., X. QIU, E. LARGE, C. P. SMITH, S. MANGO and B. L. JOHANSON, 2004 The coordinate regulation of pharyngeal development in *C. elegans* by *lin-35*/Rb, *pha-1*, and *ubc-18*. Dev Biol **271:** 11-25.

HSIEH, J., J. LIU, S. A. KOSTAS, C. CHANG, P. W. STERNBERG and A. FIRE, 1999 The RING finger/B-box factor TAM-1 and a retinoblastoma-like protein LIN-35 modulate context-dependent gene silencing in *Caenorhabditis elegans*. Genes Dev **13:** 2958-2970.

LEHNER, B., A. CALIXTO, C. CROMBIE, J. TISCHLER, A. FORTUNATO, M. CHALFIE and A. G. FRASER, 2006 Loss of LIN-35, the *Caenorhabditis elegans* ortholog of the tumor suppressor p105Rb, results in enhanced RNA interference. Genome Biol **7:** R4.

MELENDEZ, A., and I. GREENWALD, 2000 *Caenorhabditis elegans lin-13*, a member of the LIN-35 Rb class of genes involved in vulval development, encodes a protein with zinc fingers and an LXCXE motif. Genetics **155:** 1127-1137.

NIELSEN, P. R., D. NIETLISPACH, H. R. MOTT, J. CALLAGHAN, A. BANNISTER, T. KOUZARIDES, A. G. MURZIN, N. V. MURZINA and E. D. LAUE, 2002 Structure of the HP1 chromodomain bound to histone H3 methylated at lysine 9. Nature **416:** 103-107.

PALACIOS, A., P. GARCIA, D. PADRO, E. LOPEZ-HERNANDEZ, I. MARTIN and F. J. BLANCO, 2006 Solution structure and NMR characterization of the binding to methylated histone tails of the plant homeodomain finger of the tumour suppressor ING4. FEBS Lett **580:** 6903-6908.

REDDY, K. C., and A. M. VILLENEUVE, 2004 *C. elegans* HIM-17 links chromatin modification and competence for initiation of meiotic recombination. Cell **118:** 439-452.

SEELIG, H. P., I. MOOSBRUGGER, H. EHRFELD, T. FINK, M. RENZ and E. GENTH, 1995 The major dermatomyositis-specific Mi-2 autoantigen is a presumed helicase involved in transcriptional activation. Arthritis Rheum **38:** 1389-1399.

UNHAVAITHAYA, Y., T. H. SHIN, N. MILIARAS, J. LEE, T. OYAMA and C. C. MELLO, 2002 MEP-1 and a homolog of the NURD complex component Mi-2 act together to maintain germline-soma distinctions in *C. elegans*. Cell **111:** 991-1002.

VON ZELEWSKY, T., F. PALLADINO, K. BRUNSCHWIG, H. TOBLER, A. HAJNAL and F. MULLER, 2000 The *C. elegans* Mi-2 chromatin-remodelling proteins function in vulval cell fate determination. Development **127:** 5277-5284.

WANG, D., S. KENNEDY, D. CONTE, JR., J. K. KIM, H. W. GABEL, R. S. KAMATH, C. C. MELLO and G. RUVKUN, 2005 Somatic misexpression of germline P granules and enhanced RNA interference in retinoblastoma pathway mutants. Nature **436:** 593-597.

WOOD, W. B., 1988 The Nematode *Caenorhabditis elegans*.

XUE, Y., J. WONG, G. T. MORENO, M. K. YOUNG, J. COTE and W. WANG, 1998 NURD, a novel complex with both ATP-dependent chromatin-remodeling and histone deacetylase activities. Mol Cell **2:** 851-861.

ZHANG, Y., G. LEROY, H. P. SEELIG, W. S. LANE and D. REINBERG, 1998 The dermatomyositis-specific autoantigen Mi2 is a component of a complex containing histone deacetylase and nucleosome remodeling activities. Cell **95:** 279-289.

Table 1: Defects associated with the *let-418(n3536)* temperature-sensitive strain.

temperature (°C)	phenotype
20	no obvious abnormalities
22.5	weakly penetrant multivulva and sterile
25	100% penetrant L1 larval lethality

Table 2: Suppressors of the larval-lethal phenotype of *let418(n3536)*

isolates	identified by…
n4481, *n4482*, *n4483*	Divya Mathur
n4644, *n4645*, *n4646*, *n4647*, *n4648*, *n4649*, *n4650*	Sebastian Treusch